

University of Bath



**PHD**

**Insulin-like growth factor 2: Escape from imprinted regulation in the choroid plexus of the mouse**

Menheniott, T. R.

*Award date:*  
2004

*Awarding institution:*  
University of Bath

[Link to publication](#)

**General rights**

Copyright and moral rights for the publications made accessible in the public portal are retained by the authors and/or other copyright owners and it is a condition of accessing publications that users recognise and abide by the legal requirements associated with these rights.

- Users may download and print one copy of any publication from the public portal for the purpose of private study or research.
- You may not further distribute the material or use it for any profit-making activity or commercial gain
- You may freely distribute the URL identifying the publication in the public portal ?

**Take down policy**

If you believe that this document breaches copyright please contact us providing details, and we will remove access to the work immediately and investigate your claim.

Download date: 13. May. 2019


*Insulin-like Growth Factor 2: Escape from  
Imprinted Regulation in the Choroid Plexus of  
the Mouse*

Submitted by T. R. Menheniott  
for the degree of PhD of the University of Bath  
2004

**COPYRIGHT**

Attention is drawn to the fact that copyright of this thesis rests with the author. This copy of the thesis has been supplied on condition that anyone who consults it is understood to recognise that its copyright rests with the author and that no quotation from the thesis and no information derived from it may be published without the prior written consent of the author.

This thesis may be made available for consultation within the University library and may be photocopied or lent to other libraries for the purposes of consultation.

Signed  .....

**T R Menheniott**

UMI Number: U602178

All rights reserved

INFORMATION TO ALL USERS

The quality of this reproduction is dependent upon the quality of the copy submitted.

In the unlikely event that the author did not send a complete manuscript and there are missing pages, these will be noted. Also, if material had to be removed, a note will indicate the deletion.



UMI U602178

Published by ProQuest LLC 2014. Copyright in the Dissertation held by the Author.  
Microform Edition © ProQuest LLC.

All rights reserved. This work is protected against  
unauthorized copying under Title 17, United States Code.



ProQuest LLC  
789 East Eisenhower Parkway  
P.O. Box 1346  
Ann Arbor, MI 48106-1346

UNIVERSITY OF BATH  
LIBRARY  
SS 23 AUG 2005  
Ph.D.



## ABSTRACT

The *Igf2* and *H19* genes are tightly linked and oppositely imprinted. Both genes are situated at the distal region of mouse chromosome 7 and display conserved linkage in humans on chromosome 11p15.5, a region strongly implicated in the paediatric overgrowth disorder Beckwith-Weidemann Syndrome (BWS). Loss of imprinting, leading to biallelic expression of *Igf2*, is the most frequent molecular defect associated with BWS and is observed in the majority of all tumours. *Igf2* and *H19* are widely expressed in mesodermal and endodermal lineages during embryogenesis, with monoallelic expression of the two genes primarily dependent upon a differentially methylated domain (DMD) situated immediately 5' of *H19*. The DMD exists in two epigenetic states, dependent upon its parental origin, functioning on the maternal allele as a chromatin insulator to prevent access of 3' enhancers to *Igf2*, and on the paternal allele as a silencer that confers a heterochromatic state upon *H19 in cis*. Differential methylation at sites proximal to *Igf2*, is established by interaction with the DMD, in hierarchical fashion, and provides additional imprinting control at this locus. *Igf2* escapes imprinted regulation and is biallelically expressed in the choroid plexus and leptomeninges of the brain. An enhancer that confers *Igf2* expression in the choroid plexus, identified within a central conserved domain (CCD) situated 5' of the DMD, and therefore unaffected by insulator activity, provides one mechanism for biallelic expression in this tissue. This work aimed to further elucidate this atypical imprinting, by study of gene expression during choroid plexus development and functional analysis of the critical *cis*-elements. It was found that *Igf2* is biallelically expressed in the developing choroid plexus epithelium, but imprinted in the stroma, thus suggesting that epigenetic modifications are established differently in the two components of this organ. Immortalised choroid plexus epithelial cell lines were derived to test this hypothesis in a homogenous system. The cell lines proliferated rapidly in culture and presented morphological and biochemical features of choroid plexus epithelium. Epigenetic analysis of the cells revealed that DMRs proximal to *Igf2* were uncharacteristically methylated upon both alleles, yet differential methylation at the DMD was preserved, implicating a DMD-independent mechanism in this process. The data argues that the long-range DMR interactions that occur in imprinted tissues are potentially decoupled in the choroid plexus epithelium, thus providing an additional mechanism for biallelic *Igf2* expression in this tissue.

## ACKNOWLEDGEMENTS

I would like to thank first and foremost, Dr Andrew Ward, who has been an outstanding supervisor and an unerring source of guidance and support throughout, in matters both professional and personal. I am grateful to a number of people for providing DNA constructs and probes; Prof. Michael Skinner (Washington State University, USA) provided -3kb and -581bp mouse *Transferrin* promoter constructs, Prof. Robert Costa (University of Illinois, USA) provided the pTTR-7kbexV3 plasmid containing the mouse *Transthyretin* probe, Dr Susan McConnell (Stanford University, California, USA) provided the mouse *Msx1* probe and Prof. Hiroyuki Sasaki (National Institute of Genetics, Mishima, Japan) provided the mouse *CTCF* probe. I am grateful to a number of people for kindly providing strains of transgenic mice; Prof. Wolf Reik (Babraham Institute, Cambridge, UK) provided the *lacZDMR2* (*Igf2* knockout) mice, Prof. Terry Van Dyke (University of North Carolina, USA) provided the T<sub>121</sub> mice, Dr Luisa Dandolo (Institut Cochin de Genetique Moleculaire, Paris) provided embryos derived from the *H19Δ3* knockout strain and Dr Alan Clarke (CRC laboratories, University Medical School, Edinburgh) provided the *p53* knockout mice. I am especially grateful to Dr Marika Charalambous, as this work has benefited enormously from her technical and intellectual input, not to mention those lengthy afternoon discussions and wild conjecture! Thanks are also given to Dr David Tosh for showing me how to perform immunofluorescence, for providing access to primary antibodies and for performing countless hours of confocal microscopy, to Dr James Dutton for imparting his vast scientific knowledge, to Dr Stone Elworthy for divulging his secrets to successful molecular biology and to Louise Anderson and technicians in the animal unit for their considerable efforts on my behalf. I express the most sincere gratitude to my friend and colleague Florentia Smith for being a great 'partner in crime' and for sharing this experience over the past few years, especially during the protracted and at times lonely writing-up process. Finally, thanks to all other members of lab 0.76 for providing a wonderfully informal working environment, none more so than Dr Valentina Svetić with whom I have shared so much and also to Dr Sharon Kelly for generous supply of wine and Alastair Garfield for keeping me entertained and for 'tying up a few loose ends'. This work was funded by the Association for International Cancer Research.

This work is dedicated to my parents,

*“The heights of great men reached and kept  
Were not achieved by sudden flight,  
But they, while their companions slept,  
Were toiling upward in the night”.*

Henry Wadsworth Longfellow, from  
‘The Ladder of St Augustine’

## TABLE OF CONTENTS

TABLE OF CONTENTS .....	5
LIST OF FIGURES .....	8
LIST OF TABLES .....	12
LIST OF ABBREVIATIONS .....	13
<b>CHAPTER 1: INTRODUCTION.....</b>	<b>15</b>
GENOMIC IMPRINTING .....	15
<i>Background</i> .....	15
<i>Epigenetic Modifications</i> .....	16
<i>Features of imprinted genes</i> .....	21
<i>Genetic conflict and the evolution of imprinting</i> .....	27
THE IGF2/H19 LOCUS.....	30
<i>Tissue specific expression</i> .....	36
<i>Cis-elements required for Igf2/H19 expression</i> .....	38
<i>Differentially methylated regions at Igf2/H19</i> .....	44
THE CHOROID PLEXUS .....	52
<i>Development of the choroid plexus</i> .....	55
<i>In vitro culture systems</i> .....	58
<i>Summary</i> .....	58
<i>Aims</i> .....	60
<b>CHAPTER 2: MATERIALS AND METHODS .....</b>	<b>63</b>
MOLECULAR CLONING TECHNIQUES .....	63
MICE .....	67
SOUTHERN ANALYSIS .....	69
NORTHERN ANALYSIS .....	71
REVERSE TRANSCRIPTION AND POLYMERASE CHAIN REACTION (RT- PCR).....	72
TRANSIENT EXPRESSION ASSAYS.....	73
GENERATION OF IMMORTAL CHOROID PLEXUS EPITHELIAL CELL LINES .....	76
IN SITU EXPRESSION ANALYSIS IN CULTURED MAMMALIAN CELLS .....	78
IN SITU EXPRESSION ANALYSIS IN WHOLE MOUNT PREPARATIONS.....	79
<i>Whole mount mRNA in situ hybridisation</i> .....	79

<i>Whole mount staining for <math>\beta</math>-galactosidase in situ</i> .....	82
IN SITU EXPRESSION ANALYSIS IN HISTOLOGICAL PREPARATIONS .....	83
<i>Slide mRNA in situ hybridisation</i> .....	83
<i>Immunohistochemistry</i> .....	84
<b>CHAPTER 3: DEVELOPMENTAL GENE EXPRESSION ANALYSIS.....</b>	<b>86</b>
INTRODUCTION .....	86
MATERIALS AND METHODS .....	92
RESULTS .....	96
<i>Allele-specific lacZDMR2<sup>-</sup> reporter gene assays</i> .....	96
<i>Comparison of lacZDMR2<sup>-</sup> and endogenous Igf2 expression</i> .....	111
<i>H19 expression in the developing choroid plexus</i> .....	112
<i>Analysis of differentiation markers in the developing choroid plexus</i> .....	120
<i>A potential involvement of Notch signalling in regulating variegated Igf2 expression</i> .....	126
CONCLUSIONS .....	135
<b>CHAPTER 4: IN VITRO INVESTIGATION OF CHOROID PLEXUS CIS REGULATORY ELEMENTS.....</b>	<b>148</b>
INTRODUCTION .....	148
MATERIALS AND METHODS .....	150
RESULTS .....	152
<i>Primary culture of choroid plexus epithelial cells</i> .....	152
<i>PCR-amplification of Intergenic conserved elements</i> .....	154
<i>Generation of Igf2-Luciferase reporter constructs</i> .....	159
<i>Transient expression assays</i> .....	164
CONCLUSIONS .....	180
<b>CHAPTER 5: GENERATION AND CHARACTERISATION OF IMMORTAL CHOROID PLEXUS EPITHELIAL CELL LINES .....</b>	<b>187</b>
INTRODUCTION .....	187
MATERIALS AND METHODS .....	195
RESULTS .....	198
<i>Generation of immortal choroid plexus epithelial cell lines</i> .....	198
<i>Characterisation of immortal choroid plexus epithelial cell lines</i> .....	202

<i>Gene expression at the Igf2/H19 locus</i> .....	227
<i>Allele-specific Igf2 expression in situ</i> .....	230
<i>DNA methylation at the Igf2/H19 locus</i> .....	236
CONCLUSIONS .....	246
<b>CHAPTER 6: CONCLUSIONS</b> .....	<b>260</b>
DEVELOPMENTAL EXPRESSION ANALYSIS .....	260
TRANSIENT EXPRESSION ASSAYS .....	264
IMMORTAL CHOROID PLEXUS EPITHELIAL CELL LINES .....	266
FUTURE WORK .....	271
<b>REFERENCES</b> .....	<b>273</b>
<b>PUBLICATIONS ARISING</b> .....	<b>297</b>

## LIST OF FIGURES

<i>Figure</i>	<i>Description</i>	<i>Page</i>
<b>Figure 1</b>	The <i>Igf2/H19</i> locus in the mouse	31
<b>Figure 2</b>	<i>Igf2/H19</i> expression during mouse embryogenesis	37
<b>Figure 3</b>	The choroid plexus	54
<b>Figure 4</b>	PCR optimisation protocol	68
<b>Figure 5</b>	The <i>lacZDMR2</i> <sup>-</sup> genomic region	89
<b>Figure 6</b>	Allele-specific <i>lacZDMR2</i> <sup>-</sup> reporter gene expression assays, e9.5 and e10.5 embryos	99
<b>Figure 7</b>	Allele-specific <i>lacZDMR2</i> <sup>-</sup> reporter gene expression assays, e12.5 and e14.5 embryos	102
<b>Figure 8</b>	Allele-specific <i>lacZDMR2</i> <sup>-</sup> reporter gene expression assays, adult brain	105
<b>Figure 9</b>	Allele-specific <i>lacZDMR2</i> <sup>-</sup> reporter gene expression assays, choroid plexus development	107
<b>Figure 10</b>	Allele-specific <i>in situ</i> hybridisation analysis of <i>Igf2</i> expression, choroid plexus	113
<b>Figure 11</b>	Allele-specific <i>in situ</i> hybridisation analysis of <i>Igf2</i> expression and <i>lacZDMR2</i> <sup>-</sup> reporter gene expression, brain capillary endothelium	115
<b>Figure 12</b>	Allele-specific <i>in situ</i> hybridisation analysis of <i>H19</i> expression, choroid plexus	118
<b>Figure 13</b>	Immunohistochemistry analysis of differentiation markers in the choroid plexus epithelium	121
<b>Figure 14</b>	<i>In situ</i> hybridisation analysis of <i>FoxJ1</i> expression in the choroid plexus epithelium	123

<b>Figure 15</b>	RT-PCR analysis of <i>Notch</i> , <i>Delta</i> and <i>Jagged</i> gene expression in the choroid plexus	127
<b>Figure 16</b>	<i>In situ</i> hybridisation analysis of <i>Notch</i> , <i>Delta</i> and <i>Jagged</i> gene expression in the choroid plexus	132
<b>Figure 17</b>	Primary choroid plexus cultures, morphological analysis	155
<b>Figure 18</b>	Primary choroid plexus cultures, Northern analysis of <i>Igf2</i> and <i>TTR</i> expression	157
<b>Figure 19</b>	Primary choroid plexus cultures, immunofluorescence analysis of TTR and E-cadherin expression	158
<b>Figure 20</b>	Genomic location of <i>Igf2/H19</i> intergenic conserved regions	160
<b>Figure 21</b>	PCR-amplification of <i>Igf2/H19</i> intergenic conserved regions	162
<b>Figure 22</b>	<i>Igf2</i> promoter 3 (P3) <i>Luciferase</i> reporter constructs used in transient expression assays	166
<b>Figure 23</b>	<i>Luciferase</i> expression levels following transfection of CCD deletion constructs, primary choroid plexus cells	171
<b>Figure 24</b>	<i>Luciferase</i> expression levels following transfection of CCD deletion constructs, HepG2 cells	173
<b>Figure 25</b>	<i>Luciferase</i> expression levels following transfection of intergenic conserved region constructs, primary choroid plexus cells	175
<b>Figure 26</b>	<i>Luciferase</i> expression levels following transfection of intergenic conserved region constructs, HepG2 cells	177
<b>Figure 27</b>	<i>Luciferase</i> expression levels following transfection of enhancer synergism constructs, primary choroid plexus cells	179
<b>Figure 28</b>	Structure of the SV40-T <sub>121</sub> transgene	191



<b>Figure 29</b>	PCR genotyping analysis, identification of $T_{121}; p53^{+/-}; lacZDMR2^{+/mat}$ mutants	199
<b>Figure 30</b>	Comparison of CPlacZ cell lines and primary choroid plexus cultures, morphological analysis	204
<b>Figure 31</b>	PCR genotyping analysis, CPlacZ cell lines	206
<b>Figure 32</b>	Comparison of CPlacZ cell lines and primary choroid plexus cultures, cell growth in relation to $T_{121}$ expression and <i>p53</i> function	208
<b>Figure 33</b>	Northern analysis of <i>TTR</i> , <i>Foxj1</i> and <i>Msx1</i> expression in CPlacZ cell lines	211
<b>Figure 34</b>	Immunofluorescence: comparison of CPlacZ cell lines and primary choroid plexus cultures, hepatocyte/choroid plexus differentiation markers	215
<b>Figure 35</b>	Immunofluorescence: comparison of CPlacZ cell lines and primary choroid plexus cultures, epithelial cell differentiation markers	217
<b>Figure 36</b>	Immunofluorescence: analysis of HepG2 cells, hepatocyte/epithelial cell differentiation markers	219
<b>Figure 37</b>	RT-PCR analysis of E-cadherin expression in CPlacZ cell lines	223
<b>Figure 38</b>	<i>TFN</i> promoter <i>trans</i> -activation assays: comparison of CPlacZ cell lines and HepG2 cells	225
<b>Figure 39</b>	Northern analysis of <i>Igf2</i> , <i>H19</i> and <i>CTCF</i> expression in CPlacZ cell lines	228
<b>Figure 40</b>	RT-PCR analysis of <i>Igf2</i> ( <i>lacZDMR2</i> <sup>-</sup> ) expression in CPlacZ cell lines	232
<b>Figure 41</b>	Allele-specific analysis of <i>Igf2</i> ( <i>lacZDMR2</i> <sup>-</sup> ) expression <i>in situ</i> , CPlacZ cell lines	234

<b>Figure 42</b>	Restriction map of the <i>H19</i> locus	238
<b>Figure 43</b>	Restriction map of the <i>Igf2</i> locus	240
<b>Figure 44</b>	Methylation analysis of the DMD and <i>H19</i> promoter-proximal region in CPlacZ cell lines	242
<b>Figure 45</b>	Methylation analysis of <i>Igf2</i> DMR1 in CPlacZ cell lines	244
<b>Figure 46</b>	Proposed mechanisms of biallelic <i>Igf2</i> expression in the choroid plexus epithelium	269

## LIST OF TABLES

<i>Table</i>	<i>Description</i>	<i>Page</i>
<b>Table 1</b>	RNA probes used for <i>in situ</i> hybridisation analysis	93
<b>Table 2</b>	Primary antibodies used for immunohistochemistry	94
<b>Table 3</b>	Primers used for RT-PCR analysis of <i>Notch</i> , <i>Delta</i> and <i>Jagged</i> expression	95
<b>Table 4</b>	Summary of allele-specific <i>lacZDMR2</i> <sup>-</sup> reporter gene assays	110
<b>Table 5</b>	Summary of differentiation marker expression analysis	125
<b>Table 6</b>	Summary of <i>Notch</i> , <i>Delta</i> and <i>Jagged</i> <i>in situ</i> hybridisation analysis	134
<b>Table 7</b>	Primers used to PCR-amplify conserved elements from the <i>Igf2/H19</i> intergenic region	151
<b>Table 8</b>	Summary of transient expression data for CCD deletion constructs, primary choroid plexus cells	171
<b>Table 9</b>	Summary of transient expression data for CCD deletion constructs, HepG2 cells	173
<b>Table 10</b>	Summary of transient expression data for intergenic conserved region constructs, primary choroid plexus cells	175
<b>Table 11</b>	Summary of transient expression data for intergenic conserved region constructs, HepG2 cells	177
<b>Table 12</b>	Summary of transient expression data for enhancer synergism constructs, primary choroid plexus cells	179
<b>Table 13</b>	Primary antibodies used for immunofluorescence cytochemistry	196
<b>Table 14</b>	Primers used for RT-PCR expression analysis	197

## LIST OF ABBREVIATIONS

<i>Air</i>	<i>Antisense insulin-like growth factor receptor transcript</i>
AS	Angelman Syndrome
AVP	arginine vasopressin
Aza-C	5'-aza-2'-deoxycytidine
$\alpha$ -	anti-
bp	base pair
BMP	bone morphogenetic protein
BSA	bovine serum albumin
BWS	Beckwith Weidemann Syndrome
CAF	cytosine arabinofuranoside
CCD	centrally conserved domain
cDNA	complementary deoxyribonucleic acid
CNS	central nervous system
CpG	cytidine and guanidine containing dinucleotide unit
CSF	cerebrospinal fluid
CTCF	CCCTC-binding factor
<i>Dlk1</i>	<i>Delta-like homologue 1</i>
DIC	differential interference contrast
DMD	differentially methylated domain
DMR	differentially methylated region
DNA	deoxyribonucleic acid
Dnmt	De-novo methyltransferase
e(x)	embryonic day x
ECM	extracellular matrix
<i>Eed</i>	<i>Embryonic ectoderm development</i>
<i>E[z]</i>	<i>Enhancer of zeste</i>
ES cells	embryonic stem cells
FBS	foetal bovine serum
FGF	fibroblast growth factor
FITC	fluorescein isothiocyanate
<i>Grb10</i>	<i>Growth factor receptor bound protein 10</i>

HDAC	histone deacetylase
<i>Hpy</i>	<i>Hydrocephalus and polydactyl</i>
HS	hypersensitive site
ICR	imprinting control region
<i>Igf2</i>	<i>Insulin-like growth factor 2</i>
<i>Igf2r</i>	<i>Insulin-like growth factor 2 receptor</i>
kb	kilobase
LOI	loss of imprinting
Mb	megabase
MeCP2	5' methyl cytosine binding protein 2
M	mole
mRNA	messenger ribonucleic acid
<i>Msx1</i>	<i>Msh-like homeobox gene 1</i>
PBS	phosphate buffered saline
PcG	polycomb group
PCR	polymerase chain reaction
PGC	primordial germ cell
PMEF	primary embryonic mouse fibroblast
<i>Psc</i>	<i>Posterior sex combs</i>
PWS	Prader-Willi Syndrome
P3	<i>Igf2</i> promoter 3 region
RNA	ribonucleic acid
RNAi	ribonucleic acid interference
RT	reverse transcription
SINE	short interspersed repeat element
<i>TFN</i>	<i>Transferrin</i>
TRITC	tetramethyl-rhodamine isothiocyanate
TSA	trichostatin A
<i>TTR</i>	<i>Transthyretin</i>
UPD	uniparental disomy
WT	wild type
<i>Xt</i>	<i>Extra toes</i>
YAC	yeast artificial chromosome

## CHAPTER 1: INTRODUCTION

### ***Genomic Imprinting***

#### **Background**

Embryogenesis in mammals requires a contribution of paternal and maternal genomes for development to term. Nuclear transplantation experiments in the mouse have demonstrated that reconstituted diploid embryos, derived from two paternal, or two maternal pronuclei, are not viable (McGrath 1984; Surani *et al.* 1986). Such uniparental embryos exhibit reciprocal developmental abnormalities, where those of entirely paternal derivation display overabundance of the extraembryonic tissues and severe growth retardation in embryonic lineages, whilst in embryos of maternal derivation the converse situation is seen (Barton *et al.* 1984; Barton *et al.* 1985). Similarly, in humans hydatidiform moles, which are derived entirely from paternal chromosomes generate placental tissue, whilst maternally derived ovarian dermoid cysts have a predominant embryonic component (Jirtle 1999)(and references therein). The parental genomes are therefore functionally nonequivalent. Genetic studies utilising mice in which individual chromosomes or chromosomal regions were inherited uniparentally demonstrated that this functional non-complementation is not manifested by the entire genome, but resides within specific chromosomal domains (Cattanach and Kirk 1985).

The breakthrough in understanding this phenomenon came with the discovery of imprinted genes, that is those genes differentially activated or silenced dependent upon the sex of the transmitting parent (Barlow *et al.* 1991; Bartolomei *et al.* 1991; DeChiara *et al.* 1991). It is thought that imprinted genes acquire their parent-of-origin specific mode of expression by means of heritable epigenetic marks established in the respective parental germlines. This marking discriminates the alleles as being of maternal or paternal origin and determines which copy will be active in the embryo. Imprinted genes play fundamental roles during development with particular emphasis upon the regulation of foetal and placental growth/viability and influence of postnatal behaviour. More than 70 genes with this mode of non-Mendelian expression have been identified in the mouse, although it is postulated the total number could be far greater (Falls 1999; Beechey *et al.* 2003). Both the genomic organisation and parental origin-specific expression of many imprinted genes are conserved in humans. Non-

compliance with Mendelian inheritance, it has been suggested, may render imprinted genes particularly susceptible to the effects of mutation and consistent with this proposal their misregulation is frequently observed in many human cancers and the congenital disorders Prader-Willi/Angelman Syndrome (PWS/AS) and Beckwith Weidemann Syndrome (BWS), which causes pre- and postnatal overgrowth and childhood tumour susceptibility (Nicholls *et al.* 1998; Jirtle 1999; Pulford *et al.* 1999; Maher 2000; Walter 2003).

### **Epigenetic Modifications**

The nucleotide sequence of autosomal DNA is identical between the paternal and maternal genomes. The parental-origin specific mode of expression exhibited by imprinted genes must therefore be a consequence of epigenetic marking, or 'imprinting' of DNA in a manner that allows the parental alleles to be distinguished. The imprinting mark must be heritable (and stable) through successive cell divisions, such that it is retained in cell progeny, but must also be able to alter the transcriptional activity of the genes that it regulates. Importantly, an imprinting mark must be reversible such that upon germline passage it may be erased and reset in a manner appropriate to the sex of the transmitting parent.

#### *DNA methylation*

In mammals, DNA methylation occurs principally by the covalent attachment of a methyl group to the 5'carbon of the cytosine residue within symmetrical cytosine/guanine (CpG) dinucleotides. This symmetry together with the preference of the principle mammalian methyltransferase, Dnmt1, for hemimethylated DNA as a substrate provides a basis by which methylation patterns are stably inherited through successive cell generations. In general, DNA methylation is thought to regulate specific genes by the recruitment of methyl-CpG binding domain (MBD) proteins and histone deacetylases (HDACs), which confer transcriptional repression by induction of the heterochromatic state (Bird 1999). Methylation is also thought to be necessary for silencing of CpG-rich retrotransposons, the activity of which can lead to genome instability (Greally 2002; Bourc'his and Bestor 2004). DNA methylation therefore maintains normal genome functioning, by modulating gene expression and influencing structural integrity.

Manipulation of the *Dnmt1* gene in loss- and gain-of-function studies has demonstrated an essential role for correct genome methylation in both embryonic development and genomic imprinting. Inactivation of *Dnmt1* in mice results in growth arrest and embryonic lethality at the 8-somite stage (Li *et al.* 1992). Deregulation of imprinted gene expression also occurs in *Dnmt1*-deficient embryos, with reactivation of the normally silent paternal *H19* allele and silencing of both alleles at the *Igf2* and *Igf2r* loci (Li 1993). Similarly, embryonic lethality and the inappropriate expression of several imprinted genes results from the overexpression of *Dnmt1* in mice (Biniszkiwicz 2002). These experiments provide unequivocal evidence that DNA methylation is required for the imprinting process. An exception is provided by the *Mash2* gene, whose imprinted expression persists in *Dnmt1*<sup>-/-</sup> embryos despite extensive genome demethylation (Tanaka 1999). Therefore, the imprinting of *Mash2* is probably dependent upon modifications other than DNA methylation.

How does methylation upon CpG dinucleotides convey parental identity such that differential expression of the alleles arises in somatic cells? CpGs occur in vertebrate genomes at less than one quarter of the expected frequency. Exceptions to this gross underrepresentation are short CpG-rich regions termed CpG islands. The term CpG island defines genomic regions that are greater than 200 bp in length, with a GC content greater than 50% and a CpG dinucleotide observed to expected ratio (based on GC content) greater than 0.6 (Gardiner-Garden 1987; Strichman-Almashanu 2002). It is generally thought that CpG islands are not methylated, however exceptions are provided by the existence of CpG islands that map to the inactive X-chromosome and imprinted regions (Yen 1984; Mann 2000)(and references therein). In support of a role for DNA methylation in the imprinting process, CpG islands located within the vicinity of most, but not all imprinted genes are overlapped by regions of parent-specific differential methylation (DMRs) and it is generally accepted that this modification constitutes at least part of the marking process that discriminates the parental origin of the alleles (Reik 2001b)(and references therein). Additionally, consistent with a methylation independent mechanism of imprinting implicated by *Dnmt1* knockout studies, *Mash2* does not appear to be differentially methylated or associated with a DMR (Tanaka 1999).



As already discussed, DNA methylation is generally thought to be a stable and heritable epigenetic mark that regulates key aspects of genome function. There are, however, two principal developmental stages, primordial germ cells (PGCs) and the pre-implantation embryo, in which DNA methylation levels are highly variable, with major differences apparent between the parental genomes (reviewed in (Reik 2001a)). Functional imprinting requires that differential methylation marks are correctly established in germ cells and stably maintained postzygotically, a seemingly unremarkable process, if it were not for successive waves of demethylation and subsequent *de novo* methylation that sweep the genome at pre-implantation stages. Specific mechanisms must then exist which protect parental origin-specific methylation marks during these early stages of development.

The genomes of the egg and sperm become highly methylated during maturation, however both become demethylated following fertilisation by both active and passive mechanisms (Reik 2001a)(and references therein). Demethylation is initially confined to the paternal genome, which commences following sperm entry to the egg cytoplasm and is completed prior to the first zygotic division, providing strong evidence of an active demethylation mechanism. Intriguingly, the maternal genome is not itself affected by this ‘demethylase’ activity and remains highly methylated, even at syngamy (Santos 2002). The paternal genome is therefore targeted for active demethylation, with factors in the egg environment potentially mediating this process. *In vitro* work has implicated the methyl-CpG binding protein, MBD2, in this process (Bhattacharya *et al.* 1999), however demethylation occurs normally in MBD2-deficient oocytes, demonstrating that MBD2 is not required for demethylation *in vivo* (Santos 2002).

During subsequent cleavage divisions methylation levels steadily decline in the embryo, reaching their lowest point at the blastocyst stage. This represents the passive phase of demethylation, probably mediated by the exclusion of the maintenance methyltransferase, Dnmt1, from the nucleus in embryos at preimplantation stages (Howell *et al.* 2001). Intriguingly, many imprinted genes and some direct repeat sequences are not demethylated during this phase. For example, paternal-specific methylation imprints are maintained at both *Rasgrf1* and *H19*, but not at *Igf2*, suggesting a mechanism that confers specific protection of some loci but not others

(Brandeis *et al.* 1993; Tremblay *et al.* 1997; Reik 2001a). Genetic studies implicate the oocyte and preimplantation Dnmt1 variant, Dnmt1o, in this process (Howell *et al.* 2001). Dnmt1o is expressed at high levels in the oocyte and preimplantation embryo and replaces the somatic Dnmt1 variant at these stages. Though excluded from the nucleus prior to fertilization, in 8-cell embryos, Dnmt1o transiently relocates to the nucleus for a single replication cycle. Analysis of embryos deficient in this preimplantation form of Dnmt1 revealed that the methylated alleles of imprinted genes had lost 50% of their methylation at later stages, demonstrating that the maintenance methylation function of Dnmt1o, possibly acting at the 8-cell stage, is crucial for the preservation of methylation imprints (Howell *et al.* 2001). That only 50% methylation is lost at imprinted loci, suggests that additional methylation protective mechanisms are also likely to be involved.

By the blastocyst stage of development and unlike earlier stages where gross differences are apparent, the parental genomes cannot be distinguished on the basis of their methylation levels, with both being almost completely demethylated. Genome remethylation commences shortly after implantation and levels gradually increase as development proceeds (Monk 1987). This occurs in a lineage-specific manner, where *de novo* methylation is restricted to the inner cell mass (ICM) appear, whilst the trophoectoderm remains almost devoid of methylation (Santos 2002). Rising genome methylation levels mount a further challenge to the perpetuation of imprinting marks, as unmethylated alleles within DMRs must be protected from *de novo* methylation. Studies at the *H19* locus, which bears a paternal methylation imprint (Tremblay *et al.* 1997) implicate the local chromatin conformation in the exclusion of methylation from the unmethylated maternal allele (Khosla *et al.* 1999; Kanduri 2000a). More recent evidence indicates, that this specific protection against *de novo* methylation may be conferred upon *H19*, entirely by binding of the chromatin insulator protein, CTCF (Schoenherr *et al.* 2003; Fedoriw *et al.* 2004; Pant 2004). Therefore, it seems likely that imprinted genes require additional epigenetic marks and the recruitment of *trans*-imprinting factors, in order to attract, or to be protected against *de novo* methylation during postimplantation development.

Precisely how methylation imprints are established *de novo* is not clearly understood, principally because the DNA methyltransferases have little or no sequence specificity

other than for CpG dinucleotides. Genome wide demethylation takes place at an early stage of PGC development in mice and reaches completion by e13-14 in both male and female germlines, though prior to this stage PGCs in both sexes are methylated and display monoallelic expression at imprinted loci (Reik 2001a) (and references therein). *De novo* methylation of both parental germlines is initiated several days later, though the process in males occurring in prospermatogonia between e15-16 (Kafri 1992; Brandeis *et al.* 1993) precedes that in females, which is initiated after birth during oocyte growth (Kafri 1992).

Current evidence assigns the function of maintenance methylation to the protein Dnmt1 and its oocyte variant, Dnmt1o, and whilst there is some evidence that Dnmt1 can perform *de novo* methylation *in vitro*, it seems unlikely that this enzyme can initiate *de novo* methylation *in vivo*. *De novo* methyltransferase activity for the variant, Dnmt1o has also been excluded (Howell *et al.* 2001).

The activity of *de novo* methylation *in vivo* is thought to be a property of Dnmt3 family proteins, consisting of Dnmt3a, Dnmt3b and Dnmt3L (Bestor 2000). Targeted mutagenesis of the *Dnmt3a* and *Dnmt3b* genes led to embryonic (*Dnmt3b*) and postnatal (*Dnmt3a*) lethality, thus both are required for normal development. Compound (*Dnmt3a*<sup>-/-</sup>/*Dnmt3b*<sup>-/-</sup>) mutants did not undergo genome remethylation during postimplantation development and were subject to growth arrest at the presomite stage. Therefore, these proteins are required for *de novo* methylation during early embryogenesis. Imprinted gene expression was maintained in the compound mutants, providing clear evidence that *de novo* activity of Dnmt3a and 3b is not required to maintain imprinting at post-zygotic stages (Okano 1999). The lethal effects of these mutations prevented further analysis in the germline context.

In a recent study, germline-specific deletions of *Dnmt3a* and *Dnmt3b* were created by *cre-loxP* mediated conditional mutagenesis, to address the question of whether these proteins are required to establish methylation imprints. Females homozygous for the conditional *Dnmt3a* mutation were viable and normal, however heterozygous progeny of these females died at, or prior to e10.5 of gestation, with disruption of maternal methylation imprints and misexpression of several imprinted genes. The role of *Dnmt3a* in the context of the male germline could not be directly addressed, as male

mice homozygous for the *Dnmt3a* mutation were azoospermic. However analysis of spermatogonia dissected from these mice revealed that paternal methylation imprints had similarly been disrupted. By contrast, the conditional *Dnmt3b* mutation had no effect upon methylation in either germline (Kaneda *et al.* 2004). Therefore, *Dnmt3a*, but not *Dnmt3b* is required for establishment of methylation imprints in both male and female germlines.

Dnmt3L (for Dnmt3-like) shares homology with Dnmt3 methyltransferases, but lacks the catalytic methyltransferase domain, setting it apart from the other Dnmt3 family members and suggesting that it does not possess intrinsic methyltransferase activity (Bourc'his *et al.* 2001). Disruption of *Dnmt3L* in mice resulted in a maternal-effect phenotype that was indistinguishable from that of the conditional *Dnmt3a* mutation (Bourc'his *et al.* 2001; Hata 2002). Intriguingly, Dnmt3L has also been shown to interact and colocalise with both Dnmt3a and Dnmt3b in tissue culture cells (Hata 2002). Therefore, whilst Dnmt3L is unlikely itself to mediate *de novo* methylation in the germline, it appears to co-operate with the other Dnmt3 proteins in this process imprint establishment. Taken with the findings of other studies, this indicates that Dnmt3 family proteins (Dnmt3a and Dnmt3L) are the major factors responsible for the establishment of germline methylation marks essential to genomic imprinting.

### **Features of imprinted genes**

Parental origin-specific expression or silencing of the alleles is the defining feature of an imprinted gene. It is now generally accepted that most imprinted genes are characterised by a number of other distinguishing features that sets them apart from autosomal genes not subject to this unusual form of regulation. These features are discussed below.

#### *Differential methylation*

As discussed above, genome methylation is essential for correct imprinted gene expression (Li 1993) and most imprinted genes or their flanking sequences are marked by regions of parental origin-specific differential methylation (DMRs). The function of DMRs with respect to the mechanism of imprinted gene expression will be later discussed in detail in the context of the *Igf2/H19* locus, upon which this study is based.

### *Clustering of Imprinted genes*

One of the most striking properties of imprinted genes is that, in most cases, other imprinted genes are located in close proximity. A significant proportion of known imprinted genes are organised in clusters, which argues for the existence of region-wide regulatory mechanisms such as *cis*-acting imprinting control regions or local chromatin structure. An intensively studied imprinted gene cluster is situated within the Beckwith-Weidemann Syndrome (BWS) region, which lies on chromosome 11p15.5 in humans and shows conserved linkage on distal chromosome 7 in the mouse (Beechey 2003). The cluster spans approximately 1Mb in both species. In the mouse, this region contains at least 15 imprinted genes, which display both paternal-specific (*Igf2*, *Igf2AS/Peg8*, *Ins2*, *Kvlqt1AS/Lit1*) and maternal-specific (*H19*, *Cd81*, *Ascl2/Mash2*, *Tssc4*, *Kvlqt1*, *p57<sup>KIP2</sup>/Cdkn1c*, *Msuit*, *Ipl/Tssc3*, *Slc22a11*, *Obph1*, *Nap114*) monoallelic expression (Paulsen 2000; Beechey 2003). The genomic arrangement and transcriptional orientation of this cluster is largely conserved in humans, although not all of the human orthologues demonstrate imprinting, with *CD81* and *TSSC4* biallelically expressed. Conversely, the *LTRPC5/Ltrpc5* gene is imprinted in humans, but not in mice (Paulsen 2000)(and references therein). In humans and mice, the proximal and distal extent of the cluster is respectively defined by the flanking genes *NAP1L4/Nap114* and *RRPL23L/Rrpl23l*, which are biallelically expressed in both species (Paulsen 1998). A further difference between the species occurs in the orientation of the cluster with respect to the centromere, with *H19* representing the most telomeric imprinted gene in humans and the most centromeric gene in mice (Casparly *et al.* 1998).

Paternal uniparental disomy (UPD) of 11p15.5 is observed in a small number of BWS cases and loss of maternal 11p15.5 is a frequent occurrence in the tumours, most commonly Wilms tumour, to which BWS predisposes (Jirtle 1999)(and references therein). The most frequently observed defect in cases of BWS (where no cytogenetic rearrangements are detected) is biallelic expression caused by loss of imprinting (LOI) at the *IGF2* locus. This is often associated with aberrant epigenetic modification and silencing of the neighbouring *H19* gene, although in many other cases no modification of *H19* is apparent (Reik *et al.* 1995; Catchpoole *et al.* 1997). Mutations in *KvLQTI* and the overlapping *LIT1* antisense transcript are also prominent in BWS and have been associated with biallelic *IGF2* expression in some cases (Smilnich *et al.* 1999).

Two imprinting control regions (ICR) that confer imprinting upon distinct subdomains within this cluster have been formally identified by gene targeting studies in mice. One of these is located in the 5' flank of the *H19* gene and regulates the imprinting of *Ins2*, *Igf2*, and *H19* by functioning, in part, as a chromatin insulator that prevents access to shared enhancers (Thorvaldsen *et al.* 1998; Bell 2000; Hark *et al.* 2000). The function of this ICR and its implications for *Igf2/H19* imprinting is discussed at length in a later section of this chapter. A second ICR is located within the body of the *Kvlqt1* gene and is overlapped by the *Lit1* antisense transcript (Smilinich *et al.* 1999). Deletion of this region leads to loss of imprinting of several genes including *Ipl*, *p57<sup>KIP2</sup>* and *Ascl2*, again with chromatin insulator activity possibly mediating at least part of this function (Fitzpatrick 2002; Kanduri 2002). Therefore, this region (and possibly the *Lit1* transcript) is required to imprint a subset of genes within this cluster. Regional imprinting control conferred by two ICR elements thus partitions the BWS cluster into *Igf2/H19* and *p57<sup>KIP2</sup>/Lit1* regulatory subdomains.

Another example of regional imprinting control has been revealed by studies of the Prader-Willi Syndrome/Angelman Syndrome (AS/PWS) imprinted region, which maps to human chromosome 15q11-q13. The cluster is characterised by the paternally expressed *SNRPN/SNURF*, *ZNF127*, *NDN*, *IPW* genes and the maternally expressed *UBE3A* gene. The homologous region in the mouse is located on proximal chromosome 7 with conservation of gene order and imprinted features (Nicholls 1998). The most frequent event in the pathogenesis of PWS/AS is a 4Mb deletion at 15q11-q13, which removes the entire cluster. The deletion is paternal in origin for PWS, and results in loss of expression of several paternally expressed genes, and maternal in origin for AS, resulting in loss of *UBE3A* expression, which it is proposed, is the single cause of this disorder. Mutational studies in PWS and AS families, have defined a bipartite ICR element that occupies a 4kb region spanning the 5' promoter region and exon 1 of the bicistronic *SNRPN/SNURF* locus and a second 880bp region situated 40kb further proximal. Microdeletions that disrupt the 5' region of the *SNRPN/SNURF* locus have been observed in a subset of PWS patients that present biparental inheritance of 15q11-q13, but display an abnormal epigenotype (Ohta 1999). Moreover, deletion of this region in mice leads to the loss of expression of the paternally expressed *Znf127*, *Ndn* and *Ipw* genes and manifestation of the PWS

phenotype (Yang 1998). Deletions affecting the second and more proximal of the two ICR elements are frequently observed in AS families (Buiting *et al.* 1999). Analysis of this region in a transgenic context demonstrated that this element was required for imprinting of mouse *Snrpn* minitransgenes including the 5' promoter element, providing formal evidence in support of a functional imprinting role (Kantor 2004).

### *Repeat elements*

Mounting evidence indicates that DNA methylation constitutes a primary imprinting mark and therefore the processes establishing this modification putatively represent the primary imprinting mechanisms. Whilst major *trans*-imprinting factors (DNA methyltransferases) have been discovered, proteins that target the establishment of parental-origin specific methylation patterns in a sequence-specific manner have not been identified. GC-rich tandem repeats are often observed in association with regions of differential methylation (DMRs) of imprinted genes and have been proposed to play a role in the imprinting mechanism by attracting methylation to DMRs (Szebenyi 1994; Neumann 1995). *Trans*-imprinting factors expressed in the germ line of one sex but not the other are likely to be involved, and their ability to methylate in primary DMRs may be mediated, in part, through interactions with the repeat elements themselves. Consistent with this proposal, a tandem repeat region located 5' of the *Rasgrf1* locus has been shown to function in such a role. While not itself differentially methylated, this region is required *in cis* to direct differential methylation within an adjacent DMR and for imprinted expression of *Rasgrf1* (Yoon 2002). By contrast, at the *Igf2/H19* locus the deletion of two regions containing tandem repeats respectively situated 5' and 3' of the *H19* DMD had no effect upon either differential methylation within the DMD or the imprinted expression of *H19* (or *Igf2*) (Thorvaldsen *et al.* 2002; Lewis 2004). Whilst a definitive role for direct repeat elements in imprinting has yet to be established, current evidence (*Rasgrf1*) supports their participation in establishment of parental-origin expression and epigenetic modifications at some imprinted loci.

Imprinted chromosomal domains have also been found to be associated with significantly reduced numbers of short interspersed transposable elements (SINEs) a characteristic that is conserved between humans and mice (Engemann 2000; Greally 2002; Ke 2002). This correlate supports the hypotheses that there is either active

selection against SINE elements in imprinted regions or alternatively, that there is a lower rate of insertion of these elements. SINE elements have been reported to attract DNA methylation and mediate its spread into adjacent flanking sequence (Hasse 1994). The methylation-nucleating effect mediated by SINEs could have severe consequences at imprinted loci where aberrant methylation could lead to the ectopic expression or silencing of imprinted genes. This suggests a possible mechanism by which SINE insertion events could be selected against at imprinted loci (Greally 2002). In support of this hypothesis, a paucity of SINE elements has also been observed on the X-chromosome, another region of the genome where monoallelic expression is regulated by methylation (Boissinot 2001). Whilst the precise functional significance of SINEs, if any, remains unclear, these elements may provide genomic markers for the discrimination of imprinted and non-imprinted regions.

### *Antisense transcripts*

Natural antisense transcripts that overlap imprinted protein coding transcripts have been identified at numerous imprinted loci, examples of which are *Igf2*, *Igf2r*, *Kvlqt1*, *Ube3a*, *Wt1*, *Xist* and *Gnas* (Malik 1995; Moore *et al.* 1997; Rougeulle 1998; Lee 1999; Smilinich *et al.* 1999; Lyle *et al.* 2000; Wroe 2000) with conservation between humans and mice in many cases. These antisense transcripts are always imprinted, in most cases oppositely to the protein-coding transcripts with which they overlap. In addition, antisense transcripts usually co-localise with the overlapping protein coding transcript in a tissue-specific manner. Antisense RNA expression from one parental allele therefore correlates with silencing of the protein-coding gene *in cis*. Transcriptional overlap occurring in the same nucleus, it is proposed, may constitute one mechanism by which antisense RNA could confer silencing of coding genes *in cis* (Barlow 1997). However, studies at the murine *Igf2r* locus establish that such a mechanism may not mediate silencing in all cases. The antisense to *Igf2r* (*Air*) transcript is paternally expressed and emanates from a CpG island located within intron 2 of the maternally expressed *Igf2r* gene, with which it exhibits overlap (Wutz 1997). Paternal-specific expression of *Air* correlates with paternal-specific silencing at *Igf2r* and at the flanking *Slc22a2* and *Slc22a3* loci (Zwart 2001). Disruption of *Air* in mice, by insertion of a polyadenylation sequence thereby truncating 96% of the mature transcript, led to reactivation *in cis* of the normally repressed, overlapping paternal allele of *Igf2r* and that of the neighbouring *Slc22a2* and *Slc22a3* genes, with



which it does not overlap. The *Air* transcript is therefore required to imprint the *Igf2r*, *Slc22a2* and *Slc22a3* genes (Sleutels *et al.* 2002). The mechanism by which this occurs is currently unknown, but does not appear to involve overlap between the *Igf2r* promoter and *Air* (Sleutels 2003).

### *DNA replication timing*

The timing of DNA replication of S-phase nuclei is strongly correlated with chromatin structure and transcriptional activity, with active euchromatic regions typically replicating earlier than inactive heterochromatin blocks (Kitsberg *et al.* 1991; Selig *et al.* 1992). Many imprinted regions are characterised by asynchronous DNA replication timing of the parental alleles. Parental-origin specific differences in replication timing have been observed at *Snrpn*, *Igf2*, *H19* and *Igf2r* in humans and mice, with the paternal allele replicating early in each case (Kitsberg 1993). Asynchronous replication is also consistently associated with non-imprinted modes of monoallelic expression in immunoglobulin genes, olfactory receptor genes and (in females) X-linked genes (Takagi 1980; Chess *et al.* 1994; Mostoslavsky *et al.* 2001). Asynchronous replication at imprinted loci is established in the gametes, maintained postzygotically and is apparent in a number of differentiated cell types, which argues for its functioning as a primary imprint that distinguishes the parental alleles (Simon 1999). Consistent with this proposal, deletion of the *H19* gene and its 5' flank (containing the *Igf2/H19* ICR), led to synchronous replication of the alleles at this locus (Greally 1998). The ICR is therefore required for asynchronous replication at the *Igf2/H19* locus. However a recent study in the mouse mutant, *Minute (Mnt)*, found that paternal methylation imprints can be established within the ICR, whilst maintaining asynchronous replication timing of the alleles (Cerrato *et al.* 2003). This suggests that asynchronous replication of the alleles is probably independent of DNA methylation at *Igf2/H19*. This also appears to be the case at other imprinted loci. Asynchronous replication of the alleles has been demonstrated in *Dnmt1* or *Dnmt3L* deficient ES-cells that exhibited genome hypomethylation and widespread loss of imprinted gene expression (Gribnau 2003). It appears that replication timing is neither a determinant, nor a consequence of the epigenetic modifications (DNA methylation) likely to directly mediate imprinting. It is possible that asynchronous replication timing of the alleles could reflect heritable differences in chromatin structure that exist between the alleles of some imprinted loci. Indeed, experimental interference

with chromatin structure by treatment of cultured cells with histone deacetylase inhibitors results in synchronous replication timing of imprinted regions (Bickmore 1995).

### **Genetic conflict and the evolution of imprinting**

The existence of genomic imprinting was first implied by the observation that parthenogenetic embryos do not survive to term (McGrath *et al.* 1984; Surani *et al.* 1986). Subsequently, the observation of reciprocal phenotypes in embryos with either paternal or maternal uniparental disomy (UPD) of certain chromosome regions and in gynogenetic and androgenetic embryos, suggested that maternal or paternal duplications lead to reduced or increased growth respectively (Barton *et al.* 1984; Barton *et al.* 1985). These early observations led to the proposal of the widely documented and accepted genetic conflict theory of imprinting (Moore and Haig 1991). The theory proposes that imprinted genes will arise as a consequence of conflicting interests between males and females in a mammalian polyandrous species, that is where the occurrence of mixed paternity in reproduction reduces the likelihood that paternal alleles in a given fetus will be related to paternal alleles in future siblings. Since the female is equally related to all her offspring, she will try to allocate resources sufficient for the survival of the current brood without compromising her ability to meet the demands of future pregnancies. However, the male has no interest in future offspring produced by a mate, as they are unlikely to be sired by him, rather he will seek maximum investment of the females limited resources in his offspring, even at the expense of that females future reproductive fitness. The conflict theory therefore predicts that paternal alleles will function to increase maternal investment in offspring and promote growth, whilst maternal alleles will act in an opposite manner and limit maternal investment, thus functioning in growth restraint. That is, growth promoting genes will be selected for paternal-specific monoallelic expression and growth inhibitory genes, maternal specific expression. Those genes that do not influence maternal investment or that are expressed exclusively at adult stages would, according to genetic conflict, not be expected to undergo selection for imprinting (Moore and Haig 1991). The first imprinted genes to be identified in the mouse, the oppositely imprinted *Igf2* (DeChiara *et al.* 1991) and *Igf2r* (Barlow *et al.* 1991) genes, the products of which interact antagonistically in the embryo and confer directly opposing effects upon growth, support the prediction.

This is perhaps unsurprising, given that most of what is known about embryonic growth relates to insulin/insulin like growth factor (Ins/Igf) signalling (reviewed in (Efstratiadis 1998)), though on the other hand if the genetic conflict theory is correct, then genes participating in other embryonic growth control pathways would also be expected to undergo selection for imprinting. Consistent with this assertion, in recent work targeted mutagenesis of the maternally expressed *Grb10* gene resulted in significant embryonic and placental overgrowth that, intriguingly, was also shown to be independent of *Igf2* signalling (Charalambous *et al.* 2003). Therefore disruption of *Grb10* in mice provides evidence of the existence of a second, Ins/Igf independent, major growth axis that has also been selected for genomic imprinting. Taken together, these and other studies (reviewed in (Reik *et al.* 2001)), provide compelling experimental evidence of a strong correlation between preferential paternal-specific expression of imprinted genes that promote growth and preferential maternal-specific expression of those involved in growth restraint.

The placenta is the site of nutrient exchange between the mother and fetus, thus it has been argued that this tissue should therefore constitute a principal site for parental conflict and imprinted gene function (Moore and Haig 1991). If the conflict theory holds, then imprinted genes expressed in the placenta should function to appropriately enhance or restrict the availability of maternal resources to the developing embryo. Consistent with this expectation, recent work has shown that a paternal deletion of an *Igf2* (P0) transcript, specifically expressed in the labyrinthine trophoblast of the placenta, led to placental and embryonic growth restriction, with an associated failure of active and passive transport mechanisms (Constancia *et al.* 2002), providing evidence for imprinted gene function in the placenta that directly regulates the supply of maternal nutrients to the fetus.

The argument for genetic conflict is not as straightforward as the previous examples would suggest, as there exists a gene, *Mash2*, which encodes a maternally expressed transcription factor that promotes placental growth. Targeted deletion of *Mash2* in mice led to placental failure, severe embryonic growth retardation and early lethality (Guillemot *et al.* 1995). Therefore the directionality of *Mash2* imprinting and its effect upon growth appear to contradict the conflict hypothesis. However, it may be naïve to assume that a large placenta will always make a large embryo, as illustrated

by some paternal UPD embryos, which are smaller than normal embryos, yet have larger than normal placentae (Hurst 1997). The implication is that placental overgrowth may negatively affect placental function and nutrient flux between mother and fetus, possibly limiting rather than promoting embryonic growth. These considerations do not necessarily exclude genetic conflict as a determinant of imprinted gene evolution but rather suggest it may operate in a more complex manner than previously thought.

As a further cautionary note, it seems likely that many hundreds or possibly thousands of genes regulate embryonic growth, yet the number of imprinted genes is small with around 70 examples identified to date (Efstratiadis 1998; Moore 2001; Beechey 2003). A perceived inconsistency of genetic conflict, questions why most embryonic growth factors are not selected for imprinting as exemplified by the *Igf1* gene, which encodes a potent embryonic and postnatal growth factor yet is not imprinted (Liu 1993; Hurst 1997; Efstratiadis 1998). Proponents of genetic conflict explain this problem in terms of a cost/benefit argument. For example, when a new imprinted paternal allele arises, it will be exposed to severe negative selection and will only persist if it receives a pay-off in terms of increased investment of maternal resources in offspring that exceeds the cost of effectively being functionally haploid (Moore and Haig 1991; Moore 2001). In other words, the benefits conferred by changes in maternal resource allocation may not be sufficient to select for imprinting in all cases.

Genetic conflict predicts that imprinted genes will arise only in those species where the nutritional requirements of the developing embryo are provisioned by direct contact with maternal tissues, an assertion supported by the occurrence of imprinted genes in placental mammals, marsupials and angiosperm plants (Moore and Haig 1991). However, recent studies have revealed the existence of imprinting in *Drosophila* (reviewed in (Lloyd 2000)), a finding inconsistent with genetic conflict in its current form. Whilst other theories have been proposed to account for the evolution of imprinting (reviewed in (Hurst 1997)) and despite some inconsistencies, the theory of genetic conflict currently provides the most tenable description of imprinted gene evolution and function.

## **The *Igf2/H19* locus**

### *Igf2*

Insulin-like growth factor 2 (IGF2) is an embryonic growth factor structurally related to insulin (Milner 1984). The *Igf2* gene is widely expressed in the mesoderm and endoderm lineages at postimplantation stages of development, with expression predominantly occurring from the paternally inherited allele (DeChiara *et al.* 1991). Germline knockout experiments demonstrate that *Igf2* is required for embryonic growth, such that mice inheriting a paternal deletion in the *Igf2* gene display severe embryonic growth retardation, with only 60% of the bodyweight of wild type littermates at birth (DeChiara *et al.* 1990; DeChiara *et al.* 1991). An identical phenotype was observed in mice homozygous for the deletion, though consistent with the imprinted status of the endogenous gene, animals that inherited the *Igf2* deletion maternally were phenotypically indistinguishable from wild-type littermates (DeChiara *et al.* 1990; DeChiara *et al.* 1991). Therefore, physiological deficiency in IGF2 results in embryonic growth retardation.

The structure of the *Igf2* gene is largely conserved in humans and mice, with transcription initiating from four promoters in each species (termed P1-P4 in humans and P0-P3 at the mouse locus, see **Figure 1**) although there are some contrasting features. Human P1, from which transcripts are initiated upon both alleles specifically in the adult liver, does not have a representative homologue at the mouse locus (Ekstrom *et al.* 1995). Mouse P0, from which a placental-specific transcript is produced, is absent from the human sequence (Moore *et al.* 1997). P2-P4 in humans and P1-P3 in the mouse, are functionally equivalent and are expressed in co-ordinate fashion during development (Feil 1997).

The *Igf2* gene maps to mouse distal chromosome 7 in a cluster of imprinted genes that include *H19*, *Ins2*, *Mash2* and *P57<sup>KIP2</sup>* and shows conserved linkage in humans, on chromosome 11p15.5 (Paulsen 1998; Paulsen 2000), a region associated with the rare paediatric overgrowth disorder Beckwith Weidemann Syndrome (BWS) that affects 1 in 11700 live births on average. Individuals with the disease present a complex array of clinical features, including somatic overgrowth, placentomegaly, visceromegaly, macroglossia, cleft palate, omphalocele, polydactyly and a predisposition to childhood tumours (Weksberg 1996) (and references therein).

**Figure 1. The *Igf2/H19* locus in the mouse.** Map of the 100kb region showing the genomic arrangement of the *Igf2* and *H19* genes and surrounding *cis*-elements. Open boxes represent exons of the genes. The *Igf2* gene is comprised by eight exons in total, including placental specific exons 1 and 2 (u1 and u2) and six other exons. The *H19* gene is comprised of five short exons interspersed by 4 very short introns. Differentially methylated regions (DMRs) are represented as arrows; at *Igf2*, differentially methylated regions 0, 1 and 2 (DMR0, DMR1, DMR2); at *H19*, differentially methylated domain (DMD) and *H19* promoter proximal region. Regions that confer enhancer activity at this locus are represented as ovals; *Igf2/H19* centrally conserved domain (CCD); *H19* endoderm-specific enhancers (EE); skeletal muscle-specific enhancers (SME).

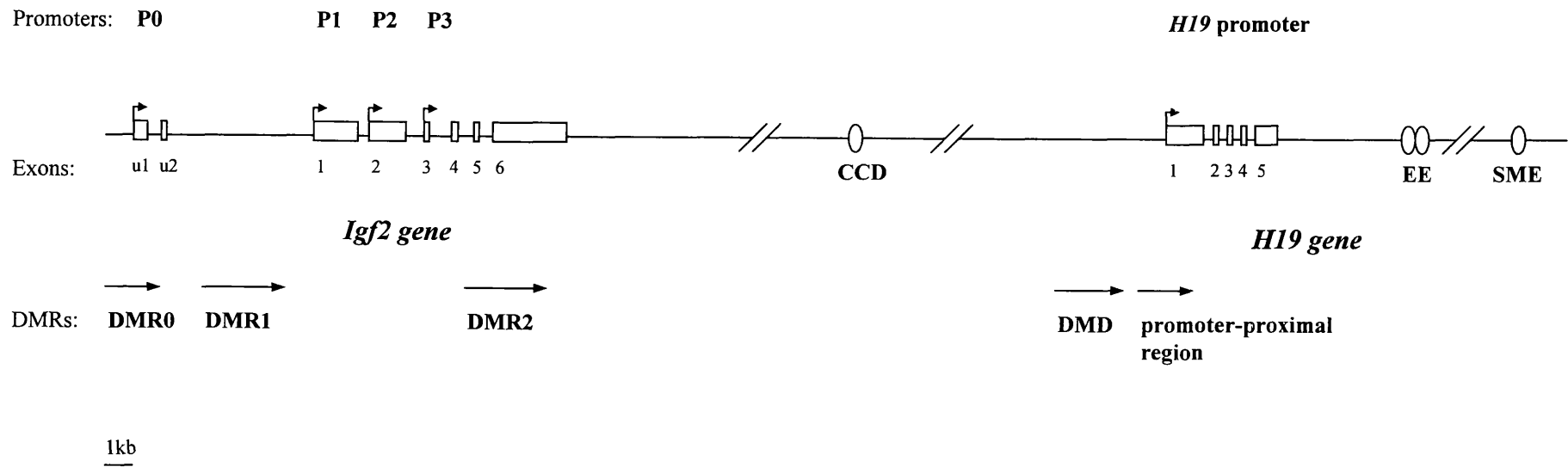


**Figure 1. The mouse *Igf2/H19* locus.**

Dosage of imprinted gene products is critical for normal development and the available evidence suggests that loss of imprinting (LOI) mutations leading to biallelic expression of *IGF2*, a frequent observation in BWS patients, have a causal role in the disease by generating abnormally high levels of IGF2 (Weksberg 1993). The majority of BWS cases arise sporadically, though about 15% of cases show an autosomal-dominant pattern of inheritance. In addition, most patients present no obvious cytogenetic abnormalities, but in a small number of cases paternal UPD of 11p15.5 is correlated with biallelic *IGF2* expression (Weksberg 1996) (and references therein). BWS is genetically heterogeneous and multiple imprinted genes located within the 11p15.5 critical region are probably involved in the pathogenesis of the disease. In particular, biallelic expression of the *KVLQT1* antisense transcript, *LIT1*, which normally displays paternal-specific expression, is the most common molecular defect in found in BWS (Lee *et al.* 1999). In addition, mutations affecting the maternally expressed *P57<sup>KIP2</sup>* gene, which encodes a cyclin-dependent kinase inhibitor, are also found, but occur at a much lower frequency (Engel *et al.* 2000; Gaston 2000; Li 2001b). Almost all of the clinical features of BWS can be recapitulated in a mouse model in which loss of *p57<sup>KIP2</sup>* function is lost and *Igf2* is overexpressed, therefore supporting a causal role for *P57<sup>KIP2</sup>* in this disease (Zhang 1997; Caspary *et al.* 1999). In addition, recent work has revealed the presence of an inherited microdeletion in familial BWS, which disrupts expression of the *LIT1* transcript and leads to concomitant silencing of *P57<sup>KIP2</sup>* providing direct evidence of a mechanistic route to the disease (Niemitz 2004).

Aside from an association with overgrowth in BWS, biallelic *IGF2* expression is found in greater than 70% of all tumours examined and is frequently observed in Wilms' tumour, a familial and sporadic paediatric tumour of the kidney, a neoplasm often manifested in BWS (reviewed in (Reeve 1996)). In addition, biallelic *IGF2* expression has also been shown to occur frequently in colorectal cancer (Takano 2000).

Although not formally substantiated in humans, a causal role for *IGF2* in the overgrowth features of BWS and in many instances of cancer is supported indirectly by evidence from mouse models. Transgenic overexpression of *Igf2* in mice under the control of a bovine keratin promoter, which directs transgene expression to the skin,



gut and uterus, resulted in disproportionate overgrowth of those tissues (Ward *et al.* 1994). Similarly, mice carrying a deletion of the *H19* gene and its 5' flanking sequence, which leads to biallelic *Igf2* expression, were found to be 27% heavier than wild-type littermates at birth, consistent with an excess of IGF2 (Leighton 1995). In further transgenic work, overexpression of *Igf2* manifested key aspects of the BWS phenotype, including somatic overgrowth, tongue overgrowth and skeletal abnormalities (Sun *et al.* 1997). These experiments provide clear evidence that abnormal excess of IGF2 can lead to both local and systemic overgrowth, thus establishing the *Igf2* gene as an important determinant of BWS and tumour progression.

IGF2 exerts its growth effects primarily by signalling through the *type 1* insulin-like growth factor receptor (*Igf1r*) and to a lesser extent via the structurally related insulin receptor (*Insr*) (Liu 1993; Louvi 1997; Efstratiadis 1998). Its cognate receptor, the *type 2* insulin-like growth factor receptor (*Igf2r*) that also functions as the cation-independent mannose-6-phosphate receptor, is not thought to have a signalling role, but rather removes excess IGF2 by receptor-mediated endocytosis (Wang *et al.* 1994). Intriguingly, *Igf2r* is encoded by the imprinted and maternally expressed *Igf2r* gene (Barlow *et al.* 1991), and consistent with a role that is antagonistic to *Igf2* function, mice inheriting a maternal deletion in the *Igf2r* gene displayed embryonic overgrowth, weighing 130% of wild-type littermates at birth (Lau 1994; Wang *et al.* 1994). Double mutant embryos carrying a maternal deletion of *H19* and proximal flanking sequences, such that *Igf2* was biallelically expressed and in addition carry a maternal deletion in *Igf2r*, such that IGF2 turnover is compromised, accumulated IGF2 protein to extremely high levels. This excess of IGF2 caused somatic overgrowth, visceromegaly, placentomegaly, omphalocele, and cardiac and adrenal defects, all of which are consistent with the BWS phenotype (Eggenschwiler *et al.* 1997).

### ***H19***

The *H19* gene is thought to produce one of the most abundant transcripts known (Brannan 1990). *H19* RNA behaves as a classical mRNA, in that it is transcribed by RNA polymerase II, 5' capped, polyadenylated, spliced and exported to the cytoplasm (Brannan 1990). The structure of the *H19* gene is highly similar in humans and mice (**Figure 1**) consisting of 5 exons separated by four small introns, with transcription

initiated from a single promoter in both cases (Pachnis *et al.* 1988). The *H19* gene is tightly linked to *Igf2* in humans and mice, with the two genes separated by approximately 90kb of intervening sequence in the mouse (Zemel *et al.* 1992). *H19* is oppositely imprinted to *Igf2* in both species, showing predominant expression from the maternal allele in most tissues (Bartolomei *et al.* 1991; Zhang 1992).

Overall, the human and mouse *H19* homologues share 77% identity at the DNA sequence level, with several open reading frames (ORFs) identified in both species, of which the largest example in the mouse is sufficient to encode a protein of 14kDa, yet strikingly, no ORF conserved along its entire length exists between the two species (Pachnis *et al.*; Brannan 1990). To date, no description of a protein coding function for *H19* has emerged and the gene is widely held to function as an RNA.

Several targeted deletions of *H19* have been described in mice, though none reveal clear evidence of a functional role for this gene (Leighton 1995; Ripoche *et al.* 1997; Schmidt *et al.* 1999), however evidence from an *in vitro* study implicates tumour suppressor activity for *H19* RNA, possibly consistent with a role in negatively regulating growth (Hao 1993). The tight linkage, reciprocal imprinting and overlapping spatio-temporal expression of *H19* with *Igf2* has led to speculation that the two genes might be functionally coupled. *H19* RNA has been observed to co-localise with *Igf2* mRNA on polysomes and other *in vitro* work has shown that a region encoded by exons 4 and 5 of the mature transcript was required both for interaction with the *Igf2* mRNA binding protein (IMP) and for its own targeting to cytoplasmic sites where IMP is localised (Li *et al.* 1998; Runge *et al.* 2000). These studies point to an attractive hypothesis where *H19* RNA co-localises with *Igf2* mRNA in the cytoplasm, potentially regulating *Igf2* expression *in trans* by a posttranscriptional mechanism. In the absence of firm *in vivo* evidence supporting this proposal, the function of the *H19* gene remains obscure, though the high levels to which *H19* RNA accumulates and its conservation across several species suggest that a functional role may yet be proven (Hurst 1999).

## Tissue specific expression

### *Peripheral tissues*

The *Igf2* and *H19* genes are widely expressed in both the mouse embryo and extraembryonic tissues during development and strikingly, display almost identical spatio-temporal expression patterns (**Figure 2**). It is generally accepted that both genes are highly expressed in derivatives of endoderm, mesoderm and neural crest from early stages of development and in each case transcripts become highly abundant in most major organ systems during their formation (Beck 1987; Stylianopoulou *et al.* 1988a; DeChiara *et al.* 1991; Poirier 1991). *Igf2* and *H19* expression is confined to embryonic stages of development and declines sharply in most tissues shortly after birth, though *H19* expression in mice has been reported to persist at low levels in skeletal muscle postnatally (Poirier 1991). Whilst the spatio-temporal characteristics of *IGF2* and *H19* expression in humans are similar to that of the mouse (Lustig 1994; Ohlsson *et al.* 1994), there are some exceptions. Most notably, in humans *IGF2* expression persists at high levels in the liver of adults where it occurs from both alleles (Ekstrom *et al.* 1995), whilst in mice, *Igf2* expression is lost from the liver during early postnatal stages and does not occur in the adult.

### *Brain*

Early investigations that utilised an *in situ* hybridisation approach revealed a stark contrast in *Igf2/H19* gene expression levels between peripheral mesoderm and endoderm derivatives, in which both genes found to be broadly and abundantly expressed and the central nervous system (CNS), where expression appeared to be almost completely absent (Beck 1987; Stylianopoulou *et al.* 1988a; Stylianopoulou *et al.* 1988b; DeChiara *et al.* 1991; Poirier 1991)(and see **Figure 2**). Though *Igf2* expression was not generally apparent, intense hybridisation signals were noted at highly discrete sites, which corresponded to the choroid plexi, projecting into each of the four cerebral ventricles (Stylianopoulou *et al.* 1988b). *Igf2* expression localised both to the choroid plexus epithelium, a neuroectodermal derivative and the stromal core of this organ, which arises principally from mesoderm (Stylianopoulou *et al.* 1988b; DeChiara *et al.* 1991; Catala 1998). The structure and development of the choroid plexus is discussed more fully in a later section of this chapter. *Igf2* expression was also found in the two innermost membranes surrounding the brain and spinal cord, the pia mater and arachnoid mater, known collectively as the

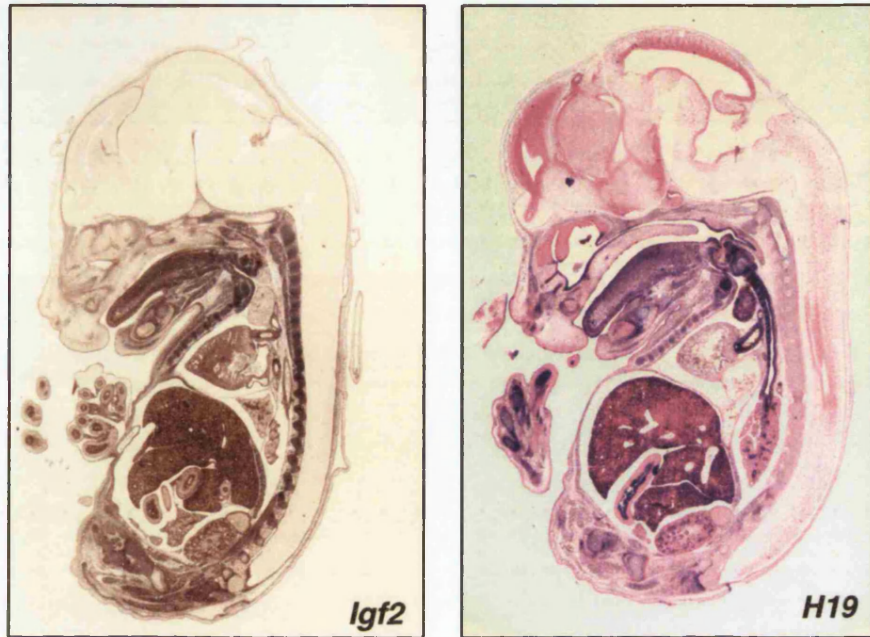


**Figure 2.** *Igf2* and *H19* mRNA expression during embryogenesis. *In situ* hybridisation in embryos at e14.5 of gestation shows expression of the *Igf2* and *H19* genes (dark purple staining) in a closely overlapping distribution, that principally involves the mesodermal and endodermal lineages. Magnifications  $\times 12$ .

leptomeninges and in addition, was detected in the trabeculae, the cytoplasmic processes that interconnect these membranes (Stylianopoulou *et al.* 1988b; DeChiara *et al.* 1991). *Igf2* is not imprinted and is biallelically expressed at these sites, with expression from both alleles continuing at adult stages, contrary to all other sites where its expression is imprinted and downregulated shortly after birth (DeChiara *et al.* 1991; Svensson 1995). That is, *Igf2* escapes imprinted regulation in the choroid plexus and leptomeninges.

More recent work has established that biallelic *Igf2* expression occurs in further derivatives of neuroectodermal origin, in mid to late gestation embryos, including the neuroepithelium in the vicinity of the optic recesses and in bilateral stripes running through the neuroepithelium parallel to the ventral medial region of the hindbrain (Hemberger 1998). *Igf2* expression has also been observed in the granule cell layer of the cerebellum at postnatal stages, though in contrast to other sites of brain expression, this was reported to occur predominantly from the paternal allele (Hettis 1997). As might be expected on the premise of its co-expression with *Igf2* in most other tissues, *H19* expression has also been reported in the choroid plexus and leptomeninges of the developing brain, but in contrast to *Igf2*, maintains imprinting with maternal-specific expression at these sites (Svensson 1995).

Biallelic *IGF2* expression has been described in the choroid plexus and leptomeninges of the developing human fetus (Ohlsson *et al.* 1994; Pham 1998) and at several other sites including the pons, Raphe nucleus and hypothalamus (Pham 1998) though in contrast to the mouse, *H19* expression, where examined, has not been detected at these sites (Ohlsson *et al.* 1994). However, biallelic *H19* expression has been observed in whole human fetal brain analyses (Pham 1998). The reasons for this discrepancy are unclear but could be explained by the slightly different developmental stages that were analysed by the two groups.

### **Cis-elements required for *Igf2/H19* expression**

The overlapping expression patterns, reciprocal imprinting and tight linkage of *Igf2* and *H19* has led to the suggestion that the two genes are co-ordinately regulated. Numerous molecular studies have identified and characterised several *cis*-acting regulatory elements surrounding the *Igf2/H19* locus that are required for the correct

tissue-specific expression of both genes (for review see (Arney 2003)). Elements that confer gene expression in derivatives of each of the three principal embryonic layers, endoderm, mesoderm and ectoderm (brain) will be briefly discussed.

### *Endoderm-specific elements*

Co-expression of *Igf2* and *H19* in endoderm tissues is attributed to a pair of shared enhancers, termed here as the *H19* enhancers, situated in a region +9 to +11kb relative to the *H19* transcription start site (Yoo-Warren *et al.* 1988)(and see **Figure 1**). The tissue-specific function of this region was originally identified with an *in vitro* approach, which revealed enhancer activity in liver derived cell lines but not HeLa cells (Yoo-Warren *et al.* 1988). Analysis of this region within the context of a germline deletion corroborated the tissue-specific enhancer activity of these elements observed in the earlier *in vitro* analysis. Upon paternal transmission of the deletion, *Igf2* expression, but not *H19* expression, was substantially downregulated in tissues having a significant endoderm component, in particular the liver and gut, yet there was little or no change in the level of expression in skeletal muscle or brain. Upon maternal transmission, a reciprocal phenotype was observed with *H19* expression reduced in an identical range of tissues and *Igf2* expression unaffected (Leighton *et al.* 1995). Therefore, the endoderm-specific expression of both *Igf2* and *H19* is dependent upon a shared enhancer region.

Mouse transgenic studies indicate that, in addition to functioning in endoderm, regional activity of the *H19* enhancer pair may also encompass non-endodermal tissues. Consistent with the transient and knockout experiments, these elements reproducibly conferred upon *H19* promoter-*lacZ* reporter transgenes, expression in liver and gut endoderm, but were also able to drive reporter gene expression in the sclerotome compartment of the somites, a mesoderm derivative that later generates the spinal vertebrae (Brenton *et al.* 1999). More recent analysis of each of the two elements separately upon distinct transgenes, indicates that the property of endoderm specific activity resides entirely in the 3' most element, with enhancer activity in sclerotome conferred by the 5' most element of the pair (Ishihara and Jinno 2000). Therefore, the *H19* enhancer region principally upregulates *Igf2* and *H19* expression in tissues of endoderm origin, but may also have some activity in a subset of mesodermal tissues.

### *Mesoderm-specific elements*

As discussed, whilst a subset of *Igf2/HI9* mesoderm-specific expression may be attributed to activity within the *HI9* enhancer region, this is clearly not sufficient to account for the complete range of mesodermal expression exhibited by the two genes, thus arguing for the existence of additional enhancer elements at this locus. The co-expression of *Igf2* and *HI9* in mesoderm argues that the two genes might share elements conferring expression in this lineage, as is the case for the endoderm enhancers. In pioneering work, a 130kb yeast artificial chromosome (YAC) transgene that contained sequences inclusive of *Igf2* exon 1 to a position +36kb relative to the *HI9* transcription start site (represented in **Figure 1**), was shown when present at low copy number, to confer appropriate expression of a *lacZ* reporter gene in a range of mesodermal tissues including skeletal muscle, consistent with the known expression profile of the endogenous *Igf2* gene, though expression in cardiac muscle was not conferred by the YAC (Ainscough *et al.* 1997). The authors concluded that elements conferring gene expression in mesodermal tissues and skeletal muscle, but not cardiac muscle must be located within the boundaries of the 130kb domain defined by the YAC. A subsequent study that utilised the same large YAC, provided evidence that at least three distinct enhancer regions are required for correct *HI9* expression and that expression of the gene in skeletal muscle is conferred by an activity that is separable from that driving expression in the remaining mesoderm tissues (Ainscough *et al.* 2000a). These early experiments provided the first indication that mesodermal expression of *Igf2/HI9* is unlikely to be under the control of a single region, therefore implicating the involvement of multiple elements for correct expression in this lineage.

A subsequent study identified three putative enhancer elements situated in the +22kb to +28kb interval with respect to the *HI9* gene, which were subsequently shown to confer upon *Igf2* promoter-*lacZ* reporter transgenes, expression in several mesodermal derivatives, consistent with the findings of the large YAC transgene (Ishihara and Jinno 2000). In an independent study, elements from within this region demonstrated enhancer activity in muscle-derived cell lines, thus supporting the transgenic data (Kaffer 2000). The requirement for these elements in directing *Igf2* and *HI9* expression in skeletal muscle and other mesodermal tissues was formally addressed by creation of 24kb deletion that removed a region spanning +10kb to +34kb relative

to *H19*, including the putative enhancers. Maternal transmission of the deletion led to a dramatic reduction of *H19* expression in skeletal muscle and tongue, but not in other mesodermal tissues such as heart, lung, kidney or placenta. Paternal inheritance of the deletion led to a qualitatively identical reduction in *Igf2* expression, though the quantitative effects of the deletion were not as significant as those observed for *H19* (Kaffer *et al.* 2001). This study nonetheless confirmed the expectation that *Igf2* and *H19* utilise shared skeletal muscle enhancers located downstream of *H19* (see **Figure 1**), consistent with the expression pattern of the large YAC transgene (Ainscough *et al.* 1997). This work also indicated that elements governing expression in other mesodermal tissues (heart, lung, kidney, placenta) must lie outside of the region deleted.

Recent work in the context of the mouse mutant, *minute (mnt)*, which carries a small chromosomal inversion, has clarified the issue of these elusive elements. Genomic analysis mapped the first breakpoint of the *mnt* inversion to a region approximately 25kb downstream of *H19*, where the skeletal muscle enhancers are located. It was perhaps then unsurprising that paternal inheritance of *mnt* led to severely reduced *Igf2* expression in skeletal muscle and tongue, however, almost all other tissues with a mesodermal component including heart, kidney, lung and placenta were similarly affected (Davies *et al.* 2002). The authors concluded, when considered with prior transgenic and knockout experiments, evidence from the *mnt* study indicates that the additional mesodermal elements lie further 3' of the skeletal muscle enhancers. Collectively, the evidence from studies of YAC transgenes, germline deletions and the *mnt* mutant indicate that the majority of elements conferring *Igf2* and *H19* expression in tissues of mesoderm and endoderm origin, where both genes are imprinted, are located 3' of *H19*. There are, however, important exceptions to this rule as recent transgenic studies provide evidence that additional enhancers with some activity in mesoderm derivatives, possibly specific to *Igf2*, reside within two distinct regions situated 5' of *H19* in the *Igf2/H19* intergenic region (Drewell *et al.* 2002a; Charalambous *et al.* 2004).

### ***Brain-specific elements***

*Igf2* is biallelically expressed in the exchange tissues of the brain, the choroid plexus and leptomeninges of the brain (DeChiara *et al.* 1991) though mechanisms regulating



its expression at these sites are not fully understood. Whilst several tissue-specific enhancer regions exist 3' of the *H19* gene, it seems unlikely that these elements are sufficient for regional enhancement of *Igf2* expression in the brain, although that the choroid plexus stroma and leptomeninges are comprised of a significant mesoderm component, a lineage in which the 3' enhancers are active, argues that these elements might play a minor role (Catala 1998).

### The CCD

The centrally conserved domain (CCD) was originally identified by Koide *et al.* (Koide *et al.* 1994) in a study of a 130kb genomic region that included both *Igf2* and *H19* genes. The CCD, a 2kb region of GC-rich sequence, is located approximately 32kb 5' of the *H19* gene in the mouse (see **Figure 1**) and is conserved in mammals. In all tissues examined, the CCD has been found to be unmethylated and in addition, the region exists in open chromatin conformation, as evidenced by the presence of three sites of strong hypersensitivity to the nuclease, DNaseI, a feature that is highly suggestive of a functional role (Koide 1994).

A more recent study refined the earlier analysis of this region, identifying two blocks of sequence, region 1 and region 2 that are highly conserved between humans and mice. Region 1 exhibits 86% similarity between the two species over 100bp and coincides with the three sites of DNaseI hypersensitivity observed previously (Koide 1994). Deletion of the 5' most 1kb of the CCD within the context of a large YAC transgene, which removed region 1 and the hypersensitive sites resulted in reactivation of the maternal *Igf2* allele in a subset of tissues with a significant skeletal muscle component, including the tongue, after e17.5 of development, continuing at postnatal stages (Ainscough *et al.* 2000b). That is, region 1 contains a muscle-specific silencer element that functions in late embryogenesis and in postnatal development.

Region 2 displays 87% similarity between humans and mice over approximately 200bp, and intriguingly, contains an ORF that is conserved along its entire length in mouse, rat and human sequence, though three independent studies have failed to detect transcripts from this region (Koide *et al.* 1994; Ainscough *et al.* 2000b; Charalambous 2000).

Several lines of evidence demonstrate that enhancer elements conferring *Igf2* expression in the choroid plexus and leptomeninges reside within the CCD. Ward *et al.* (Ward *et al.* 1997) observed that the CCD, when present upon an *Igf2* promoter (P3)-*Luciferase* reporter transgene, increased reporter gene activity in whole brain lysates by greater than 40-fold compared against that of a control transgene containing P3-*Luciferase* alone. More detailed analysis of P3-*Luciferase*-CCD lines revealed that reporter gene expression levels were more than 20-fold enriched in pooled lysates of dissected choroid plexus and leptomeninges, compared with lysates prepared from whole brain tissue depleted of these tissues, thus indicating that the CCD specifically upregulates *Igf2* promoter activity at these sites (Ward *et al.* 1997). A recent study demonstrated that the CCD, when placed in *cis* to a P3-*lacZ* reporter transgene, reproducibly conferred reporter gene expression in the choroid plexus and leptomeninges, thus corroborating the findings of the earlier transgenic analysis. In the same study, the CCD was reported to confer reporter gene expression in additional tissues, where *Igf2* is imprinted, including the dorso-lateral compartment of the somites, the intrinsic muscles of the tongue and a range of neural crest derivatives (Charalambous *et al.* 2004).

The function of the CCD has also been tested within the context of a 12kb germline deletion, in which a substantial decrease in the level of *Igf2* expression was observed specifically in the choroid plexus and leptomeninges, whether the deletion was inherited from either parent. Therefore, the CCD acts as an enhancer of *Igf2* expression upon both parental alleles in the exchange tissues of the brain. Interestingly, the deletion did not completely eliminate *Igf2* expression from these sites, suggesting that additional elements, presumably located outside of the 12kb deletion, are required for quantitatively normal expression in these tissues. By contrast, no change in the level of *H19* RNA was reported, either in the brain or at any other site, suggesting that the CCD, when present at its normal endogenous position, does not mediate expression of *H19* (Jones *et al.* 2001). In addition to the effects upon *Igf2* in the brain, a slight relaxation of *Igf2* imprinting was observed in skeletal muscle and tongue upon maternal inheritance of the deletion (Jones *et al.* 2001), an observation consistent with the presence of a maternal allele-specific muscle silencer described at the CCD in an earlier report (Ainscough *et al.* 2000b).

Current evidence therefore supports a multifunctional role for the CCD, principally as a regional enhancer of *Igf2* expression in the choroid plexus and leptomeninges (Ward *et al.* 1997; Jones *et al.* 2001; Charalambous *et al.* 2004), where the gene is biallelically expressed, but also as an allele-specific silencer with activity in muscle, where *Igf2* is imprinted (Ainscough *et al.* 2000b; Jones *et al.* 2001). Deletion experiments assign the silencer function of the CCD to the first of two blocks of conserved sequence, region 1. Since no change in the level of *Igf2* expression was reported in the choroid plexus and leptomeninges following the deletion of region 1, the most likely location for the exchange tissue enhancers is region 2, the function of which remains to be verified (Ainscough *et al.* 2000b).

### **Differentially methylated regions at *Igf2/H19***

Correct genome methylation was shown to be essential for imprinting of the *Igf2* and *H19* genes, by analysis of embryos homozygous for a mutation in the *Dnmt1* gene, where *H19* was biallelically expressed and *Igf2* silenced upon both alleles (Li 1993). That is, methylation regulates both genes, but in a directly opposing manner. As already discussed, regions of differential methylation (DMRs) have been shown to overlap CpG-rich sequences located in the vicinity of imprinted genes, but not non-imprinted loci, and it is generally accepted that this modification constitutes at least part of the marking process that distinguishes the parental origin of the alleles (Reik 2001b)(and references therein).

For differential methylation to meet the criteria of a primary imprinting mark that distinguishes the parental alleles, this modification must be established in the gametes, whilst the parental genomes are separated, then be maintained postzygotically such that the methylated allele withstands demethylation at preimplantation stages and the unmethylated allele is protected against *de novo* methylation during early post implantation development, with the marks sustained in somatic tissues thereafter. Several DMRs have been identified in sequences surrounding the *Igf2* and *H19* genes and as will become evident from the following text, these regions contain regulatory elements that either promote or repress gene expression dependent upon their methylation status.

### *Differential methylation at H19*

The *H19* gene is hypermethylated upon the inactive paternal allele in a region that encompasses the gene body and 4kb of immediate 5' flanking sequence, in sperm and in somatic tissues (Bartolomei *et al.* 1993; Brandeis *et al.* 1993; Ferguson-Smith 1993). However, the maintenance of differential methylation throughout the entire course of pre- and postimplantation development, is restricted to a 2kb region positioned -2 to -4 kb relative to the *H19* transcription start site, consistent with the qualities of an imprinting mark (Tremblay *et al.* 1995; Tremblay *et al.* 1997). By contrast, the immediate promoter-proximal region and the structural gene are demethylated in the blastocyst and reacquire differential methylation during subsequent post implantation development (Brandeis *et al.* 1993; Tremblay *et al.* 1995; Tremblay *et al.* 1997), indicating that these regions do not act to distinguish the alleles.

### The DMD

As described above, the differentially methylated domain (DMD) positioned -2kb to -4kb upstream relative to *H19* (see **Figure 1**), bears epigenetic features consistent with functioning as a primary imprinting signal, in that its paternal-specific methylation is established in the gametes and is not altered by waves of demethylation and *de novo* methylation that successively sweep through the genome during pre-implantation development (Tremblay *et al.* 1995; Tremblay *et al.* 1997). In addition to these modifications, the DMD is also marked by parental origin-specific differences in chromatin structure between the alleles. Sites of hypersensitivity to nucleases, map within two blocks of sequence, HS1 and HS2, located approximately -3.8kb and -2.5kb relative to the *H19* transcriptional start site and are specific to the unmethylated maternal allele (Hark and Tilghman 1998). Subsequent analyses of this region observed that the maternal allele bears an unusual chromatin conformation, consistent with local displacement of the nucleosomal array by non-histone protein-DNA interactions (Khosla *et al.* 1999; Kanduri 2000a). Therefore the DMD exists in alternate epigenetic states, dependent upon its parental origin. Subsequent studies have established that it constitutes an imprinting control region (ICR) with the paternal epigenotype (methylation) and the maternal epigenotype (chromatin insulator) respectively required for the monoallelic expression of the *H19* and *Igf2*

genes. The work that has elucidated these functions of the DMD is discussed in the text below.

Early transgenic experiments provided evidence that the DMD contained sequences sufficient to direct imprinting at the *H19* locus. A 14kb transgene, which included 4kb of the *H19* 5' flanking sequence, an internally deleted *H19* gene and an 8kb portion of the 3' region including the endodermal enhancers, displayed imprinted expression and parental origin-specific methylation in a manner consistent with that of the endogenous *H19* locus (Bartolomei *et al.* 1993). That is, the transgene was expressed and hypomethylated upon maternal transmission, but silenced and hypermethylated upon paternal transmission. When a 2kb region (containing the DMD) was deleted from the 5' flanking region, the transgene was expressed and hypomethylated, irrespective of the sex of the transmitting parent (Elson and Bartolomei 1997). Therefore, the DMD contains sequences sufficient to confer imprinting, at the levels of both parental allele specific expression and methylation, at ectopic loci.

As discussed earlier, the almost identical spatio-temporal expression patterns and reciprocal imprinting of the *Igf2* and *H19* genes is suggestive of a functional link between the two genes. Deletion of distinct enhancer regions located 3' of *H19* has established that the expression of both genes is, in endodermal and some mesodermal tissues, dependent upon shared elements (Leighton *et al.* 1995; Kaffer *et al.* 2001). Deletions encompassing the *H19* gene region provided the first indications that the imprinting of the two genes might also be functionally coupled. When the *H19* gene was deleted along with its 5' flank (which contains the DMD) from the maternal chromosome, reactivation of *Igf2* was observed in *cis* (Leighton 1995). Analysis of a smaller deletion that removed the *H19* structural gene, but not the 5' flank, showed that whilst *Igf2* was again reactivated, the effect was minor in comparison with that observed in the large deletion (Ripoche *et al.* 1997), thus arguing that the 5' flank of *H19* (and hence the DMD) plays a functional role in silencing at the *Igf2* locus.

The necessity of the DMD at its endogenous location for both *Igf2* and *H19* imprinting was formally demonstrated by deletion of a 1.6kb region between -3.7kb and -2.1kb upstream of *H19*, which removed most of the differentially methylated sequences and the hypersensitive sites. Paternal transmission of this deletion led to

reactivation of *H19* expression in a subset of tissues, including liver and gut endoderm and skeletal muscle, with a concomitant loss of methylation in the adjacent promoter-proximal region and structural gene. Upon maternal transmission, the reciprocal situation was seen, with reactivation of the normally silent *Igf2* allele (Thorvaldsen *et al.* 1998). The DMD is therefore required for the imprinted expression of both genes.

Whilst the work of Thorvaldsen *et al.* demonstrated the requirement of the DMD for imprinting at *Igf2/H19*, it failed to differentiate between a role in establishment or maintenance of imprinting. To discern the exact role of the DMD, a subsequent study utilised the approach of *cre-loxP* mediated conditional mutagenesis to delete this region at three different developmental stages, in the germline, in the zygote and in differentiated tissue. Paternal deletions of the DMD in the germline and zygote, led to reactivation of *H19* expression in *cis* and loss of methylation in the adjacent promoter-proximal region, therefore demonstrating a requirement of this region for establishment of imprints in the germline and for maintenance during post-zygotic development. However, following deletion of the DMD in differentiated tissues, paternal-specific silencing and methylation of *H19* was maintained. Deletion of the DMD on the maternal chromosome resulted in reactivation of *Igf2* in *cis*, irrespective of whether the deletion was imposed in the germline, the zygote or in differentiated tissue (Srivastava 2000). The DMD was therefore proposed to contain two distinct functions. The first is required to establish silencing of the paternal *H19* allele during early development by directing methylation of its promoter region (and possibly induction of heterochromatin), but is dispensable for maintenance of *H19* silencing in differentiated tissues. By contrast, the presence of a second silencing function is required at all stages of development to repress the maternal *Igf2* allele. Both functions are discussed below.

#### *Silencer function of the DMD*

The conclusion of Srivastava *et al.* that silencing of *Igf2* and *H19* is conferred by separate mechanisms is supported by analysis of a smaller 1.2kb deletion within the DMD, that removed sequences between -2.9kb to -1.7kb, including the hypersensitive site, HS2. Paternal transmission of this deletion led to reactivation of *H19* in *cis*, in a subset of endodermal tissues, though there was no effect upon *Igf2* following maternal transmission of the deletion, indicating that the sequences necessary for its imprinting

were intact. Surprisingly, the deletion did not affect the differential methylation of the remaining DMD sequences or the adjacent *H19* promoter-proximal region (Drewell *et al.* 2000). The authors concluded that the 1.2kb element acts specifically to silence the paternal *H19* allele in a subset of tissues by a mechanism that appeared to be independent of DNA methylation. This conclusion is consistent with an earlier study in which the same 1.2kb mouse element conferred silencing upon reporter genes in transgenic *Drosophila*, a species that lacks genome methylation (Lyko *et al.* 1997). However at its endogenous location, the silencer is methylated exclusively upon the paternal allele, therefore this modification could play some role in the allele-specific activity of this element. A subsequent study has demonstrated that the methyl-binding domain (MBD) containing repressor, MeCP2, is recruited to the silencer *in vivo*, with this protein and HDAC activity required for DMD-mediated silencing of a reporter gene *in vitro* (Drewell *et al.* 2002b).

The silencing of the paternal *H19* allele is therefore likely to be mediated by paternal-specific methylation of the DMD, which spreads into the *H19* promoter region during postimplantation development and initiates a stable heterochromatic state. This appears to be directed by the protein MeCP2, but possibly involves a methylation-independent silencing mechanism.

#### *Insulator function of the DMD*

Chromatin insulators are thought to define distinct transcriptional domains in the genome, preventing inappropriate gene silencing or activation by restricting the expansion of heterochromatin and blocking promoter-enhancer interactions (reviewed in (Bell 1999a)). To be functional, an insulator must be positioned between a promoter and an enhancer to prevent the enhancer activating transcription. Insulator elements therefore block promoter-enhancer communication in a position dependent manner.

Two lines of evidence suggested that insulator activity might be present within the DMD, possibly involved in silencing *Igf2* by blocking access to shared enhancers located 3' of *H19*. Relocation of the *H19* endoderm enhancers from their endogenous location to a position 5' of *H19* in the intergenic region resulted in reactivation of the maternal *Igf2* allele in tissues where these enhancers are normally active (Webber *et*

*al.* 1998). In further work, the DMD was relocated to a position between the endodermal and skeletal muscle enhancers, where upon maternal inheritance of this mutation, *H19* expression was drastically reduced in muscle but unaffected in endodermal tissues (Kaffer 2000). Location of enhancers relative to the DMD is therefore a critical determinant of imprinting mechanisms at the *Igf2/H19* locus. The dependence of *Igf2* and *H19* expression on the position of enhancers relative to the DMD could be explained by a model proposing the existence of an insulator within this region.

*In vitro* studies have examined the insulator function of the DMD, when in isolation from its genomic context. As such the full length DMD was shown to confer position dependent silencing upon reporter gene constructs consistent with having insulator function. (Bell 2000; Hark *et al.* 2000; Kanduri 2000a; Holmgren 2001). Analysis of smaller fragments of the DMD mapped this activity to the hypersensitive sites, HS1 and HS2, identified within this region by an earlier study (Hark and Tilghman 1998).

Binding sites for the protein, CTCF, a critical regulator of the chicken  $\beta$ -globin insulator (Bell 1999b), were identified within these hypersensitive sites (Bell 2000; Hark *et al.* 2000). Experiments performed *in vitro* established that insulator activity is dependent upon CTCF binding at these sites, and that this binding occurs in a methylation-dependent manner. Methylation of CpGs within the CTCF-binding sites eliminated binding of CTCF *in vitro*, and deletion of these sites from the context of the DMD resulted in loss of enhancer-blocking activity in tissue culture cells, thereby permitting expression of a reporter gene (Bell 2000; Hark *et al.* 2000). Therefore, activity of the insulator is mediated by the protein, CTCF, and is restricted to the unmethylated maternal allele of the DMD.

In more recent work, targeted mutagenesis was employed to introduce point mutations into each of the four CTCF binding sites within the DMD, thus testing the requirement for CTCF in *Igf2* imprinting *in vivo*. Maternal transmission of this mutation led to reactivation of *Igf2* expression, consistent with disrupted CTCF binding and loss of insulator function on the maternal allele. Methylation analysis of the mutated DMD revealed that whilst the correct unmethylated state was essentially



maintained in oocytes and blastocysts, abnormal methylation of this region was observed in differentiated tissues. Therefore, in addition to its role in activating the insulator, CTCF binding also is required to maintain the maternally unmethylated state of the DMD during postimplantation development (Schoenherr *et al.* 2003). A recent report describing disruption of CTCF function in oocytes by an RNAi-mediated approach, provided evidence in support of a role for CTCF in maintaining the unmethylated state of the DMD in this tissue (Fedoriw *et al.* 2004), contrary to the findings of Schoenherr *et al.* Despite this inconsistency, both studies point to an additional role for CTCF in conferring protection against aberrant *de novo* methylation during development.

In summary, imprinted expression of *Igf2* is mediated, principally, by a methylation-dependent insulator function of the DMD. In the unmethylated state, the insulator blocks interaction of *Igf2* promoters with tissue specific enhancers located 3' of *H19*, thus explaining the silence of the maternal *Igf2* allele. Paternal-specific methylation of the DMD abolishes insulator activity, allowing enhancers to engage the *Igf2* promoters, leading to transcription of the paternal *Igf2* allele. Bound CTCF protein appears to be required to maintain the unmethylated state of the DMD that is crucial for this insulator function. An anticipated consequence of this insulator activity is that enhancers driving *Igf2* expression in imprinted tissues will be located 3' of the DMD and their activity thus blocked on the maternal allele. As discussed in an earlier section of this chapter, the majority of enhancers conferring expression in imprinted endodermal and mesodermal tissues are located 3' of the *H19* gene (Leighton *et al.* 1995; Kaffer *et al.* 2001), thus supporting this assertion. By the same argument, this model of imprinting predicts that enhancers driving non-imprinted, or biallelic expression will be located 5' of the DMD, thereby avoiding the influence of the insulator. The identification of an enhancer, the CCD, which is located 5' of the DMD in the intergenic region and drives biallelic *Igf2* expression in the choroid plexus and leptomeninges, fulfils this prediction (Jones *et al.* 2001; Charalambous *et al.* 2004).

### *Differential methylation at Igf2*

Three regions of differential methylation mark the *Igf2* gene (see **Figure 1**). DMR0, which overlaps *Igf2* promoter 0 (P0), the site of initiation of a placental-specific

transcript, displays maternal allele specific methylation exclusively in the placenta but is biallelically methylated in embryonic tissues (Moore *et al.* 1997).

DMR 1 overlaps a 600bp region located approximately 3kb 5' of *Igf2* promoter 1. A further region, DMR2, is located within the *Igf2* structural gene and covers a 2.4kb region spanning exons 4-6. Both DMRs display predominant methylation of the paternal chromosome in the majority of tissues. However, these modifications though present in sperm, are lost during pre-implantation development and re-established at later stages and therefore are not thought to represent primary imprinting marks (Sasaki *et al.* 1992; Brandeis *et al.* 1993; Feil *et al.* 1994; Moore *et al.* 1997). Intriguingly, both regions are highly methylated upon both parental alleles in the adult choroid plexus, a tissue where *Igf2* is biallelically expressed, providing evidence of an epigenetic basis to this non-imprinted mode of expression (Feil *et al.* 1994). A detailed study of these regions during embryogenesis revealed that their differential methylation is most pronounced in tissues with a significant mesodermal component, with the exception of skeletal muscle, in which both regions are methylated equivalently until birth (Weber 2001). Additionally, the correlation between paternal-specific methylation of these DMRs and the exclusive paternal-specific expression of *Igf2* in many tissues has led to the hypothesis that these regions harbour silencer elements that are inactivated by methylation.

The requirement of DMR1 for *Igf2* imprinting was tested within the context of a 5kb germline deletion. Upon maternal transmission of the deletion, *Igf2* expression was reactivated in most mesodermal tissues, but not skeletal muscle. Paternal or maternal transmission of the deletion led to continued expression of *Igf2* postnatally, in contrast to the wild type gene, which is silenced shortly after birth in most tissues. In addition the deletion had no effect upon the expression or imprinting of *H19* (Constancia *et al.* 2000). Therefore, DMR1 contains a methylation-dependent silencer element that is, required for imprinting of *Igf2* in mesodermal tissues, with the exception of skeletal muscle. In further work, an additional silencer element was identified within this sequence, with its silencing function mediated by methylation-dependent binding of the repressor protein, GCF2, though this activity was not shown to be tissue specific (Eden *et al.* 2001).

The necessity of DMR2 for imprinting at *Igf2* was addressed by insertion of a *lacZ* reporter gene cassette, replacing a 4.65kb region between exons 4-6 that included DMR2. However, deletion of this region did not lead to reactivation of the maternal *Igf2* allele, as assayed by examination of reporter gene expression following maternal transmission of the mutation. Therefore, in contrast to the role demonstrated for DMR1, DMR2 is not required to silence the maternal *Igf2* allele. However, in the same study, deletion of an intensely methylated 54bp core element located within DMR2 led to decreased *Igf2* expression, consistent with a function in activating transcription. Analysis of this region *in vitro* revealed that the activating function of this element was regulated by its methylation (Murrell *et al.* 2001). Therefore, a core element within the DMR2 region activates *Igf2* expression in a methylation-dependent manner.

The role of DMR1 and DMR2 in mediating *H19*-independent silencing and activation respectively, argues for the existence of imprinting controls distinct from that provided by the DMD. Interestingly, recent work indicates that correct parental origin-specific methylation within both *Igf2* proximal DMRs is directed by modifications at the DMD acting *in cis*. Whilst paternal-specific methylation in these DMRs is normally established after implantation, both DMR1 and DMR2 were incorrectly *de novo* methylated upon the maternal chromosome following deletion of the DMD *in cis*. In addition, DMR2, but not the DMD, became methylated upon the maternal chromosome following deletion of DMR1 (Lopes *et al.* 2003). Therefore, the DMD is required on the maternal allele to protect DMR1 and 2 from methylation, and DMR1 is required to protect DMR2, but not the DMD, from methylation suggesting that the establishment of epigenetic modifications within these DMRs is coordinated in a hierarchical fashion.

### **The Choroid Plexus**

There are four choroid plexuses in the brain, the two largest being found in the lateral ventricles, a smaller structure in the third ventricle and a morphologically distinct structure occurring in the fourth ventricle. The choroid plexuses are the major sites of cerebrospinal fluid (CSF) production that circulates through the ventricles and out into the subarachnoid space, providing both buoyant protection and nourishment to the brain and spinal cord (reviewed in (Speake 2001)). The choroid plexuses, together

with the leptomeninges, comprise the major blood-CSF interface, mediating the exchange of biologically important molecules such as hormones and growth factors between peripheral circulation and the central nervous system (CNS) (reviewed in (Segal 2001)).

The choroid plexus is formed by the apposition of two principal components, an outer secretory epithelium and a capillary-rich stromal core (see **Figure 3**). The epithelium consists of modified ependyma, a morphologically uniform cuboidal cell layer that lines the cerebral ventricles with which it is continuous and sits upon a basement membrane that contacts its basal surface. The epithelial cells are connected at their lateral surfaces by an occluding band of tight junctions that prevent passive exchange between the blood and the CSF by the pathway between the cells (Brightman and Reese 1969). In addition, choroid plexus epithelial cells display abundant mitochondria, rough endoplasmic reticulum and secretory vesicles, thus suggesting a significant involvement in secretion (Sturrock 1979).

Transmission electron microscopy (TEM) imaging of the choroid plexus epithelium reveals that the cells are distinctly polarised, with numerous apical microvilli and basally located nuclei, features again consistent with a role in secretion. The surface of these cells is covered with cilia, the beating of which is thought to facilitate mixing and movement of CSF through the ventricular system. Interestingly, electron lucent and dense (light and dark) cells have been observed in the choroid plexus epithelium of several mammalian species (Dohrmann 1970; Sturrock 1979). Sturrock, in a study of the developing mouse choroid plexus showed that these cells first become apparent at e14.5 of development and provided quantitative evidence that the light cells predominate with the number of dark cells comprising approximately 11% of total epithelial cell number at all stages examined thereafter. It was proposed that dark cells contain a greater number of subcellular organelles such as mitochondria and ribosomes and it was suggested that these cells are engaged in distinct metabolic activities. To date, it remains unclear whether this morphological dichotomy translates into functional differences, for example in protein synthesis or secretion, or represents a mechanism of cell-turnover (Sturrock 1979). That differentiated choroid plexus epithelial cells lack the ability to proliferate would seem to exclude a mechanism of senescence in the manifestation of these cell types (Saenz Robles *et al.* 1994). Other

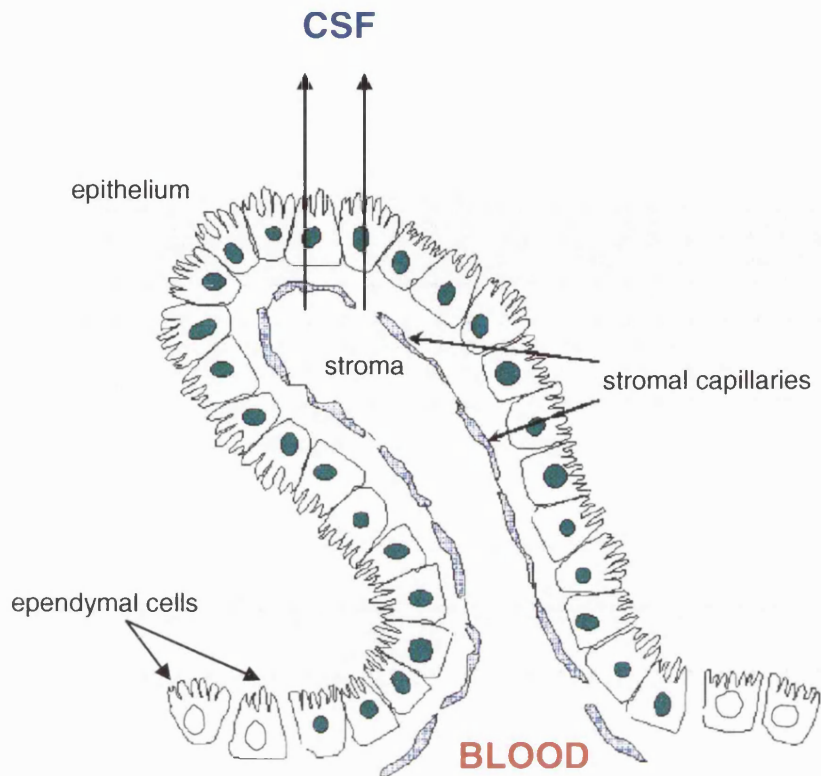


**Figure 3. The choroid plexus.** The structure of the choroid plexus is represented schematically. The simple columnar epithelium (green nuclei) of the choroid plexus is highly folded and is continuous with the ependymal cell layer (white nuclei) which lines the ventricles. The epithelial cells are polarised and display numerous microvillae upon their apical surface which faces the ventricle lumen. The epithelium surrounds the capillary rich stromal component of this organ, with which it is intimately associated. The principal function of the choroid plexus is the synthesis and secretion of CSF and this organ constitutes a major blood-CSF interface. The directional movement of CSF across the epithelium is indicated by large vertical arrows.

studies implicate a function in fluid homeostasis, as dark cell frequency is increased in mice homozygous for the *hydrocephalus and polydactyl (hpy/hpy)* mutation and also in water deprived wild-type mice (Shuman 1991).

The stromal mesenchyme of this organ is completely enveloped by the epithelial component and is principally comprised by the leptomeningeal cells of the pia mater, but also contains many other cell-types including fibroblasts, macrophages, neuronal termini and importantly, an extensive network of capillary endothelium. Capillaries in the choroid plexus stroma are unusual in that they have numerous fenestrations that permit access of blood-plasma components to the basal side of the epithelium, contrary to the majority of cerebral capillaries, which have a tight structure and constitute the blood brain barrier (Brightman and Reese 1969).

### **Development of the choroid plexus**

The development of the choroid plexus has been studied in a number of species (reviewed in (Catala 1998)). Cell lineage studies performed in the chick-quail chimaera system reveal that this organ has a dual embryonic origin. The epithelial component arises entirely from the embryonic neuroepithelium that lines the lumen of the neural tube, whilst the mesenchymal and vascular components of the stroma are derived from cephalic paraxial mesoderm (Wilting 1989).

Morphogenesis of the choroid plexus in the mouse commences shortly after neural tube closure at e10, where a thinning becomes evident in regions of the neuroepithelium destined to form the choroid plexus epithelium. During the next two days, these regions extend outwards into the ventricle lumen, the motive force for which is thought to involve the rapid invasion of stromal mesenchyme from beneath. As the evagination of the choroid plexus continues it becomes rigorously folded and by e14.5 of development has assumed its characteristic lobulate morphology (Sturrock 1979). The choroid plexus appears first in the fourth ventricle, shortly followed by those occupying the lateral and third ventricles, with this order a consistent feature of all species examined so far (Dziegielewska 2001) (and references therein). As the epithelium cells mature, they undergo transition from a pseudostratified to a tall columnar morphology and this morphological differentiation is accompanied by the expression of a number of diagnostic biochemical markers including the thyroid

hormone transport protein, transthyretin (TTR) and numerous enzymes, consistent with a central metabolic role for these cells in the CNS (Murakami 1987; Catala 1998) (and references therein).

### *Genes regulating choroid plexus development*

The molecular and genetic basis of choroid plexus morphogenesis is poorly understood and in addition, most of what is known has emerged serendipitously in studies of neural fate specification. In rat embryos, expression of the actin-regulatory protein, tropomyosin, in the neuroepithelium layer defines future sites of choroid plexus formation before the characteristic folded morphology of this organ can be detected (Nicholson-Flynn *et al.* 1996). It was proposed that the early appearance of tropomyosin expression, which reportedly preceded even that of *TTR*, reflects the active rearrangement of cytoskeletal elements in preparation for the morphogenetic movements that later generate this organ (Murakami 1987; Nicholson-Flynn *et al.* 1996). These observations suggest that the choroid plexus phenotype is specified at an early stage of neuroectodermal differentiation.

The intrinsic capacity of early neuroectoderm to differentiate into choroid plexus epithelial cells has been examined using an *in vitro* approach to culture explanted mouse neuroectoderm tissue. Using *TTR* expression as a differentiation marker, it was found that the potential of the explants to differentiate into choroid plexus epithelial cells was widespread in rostral regions prior to neurulation at e8.5, but demonstrated progressive spatial restriction to domains that eventually give rise to the choroid plexus, in embryos at e9.5 and e10.5 (Thomas 1993). Therefore, the specification of the choroid plexus epithelium fate represents an early step in the regionalisation of the neural tube and is likely to be dependent upon dynamic positional cues.

Recent work provides evidence that bone morphogenetic proteins (BMPs), a family of secreted factors encoded by *Bmp* genes, are involved in this process. Co-expression of *Bmp2* and *Bmp4* marks the dorso-medial neuroepithelium of the telencephalon, a region from which the choroid plexus epithelium later arises, thus implicating a role for these genes in the specification of this tissue (Furuta 1997). The widespread expression of BMP receptor genes in the dorsal neural tube, encompassing regions destined to form the choroid plexus is consistent with this hypothesis (Dewulf 1995).

The necessity of BMP signalling for the specification of dorsal telencephalic fates was tested in a recent study using *cre-loxP*-mediated conditional mutagenesis to create a telencephalon-specific deletion of the *Bmpr1a* gene, which encodes the BMPRI1A receptor. Embryos homozygous for this mutation failed to generate the choroid plexus structure in the lateral ventricles of the brain. Instead choroid plexus epithelial precursors remained in a proliferative state throughout development, lacked expression of tissue-specific marker, *TTR*, and showed reduced expression of *Msx1*, a BMP-responsive dorsal midline marker (Hebert 2002). BMP signalling is therefore required to correctly specify and differentiate the choroid plexus. In subsequent work, disruption of the *Bmp4* gene in the telencephalon did not, however, reveal any patterning defects and the choroid plexus developed normally (Hebert 2003). The absence of an effect following loss of *Bmp4*, together with the role of the BMPRI1A receptor with which BMP4 is thought to interact, argues that loss of *Bmp4* function was compensated for by other *Bmp* genes acting in a redundant manner. At least one other BMP ligand, possibly acting in concert with BMP4, therefore appears to be required for normal development of the choroid plexus.

Studies of the mouse mutant, *extra-toes* (*Xt/Xt*), have provided a further insight into the nature of signals potentially regulating choroid plexus development. The *Xt* allele carries a deletion in *Gli3*, a vertebrate homologue of the *Drosophila* gene, *cubitus interruptus* (*ci*), a transcription factor that regulates *wingless*, the canonical member of the Wnt family of secreted morphogens (Franz 1994; Von Ohlen 1997). The choroid plexus of the lateral ventricles fails to form in *Xt/Xt* embryos (Franz 1994). However, this failure was thought not to be a direct consequence of *Xt*, as *Gli3* expression, whilst widespread in the dorsal telencephalon, does not occur in the choroid plexus. Instead this was attributed to loss of a *Gli3*-dependent Wnt-rich signalling centre, the cortical hem, a tissue thought to provide dorsalising cues necessary to pattern the adjacent choroid plexus (Grove 1998). More detailed examination of these embryos revealed that, whilst some thinning of the neuroepithelium was detected, consistent with progress to the earliest stages of choroid plexus morphogenesis, these precursor cells remained in a proliferative state and did not express the marker TTR, bearing a striking similarity to observations made in *Bmpr1a* mutants (Grove 1998; Hebert 2002). A further study demonstrated loss of expression of multiple *Bmp* genes, including *Bmp4*, from the cortical hem in *Xt/Xt* embryos suggesting that BMP



signalling, acting downstream of *Gli3*, is also involved in the choroid plexus phenotype of this mutant (Tole 2000).

These studies indicate that in the absence of BMP, and possibly Wnt signalling, choroid plexus development is blocked at an early stage, prior to the establishment of the characteristic columnar, *TTR*-expressing epithelium. That this effect is limited to the choroid plexus of the lateral ventricle (choroid plexi at other sites develop normally in *Bmpr1a*-deficient and *Xt/Xt* mice) suggests that distinct, and as yet unidentified positional signals are required to pattern the third and fourth ventricle choroid plexi of the brain.

### ***In vitro* culture systems**

Scientific investigation of the choroid plexus is often limited because of the small size and inaccessibility of this organ. *In vitro* approaches involving primary culture systems have been essential in order to overcome these limitations. For the purposes of primary culture, choroid plexus epithelial cells are preferred because they perform most of the biological secretory and exchange functions of the choroid plexus that researchers wish to investigate. Moreover, the epithelium is the more homogeneous tissue, hence better suited to studies where variability might detrimentally affect quantitative analysis. Cultured choroid plexus epithelial cells faithfully reproduce morphological and biochemical features that are characteristic of the choroid plexus epithelium *in vivo* (Villalobos *et al.* 1997). As such, choroid plexus cell cultures have allowed biological questions to be rapidly and reliably tested, particularly those investigations that use the cells to recapitulate *in vitro* the barrier functions of the choroid plexus epithelium *in vivo*, for example the study of transport of novel drugs, organic substrates and proteins across the blood-CSF barrier (reviewed in (Gherzi-Egea 2001)).

### **Summary**

The *Igf2* and *H19* genes are widely expressed in the mesodermal and endodermal lineages during development. *Igf2* is, with the exception of the choroid plexus and leptomeninges, predominantly expressed from the paternally inherited allele (DeChiara *et al.* 1991), whilst for *H19*, it is transcription of the maternal allele that predominates in the majority of tissues (Bartolomei *et al.* 1991). The correct

monoallelic expression of *Igf2* is frequently disrupted in the paediatric overgrowth disorder, BWS, with biallelic expression of the gene observed in many cases.

Current evidence favours an insulator model to explain imprinting at the *Igf2/H19* locus. This involves complex interactions between an imprinting control region (ICR), situated within a differentially methylated domain (DMD) 2-4kb 5' of *H19* and an array of *cis*-acting enhancer elements, principally located in sequences 3' of the *H19* gene, which confer expression in a tissue-specific manner. The DMD exists in two epigenetic states, dependent upon its parental origin. Following transmission through the paternal germline, it is hypermethylated, and is required to initiate, but not maintain, silencing of the *H19* gene by establishment of secondary methylation imprints and a closed chromatin conformation over the promoter region. After maternal transmission, it is devoid of methylation, exists in an open chromatin conformation and is required to initiate and also maintain silencing of *Igf2* *in cis* (Tremblay *et al.* 1997; Srivastava 2000). The DMD contains a chromatin boundary or insulator element that acts to block the interaction of *Igf2* promoters with mesoderm- and endoderm-specific enhancer regions that lie 3' of *H19*, providing an epigenetic basis to imprinted gene expression in tissues where these enhancers are active (Bell 2000; Hark *et al.* 2000; Szabo 2000).

*Igf2* escapes imprinted regulation and is biallelically expressed in the choroid plexus and leptomeninges, thus reflecting the situation often seen in BWS, though *H19* maintains maternal-specific expression at these sites. Imprinting of the two genes therefore appears to be dissociated, suggesting that distinct mechanisms may govern expression from each locus in this tissue. Whilst the *cis*-elements responsible for correct imprinting and expression of *Igf2/H19* in endodermal and mesodermal tissues have been identified, those required to initiate and maintain biallelic *Igf2* expression in the choroid plexus have not been fully characterised. One such element, an enhancer driving *Igf2* expression in the choroid plexus, is located at the CCD, situated 5' of the DMD, a position presumably unaffected by insulator activity and provides one mechanism for biallelic expression in this tissue.

Regions of paternal specific hypermethylation, DMR1 and DMR2, situated proximal to *Igf2*, that respectively confer methylation dependent silencing and activation are

uncharacteristically hypermethylated on both alleles in the choroid plexus, suggesting a possible epigenetic route to biallelic *Igf2* expression in this tissue. To date, no attempt has been made to examine the methylation status of the DMD in the choroid plexus, though the central role played by this region in the initiation and maintenance of imprinting and its hierarchical influence upon *Igf2* proximal DMRs is suggestive of its participation at non-imprinted sites of *Igf2* expression.

## **Aims**

The purpose of this study is to elucidate *cis*-elements and mechanisms that confer biallelic *Igf2* expression in the choroid plexus. Current evidence is not informative of whether *Igf2* expression is initially imprinted in the primitive choroid plexus, becoming biallelic as development proceeds, or alternatively whether both alleles are active from the onset of expression. Resolving these questions by allele-specific analysis at the whole organ level would not be straightforward, as the choroid plexus is small and inaccessible at all stages of its development, thus requiring repeated microdissection from many animals. In addition, a whole organ approach makes over simplistic assumptions about the composition of the choroid plexus, which is comprised by a variety of distinct cell types arising from both neuroectodermal and mesodermal lineages, thus further complicating the analysis. Therefore allele-specific analysis to examine the imprinting status of *Igf2* expression during choroid plexus development will be performed *in situ*, using a combined approach of *in situ* hybridisation analysis and *lacZ* reporter gene expression assays. It is hoped that this dual methodology will provide detailed information upon the developmental timing of *Igf2* expression in the choroid plexus, its imprinting status and resolve the precise cell types, for example the epithelium or stroma, in which the gene becomes expressed during development.

Is the CCD the sole element driving biallelic expression in the choroid plexus, or as implicated by previous work (Jones *et al.* 2001), are other elements also required? If the insulator model of imprinting is correct, novel enhancer elements would be expected to be situated 5' of the DMD, an arrangement thought permissive for promoter-enhancer communication upon both alleles. A mouse transgenic system provides one of the most robust approaches to the identification and characterisation of *cis*-elements required for tissue and developmental stage specific gene expression

*in vivo*. However, the establishment of transgenic lines is labour intensive, time consuming and subject to ethical considerations. In this study, primary cultures derived from the choroid plexus epithelium will be used as a preliminary means to test the function of putative regulatory elements isolated from the *Igf2/H19* locus, by their use in transient reporter gene expression assays. Although not a replacement for the *in vivo* approach, *in vitro* studies permit a reduction in the number of animals used and, it is hoped, will allow rapid evaluation of *cis*-elements potentially involved in biallelic *Igf2* expression in the choroid plexus. Any regions identified as showing tissue-specific enhancer activity in the primary cultures would provide good candidates for subsequent analysis in a transgenic system.

Are epigenetic factors involved in the mechanism of biallelic *Igf2* expression in choroid plexus tissue? As already discussed, DMR1 and DMR2 are uncharacteristically methylated upon both alleles in the choroid plexus. Whether this is a determinant factor or a consequence of biallelic *Igf2* expression in this tissue will be addressed with an *in vitro* approach, by treatment of cultured choroid plexus cells with the DNA methyltransferase inhibitor, 5-aza-2'-deoxycytidine. Primary choroid plexus cultures discussed above could be used for such imprinting manipulation studies, although an immortal mouse choroid plexus epithelial cell line would be far better suited to this purpose. As no cell line of this description exists, derivation of immortal cell lines from the choroid plexus epithelium will form a primary aim of this study. A line of transgenic mice that overexpress SV40 large T-antigen protein in the choroid plexus epithelium have been obtained (described in Chapter 5) and will provide a resource from which, it is hoped, an immortal choroid plexus epithelial cell line can be created. The cell line will also carry suitable DNA polymorphisms such that the identity of the parental alleles can be distinguished for the purposes of gene expression and methylation analysis.

What is the role of the DMD? Methylation analysis of this region will be carried out to ascertain whether it bears characteristic paternal-specific hypermethylation marks in choroid plexus tissue or, as shown for DMR1 and DMR2, if it is highly methylated on both alleles. This will be conducted at the whole organ level, as was done previously by others for DMR1 and DMR2, but could also be performed in one, or both of the *in vitro* culture systems discussed above, which it is presumed, would bear

epigenetic marks appropriate to the choroid plexus. The methylation status of the DMD in the choroid plexus could be informative of a potential role in biallelic *Igf2* expression in this tissue.

## **CHAPTER 2: MATERIALS AND METHODS**

### ***Molecular Cloning Techniques***

#### ***Digestion of plasmid DNA with restriction enzymes***

Plasmid DNA up to 1µg amounts was digested according to the supplier's instructions (Promega) and as described in the Protocols and Applications Guide. Typically digests were carried out in 20µl reactions that contained the DNA, 2µl of 10x buffer and 10 units of enzyme made to volume with water. Larger quantities of plasmid DNA were digested in reaction volumes scaled up as appropriate. Digests were incubated at 37°C for at least 1 hour. The efficiency of the digests was checked by electrophoresis of small aliquots through agarose gels as described (Sambrook 1989).

#### ***Purification of DNA from solutions and agarose gels***

DNA fragments were purified from agarose gels or from enzymatic reactions prior to cloning with the Qiaquick gel purification or nucleotide removal kits respectively (Qiagen). The kits were used according to the manufacturers instructions.

#### ***Conversion of 5' and 3' recessed ends to blunt ends***

If required prior to ligation, 5' and 3' recessed plasmid vector and insert DNA ends were filled-in or removed by treatment with T4 DNA polymerase as described in the Protocols and Applications Guide (Promega). In brief, reactions were carried out in volumes of 50-100µl containing an appropriate volume of 10× reaction buffer, 100µM of each dNTP and 5 units of T4 DNA polymerase for each 1µg of template DNA. Reactions were incubated at 37°C for 10 mins and the enzyme inactivated by incubating at 75°C for 10 mins.

#### ***Dephosphorylation of plasmid ends***

To prevent self-ligation of linear plasmid DNA during ligation reactions, shrimp alkaline phosphatase (SAP) was used according to the manufacturers instructions (UpState Biotechnologies, USA). In brief, restriction digests of plasmid DNA were made to twice the original volume with water also incorporating an appropriate amount of 10× SAP reaction buffer and 0.5-1 units of SAP enzyme. Reactions were then incubated for 1 hour at 37°C after which the SAP enzyme was inactivated by incubating at 65°C for 15 mins.

### *DNA precipitation*

DNA solutions were precipitated by addition of 0.1 volume of 3M sodium acetate pH5.2 and 0.7 volumes of isopropanol, then incubated at RT for 10 mins. DNA was pelleted by centrifugation for 15 mins at RT, then washed with 70% Ethanol. DNA was centrifuged for a further 2 mins, the wash discarded and the pellet air-dried at RT and resuspended in an appropriate volume of water or TE Buffer (10mM Tris-HCl pH8, 1mM EDTA).

### *DNA and RNA quantification*

For those samples expected to contain limited amounts of DNA, for instance fragments obtained following purification from agarose gels were quantified by agarose gel electrophoresis. This was done by comparison of band intensities of unknown samples with bands of known concentration in either 1kb or 100bp quantitative DNA ladders (New England Biolabs) electrophoresed in adjacent lanes. Gels were stained with ethidium bromide (Sigma) and visualised with an ultraviolet transilluminator (UVP). Large-scale plasmid DNA, genomic DNA and total RNA preparations were analysed using a Beckman DU<sup>®</sup>530 Life Science UV-visible spectrophotometer with pre-programmed DNA/ RNA quantitation (Beckman-Coulter). Prior to analysis, DNA samples were diluted 1:100 fold in TE buffer. Aliquots of 100µl were taken from the diluted samples and readings taken in a 100µl quartz cell at 260nm wavelength, using TE buffer to calibrate the zero point.

### *Ligation of plasmid vector with insert DNA fragments*

Ligations were performed using reagents and protocols from Promega. Reactions were set up in 10µl volumes that contained 50-100ng purified plasmid vector DNA mixed with a 2-3 fold molar excess of insert DNA and incubated overnight at 4°C. Molar ratios of plasmid vector:insert DNA were calculated as follows:-

$$\frac{\text{ng vector DNA}}{\text{kb size of vector}} \times \frac{\text{kb size insert DNA}}{\text{molar ratio of insert vector}}$$

### *Oligonucleotide linker synthesis*

Approximately 500pM of complementary oligonucleotides were made to 50µl volumes in annealing buffer (10mM Tris; 10mM MgCl<sub>2</sub>), denatured by incubating at 80 °C for 10 mins, then annealed by slowly cooling to room temperature. Prior to ligation into plasmid vectors, annealed fragments were 5'-phosphorylated using polynucleotide kinase (Promega) in the presence of dATP according to the manufacturers instructions.

### *Preparation of competent E. coli cells*

Competent cells for molecular cloning were made using a rapid protocol (Nishimura 1990). A culture was set up by inoculating 0.5ml of an *E.coli* DH5α starter culture into 50mls LB broth (supplemented with 10mM magnesium sulphate and 0.2% glucose) and then grown with aeration to mid log phase. The culture was incubated on ice for 10 min and centrifuged at 1500g for 10 min at 4°C and the supernatant discarded. The cell pellet was gently resuspended in 0.5 ml of ice-cold LB broth and then 2.5 ml storage solution was added (36% glycerol; 12% PEG 7500; 12mM magnesium sulphate in LB broth sterilised by filtration). The cell suspension was gently mixed by pipetting, divided into 100µl aliquots and stored at -80°C.

### *Transformation of competent E.coli with recombinant plasmids*

Frozen aliquots of competent *E.coli* DH5α cells were thawed on ice and mixed with 1-5µl of plasmid DNA or a ligation reaction and incubated on ice for 15 to 30 mins. The cells were heatshocked at 42°C for 60 secs then immediately returned to ice for 1-2 mins, diluted 10-fold in SOC medium (Sambrook 1989) (pre-warmed at 37°C) and incubated at 37°C for 1 hour with rapid shaking (200 rpm) to allow expression of antibiotic resistance. Aliquots of 50-100µl were taken from each transformation, spread out on LB agar plates (Sambrook 1989) containing 50µg ml<sup>-1</sup> of carbenicillin (Sigma) and incubated overnight at 37°C. For blue/white selection of non-recombinant versus recombinant clones, 100µl of 200mg ml<sup>-1</sup> isopropyl-β-D-thiogalactopyranoside (IPTG; Melford Laboratories, UK) and 500µl of a 40mg ml<sup>-1</sup> solution of 5-bromo-4-chloro-3-indolyl-β-D-galactoside (X-gal; Melford Laboratories, UK) in di-methyl formamide (Sigma) were incorporated into 500 ml molten LB agar.



### *Isolation of plasmid DNA*

Small-scale plasmid DNA preparations (minipreps) as required for screening recombinant clones were performed with the Wizard MiniPreps Kit (Promega) according to the manufacturers instructions. Large-scale preparation of high-quality plasmid DNA as required for transfection of mammalian cells or for *in vitro* transcription of RNA probes, was done with the CONCERT Maxiprep system (Invitrogen) according to the manufacturers instructions.

### *Isolation of high-purity genomic DNA from mouse tissues*

The DNeasy genomic DNA purification kit (Qiagen) was used according to the manufacturers instructions to isolate high-purity DNA from mouse tissues or cultured cells suitable for PCR amplification of long or GC-rich DNA templates.

### *DNA sequencing*

All samples for DNA sequencing were analysed by automated fluorescent sequencing by Paul Jones at the Core Sequencing Facility in the Dept. Biology and Biochemistry at the University of Bath. In brief, between 150-250ng plasmid DNA was mixed with 10pM of sequencing primer and made to a total volume of 6µl with water. Sequencing reactions were then done with ABI Big-Dye termination reagents using various primers (shown below) and the reactions analysed with ABI 377 DNA sequencer (Applied Biosystems).

T7 (Invitrogen)      5' CGGGATATCACTCAGCATAATG-3'

T3 (Invitrogen)      5' AATTAACCCTCACTAAAGGG-3'

SP6 (Invitrogen)      5' ATTTAGGTGACACTATAGAATAC-3'

M13 -20 (Stratagene) 5' GTAAAACGACGGCCAGT-3'

M13 R (Stratagene) 5'GGAACAGCTATGACCATG-3'

### *Polymerase chain reaction (PCR)*

Standard PCR reactions were done in 20µl reactions in an MJ research thermal cycler using 1.1× Reddy Mix PCR buffer with 1.5mM MgCl<sub>2</sub> according to the manufacturers instructions (AB-Gene) with primers at 0.2µM. In some instances where genomic or cDNA fragments in excess of 1kb were amplified, more specific reaction conditions

were required. These reactions were done with variable (1-2.5mM)  $Mg^{2+}$  concentration, 2mM dNTPs and 1 unit Thermoprime Taq polymerase in 1× Thermoprime reaction buffer (AB-Gene). Unless stated otherwise in the relevant Results chapters cycling conditions were 94°C for 5 mins; then 94°C for 1 min, 60°C for 1 min, 72°C for 1 min for 35 cycles; with a final cycle of 72°C for 5 min. For amplification of long DNA templates (>5kb) the Expand high-fidelity polymerase kit (Roche) was used according to the manufacturers instructions. An optimisation protocol was used to determine specific reaction conditions (concentration of  $Mg^{2+}$ , dNTPs and primers) for standard and long template PCR (shown in **Figure 4**) Completed PCR reactions were analysed by agarose gel electrophoresis.

## **Mice**

### *Inbred laboratory strains*

Unless stated otherwise, F<sub>1</sub> mice derived from C57BL/6J × CBA crosses and embryos derived from F<sub>1</sub> crosses were used in all protocols. Mice were maintained on a 12-hour light/dark cycle in all cases.

### *Transgenic mice*

The *lacZDMR2*<sup>-</sup> mice, which carry a *lacZ*-neomycin cassette insertion at the *Igf2* locus were created in previous work and were maintained on an F<sub>1</sub> background (Murrell *et al.* 2001).

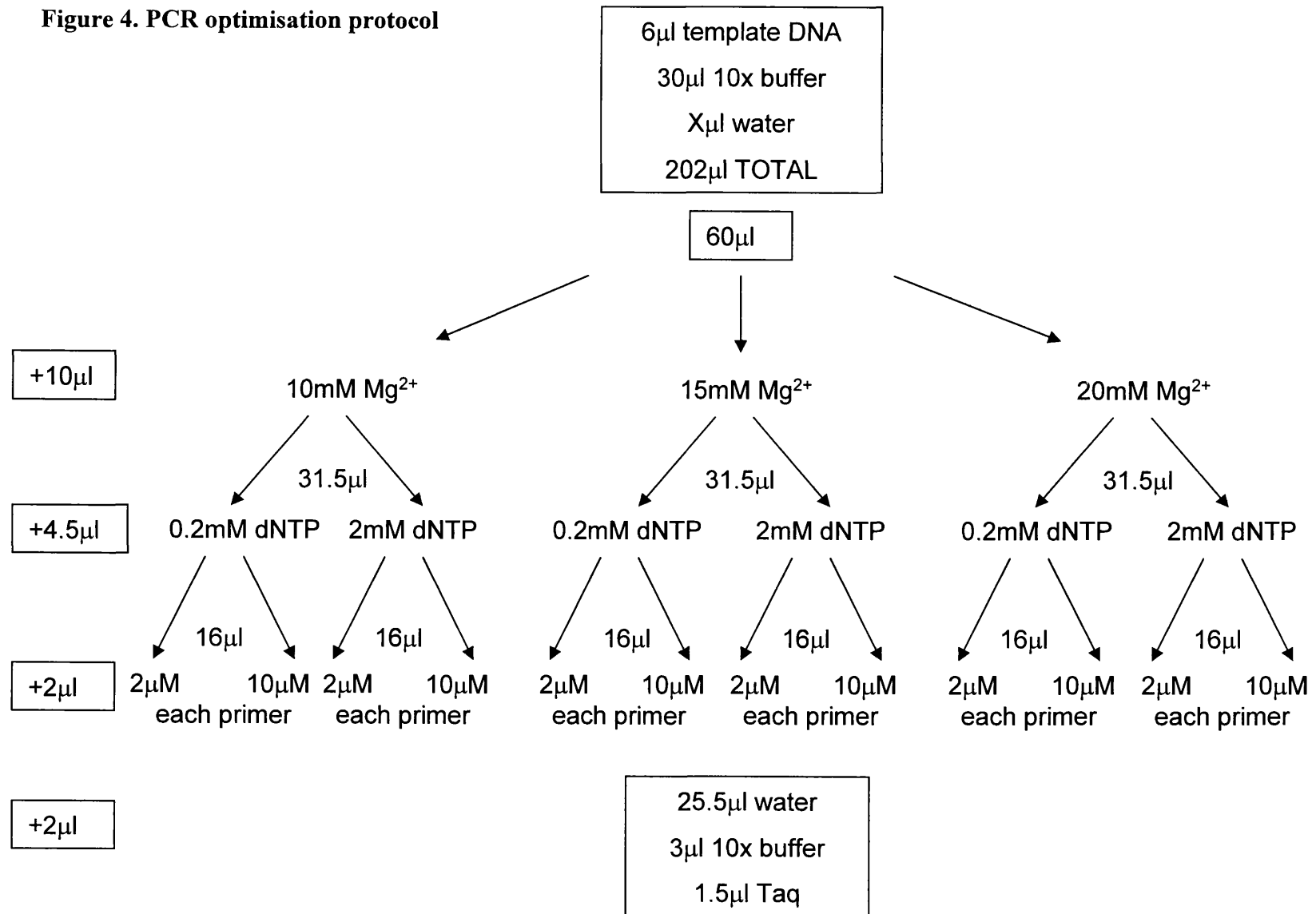
The T<sub>121</sub> mice, which carry a transgene for overexpression of a truncated SV40 large T-antigen protein in the choroid plexus epithelium were created in previous work (Saenz Robles *et al.* 1994) and were maintained as homozygotes on an F<sub>1</sub> (C57BL/6J × DBA) background.

The *p53* knockout mice, which carry a targeted deletion at the *p53* locus were created in previous work (Clarke 1993) and were maintained on an F<sub>1</sub> background.

### *Genotyping transgenic mice by PCR*

For rapid genotyping of transgenic lines a PCR based assay was used. Crude tissue lysates were made by incubating yolk sacs, ear punches or tail tip biopsies at 100°C for 10 mins in 600µl 50mM NaOH. Lysates were made pH neutral by adding 50µl of

**Figure 4. PCR optimisation protocol**



1M Tris-HCl (pH8) after which 1µl aliquots was taken from each and PCR-amplified in 20µl reactions (see section describing PCR) using primers appropriate to the strain.

For the *lacZ*<sup>DMR2</sup> mice, two pairs of primers were used to distinguish animals that were either WT, heterozygous or homozygous for the mutation. Primers internal to the *lacZ* reporter gene were used to amplify a 206bp product from the disrupted *Igf2* allele:- forward 5'-CTG TGA GAA CCT TCC AGC CTT TTC-3'; reverse 5'-CAA GGC GAT TAA GTT GGG TAA CGC C-3'. The second pair of primers which span the 3' end of intron 3 to the 5' end of exon 4 of the mouse *Igf2* gene were used to amplify a 190bp product from the WT *Igf2* allele:- forward 5'AGA GGA GTG TTG TTT CCG TAG C-3'; reverse 5'GTC CCA TTA CAG GTA GAG GTG C-3'. These primer pairs were run in separate reactions. For the T<sub>121</sub> mice, primers internal to the LPV-SV40 transgene were used to amplify a 170bp product in individuals positive for the transgene:- forward 5'CTA GTG ATG ATG AGG CTA CTG-3' reverse 5'TTC TTG TAT AGC AGT GCA GC-3'. For the *p53* knockout mice, primers used to distinguish animals that were either WT, heterozygous or homozygous are described (Malcolmson 1997). In all cases, the cycling profile was 94°C for 5 mins; then 94°C for 1 min, 60°C for 1 min, 72°C for 1 min for 34 cycles; with a final cycle of 72°C for 5 mins.

### ***Southern Analysis***

Southern (DNA blotting) analysis was performed according to standard protocols (Sambrook 1989) with modifications described below.

### ***Genomic DNA extraction from tissue***

Tissue biopsies were placed in tubes and digested by incubating with 525µl tail buffer (50mM Tris-HCl pH8, 100mM EDTA 100mM Sodium chloride, 1% SDS in water) and 35µl of a 10mg ml<sup>-1</sup> Proteinase K solution at 55°C overnight. To remove total RNA, the digests were incubated with 2µl 0.2mg ml<sup>-1</sup> RNase A at 37°C for 1 hour. Proteins were removed by addition of 200µl 5M Sodium chloride and 700µl chloroform: isoamyl alcohol followed by gentle mixing for 2 hours on a rocking platform, then centrifugation at 10000 rpm for 10 mins to separate the aqueous and organic phases. The aqueous layer was transferred to a clean tube, the genomic DNA

precipitated by addition of 700µl of isopropanol and then pelleted by centrifugation at 10000 rpm for 10 mins. DNA pellets were washed with 300µl 70% (v/v) ethanol at 4°C for 1h, spun briefly, the ethanol removed and the pellets air-dried. DNA was resuspended in 200µl TE buffer (10mM Tris-HCl, 1mM EDTA) then incubated with gentle agitation overnight to dissolve.

#### *Synthesis of $\alpha$ -<sup>32</sup>P(dCTP)-labelled DNA probes.*

Probes were synthesised using the Hi-Prime random priming kit (Roche) according to the manufacturers instructions. In brief, 20ng of a gel purified probe DNA fragment was made to 13.5µl with water then heat denatured at 100°C for 5 mins, chilled on ice for 5 mins, then incubated with 4µl of Hi-prime polymerase mix and 2.5µl  $\alpha$ -<sup>32</sup>P(dCTP) nucleotide (Amersham) in a total volume of 20µl for 1 hour at 37°C. Labelled probes were purified from the unincorporated nucleotide by centrifugation through sephadex G-50 columns in 200µl of TE buffer. Probes were heat denatured a second time, and chilled on ice until required.

#### *Blotting and hybridisation*

Approximately 10µg amounts of genomic DNA samples were digested with various restriction enzymes, size fractionated by electrophoresis through a 1% agarose gel, blotted onto N+ nylon membranes (Osmonics, USA) and crosslinked with a CL-1000 ultraviolet crosslinker (UVP). For the hybridisation, a modification of the protocol described by Church and Gilbert was used (Church 1984). The buffer used for pre-hybridisation and hybridisation was identical (0.5M sodium di-hydrogen orthophosphate, 1mM EDTA, 7% sodium dodecyl sulphate (SDS), 1% bovine serum albumin (BSA)). In each case immediately before use, 100µg ml<sup>-1</sup> sonicated and heat-denatured salmon sperm was added. Membranes were placed in glass hybridisation tubes containing 15ml of pre-heated hybridisation buffer then pre-hybridised for 4 hours at 65°C. For the hybridisation,  $\alpha$ -<sup>32</sup>P(dCTP) labelled probes were synthesised as described and added to the hybridisation tubes containing 15mls fresh pre-heated church buffer and hybridised to the membranes overnight at 65°C. Post hybridisation washes were carried out in 150ml volumes with the following solutions. Wash1 (40mM sodium di-hydrogen orthophosphate, 1mM EDTA 5% SDS, 0.5% BSA). Wash 2 (40mM sodium di-hydrogen orthophosphate, 1mM EDTA 1% SDS). Both

washes were done twice each for 30 mins at 65°C. Membranes were covered in saran wrap and autoradiographed at -80°C with intensifying screens using BIOMAX MS-1 film (Kodak). Exposure times were varied depending on the intensity of the hybridisation signal.

## ***Northern Analysis***

### ***DEPC-treatment of reagents***

All reagents for RNA analysis (excluding Tris-based buffers) were made RNase-free by incubating overnight with 0.05% di-ethyl pyrocarbonate (DEPC; Sigma) at RT. Excess DEPC was removed from the reagents by autoclaving.

### ***Isolation of Total RNA***

Tissue for RNA extraction was homogenised in TRI reagent (Sigma) using an Ultra-Turrax homogeniser. Homogenates were then either stored at -70°C or processed immediately. The homogenates were centrifuged at 13000 rpm for 10 mins at 4°C, the supernatant transferred in 1 ml aliquots to clean 1.5 ml eppendorf tubes then extracted with 200µl chloroform and centrifuged at 13000 rpm for 15 mins at 4°C. The aqueous phase was transferred to a clean tube, mixed with 1/10 volume of isopropanol, centrifuged at 13000 rpm for 10 mins at 4°C. The supernatant was transferred to a clean tube, the RNA precipitated by addition of an equal volume of isopropanol and pelleted by centrifuging at 13000 rpm for 10 mins at 4°C. RNA pellets were washed with 75% ethanol, air dried and dissolved in DEPC-treated water and stored at -70°C.

### ***Northern (RNA) blotting and hybridisation***

A standard protocol was used with some modifications (Sambrook 1989) All reagents were made RNase-free. Total RNA was prepared as described. Between 6-20µg of total RNA samples were denatured by mixing with 5µl 10× MOPS buffer (0.2M 3-[N morpholino]propanesulphonic acid, 0.05M sodium acetate, 0.01M EDTA, made in DEPC-treated water and adjusted to pH7) 8.75µl 37% formaldehyde, 25µl formamide and made up to 50µl DEPC-treated water and incubated at 55°C for 15 mins. Denatured total RNA samples were separated by electrophoresis through a 1.2% agarose-MOPS-formaldehyde gel (1× MOPS, 1.1% formaldehyde) then blotted and crosslinked as described for Southern analysis.

The buffer for the pre-hybridisation and hybridisation was identical (6×SSC, 5× Denhardt's reagent, 0.5% SDS). The hybridisation buffers were prepared fresh by dilution of a 20× SSC stock (3M sodium chloride, 0.3M sodium citrate) and 100× Denhardt's reagent stock (2g each of Ficoll 400, polyvinylpyrrolidone and BSA; Sigma) in DEPC-treated water. Immediately before use 100µg ml<sup>-1</sup> sonicated and heat denatured salmon sperm DNA was added. Membranes were placed in hybridisation tubes containing 15ml hybridisation buffer then pre-hybridised for 4 hours at 65°C. For the hybridisation, α-<sup>32</sup>P(dCTP) labelled probes were generated as described then added to the hybridisation tubes containing 15ml pre-warmed hybridisation buffer and hybridised to the membranes overnight at 65°C. The post-hybridisation washes were done in large (150ml) volumes. Wash 1 (2×SSC, 0.5% SDS) and wash 2 (0.5×SSC 0.5% SDS) were each done twice for 30 mins at 65°C. Autoradiography was done as described for Southern analysis.

### *Probes*

DNA probes used for Southern and Northern hybridisation are described in the relevant results chapters.

## ***Reverse Transcription and Polymerase Chain Reaction (RT-PCR)***

### ***DNaseI treatment of total RNA extracts***

For the purposes of RT-PCR analysis, genomic DNA contamination was removed from RNA extracts by treatment with DNaseI. Total RNA in 50µl water was made to 100µl with 10µl DNase reaction buffer, 10µl 100mM DTT, 28µl water, 100 units rRNasin<sup>®</sup> ribonuclease inhibitor, 2 units RQ1 RNase-free DNase (all Promega) and incubated at 37°C for 15 mins. The digested RNA was extracted with an equal volume of phenol: chloroform: isoamyl alcohol (125:24:1, pH4.7; Sigma) and centrifuged at 13000 rpm for 2 mins. The aqueous phase was extracted a second time with chloroform then transferred to a clean tube and the RNA precipitated by addition of 0.1 volumes 3M sodium acetate and 2.5 volumes of absolute ethanol. The RNA was pelleted by centrifuging at 13000 rpm for 10 mins at 4°C and the pellets washed with 70% ethanol then air-dried, dissolved in DEPC-treated water and stored at -70°C.

### *Complementary DNA (cDNA) synthesis*

First strand cDNA was synthesised from various total RNA samples using SuperscriptII<sup>TM</sup> reverse transcriptase (Invitrogen) according to the manufacturers instructions. In brief, 4µg of total RNA was annealed with either random hexamer or Oligo-dT primers (Promega) then reverse transcribed at 42°C for 50 mins. ‘Mock’ reverse-transcribed reactions were done in parallel for each cDNA sample in which the reverse transcriptase was omitted. PCR reactions were done as described (see section describing polymerase chain reaction) using 0.3µl cDNA template. In all cases the efficacy of the cDNA synthesis and relative abundance of expressed sequences were judged by PCR-amplification of cDNA samples using primers designed to the mouse *β-actin* sequence: forward 5’ GAC CCA GAT CAT GTT TGA GAC C-3’ and reverse 5’ GTT GGC ATA GAG GTC TTT ACG G-3’. Reactions were analysed by agarose gel electrophoresis.

### ***Transient expression assays***

#### *Cell lines*

Established cell lines were obtained from the European Collection of Cell Cultures (ECACC). The human hepatocellular carcinoma-derived Hep G2 cell line (Aden 1979) was maintained in DMEM (Sigma) supplemented with 10% foetal bovine serum (FBS), 2mM glutamine, 1% non-essential amino acids, 50U ml<sup>-1</sup> penicillin, 50 µg ml<sup>-1</sup> streptomycin, 2.5µg ml amphotericin-B (all Gibco-BRL) at 37°C with 5% CO<sub>2</sub>. The mouse fibroblast NIH:3T3 cell line (Uchida 1969) was maintained in DMEM nutrient mix-F12/ glutamax II supplemented with 10% FBS, 50U ml<sup>-1</sup> penicillin, 50 µg ml<sup>-1</sup> streptomycin, 2.5µg ml amphotericin-B (Gibco-BRL) at 37°C with 5% CO<sub>2</sub>. The origin of primary choroid plexus epithelial cells is described below.

#### *Isolation and culture of primary choroid plexus epithelial cells*

A modification of the protocol described in Hoffmann *et al.* was used (Hoffmann 1996). Whole brains were removed intact from litters of neonatal mice aged between postnatal days 1-6 and transferred, under aseptic conditions to pre-warmed complete growth medium DMEM nutrient mix-F12 supplemented with 10% FBS (foetal bovine serum) 50U ml<sup>-1</sup> penicillin, 50 µg ml<sup>-1</sup> streptomycin, 2.5µg ml<sup>-1</sup> amphotericin (all



Gibco-BRL). Lateral and fourth ventricle plexuses were then dissected from the brains, washed by immersion in pre-warmed Hanks buffered salt solution (HBSS; Sigma) and collected by centrifugation. The plexi were enzymatically disaggregated by digestion with pronase enzyme as described previously (Crook 1981). Pronase enzyme (Calbiochem) was made at  $2\text{mg ml}^{-1}$  in HBSS and incubated at  $37^{\circ}\text{C}$  for 5 mins after which digestion was terminated by addition of growth medium. The digested tissue fragments were collected by centrifugation at 1000 rpm for 4 mins then re-suspended by gentle repeated pipetting in 1ml complete growth medium to generate a suspension of single cells and small cell aggregates. Cells were further diluted with an appropriate volume of complete growth medium and plated in 35mm cell culture plates or 6-well plates and incubated undisturbed at  $37^{\circ}\text{C}$  with 5%  $\text{CO}_2$  for 24 hours to allow for cell attachment. The medium containing unattached cells and debris was removed and after a single wash with PBS and replaced with fresh medium supplemented with the drug cytosine  $\beta$ -D-arabinofuranoside (CAF; Sigma) to inhibit fibroblast proliferation. Positive selection for slower growing choroid plexus epithelial cells was established by alternating the cultures between CAF and CAF-free medium every 48h thereafter.

#### *Transfection of plasmid DNA into continuous cell lines.*

High quality plasmid DNA was prepared as described (see section describing isolation of plasmid DNA). HepG2 and NIH:3T3 cells were transfected with plasmid DNA using the FuGENE 6 reagent (Roche) according to the manufacturers instructions for transient transfection of adherent cells. These cell lines were seeded in 6-well plates and each well transfected with  $1\mu\text{g}$  of various test plasmid DNA constructs. In the instance of Luciferase reporter constructs,  $1\mu\text{g}$  of pSV40- $\beta$ gal vector (Promega) was co-transfected as an internal control for variable transfection efficiency. The pBluescriptII KS+ vector (Stratagene) was transfected as a negative control for Luciferase expression.

#### *Transfection of plasmid DNA into primary choroid plexus epithelial cells*

Primary choroid plexus epithelial cells were prepared as described. To derive sufficient numbers of cells for transfection choroid plexuses were removed from 20-25 neonatal mice. Cells were plated in 6-well plates at approximately  $1 \times 10^6$  cells per

well then each well immediately transfected with 1µg supercoiled test plasmid constructs using the Effectene transfection kit (Qiagen), essentially according to the manufacturers instructions. Transfection efficiency estimation and negative controls were done as for continuous cell lines. In an optimised protocol, both the test and control constructs DNA were mixed in the bottom of 1.5ml eppendorf tubes, and diluted with EC buffer to a total volume of 75µl. Enhancer reagent was added at 8µl per µg DNA added and the tubes incubated at RT for 5 mins, 12µl Effectene reagent was added, mixed with the DNA by gentle flicking and incubated at RT for a further 10 mins to allow transfection complexes to form. The entire contents of each tube was added drop wise to individual wells and mixed with the culture medium by gently rocking the plates. Plates were incubated overnight at 37°C, 5% CO<sub>2</sub>. Medium containing the transfection complexes was aspirated, the cells washed once with PBS then fresh growth medium added and the cells incubated for a further 48 hours to allow for reporter gene expression.

#### *Assay for Luciferase-specific activity of transfected cells*

To harvest cells for analysis of *Luciferase*-specific activity, growth medium was aspirated, the cells washed twice with PBS, then lysed by the addition of 200µl cell culture lysis reagent (Promega) to each well. Lysates were collected by scraping, transferred to clean tubes, then vortexed for 10 secs and centrifuged at 13,000 rpm for 2 mins to remove cell debris. Supernatants were transferred to clean tubes and either assayed for *Luciferase* immediately or stored at -80°C until required. Lysates were loaded into a 96-well microtitre plate in 5µl quadruplicate samples and *Luciferase*-specific activity measured with the addition of 25µl of *Luciferase*-assay reagent (Promega) per well in an automated Berthold LB96V microplate luminometer. Light outputs were measured with a 10 second delay after reagent dispense. Total *Luciferase* levels were determined by expressing the raw luminescence values of unknowns against that of a *Luciferase* standard series made by serial 10-fold dilutions of a 2ng µl<sup>-1</sup> *Luciferase* standard stock (Sigma).

#### *Soluble protein and β-galactosidase assays*

Total *Luciferase* measurements per well were normalised against soluble protein levels to correct for cell mass. A 5µl aliquot taken from each cell lysate was diluted

10-fold in water. 10µl aliquots were taken from these dilutions in duplicate, loaded into 96-well microtitre plates, mixed with 200µl BioRad protein reagent then incubated at RT for 30 mins. Protein measurements were made against a series of BSA standards (Bradford 1976) by reading absorbances at 590nm in a colorimetric assay. *Luciferase* values were also normalised for transfection efficiency against relative  $\beta$ -galactosidase activity levels. Activities were determined by the conversion of ONPG substrate with absorbances read at 405nm in a colorimetric assay as described (Norton 1985).

### ***Generation of immortal choroid plexus epithelial cell lines***

#### ***Isolation and culture of choroid plexus tumour tissue***

Choroid plexus papillomas were induced genetically by crossing mice of the T<sub>121</sub> line with the *p53* knockout line. Animals were monitored daily and those showing evidence of choroid plexus tumour formation (as judged by a bulging cranium) were sacrificed, the brain dissected and held in prewarmed growth medium. Choroid plexus tumours were removed, washed twice in HBSS, chopped into small pieces (approx 2mm<sup>3</sup>) with sterile scissors then given several further washes by repeated re-suspension and centrifugation in prewarmed HBSS. The tissue was disaggregated by digestion with 2mg ml<sup>-1</sup> Pronase (Calbiochem) in HBSS at 37°C for 10 mins, then diluted in growth medium and centrifuged to collect the cells. Supernatant was removed and the cells resuspended in growth medium and plated as described for primary culture. The cells were washed in PBS and medium replaced daily for the initial 5 days to remove dead cells and debris.

#### ***Cloning cell lines by limiting dilution***

A modification of a previously described protocol was used (Freshney 1987). Two rounds of colony formation in 96-well plates was required to isolate cell clones. Epithelial cell colonies from the primary tumour cultures described previously were isolated from other cell types by trypsinising from within 5mm steel cloning rings. Isolated colonies were taken up in growth medium, disaggregated with gentle pipetting and the resulting cell suspensions then split between 8-10 wells of a 96-well plate with a final volume of 200µl of growth medium used per well. Plates containing the cells were then incubated for two weeks until cultures enriched for epithelial cell

colonies had established. Those colonies exhibiting rapid growth and good epithelial morphology were selected for further purification by the limiting dilution method. Colonies were trypsinised, re-suspended in 0.5 ml complete growth medium and disaggregated by repeated pipetting to form a suspension consisting of single cells and small cell aggregates. Estimates of cell numbers in the suspension was performed by removing 10 $\mu$ l aliquots and counting on a slide haemocytometer. The suspension was then appropriately diluted in cloning medium (identical to primary culture medium but supplemented with 20% FBS and 10ng ml<sup>-1</sup> epidermal growth factor) to give a 30ml suspension containing 5-10 cells/ aggregates ml<sup>-1</sup>. The suspension was seeded in 96-well plates at 200 $\mu$ l per well, then each well was inspected to confirm that only one cell or cell aggregate was present in each well. The plates were incubated undisturbed under standard conditions for at least 5 days, after which they were inspected again to identify wells containing established colonies. Single colonies that had formed in isolation in a well were disaggregated by mild digestion in trypsin-EDTA and allowed to re-attach as smaller fragments to accelerate their outgrowth. After a further seven to ten days morphologically homogeneous clones were re-adapted to standard growth medium containing 10% FBS with no EGF supplementation, then expanded by culturing successively through, 96-well, 24-well, and 6-well plates over a period of approximately 6 weeks. Those clones maintaining epithelial morphology and rapid growth after expansion were selected as cell lines and expanded further. Cell lines were maintained in 75cm<sup>2</sup> flasks as described for primary choroid plexus epithelial cells.

### *Growth curves*

The growth rates of choroid plexus epithelial cells in primary and immortal cultures were measured by performing cell number counts with a haemocytometer at selected time points from cell plating. A Cell suspension was counted then seeded in a 24-well plate at 1ml per well and allowed to attach overnight under standard culture conditions. Plating efficiency was estimated as the number of cells attached 24 hours after plating divided by the number seeded. Counts were performed at 48 hour intervals thereafter. The cell number at each time point was estimated from the mean count of quadruplicate wells with each well counted twice.

### ***In situ expression analysis in cultured mammalian cells***

#### ***Staining for $\beta$ -galactosidase activity in situ in cultured cells***

Mammalian cells or cell lines were grown in 35mm plates with glass coverslips. Cells were washed twice in PBS and fixed with 0.8% glutaraldehyde in PBS for 10 min at 4°C. Cells were washed three times for 5 mins in PBS, then permeabilised by incubating in 0.1% triton X-100, 2mM MgCl<sub>2</sub> in PBS for 15 min at RT. Cells were washed three times for 5 mins in PBS then stained for  $\beta$ -gal activity by incubating in X-gal staining reagent (2mM MgCl<sub>2</sub>, 5mM potassium ferricyanide, 5mM potassium ferrocyanide, 0.01% sodium deoxycholate, 1mg ml<sup>-1</sup> X-gal in PBS) overnight at 37°C. After staining, cells were rinsed in PBS and post-fixed in 0.8% glutaraldehyde in PBS for 1 hour at 4°C then washed briefly in PBS, then the coverslips removed and mounted on slides in Aquatex mounting medium (Merck) and analysed by light microscopy.

#### ***mRNA in situ hybridisation in cultured cells***

Mammalian cells or cell lines were grown in 2-well (2ml) tissue culture chamber slides (Nunc). Cells were washed once in PBS and fixed in 4% paraformaldehyde, 0.25% glutaraldehyde in PBS for 1 hour at 4°C. Slides were washed three times in PBS then stored under 70% ethanol at 4°C until required. The culture chambers were removed and the slides were taken into absolute ethanol for 5 mins then rehydrated through graded ethanols and the remainder of the protocol done as for slide mRNA *in situ* but with the Proteinase-K digestion omitted. Following the colour reaction the slides were washed in PBS and mounted with glass coverslips using Aquatex mounting medium (Merck).

#### ***Immuno-fluorescence cytochemistry***

Mammalian cells or cell lines were grown in 35mm plates on glass coverslips under standard culture conditions as described previously. Cells were washed briefly in PBS, then fixed in either 4% paraformaldehyde in PBS for 15 mins at 4°C, or if cells were to be stained for cytoskeleton proteins, fixation was done in a 1:1 mixture of acetone and methanol for 5 mins at -20°C. Cells were washed three times for 5 mins in PBS then permeabilised by incubating in 0.1% Triton-X-100 in PBS for 30 mins at RT. Cells were washed three times for 5 mins in PBS then pre-blocked in 2%

blocking buffer (Roche) in PBS for 1 hour at RT. When staining for cytoskeleton proteins an antigen retrieval step was included prior to blocking by incubating cells in 10mM citric acid (Sigma) for 1 hour at 60°C. Primary antibodies diluted in blocking reagent (various dilutions between 1:100-300), were added to the cells and incubated overnight at 4°C. Primary antibodies used and their sources are listed in the relevant Results chapters. Coverslips were removed from the dishes and washed three times for 15 mins in a large volume of PBS then incubated with fluorescein-labelled  $\alpha$ -rabbit or  $\alpha$ -mouse IgG secondary antibodies (Vector Laboratories), diluted 1:100 in blocking buffer and incubated for 3 hours in the dark at RT. Secondary antibodies were removed by washing three times for 15 mins in PBS. Coverslips were mounted onto glass slides with gelvatol and slides kept in the dark until required. Bright field and FITC images were obtained with assistance from Dr. David Tosh using a Zeiss510 Confocal Laser Scanning Microscope.

### ***In situ expression analysis in whole mount preparations***

#### **Whole mount mRNA in situ hybridisation**

##### ***Embryo collection***

Embryos were taken from pregnant female mice with gestational age estimated by daily inspection for copulation plugs (with appearance of plugs designated embryonic day e0.5). Embryos were fixed in 4% paraformaldehyde in PBS overnight at 4°C. Unless stated otherwise, all subsequent steps were performed in 2ml round bottomed tubes (Treff). All reagents for prehybridisation/ hybridisation steps were made RNase-free by treatment with DEPC as described. Embryos were washed in PBT (PBS, 0.1% Tween 20; Sigma) and dehydrated through a methanol series (10 mins each in 25%, 50% 75% and absolute methanol in PBT) then stored in absolute methanol at -20°C until required.

##### ***Synthesis of DIG-labelled RNA probes***

Approximately 20 $\mu$ g of plasmid probe template DNA was linearised by digestion with appropriate restriction enzymes then purified using the Qiaquick nucleotide removal kit (Qiagen) according to the manufacturers instructions. Digoxigenin (DIG)-UTP labelled antisense RNA probes were transcribed from the purified DNA templates using the DIG RNA labelling kit (Roche) according to the manufacturers

instructions. A complementary sense control probe was synthesised in each case. The efficacies of the transcription reactions were assayed by analysing a 2 $\mu$ l aliquot of each by agarose gel electrophoresis.

### *Prehybridisation*

Embryos were rehydrated through the same methanol series in reverse and washed  $\times 2$  in PBT at RT. Embryos were bleached in 6% hydrogen peroxide (Sigma) in PBT for 40 mins at RT, washed three times in PBT and mildly digested with 10 $\mu$ g ml<sup>-1</sup> Proteinase K in PBT for 15 mins at RT. Digestion was stopped with a wash in 2mg ml<sup>-1</sup> glycine in PBT for 5 mins at RT. Embryos were washed twice in PBT then post-fixed in 0.2% glutaraldehyde/ 4% paraformaldehyde in PBT for 20 mins at RT. Embryos were washed twice in PBT then prehybridised at 65°C for at least an hour in buffer containing 5 $\times$ SSC pH4.5, 50% formamide, 0.1% Tween 20, 50 $\mu$ g ml<sup>-1</sup> Heparin (all from Sigma).

### *Hybridisation and washes*

The hybridisation buffer was identical to that used for the prehybridisation step but also included 100 $\mu$ g ml<sup>-1</sup> each of yeast transfer RNA and herring sperm DNA (Sigma). RNA probes were synthesised as described in the section above.. Probes used are listed in the relevant Chapters. Probes were denatured at 70°C for 10 mins, chilled on ice, then added at to the hybridisation buffer at 4 $\mu$ l ml<sup>-1</sup>. Embryos were hybridised with the probes at 65°C overnight. To remove non-specifically bound probe, embryos were subjected to a series of washes and treatment with RNase A as follows. Washes at low stringency were done twice for 30 mins in solution I (5 $\times$ SSC pH4.5, 50% formamide, 1% SDS) at 65°C, once for 10 mins in a 1:1 mixture of solution I and solution II (0.5M sodium chloride, 10mM Tris pH 7.5, 0.1% Tween 20) at 65°C, then three times for 5 mins in solution II. RNase A treatment was performed by incubating twice for 30 mins in 100 $\mu$ g ml<sup>-1</sup> RNase A (Sigma) in solution II at 37°C. Embryos were washed once for 5 mins in solution II, then washed at high stringency once for 5 mins in solution III (2 $\times$ SSC pH4.5, 50% formamide), followed by washing twice for 30 mins in solution III at 60°C.

### *Preparation of mouse embryo powder*

Embryos between stages e12.5 – 14.5 dpc were dissected and washed in ice-cold PBS. The embryos were homogenised with a minimum volume of PBS, 4 volumes of ice-cold acetone were added and the resulting slurry incubated on ice for 30 mins. The slurry was pelleted by centrifuging at 10000×g for 10 mins at 4°C, the supernatant discarded, the pellet washed with ice-cold acetone and pelleted as before. The pellet was transferred to filter paper to dry then ground to a fine powder with a pestle and mortar and stored at RT.

### *Pre-absorption of anti-digoxigenin conjugate*

A small amount of mouse embryo powder (~20µl) was placed in an eppendorf tube, a suspension made in 1ml TBT and heat inactivated at 70°C for 30 mins. Powder was collected by brief centrifugation, the supernatant was discarded and the pellet cooled on ice. The powder was resuspended in 1ml of an appropriate blocking buffer and the antibody added at an appropriate dilution (for whole mount *in situ* 1ml of 1% lamb serum in TBT was used and the sheep α-digoxigenin alkaline phosphatase conjugate added at a 1:2000 dilution). The antibody in blocking buffer/ embryo powder was then incubated on a rotator for at least 1 hour at 4°C. The powder was removed from the antibody solution by centrifuging at 10000 rpm for 5 mins at 4°C and the supernatant containing the antibody/blocking buffer transferred to a clean tube and kept at 4°C until ready for use.

### *Immuno-detection of the probe and colour reaction.*

Embryos were washed three times for 5 mins in Tris-Buffered Saline (TBST; 136mM sodium chloride, 3mM potassium chloride, 25mM Tris-pH 7.5, 0.1% Tween 20). Embryos were pre-blocked prior to addition of the antibody by incubating in 10% lamb serum (Gibco) in TBST for at least 2.5 hours at RT. Embryos were then immunostained for the specifically bound probe by incubating with a sheep polyclonal α-digoxigenin alkaline phosphatase conjugate (Roche) pre-absorbed as described and diluted at 1:1000 in 1% lamb serum in TBST overnight at 4°C. Non-specifically bound antibody was removed by washing three times for 5 mins then five times for 1 hour at RT. A final TBST wash was performed overnight at 4°C. Embryos were stained using an alkaline phosphatase colour reaction as follows. Embryos were



washed three times for 10 mins in NTMT buffer (100mM Tris pH9.5, 100mM Sodium chloride, 50mM Magnesium chloride, 0.1% Tween 20) then stained by incubating at RT in colour substrate solution prepared by dissolving nitroblue tetrazolium chloride (NBT) / 5-Bromo-4-chloro-3-indolyl phosphate, toluidine salt (BCIP) tablets in water (Roche) as described in the manufacturers instructions. After the colour reaction was complete, embryos were washed twice for 10 mins in NTMT buffer. The contrast of the stained versus non-stained tissues was enhanced by washing overnight in a large volume of PBT. Embryos were post-fixed in 4% paraformaldehyde in PBS for 2 hours at 4°C, rinsed in PBT then taken through a glycerol in PBS series (50%, 80%, 100%) and photographed.

### **Whole mount staining for $\beta$ -galactosidase *in situ***

$\beta$ -galactosidase expression *in situ* was analysed as previously described (Ainscough *et al.* 1997). Embryos with gestational ages between e8.5 and e14.5 dissected from pregnant female mice, and adult brains, were washed twice in ice-cold PBS, then fixed in a solution of ice-cold 5% formaldehyde, 0.8% glutaraldehyde, 2mM MgCl<sub>2</sub>, 0.01% (w/v) sodium deoxycholate, 0.02% (v/v) Igepal (all Sigma) in PBS for 1-2 hours depending on embryo size. Fixed embryos were washed twice in PBS at RT for 15 mins each to remove traces of fixative, then stained in freshly prepared X-gal reagent containing 1mg ml<sup>-1</sup> X-gal, 2mM MgCl<sub>2</sub>, 5mM potassium ferricyanide, 5mM potassium ferrocyanide, 0.01% sodium deoxycholate in PBS for 48 hours at 30°C. To enhance reagent penetration and examine internal  $\beta$ -gal expression, embryos larger than e14.5 were fixed for 30 mins, frozen briefly on dry ice and sagittally bisected using a scalpel blade then re-fixed, washed and stained in X-gal reagent as above. After staining, embryos were washed in PBS for 30 mins at RT, post-fixed overnight at 4°C and stored in 70% ethanol. For histological analysis of X-gal staining, tissues were processed into wax blocks as described. Sections were cut at 7 $\mu$ m thickness, de-waxed by soaking in HistoClear then re-hydrated by passage through a graded ethanol series, counterstained with nuclear-fast red (Vector Laboratories) for 1 min, washed for 2 mins in tap water, then dehydrated as before and mounted under glass coverslips in DPX (BDH).

## ***In situ expression analysis in histological preparations***

### ***Paraffin embedding and sectioning***

Embryos and tissues for slide mRNA *in situ* hybridisation were fixed in 4% paraformaldehyde in PBS overnight at 4°C. For protein immunohistochemistry fixation was done with Zambonis' buffer (0.85% paraformaldehyde, 0.15% saturated picric acid (Sigma) in PBS) overnight at 4°C. Samples were rinsed in PBS then transferred into 70% ethanol and either processed immediately or stored for not longer than 1 week at 4°C. Samples were processed for paraffin histology using an automated tissue processor (Leica). In brief tissue samples were dehydrated through an ethanol series (2 hours each in 70%, 70%, 90%, 90%, 95%, 100%, 100%), cleared in HistoClear (National Diagnostics, UK) then soaked for 2 hours in molten paraffin wax before embedding in wax blocks. Blocks were cut into serial sections of varying thickness between 7-10µm. Sections were floated and collected on APTES-treated glass slides. Slides were kept dust-free at 4°C until required.

### ***Slide mRNA in situ hybridisation***

#### ***Prehybridisation***

All reagents and solutions were made RNase free by treatment with DEPC as described. Slides containing 8µM paraffin sections were de-waxed by soaking twice for 10 mins in HistoClear (National Diagnostics, UK) and were re-hydrated by passage through an ethanol in water series (100, 100%, 95%, 80%, 70%, 50%, 30%) then washed in PBS for 5 mins. Slides were fixed in 4% paraformaldehyde in PBS for 30 mins, washed twice for 5 mins in PBS then digested by incubating in 25µg ml<sup>-1</sup> Proteinase K in PBS for 10 mins. Slides were washed twice for 5 mins in PBS, twice for 5 mins in 2×SSC buffer then incubated in Tris-glycine buffer (0.5M Tris, 0.5M Glycine) for 30 mins, immersed briefly in PBS, then dehydrated by passing through the same ethanol series in reverse and air dried at RT for at least 30 mins.

#### ***Hybridisation and washes***

RNA probes were synthesised as described (see section describing RNA probe synthesis). Probes used are listed in the relevant results chapters. Probes were added to the hybridisation buffer (5×SSC, 40% formamide, 1× Denhardt's reagent (see section describing Northern hybridisation and blotting), 100µg ml<sup>-1</sup> each of Yeast

transfer RNA and Herring sperm DNA; Sigma) at  $4\mu\text{l ml}^{-1}$  and then denatured at  $95^{\circ}\text{C}$  for 5 mins, chilled on ice for 5 mins then pipetted onto the slides at  $80\mu\text{l}$  hybridisation buffer per slide. Slides were covered with strips of parafilm to prevent evaporation of the buffer, placed in a sealed humidified chamber and hybridised overnight at various temperatures between  $55\text{-}65^{\circ}\text{C}$  depending on the probe used. To remove non-specifically hybridised probe, slides were washed three times for 15 mins in  $5\times\text{SSC}$ , then washed once for 40 mins in post-hybridisation buffer (20% formamide,  $0.5\times\text{SSC}$ ) at hybridisation temperature, once for 15 mins in  $2\times\text{SSC}$ , then incubated in  $10\mu\text{g ml}^{-1}$  RNase A in  $2\times\text{SSC}$  for 30 mins at  $37^{\circ}\text{C}$ . Slides were washed once for 15 mins in  $2\times\text{SSC}$ , once for 20 mins in post-hybridisation buffer at  $5^{\circ}\text{C}$  below hybridisation temperature, then once for 15 mins in  $2\times\text{SSC}$ .

#### *Immuno-detection of the probe and colour reaction*

Slides were incubated overnight with a sheep polyclonal  $\alpha$ -digoxigenin alkaline phosphatase conjugate, 1:500 in 1% blocking buffer (Roche) in PBS overnight at  $4^{\circ}\text{C}$ . Non-specifically bound antibody was removed by washing three times for 10 mins, three times for 30 mins and twice for 1 hour in PBS. Slides were washed three times for 10 mins in NTMT buffer (100mM Tris pH9.5, 100mM Sodium chloride, 50mM Magnesium chloride, 0.1% Triton X-100; Sigma) then stained by immersing in an alkaline phosphatase colour substrate solution prepared by dissolving nitroblue tetrazolium chloride (NBT)/ 5-Bromo-4-chloro-3-indolyl phosphate, toluidine salt (BCIP) tablets in water (Roche) as described in the manufacturers instructions. Staining was performed overnight at RT. After the colour reaction was judged to be complete, slides were washed briefly in PBS, post-fixed in 4% paraformaldehyde in PBS for 1 hour at  $4^{\circ}\text{C}$ , rinsed again in PBS and mounted with glass coverslips using Aquatex mounting medium (Merck).

#### **Immunohistochemistry**

Slides were de-waxed by soaking twice for 5 mins in HistoClear (National Diagnostics, UK), then rehydrated by passage through an ethanol series (1 min each in 100%, 100%, 95%, 70%) and held in PBT at RT. An antigen retrieval step was performed by boiling the slides in 10mM citric acid (three times for 5 mins in a 650W microwave oven on full power). Slides were then incubated in 0.3% hydrogen

peroxide (Sigma) for 30 mins at RT to inactivate any endogenous peroxidase activity in the tissue. Slides were washed three times for 5 mins with PBT then pre-blocked in 10% bovine serum albumin in PBT for 1 hour at RT. Primary antibodies, their sources and concentrations at which they were used are listed in the relevant results chapters. Antibodies were applied to the slides in 200 $\mu$ l blocking solution and incubated overnight at 4°C. Slides were washed three times for 5 mins in PBT then incubated with either biotinylated  $\alpha$ -goat or  $\alpha$ -rabbit IgG secondary antibodies. Secondary antibodies were diluted 1:500 in blocking solution, applied to the slides and incubated for 1 hour at RT. Slides were washed three times for 5 mins in PBT, then covered with Vectastain ready-to-use Vector Elite ABC reagent (Vector Laboratories) and incubated at RT for 45 mins. Slides were washed three times for 5 mins in PBT and stained using the Vectastain DAB kit (Vector Laboratories) according to the manufacturers instructions. When staining was judged to be complete slides were rinsed briefly in PBS then counterstained in Mayers haematoxylin (Vector Laboratories) dehydrated through graded ethanols and mounted in DPX (BDH).

## CHAPTER 3: DEVELOPMENTAL GENE EXPRESSION ANALYSIS

### *Introduction*

The *Igf2* and *H19* genes are broadly expressed in mesodermal and endodermal tissues, where both genes are imprinted. A differentially methylated domain (DMD) located in the 5' flank of the *H19* gene regulates the imprinting of both genes by functioning, in part, as a chromatin insulator that prevents access to shared enhancers situated further 3' of *H19* (Thorvaldsen *et al.* 1998; Bell 2000; Hark *et al.* 2000). *Igf2* escapes imprinted regulation and is biallelically expressed in the exchange tissues of the brain, the choroid plexus and leptomeninges, whereas *H19* reportedly maintains imprinted expression at these sites (DeChiara *et al.* 1991; Ohlsson *et al.* 1994; Svensson 1995). Elements that confer *Igf2* expression in these tissues are anticipated to lie 5' of the DMD and therefore not be affected by insulator activity. In agreement with this proposal, a tissue specific enhancer region for expression in the choroid plexus and leptomeninges is located at the CCD, situated 5' of the DMD in the intergenic region (Ward *et al.* 1997; Jones *et al.* 2001; Charalambous *et al.* 2004). Differentially methylated regions (DMR1 and DMR2) situated proximal to *Igf2*, that respectively confer methylation dependent silencing and activation (Constancia *et al.* 2000; Eden *et al.* 2001; Murrell *et al.* 2001), are hypermethylated on both alleles in the choroid plexus, suggesting that epigenetic mechanisms are also required for biallelic expression in this tissue (Feil *et al.* 1994).

How these elements might initiate and/or maintain expression, in the choroid plexus, of the otherwise normally silent maternal *Igf2* allele is unknown. No previous attempt has been made to characterise the timing of *Igf2* expression, its imprinting status, and the precise cell types (i.e. epithelium or stroma) in which the gene becomes expressed, during choroid plexus development. Are both alleles active from the onset of expression, or as implicated by studies in the rat, is expression initially imprinted, becoming biallelic as development proceeds (Overall 1997). Clarification of these issues could be informative of when regulatory elements critical to biallelic expression are likely to act. The aim of work in this chapter was to address these questions by detailed description of allele-specific *Igf2/H19* expression patterns in the context of the developing brain, with emphasis upon the choroid plexus.

The choroid plexi are both small and inaccessible at all stages of development, thus an appropriate methodology for gene expression analysis in this organ is one which can be performed *in situ* and at single-cell resolution. Techniques that have a histological basis such as mRNA *in situ* hybridisation generally satisfy these criteria, indeed studies that initially defined the choroid plexus and leptomeninges as sites of *Igf2* expression utilised an *in situ* hybridisation approach (Stylianopoulou *et al.* 1988a; Stylianopoulou *et al.* 1988b; DeChiara *et al.* 1991). However these studies used radioactive labelling of RNA probes, which were detected by the precipitation of elemental silver over the tissue sections in a layer of photographic emulsion. Although sensitive, this method lacks resolution at the cellular level, thus for the purposes of this study, a modified non-radioactive mRNA *in situ* technique was employed. This involves the chemical labelling of RNA probes, which are detected by means of an enzyme-linked antibody conjugate, followed by a colour substrate reaction within tissue sections. This approach achieves a superior single cell resolution of mRNA than the older protocol and has also permitted the technique to be extended to analysis in whole mount preparations (Wilkinson 1992).

A second strategy for gene expression analysis involved the use of the *E.coli*-derived *lacZ* gene as a reporter gene. Previous studies have used this approach to describe the expression conferred by regulatory elements at the *Igf2/H19* locus, both in the context of ectopic transgenes and germline deletions (Ainscough *et al.* 1997; Brenton *et al.* 1999; Ainscough *et al.* 2000b; Murrell *et al.* 2001). The *lacZ* gene encodes  $\beta$ -galactosidase, an enzyme involved in lactose metabolism whose activity can be detected in cells by means of a sensitive histochemical reaction. This involves the conversion of the synthetic substrate, 5-bromo-4-chloro-3-indolyl- $\beta$ -D-galactoside (x-gal) to an insoluble intensely blue product, which produces beautifully resolved expression patterns.  $\beta$ -galactosidase is extremely stable and its activity is not adversely affected by exposure to most histological fixatives. Moreover processed tissue retains x-gal staining well enough that it may be visualised in sections and additionally this approach is not subject to the degree of tissue destruction produced by *in situ* hybridisation. Whole mount  $\beta$ -galactosidase expression assays can be problematic under certain conditions. Poor stain penetration may leave the interior structures of larger tissues unstained even after lengthy incubations in staining buffer,

although it has been found that bisection of tissues prior to staining considerably enhances stain penetration (Ainscough *et al.* 1997). Another potential disadvantage is that some mammalian cells contain an endogenous lysosomal  $\beta$ -galactosidase-like activity. This activity is only present at a low pH and may be blocked by performing the staining at a pH greater than 7.4 (Alam and Cook 1990). When performed under the correct conditions  $\beta$ -galactosidase expression assays offer the advantage of a superb single-cell resolution of gene expression that can be superior to that given by *in situ* hybridisation, as exemplified by analysis of a *lacZ* reporter gene knock-in mutation at the mouse *Delta1* (*Dll1*) locus (Beckers 1999).

In the present study, to examine the developmental profile of *Igf2* expression *in situ*, an *Igf2-lacZ* reporter gene knock-in mutant was analysed in  $\beta$ -galactosidase whole mount expression assays. The mutant line named *lacZDMR2*<sup>-</sup> was described previously, to make a deletion of the differentially methylated region 2 (DMR2), a putative imprinting element, within the *Igf2* structural gene (Murrell *et al.* 2001). To create this deletion, a 4.65kb region spanning exons 4-6, also containing the DMR2 region was replaced with a promoter-less IRES-*lacZ*-neomycin resistance cassette (Figure 5). Upon paternal transmission of *lacZDMR2*<sup>-</sup>, reporter gene expression was widespread in mesodermal and endodermal tissues, but was absent from the brain with the exception of the exchange tissues, whereas upon maternal transmission, reporter gene expression was confined to the exchange tissues, consistent with the expression profile of *Igf2* (DeChiara *et al.* 1991; Murrell *et al.* 2001). Therefore, deletion of DMR2 does not appear to perturb either the regional expression pattern or imprinting status of *Igf2*. In this mutant it is reasonable to assume that reporter gene expression reflects that of the endogenous *Igf2* gene.

An important finding of work presented in this chapter was that of variegated *Igf2* expression in the choroid plexus epithelium. This manifested finely scattered expression in isolated cells or small cell clusters and was evident from the earliest point at which *Igf2* expression could be detected in this tissue. This ‘salt and pepper’ arrangement appeared highly reminiscent of lateral inhibition (discussed below), a mechanism central to the canonical Notch signalling pathway (for review see (Lewis 1998)), known to generate asymmetric cell fates in a number of metazoan organisms.

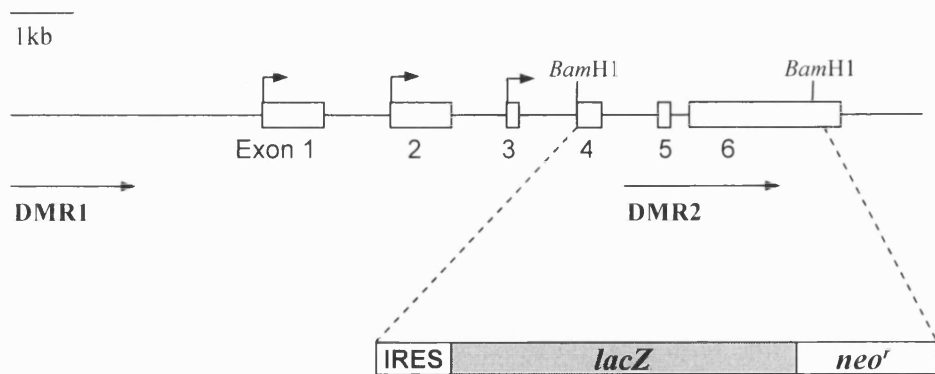


**Figure 5. The *lacZDMR2*<sup>-</sup> genomic region.** A 4.65kb region at the *Igf2* locus defined by two *Bam*H1 sites, containing the *Igf2* coding exons (4-6) and the overlapping DMR2 region was replaced with an IRES:*lacZ*-neomycin resistance cassette (Murrell *et al.*, 2002). The deleted region is shown by broken lines. DMR1 and DMR2 are represented as solid arrows; *Igf2* exons are shown as open boxes; *Igf2* promoters (initiating in the leader exons 1,2 and 3) are indicated by short arrows.



*Notch* genes encode a family of conserved transmembrane receptors that interact with the membrane bound ligands encoded by the *Delta*, *Serrate*, *Lag* (DSL) family genes (with mammalian *Serrate* genes renamed as *Jagged*) all of which were originally identified in *Drosophila*. Signalling through Notch receptors is thought to occur via direct interactions with Delta and Serrate/Jagged ligands positioned upon adjacent cells. This results in the proteolytic cleavage of the Notch intracellular domain (NICD) which translocates to the nucleus and functions as a transcriptional co-activator in concert with the transcription factor RBP-J $\kappa$ /CBF1, a mammalian homologue of the *Drosophila* gene, *Suppressor of Hairless* (*SuH*). It is thought that unbound RBP-J $\kappa$ /CBF1 mediates transcriptional repression in combination with the histone-deacetylase complex SMRT/sin3/HDAC. NICD binding to RBP-J $\kappa$ /CBF1 displaces the co-repressors and subverts RBP-J $\kappa$ /CBF1 function to activate transcription, by recruitment of histone-acetyl transferases (Kao 1998; Kurooka 2000). Activated RBP-J $\kappa$ /CBF1 promotes expression of basic helix-loop-helix (bHLH) transcriptional repressor proteins encoded by *Hes* genes, the mammalian homologues of *Enhancer of Split* genes in *Drosophila*. These molecules are thought to function as key regulators of downstream target genes, which directly mediate cell fate decisions (Jarriault 1998; Kao 1998).

These events, it is proposed, act according to the lateral inhibition model (reviewed in (Lewis 1998)). Lateral inhibition is a mechanism by which an aptly named 'salt and pepper' arrangement of different cell fates arises from a population of identical progenitor cells. This commences in a field of undifferentiated cells that uniformly express Notch receptors. Ligands encoded by *Delta* (and *Jagged*) genes present upon a small number of these cells activate Notch receptors and via intracellular signalling events involving NICD, repress the expression of Delta ligands in adjacent cells. The system is thought to be self-reinforcing, such that small differences in the number of Delta ligands present upon adjacent cells become accentuated. That is, cells with a slightly greater concentration of ligands will prevail whilst any adjacent cells with relatively less ligand will lose ligand expression altogether. Delta expressing cells are permitted to differentiate whilst those lacking Delta remain undifferentiated. Therefore, Notch signalling imposes specific fates upon isolated cells, in a Delta

dependent manner, whilst simultaneously preventing adjacent cells from following the same fate.

In mammals, four *Notch* genes (*Notch1-4*), and at least six DSL gene homologues (*Dll1*, *Dlk1*, *Dll3*, *Dll4*, *Jagged1-2*) have been identified, many of which perform essential functions during embryogenesis. Disruption of *Notch1*, *Notch2* or *Dll1* in mice results in early embryonic lethality with severe defects in somite patterning and neurogenesis (Swiatek *et al.* 1994; Hrabe de Angelis *et al.* 1997; Hamada *et al.* 1999). Recent studies also demonstrate a role for Notch signalling in patterning the vascular system. *Jagged1* null or *Notch1/Notch4* compound mutant mice die *in utero* due to severe vascular disorganisation (Loomes 1999; Krebs *et al.* 2000). In contrast, mice carrying deletions in the *Notch3* gene were reported to be viable and phenotypically normal (Krebs *et al.* 2003).

Work presented in this chapter shows that *Igf2* expression is confined to a scattered subpopulation of differentiating choroid plexus epithelial precursor cells, commencing at e10.5 of development (**Figures 6 and 9**). A Notch-dependent mechanism involved in the specification of *Igf2* positive and negative subpopulations, it is proposed, would be expected to be active in this tissue at, or immediately preceding, this stage and the expression of *Notch* and *Delta* genes in the choroid plexus epithelium, or adjacent tissue (stroma) at this time would be consistent with this expectation. *Notch*, *Delta* and *Jagged* gene expression during mouse embryogenesis is widely documented, although in only a small number of published works, describing *Notch1*, *Notch2* and *Dll1*, do the authors refer to gene expression in the choroid plexus (Higuchi 1995; Hrabe de Angelis *et al.* 1997; Hamada *et al.* 1999). However, these studies neither discriminate gene expression in the epithelial and stromal components of this tissue nor do they describe the earliest stages of choroid plexus development where variegated *Igf2* expression commences. Therefore, a second aim of the present study was to establish expression patterns for *Notch*, *Delta* and *Jagged* genes in the developing choroid plexus as a means to address a potential involvement of Notch signalling in the specification of distinct *Igf2* phenotypes amongst choroid plexus epithelial cells. This initially involved RT-PCR analysis to ask which of the *Notch*, *Delta* and *Jagged* genes are generally represented in whole choroid plexus mRNA and

was followed by *in situ* hybridisation analysis to examine expression in the epithelial and stromal components of this tissue.

## **Materials and Methods**

### **Probes**

The *Igf2* probe was a 1.5kb cDNA fragment spanning exon 6 of the mouse *Igf2* gene cloned into the Bluescript II KS+ vector (described in (Charalambous *et al.* 2004)). The *H19* probe was a 346bp cDNA fragment spanning exons 3-4 of the mouse *H19* gene, PCR-amplified from neonate liver cDNA using the primers:- 5'AAT GAG TTT CTA GGG AGG GAG G-3' and 5'GGA AAA GTG AAA GAA CAG ACG G-3' then ligated into the pGEM-T easy vector. The *FoxJ1* probe was a 1.7kb cDNA fragment spanning exons 1-2 of the mouse *FoxJ1* gene, PCR-amplified from choroid plexus cDNA using the primers:- 5'GCC CCT GAC CCA ACC ACC CCA CAC-3' and 5'CCG CCC CCT GAC GAC GTG GAC TAT-3' and cloned as for the *H19* probe. The *CTCF* probe was a 2kb cDNA fragment, cloned into the Bluescript II SK+ vector (Prof. Hiroyuki Sasaki, unpublished). The origin of *Notch*, *Delta* and *Jagged* probes is described in the results section of this chapter. For *in situ* hybridisation, plasmids containing probes were linearised by digestion with restriction enzymes and linearised fragments used in transcription reactions to synthesise RNA probes (see Chapter 2 sections describing digestion of plasmid DNA with restriction enzymes and synthesis of DIG-labelled RNA probes). Details for all probes are listed in **Table 1**.

### **Antibodies**

Commercially available primary antibodies were obtained for transthyretin (TTR) transferrin (TFN), albumin (Alb), *type1* insulin-like growth factor receptor (Igf1r), fibroblast growth factor receptor 3 (Fgfr3) and insulin for the purposes of immunohistochemistry (**Table 2**).

### **PCR Primers**

Primers corresponding to all known mouse *Notch*, *Delta* and *Jagged* homologues were designed from full-length cDNA sequences obtained from the ENSEMBL and GENBANK databases. The Genetool program (Biotools, UK) was used to select primers from these sequences (listed in **Table 3**).

<b>Probe</b>	<b>Digest</b>	<b>Orientation</b>	<b>Polymerase</b>
<i>Igf2</i>	<i>HindIII</i>	Antisense	T7
	<i>XbaI</i>	Sense	T3
<i>H19</i>	<i>SacII</i>	Antisense	SP6
	<i>SpeI</i>	Sense	T7
<i>Foxj1*</i>	<i>SpeI</i>	Antisense	T7
	<i>SpeI</i>	Sense	T7
<i>CTCF</i>	<i>EcoRI</i>	Antisense	T7
	<i>NotI</i>	Sense	T3
<i>Notch1</i>	<i>SalI</i>	Antisense	T7
	<i>XbaI</i>	Sense	SP6
<i>Notch2</i>	<i>SalI</i>	Antisense	T7
	<i>XbaI</i>	Sense	T3
<i>Notch3</i>	<i>EcoRI</i>	Antisense	T3
	<i>NotI</i>	Sense	T7
<i>Notch4</i>	<i>EcoRI</i>	Antisense	T7
	<i>BamHI</i>	Sense	T3
<i>Dll1</i>	<i>EcoRI</i>	Antisense	T3
	<i>NotI</i>	Sense	T7
<i>Dlk1</i>	<i>EcoRI</i>	Antisense	T7
	<i>BamHI</i>	Sense	T3
<i>Dll3</i>	<i>EcoRI</i>	Antisense	T7
	<i>BamHI</i>	Sense	T3
<i>Dll4</i>	<i>SalI</i>	Antisense	T7
	<i>NotI</i>	Sense	SP6
<i>Jag1</i>	<i>SalI</i>	Antisense	T7
	<i>NotI</i>	Sense	SP6
<i>Jag2</i>	<i>EcoRI</i>	Antisense	T3
	<i>NotI</i>	Sense	T7

**Table 1. RNA probes used for *in situ* hybridisation analysis.** Probes were generated by *in vitro* transcription of plasmid DNA templates. The restriction enzymes used to linearise plasmid templates, the RNA polymerases (T7, T3 or SP6) used and the orientation of the synthesised probes are shown. \*Plasmid templates with probe DNA ligated in both sense and antisense orientations were obtained for *Foxj1*.

<b>Antibody</b>	<b>Source</b>	<b>Manufacturer</b>	<b>Dilution</b>
Transthyretin (TTR) $\alpha$ -human	rabbit	DAKO	1:100
Transferrin (TFN) $\alpha$ -human	rabbit	DAKO	1:300
Albumin (ALB) $\alpha$ -human	rabbit	DAKO	1:300
Fibroblast growth factor receptor 3 (FGF-3R) $\alpha$ -mouse	goat	Santa Cruz Biotechnologies	1:300
Type-1 Insulin-like growth factor receptor (IGF-1R) $\alpha$ -mouse	rabbit	Santa Cruz Biotechnologies	1:500
Insulin (INS) $\alpha$ -mouse	guinea pig	Santa Cruz Biotechnologies	1:300

**Table 2. Primary antibodies used for immunohistochemistry.** The primary antibodies and the antigens to which they are raised are shown in the far left column. The source species in which the antibodies were raised, the manufacturer and the dilutions at which they were applied are also shown.

<b>Primer</b>	<b>Direction</b>	<b>Sequence</b>
Notch1	forward	5'CGC AAT GGG GGC ACC TGT GAC CT-3'
	reverse	5'TGG CAC GGC AGG CAC AGC GAT AG-3'
<i>Notch2</i>	forward	5'CCG CAG GGC ATG TTG GGG AAA G-3'
	reverse	5'GGG CAG TCG TCG ATA TTC CGC TCA-3'
<i>Notch3</i>	forward	5'CAC GGG GAA GGG GCA CAG GGC ACT-3'
	reverse	5'CCG CCG CCG TCG TCG CCT GAT-3'
<i>Notch4</i>	forward	5'CCC ACA CCC CCA AGC TCC CGT AGT-3'
	reverse	5'AGC GGC ACT GGA TCT GGG GGT ATG-3'
<i>Dll1</i>	forward	5'CGG GCC AGG GGA GCT ACA CAT G-3'
	reverse	5'GGC GCT CAG CTC ACA GAC CTT GC-3'
<i>Dlk1</i>	forward	5'GCC CGA GCA ACA CAT CCT GAA GGT-3'
	reverse	5'GGG GTG GGG AAC GCT GCT TAG ATC-3'
<i>Dll3</i>	forward	5'GCG GCT TGT GTG TTG GCG GTG AA-3'
	reverse	5'GCC GGC GCA GTC GTC CAG GTC-3'
<i>Dll4</i>	forward	5'CTG CGA ATG CCC CCC CAA CTT TAC-3'
	reverse	5'GGG CAC AGG GAC TTC GGG CAC AAT-3'
<i>Jagged1</i>	forward	5'CCC CGA GGA CAA CAC CAC CAA CAA-3'
	reverse	5'CCG CTG GGG GCC TTC TCC TCT C-3'
<i>Jagged2</i>	forward	5'GCG GGT TCG AGG CAG GGT CCA G-3'
	reverse	5'GGG GAG GCA GTC GTT GGG ATT GA-3'

**Table 3. Primers used for RT-PCR analysis of *Notch*, *Delta* and *Jagged* expression.**

## Results

### Allele-specific *lacZDMR2*<sup>-</sup> reporter gene assays

To separately examine expression from the paternal and maternal *Igf2* alleles at embryonic stages, timed matings were set up between male or female *lacZDMR2*<sup>-</sup> heterozygous animals and respective F<sub>1</sub> partners. The gestational stage following a successful mating was taken as e0.5 days post coitum (dpc) as judged by detection of a copulation plug, assuming a mid-dark cycle mating had occurred. Embryos were dissected at various time points between e9.5 and e14.5 of gestation, then fixed and stained for  $\beta$ -galactosidase activity *in situ* (see Chapter 2 section that describes whole mount  $\beta$ -galactosidase staining *in situ*) and genotyped for the presence of the *lacZDMR2*<sup>-</sup> allele from yolk-sac tissue (see Chapter 2 section that describes genotyping mice by PCR). Whole brains were dissected from paternal and maternal transmission *lacZDMR2*<sup>-</sup> adult mice at 3 months of age and treated as described for embryos. Where analysis in greater detail was required, stained embryos were wax embedded and sectioned as described (see Chapter 2 section that describes paraffin embedding). Positive staining was not observed in tissues derived from non-transgenic littermates at any of the embryonic or adult stages examined in this analysis (not shown).

### Expression at e9.5

#### Paternal transmission

At e9.5 reporter gene expression was widespread in mesodermal and endodermal derivatives as expected for the paternal allele of *Igf2* (**Figure 6a**). Strong staining was seen in the presomitic mesoderm, myotome and sclerotome compartments of formed somites, fore limb buds, condensing mesenchyme of the hind limb buds, developing heart, and visceral organs. In the brain, reporter gene expression appeared to be absent from the regions of neuroepithelium that later generate the choroid plexi. Analysis of sections made in the sagittal plane did not reveal any hidden staining in these regions of the neuroepithelium (not shown). Expression of the reporter was strong in blood vessels with intense staining in the carotid arteries extending upwards from the dorsal aorta, primary head veins and in the network of cerebral capillaries supplying the prosencephalon and mesencephalon (not shown). Staining was also seen in the

streams of trigeminal and facial neural crest cells migrating into the first and second branchial arches.

### Maternal transmission

Reporter gene expression was not detected in e9.5 embryos (**Figure 6b**).

### *Expression at e10.5*

#### Paternal transmission

At e10.5 expression of the reporter at peripheral sites was similar in distribution to the previous stage (**Figure 6c**). In the brain staining persisted in the carotid arteries and primary head veins and had become more widespread in the cerebral capillary network (not shown). Regional expression had commenced in the neuroepithelium of the metencephalon (the presumptive choroid plexus epithelium), although in many embryos, intense staining in the overlying surface ectoderm and mesenchymal layers made its direct observation in whole mount difficult. Analysis of these embryos in sagittal sections revealed strong staining in a scattered population of cells in this region of the neuroepithelium, with uniform staining seen in the overlying mesenchyme that later invades to form the choroid plexus stroma (**Figure 9**). Staining was also strong in Rathke's pouch, the precursor of the anterior pituitary, but was notably absent from the adjacent infundibulum, the region from which the posterior neural pituitary is formed (not shown). Stained cells were seen in the ventral aspect of the neuroepithelium lining the optic recesses and in a small area of mesenchyme overlying the antero-medial wall of the telencephalic vesicles (not shown). Staining was now evident in the trigeminal ganglion and had intensified in the streams of trigeminal and facial neural crest invading the branchial arches.

#### Maternal transmission

At e10.5, the first evidence of reporter expression was seen at several sites in the developing brain (**Figure 6d-j; Figure 9**). The neuroepithelium in the roof plate of the metencephalon was clearly stained. As upon paternal transmission this staining was restricted to a scattered population of cells and in most embryos occupied a narrow band dorsomedially, extending to wider domains more laterally. This domain of expression appeared to coincide with the choroid plaque from which the fourth ventricle choroid plexus epithelium later expands. Analysis of sections made in the



sagittal plane revealed that the staining was present exclusively in the neuroepithelium and that in contrast to paternal transmission embryos was altogether absent from the overlying mesenchyme that later forms the choroid plexus stroma. In other areas of the brain and as upon paternal transmission, a small area of mesenchyme overlying the anterior-most aspect of the medial wall separating the telencephalic vesicles was stained. Unlike paternal transmission embryos, expression of the reporter was seen in a thin dorso-medial stripe of cells running in an antero-posterior direction through the neuroepithelium of the mesencephalon. Expression of the reporter was not detected in cerebral blood vessels or in cranial neural crest derivatives at this stage.

### *Expression at e12.5*

#### **Paternal transmission**

At e12.5 (**Figure 7a**) expression of the reporter was again strong and widespread in peripheral tissues. In the evaginating fourth ventricle choroid plexus, expression of the reporter was clearly restricted to a small number of cells in the epithelium. By contrast staining was stronger and uniform in the invading stromal mesenchyme. This was particularly evident in sagittal sections (**Figure 9**). Expression had now commenced in the condensing mesenchyme of the leptomeninges surrounding the brain and the spinal cord and continued at high levels in cerebral blood vessels(not shown). Staining remained in Rathkes pouch and in the ventral neuroepithelium of the optic recesses (not shown).

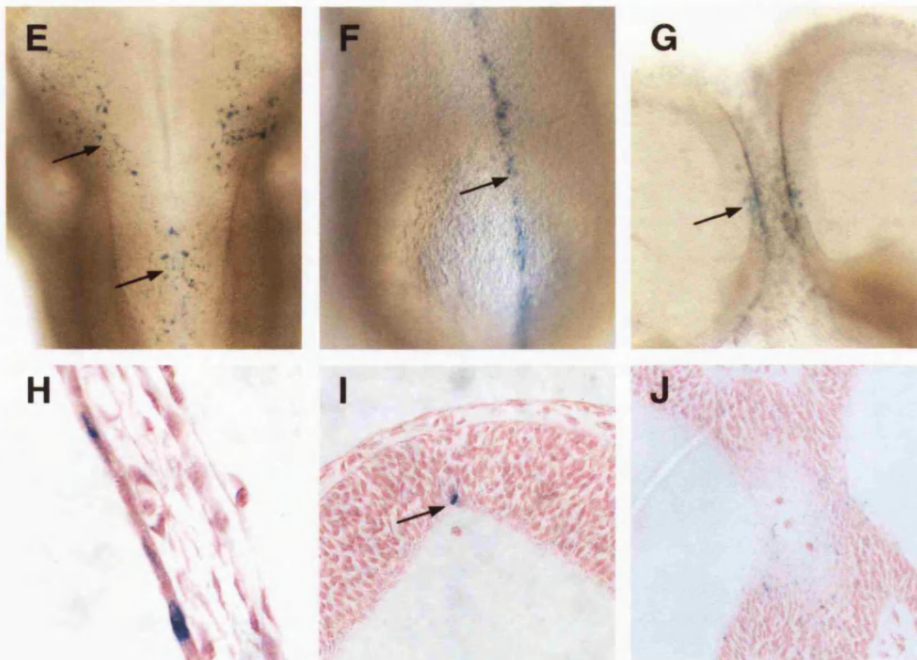
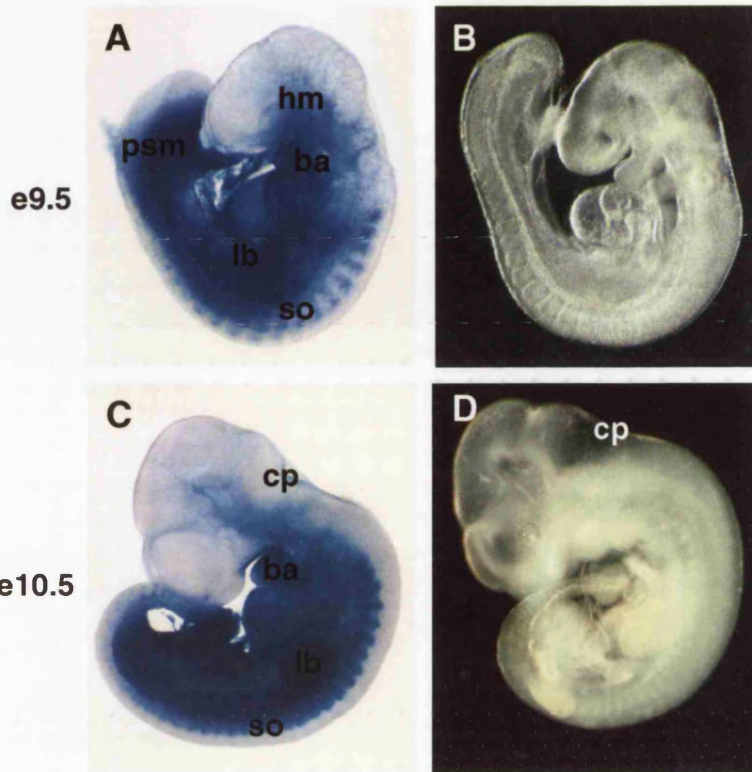
#### **Maternal transmission**

At e12.5 (**Figure 7b; Figure 9**) clear staining was seen in the evaginating choroid plexus epithelium and maintained a scattered distribution. Staining was still evident in the dorso-medial neuroepithelium of the mesencephalon but had declined from previous levels in the majority of embryos examined. Clear staining was seen for the first time in leptomeninges although in most embryos this was restricted to isolated areas underneath the ventral mid- and hind-brain regions and appeared weaker than that seen upon paternal transmission. Expression of the reporter remained absent from cerebral blood vessels and cranial neural crest derivatives (not shown).

**Figure 6. Allele-specific *lacZDMR2*<sup>-</sup> reporter gene expression assays, e9.5 and e10.5 embryos.** Embryos were fixed and stained for the presence of  $\beta$ -galactosidase activity (blue staining), then examined by light microscopy. **A,B** expression at e9.5 ( $\times 20$ ); **A** paternal transmission showed widespread expression in mesoderm and endoderm; **B** maternal transmission showed that expression was completely absent in embryos of this stage. **C,D** expression at e10.5 ( $\times 16$ ); **C** paternal transmission at e10.5 with expression generally distributed as for the previous stage; **D** expression was generally absent following maternal transmission except in those sites described below. **E,F,G** sites of expression in maternal transmission embryos at e10.5; **E** dorsal view of staining (arrows) in the roof of the metencephalon ( $\times 50$ ); **F** dorsal view of staining (arrow) along the dorsal midline of the mesencephalon ( $\times 80$ ); **G** dissected telencephalic vesicles showing staining (arrow) in the mesenchyme at their interfaces ( $\times 50$ ). **H,I,J** Detailed analysis of sites of expression described above in maternal transmission e10.5 embryos; **H** in sagittal section, sites of staining (arrows) localised in the innermost neuroepithelium layer lining the roof of the metencephalon ( $\times 400$ ); **I** in frontal section, stained cells at the dorsal midline of the mesencephalon also localised in the neuroepithelium ( $\times 100$ ); **J** in frontal section, staining (arrow) localised to mesenchyme in the medial wall separating the telencephalic vesicles ( $\times 100$ ). Detailed analysis of paternal specific *lacZDMR2*<sup>-</sup> expression is not shown. Sections were counterstained with nuclear fast red. *Abbreviations*; ba, branchial arches; cp, choroid plexus; lb, limb bud; psm, presomitic mesoderm; hm, head mesenchyme; so, somites. Magnifications are indicated.

Paternal

Maternal



### *Expression at e14.5*

#### **Paternal transmission**

At e14.5 (**Figure 7c**) reporter gene expression was similar peripherally to that of e12.5 embryos. In the brain, the reporter remained strongly expressed in the now fully differentiated choroid plexus with staining present in both the epithelium and stroma (**Figure 9**). As before, staining was restricted to a small subpopulation of epithelial cells, but was uniform in the stromal mesenchyme and pericytes of stromal capillaries. Expression had intensified in the leptomeninges with strong staining present in the pia and arachnoid mater and was also evident within interconnecting trabecular processes (not shown). Staining was also evident in small blood vessels closely associated and continuous with the pia mater. Expression in cerebral capillaries (**Figure 11**) elsewhere in the CNS although strongly evident, appeared to be declining with fewer pericytes stained in comparison with earlier stages examined. Expression continued at high levels throughout the differentiating anterior pituitary and had now appeared in the mesenchyme invading the cerebellar primordium (not shown).

#### **Maternal transmission**

At e14.5 (**Figure 7d**) reporter gene expression continued in the differentiated choroid plexus with staining in many epithelial cells. Staining remained mostly absent from the stroma, although staining in capillary pericytes was occasionally seen. As observed upon paternal transmission, expression was now present throughout the leptomeninges including regions surrounding the spinal cord. Staining had become apparent in blood vessels throughout the brain parenchyma and was particularly evident in capillaries intimately associated with the pia mater (**Figure 11**). Reporter gene expression seen in the dorso-medial mesencephalon at earlier stages had disappeared. Outside of the brain staining was seen in a cell subset of the tongue and in cartilage primordia of the clavicles, vertebrae (**Figure 7d-g**) and limbs (not shown).

### *Expression in the adult brain*

#### **Paternal transmission**

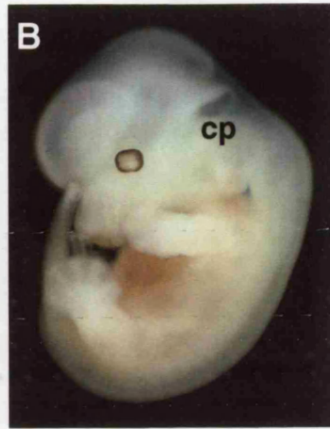
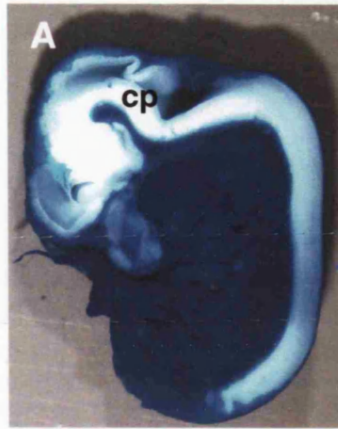
In 3 month-old whole brain analysis (**Figure 8**), staining was present in a subpopulation of choroid plexus epithelial cells, but with the exception of capillaries, was generally not seen in the stroma. Staining was evident in the pia mater (the overlying arachnoid mater was missing in most cases and was presumed to have

**Figure 7. Allele-specific *lacZDMR2*<sup>-</sup> reporter gene expression assays, e12.5 and e14.5 embryos.** Embryos were bisected, fixed and stained for the presence of  $\beta$ -galactosidase activity (blue staining), then examined by light microscopy. **A,B** expression at e12.5 ( $\times 12$ ); **A** paternal transmission showing widespread expression in mesoderm and endoderm; **B** maternal transmission with expression restricted to the developing choroid plexus. **C,D** Expression at e14.5 ( $\times 10$ ); **C** paternal transmission with expression generally distributed as for the previous stage; **D** maternal transmission with expression evident at several sites within and outside the brain. **E,F,G** Detailed analysis of sites of expression in peripheral tissues following maternal transmission embryos at e14.5, in sagittal section, **E** staining in a subset of cells in the tongue ( $\times 200$ ); **F** staining (arrows) in condensing vertebrae ( $\times 200$ ); **G** staining in epithelium (arrows) lining the aortic outflow tract of the heart ( $\times 400$ ). Detailed analysis of paternal expression is not shown. Sections were counterstained with nuclear fast red. *Abbreviations*; ao, aortic outflow tract of the heart; cl, clavicle; cp, choroid plexus; en, capillary endothelium; to, tongue. Magnifications are indicated.

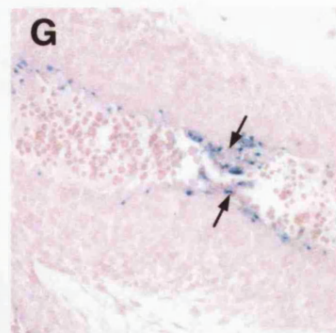
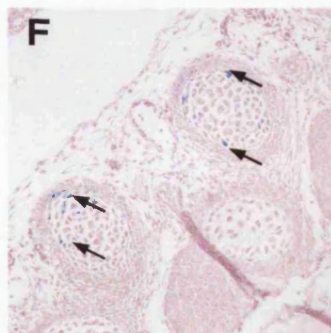
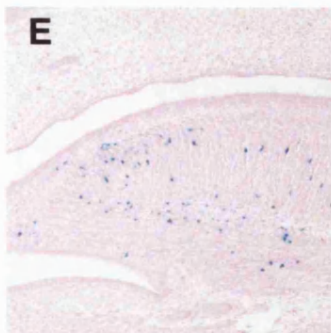
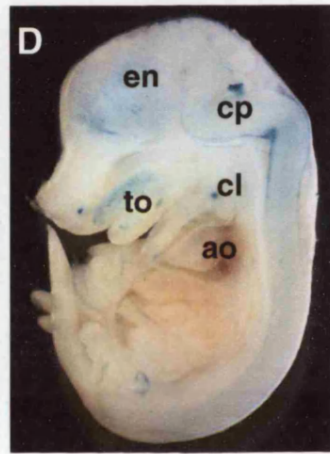
Paternal

Maternal

e12.5



e14.5



remained attached to the skull following dissection) and in capillaries associated with the pia mater and also distributed throughout the brain parenchyma (not shown). Expression was also seen at other sites, with staining evident in neurons surrounding the ventral and paraventricular regions of the hypothalamus. Neuronal staining was also seen in the giant purkinje cells of the cerebellum, but was absent from the adjacent granular cell and molecular layers (not shown, see maternal transmission).

### Maternal transmission

Reporter gene expression (**Figure 8**) was as described for paternal transmission, however staining appeared to be more intense and was noticeably more widespread in capillaries. As upon paternal transmission, some neuronal expression was present with staining seen in the giant purkinje cells of the cerebellum and in hypothalamic neurons. In contrast to paternal transmission, staining was seen in other neurons occupying the subventricular regions surrounding the lateral ventricles (not shown).

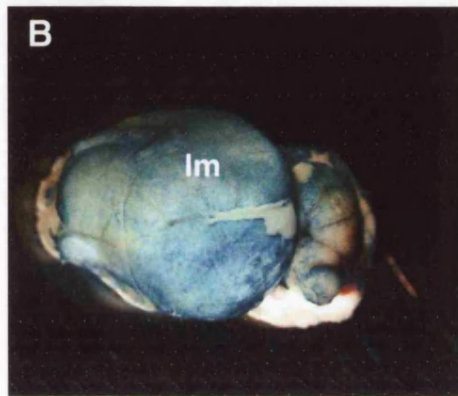
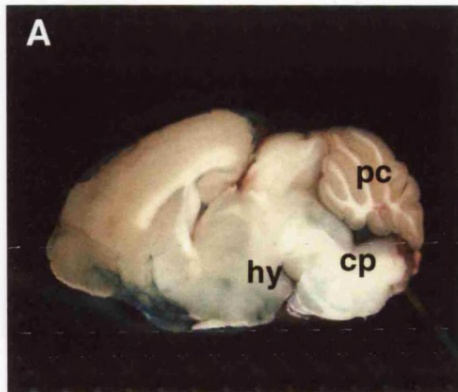
### *TTR expression in the developing choroid plexus*

Choroid plexus epithelial cells express high levels of *Transthyretin (TTR)* upon differentiation from the embryonic neuroepithelium and this gene is thus a sensitive marker for this cell type (Murakami 1987). In the *lacZDMR2<sup>-</sup>* reporter gene assays, expression was observed at e10.5, in a sheet of neuroepithelial cells lining the roof of the metencephalon, upon paternal and maternal transmission. To confirm that this reporter gene activity was associated with the presumptive choroid plexus epithelium, particularly at this early stage (e10.5) where the organ is not morphologically evident, immunohistochemistry was performed (see Chapter 2 section describing immunohistochemistry) using a primary antibody to TTR in sections of WT embryos, that contained the choroid plexus or regions destined to form the choroid plexus (**Figure 9**). At e10.5, TTR staining was seen in a domain of metencephalic neuroepithelium, apparently overlapping with the reporter gene expression described above. At e12.5 and e14.5, TTR staining was seen exclusively in the definitive choroid plexus epithelium. Notably, TTR expression was uniform in the epithelium at all stages examined, in contrast with the variegated *lacZDMR2<sup>-</sup>* reporter gene expression observed in this tissue. The region of metencephalic neuroepithelium marked by *lacZDMR2<sup>-</sup>* reporter gene expression at e10.5 was therefore populated by differentiating choroid plexus epithelial cells.

**Figure 8. Allele-specific *lacZDMR2*<sup>-</sup> reporter gene expression assays, adult brain.** Brains were bisected, fixed and stained for the presence of  $\beta$ -galactosidase activity (blue staining), then examined by light microscopy. **A-D** Staining in bisected brains ( $\times 10$ ); **A,B** paternal transmission of *lacZDMR2*<sup>-</sup> showing the internal and external views respectively  $\times 10$ . **C,D** Maternal transmission with similar views shown. **E,F** Staining in meninges of maternal transmission brains; **E** surface view showing staining (arrows) in meningeal blood vessels; **F** in sagittal section, staining (arrow) was localised in leptomeninges and capillary endothelium ( $\times 200$ ). **G** staining in the choroid plexus was confined to the epithelium, but was mostly absent from the stroma ( $\times 400$ ). **H** Staining (arrows) was also seen in the giant purkinje cells of the cerebellum but was absent from adjacent granule cell and molecular layers ( $\times 400$ ). Sections were counterstained with nuclear fast red. *Abbreviations*; cp, choroid plexus; ep, choroid plexus epithelium; s, stroma; en, capillary endothelium; lm, leptomeninges; hy, hypothalamic neurons; pc, purkinje cells; ml, molecular layer; gl, granule cell layer. Magnifications are indicated.



**Paternal**



**Maternal**

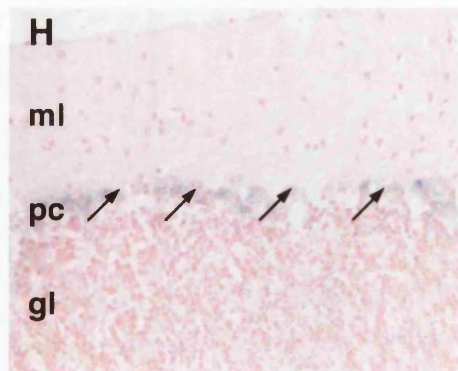
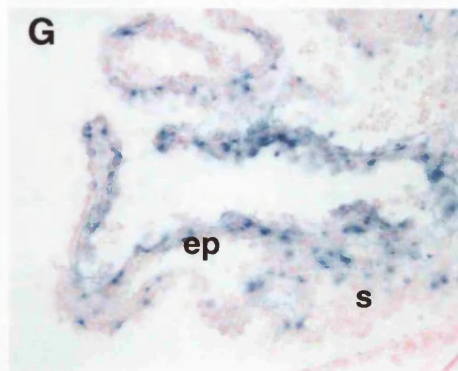
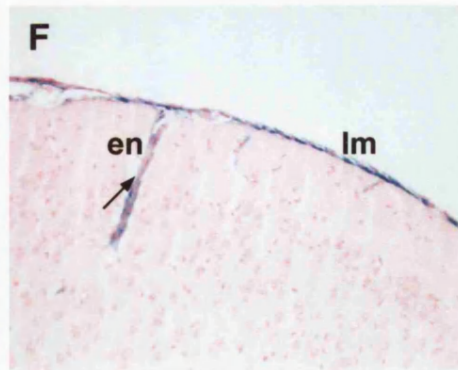
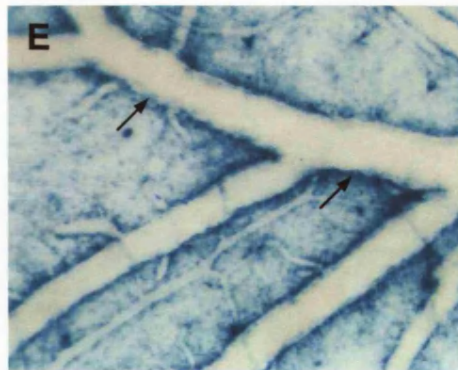
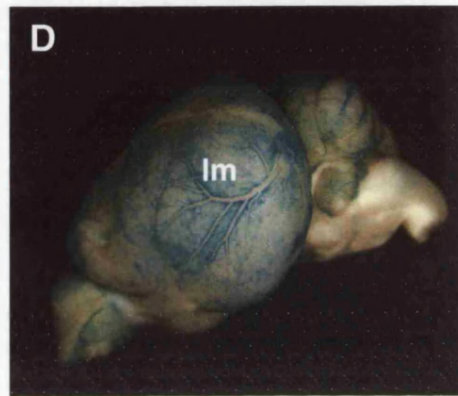
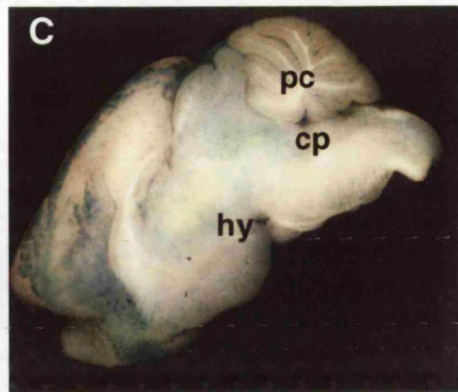


**Figure 9. Allele-specific *lacZDMR2*<sup>-</sup> reporter gene expression assays, choroid plexus development.** Embryos were fixed and stained for the presence of  $\beta$ -galactosidase activity (blue staining), sectioned in the sagittal plane and examined by light microscopy. Reporter gene expression was not detected in the presumptive choroid plexus epithelium before e10.5; **A,B** at e10.5, expression of the reporter was present, with staining in both a scattered population of ependymal cells (presumptive epithelium) following both paternal and maternal transmission but was only seen in overlying mesenchyme (presumptive stroma) following paternal transmission; **D,E,G,H** at e12.5 and e14.5, reporter gene expression was again scattered in the expanding epithelium upon both paternal and maternal transmission, but was only seen in the stroma following paternal transmission of *lacZDMR2*<sup>-</sup>. Sections were counterstained with nuclear fast red. **C,F,I** TTR protein expression in the developing choroid plexus. Sections containing the choroid plexus were prepared from WT embryos and stained for the presence of TTR and the distribution of staining visualised with brightfield microscopy. TTR positive staining (brown precipitate) was seen in the presumptive and definitive choroid plexus epithelium, but not the stroma at e10.5 (**C**); e12.5 (**F**); e14.5 (**I**). Sections were counterstained with Mayers haematoxylin. *Abbreviations:* ep, epithelium; s, stroma. All magnifications  $\times 400$ .

Paternal

Maternal

*TTR*

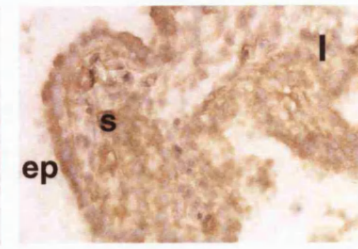
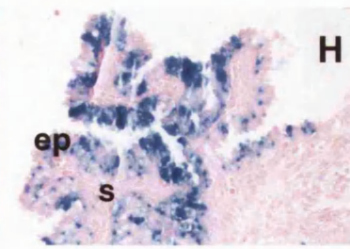
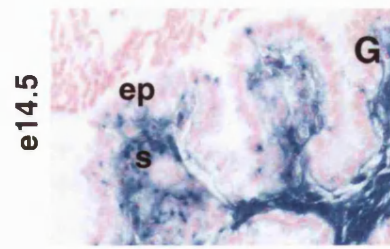
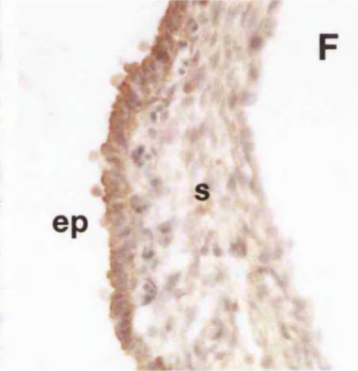
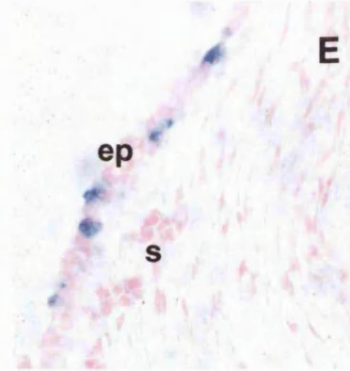
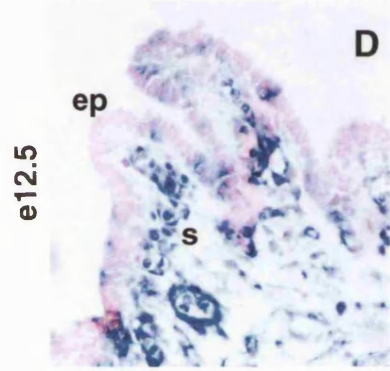
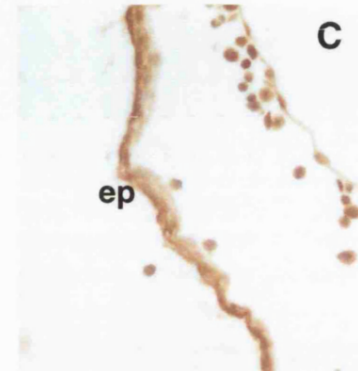
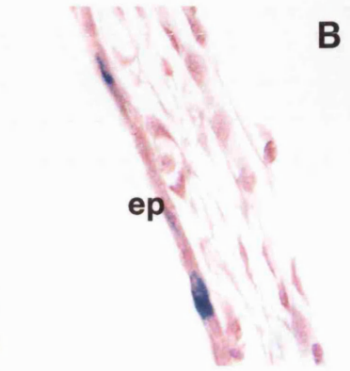
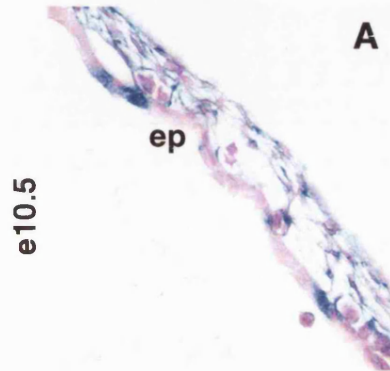


**Table 4. Summary of allele-specific *lacZDMR2*<sup>-</sup> reporter gene expression assays.** Parental transmission of *lacZDMR2*<sup>-</sup> and the developmental stages examined are given in the first and second columns respectively. Sites of expression that were found to be unique to a parental allele are shown in normal type whereas those common to both alleles (biallelic expression) are shown in either **bold type** (brain) ***bold italic type*** (peripheral tissues). *Abbreviations*; CP, choroid plexus, NC, neural crest.

<i>Transmission</i>	<i>Stage</i>	<i>Sites of lacZ expression</i>
Paternal	e9.5	Head mesenchyme, carotid arteries, primary head veins and pericytes of cerebral capillaries, migrating NC of first and second branchial arches.
	e10.5	<b>Neuroepithelium of metencephalon (CP epithelium)</b> , head mesenchyme including that overlying choroidal plaque, carotid arteries, primary head veins and pericytes of cerebral capillaries, migrating NC of 1 <sup>st</sup> and 2 <sup>nd</sup> branchial arches, trigeminal ganglion, Rathke's pouch, ventral neuroepithelium of optic recess, <b>mesenchyme overlying medial wall of telencephalic vesicles.</b>
	e12.5	<b>CP epithelium</b> and stroma (fourth and lateral ventricles) leptomeninges, carotid arteries, pericytes of blood vessels in CP stroma and brain parenchyma, Rathke's pouch, ventral neuroepithelium of optic recess, trigeminal ganglion.
	e14.5	<b>CP epithelium</b> and stroma (fourth and lateral ventricles), <b>leptomeninges</b> , pericytes of blood vessels, ventral neuroepithelium of optic recess, anterior pituitary, <b>hypothalamic neurons, aortic outflow tract of the heart, tongue, cartilage primordia of clavicles and vertebrae.</b>
	Adult brain	<b>CP epithelium (fourth and lateral ventricles), pia mater, pericytes of blood vessels, hypothalamic neurons, purkinje cells of the cerebellum.</b>
Maternal	e9.5	None detected
	e10.5	<b>Neuroepithelium of metencephalon (CP epithelium), mesenchyme overlying medial wall of telencephalic vesicles,</b> dorso-medial neuroepithelium of mesencephalon.
	e12.5	<b>CP epithelium,</b> dorso-medial neuroepithelium of mesencephalon.
	e14.5	<b>CP epithelium</b> and stroma ( <b>fourth and lateral ventricles</b> ), <b>leptomeninges</b> , pericytes of blood vessels, <b>hypothalamic neurons, aortic outflow tract of the heart, tongue, cartilage primordium of clavicles and vertebrae.</b>
	Adult brain	<b>CP epithelium (fourth and lateral ventricles), pia mater, pericytes of blood vessels, hypothalamic neurons, purkinje cells of the cerebellum, subventricular neurons.</b>

### Comparison of *lacZDMR2*<sup>-</sup> and endogenous *Igf2* expression

The detailed allele-specific *lacZ* expression data presented in the previous section revealed a number of additional sites of expression not previously reported for *Igf2* including some subtle features that may have been overlooked in other studies. In particular, this included the allele-specific choroid plexus expression analysis and the novel finding of expression in the brain capillary endothelium. Hypothetically the deletion of the DMR2 region in this mutant may have removed or otherwise perturbed *cis*-elements critical for imprinting and expression, thus leading to reporter gene expression at ectopic sites. It was therefore necessary to ask if these features of *lacZDMR2*<sup>-</sup> expression accurately reflected the expression and imprinting of the endogenous *Igf2* gene, by performing *Igf2 in situ* hybridisation.

The *lacZDMR2*<sup>-</sup> insertion removes the coding exons (4-6) and thus creates a loss-of-function mutation at the *Igf2* locus. This allele therefore cannot produce any of the natural *Igf2* transcripts that include these exons. Using an *Igf2* exon 6 probe, in embryos heterozygous for *lacZDMR2*<sup>-</sup>, any *Igf2* mRNA detected would have been produced by the reciprocal endogenous *Igf2* allele. Expression from the endogenous paternal and maternal alleles can therefore be examined separately by looking for *Igf2* mRNA in maternal and paternal transmission *lacZDMR2*<sup>-</sup> heterozygous embryos respectively. A single developmental stage, e14.5, was taken as representative for this analysis. *In situ* hybridisation was performed using a DIG-labelled antisense *Igf2* exon 6 probe (see Chapter 2 section describing slide mRNA *in situ* hybridisation), in sections made from e14.5 embryos. The comparisons were made in the choroid plexus (**Figure 10**) and in capillary endothelium (**Figure 11**). Control hybridisations with a sense probe did not produce signals.

#### *Endogenous Igf2 expression*

As expected, abundant *Igf2* mRNA was found in both the epithelial and stromal compartments of the choroid plexus (**Figure 10**) and in the leptomeninges (**Figure 11a,d**). Interestingly, expression was also evident in the pericytes of capillaries throughout the brain (**Figure 11a,d,g**). However, in contrast to the strong staining seen in the pituitary upon paternal transmission of *lacZDMR2*<sup>-</sup> at e14.5, *Igf2* mRNA was not detected at this site, with the exception of some expression in capillaries of the median eminence (not shown).

### *Paternal-specific expression (lacZDMR2<sup>+/mat</sup> heterozygotes)*

The distribution of paternal-specific *Igf2* expression resembled that of WT embryos, with expression in a small number of scattered cells in the choroid plexus epithelium and more uniform expression in the choroid plexus stroma (**Figure 10**). Expression was strong in both the pia and arachnoid mater of the leptomeninges and in pericytes of cerebral blood vessels (**Figure 11b**).

### *Maternal-specific expression (lacZDMR2<sup>+pat</sup> heterozygotes)*

Maternal-specific *Igf2* expression (paternal transmission of *lacZDMR2*<sup>-</sup>) was restricted exclusively to the choroid plexus epithelium, leptomeninges and brain capillary endothelium. In the choroid plexus epithelium, expression was highly variegated with clear positive and negative cells evident, with expression either weak or absent from the stroma (**Figure 10**). Expression was evident in capillary endothelium throughout many areas of the brain (**Figure 11c**).

### **H19 expression in the developing choroid plexus**

It was of interest to establish whether *H19* expression is similar in both its distribution and imprinting, to that of *Igf2* in the choroid plexus and capillary endothelium of the brain or whether differences exist between these genes? An *H19* knockout strain, *H19Δ3*, was obtained for this purpose and analysed by *in situ* hybridisation. This strain was created in a previous study and carries a 3kb genomic deletion that removes the *H19* structural gene (Ripoche *et al.* 1997). The *H19Δ3* allele cannot produce *H19* RNA, therefore in embryos heterozygous for the *H19Δ3* deletion, it can be presumed that any natural *H19* transcripts present must originate from the non-deleted endogenous allele. Therefore to examine total endogenous and paternal specific *H19* expression in the choroid plexus, sections of WT or *H19Δ3*<sup>+mat-</sup> heterozygous embryos respectively were hybridised with an *H19* antisense probe (see Chapter 2 section describing slide mRNA *in situ* hybridisation). Control hybridisations with a sense probe did not produce signals (not shown).

**Figure 10. Allele-specific *in situ* hybridisation analysis of *Igf2* expression, choroid plexus.** Histological sections containing the choroid plexus were prepared from WT, paternal and maternal transmission *lacZDMR2*<sup>-</sup> e14.5 embryos and hybridised with antisense and sense probes to *Igf2* and the distribution of hybridisation signals (purple staining) visualised with brightfield microscopy. **A** WT expression, staining was abundant in the epithelium and stroma; **C** paternal-specific expression (maternal transmission of *lacZDMR2*<sup>-</sup>), staining was evident in a few isolated epithelial cells and was seen throughout the stroma; **E** maternal-specific expression (maternal transmission of *lacZDMR2*<sup>-</sup>), staining was present in the epithelium, but was mostly absent from the stroma. *Igf2* expression in the choroid plexus epithelium was clearly variegated in each case. **B,D,F** maternal *lacZDMR2*<sup>-</sup>, paternal *lacZDMR2*<sup>-</sup> and WT sections hybridised with an *Igf2* sense probe. *Abbreviations*; ep, choroid plexus epithelium; s, stroma. Magnifications all ×200.



*Igf2* antisense



*Igf2* sense

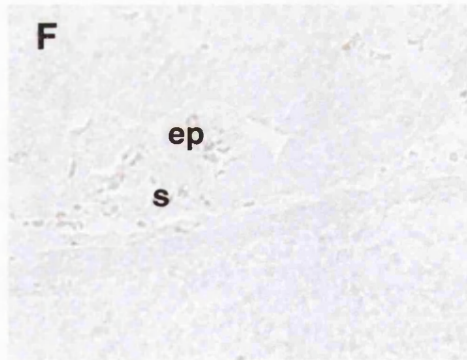
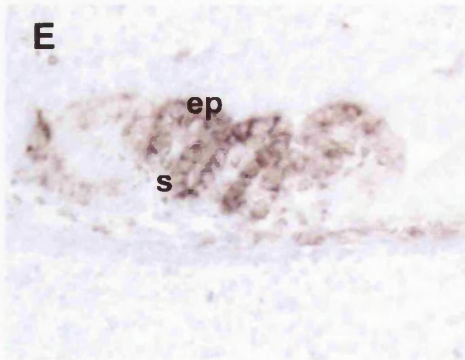
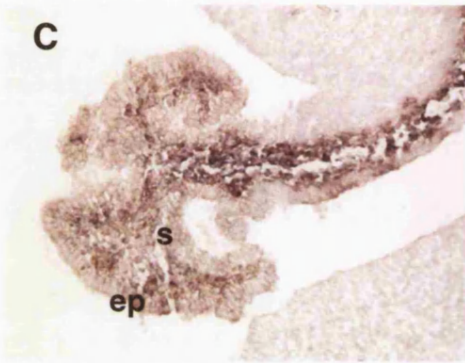
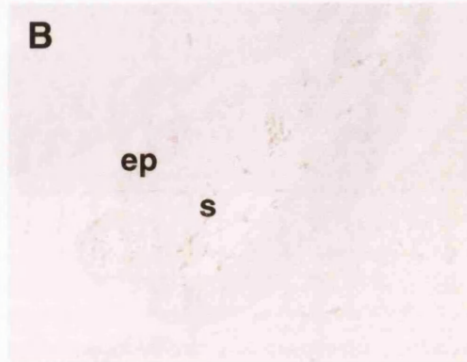
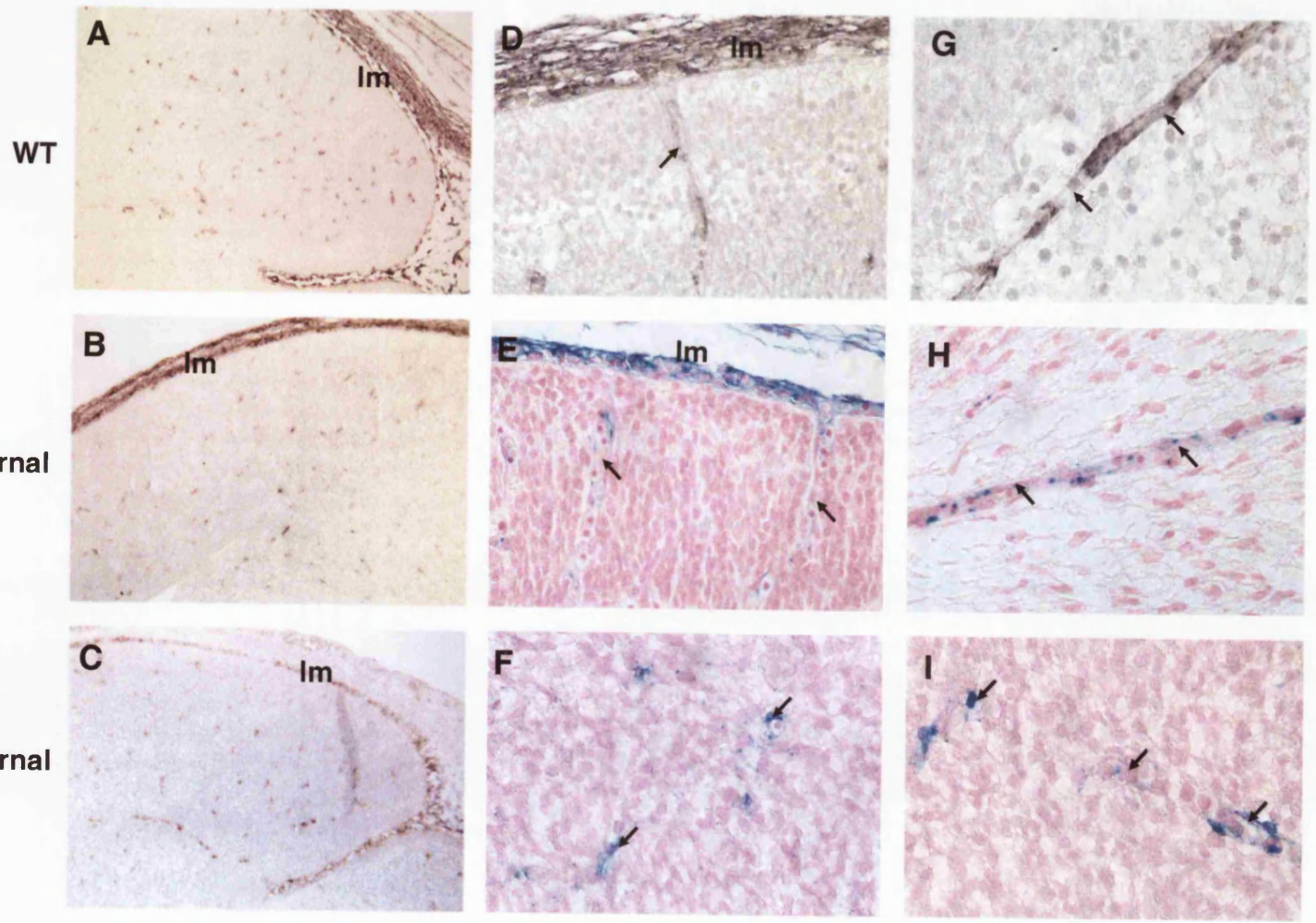


**Figure 11. Allele-specific *in situ* hybridisation analysis of *Igf2* expression and *lacZDMR2*<sup>-</sup> reporter gene expression, brain capillary endothelium. A-C, D,G** Histological sections were prepared from WT, paternal and maternal transmission *lacZDMR2*<sup>-</sup> e14.5 embryos and hybridised with antisense and sense probes to *Igf2* and the distribution of hybridisation signals (purple staining) visualised with brightfield microscopy. **A-C** Hindbrain views showing widespread *Igf2* mRNA expression in capillary endothelium **A** endogenous *Igf2* expression ; **B** paternal-specific *Igf2* expression (maternal *lacZDMR2*<sup>-</sup>); **C** maternal-specific *Igf2* expression (maternal *lacZDMR2*<sup>-</sup>). The *in situ* showed evidence of biallelic *Igf2* expression in endothelium, that is *Igf2* mRNA was present whether the embryo carried a maternal or paternal disruption of the endogenous gene; magnifications ×50. **D,G** separate views of *Igf2* mRNA expression in the endothelium of WT sections, magnifications ×400 and ×600. No signals were seen in sections hybridised with a sense control probe (not shown).

**E,F,H,I** Allele-specific *lacZDMR2*<sup>-</sup> expression. Embryos with paternal and maternal transmission of *lacZDMR2*<sup>-</sup> were fixed and stained for the presence of β-galactosidase activity (blue staining), sectioned in the sagittal plane and the staining visualised by light microscopy. Detailed views of allele specific *lacZDMR2*<sup>-</sup> expression in capillary endothelium are shown following paternal transmission (**E,H**) and maternal transmission (**F,I**) maternal transmission. This analysis provides further evidence of bi-allelic *Igf2* expression in capillary endothelium, with staining present in this tissue following transmission of *lacZDMR2*<sup>-</sup> from either parent. Sections were counterstained with nuclear fast red. Magnifications ×400 and ×600. Arrowheads indicate sites of expression in isolated capillaries. *Abbreviations*: lm, leptomeninges.



### *Endogenous H19 expression*

As expected in WT embryos *H19* expression was widespread throughout mesodermal and endodermal tissues (refer to **Figure 2**). In the brain, *H19* expression appeared to coincide with that of *Igf2* at several sites with strong staining seen in the choroid plexus stroma, but in contrast to *Igf2*, could not be detected in the choroid plexus epithelium (**Figure 12a**). Elsewhere *H19* expression was seen in the pia mater and arachnoid mater of the leptomeninges and in the ventral neuroepithelium occupying the optic recesses (not shown). *H19* expression was generally absent from brain capillary endothelium, although positive staining was occasionally seen in capillaries of the choroid plexus stroma (not shown). Although not previously reported, *H19* RNA was reproducibly detected in a subpopulation of neurons in the subventricular zones surrounding the lateral ventricles (**Figure 12c**).

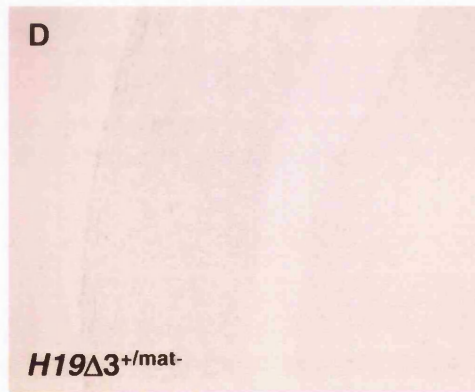
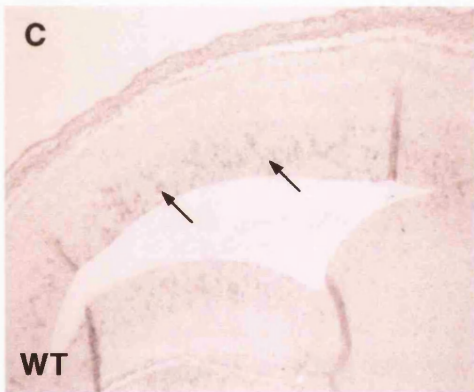
### *Paternal-specific expression ( $H19\Delta3^{+/mat-}$ heterozygotes)*

In  $H19\Delta3^{+/mat-}$  heterozygotes, paternal-specific *H19* expression was not detected in either component of the choroid plexus, in subventricular neurons or at any other site within or indeed outside of the brain (**Figure 12b,d**). A maternal *H19* deletion therefore eliminates all detectable *H19* RNA in the brain, suggesting that the gene is robustly imprinted in this tissue and developmental stage.

### *CTCF expression in the developing choroid plexus*

Expression data presented in this study provides evidence supporting biallelic *Igf2* expression and biallelic *H19* silencing in choroid plexus epithelial cells. Binding of the protein CTCF, to sites within the *H19* DMD has been shown to be a critical for the maintenance of imprinting of both genes (Bell 2000; Hark *et al.* 2000; Kanduri 2000b; Schoenherr *et al.* 2003). No attempt has previously been made to examine CTCF expression in the choroid plexus epithelium, where potentially, an absence of this factor could be consistent with deregulated *Igf2/H19* imprinting in this tissue. *In situ* hybridisation was therefore performed in embryos using an RNA probe derived from the full-length *CTCF* cDNA. Only weak signals were seen with this probe and it was not possible to determine whether expression was present or absent in the choroid plexus epithelium or at any other site (not shown).

**Figure 12. Allele-specific *in situ* hybridisation analysis of *H19* expression, choroid plexus.** Histological sections, containing the choroid plexus, prepared from WT and *H19* $\Delta$ 3<sup>+/- mat</sup> e14.5 embryos, were hybridised with an antisense probe to *H19* and the distribution of hybridisation signals (purple staining) visualised with brightfield microscopy. **A,B** *H19* expression in the choroid plexus, **A** WT, staining was seen in the stroma, but not the epithelium; **B** *H19* $\Delta$ 3<sup>+/- mat</sup>, staining was absent from both components of the choroid plexus; **C,D** *H19* expression in subventricular regions of the brain **C** WT, staining was seen in a subpopulation of neuronal cells (arrows) ; **D** *H19* $\Delta$ 3<sup>+/- mat</sup>, staining was fully absent from subventricular regions. All magnifications  $\times$ 200. *Abbreviations:* ep, epithelium; s, stroma.





## **Analysis of differentiation markers in the developing choroid plexus**

### *Immunohistochemistry analysis*

Does *Igf2* expression uniquely define a subpopulation of choroid plexus epithelial cells or are other genes similarly regulated in this tissue? Sections of WT e14.5 embryos, containing the choroid plexus, were made and stained with primary antibodies (see Chapter 2 section describing immunohistochemistry) to proteins known to be expressed in this tissue, Transferrin (TFN), Albumin (Alb), *type 1* Insulin-like growth factor receptor (*Igf1r*), fibroblast growth factor receptor 3 (shown in **Figure 13**) (Chodobski 2001) (and references therein). Positive staining with a uniform distribution was observed in the choroid plexus epithelium in all cases. Uniform TTR staining in this tissue (previously presented in **Figure 9**) is also shown for comparison. Staining for Insulin (expected to be absent from the choroid plexus epithelium) provided a negative control. Staining was not observed in sections incubated with the secondary antibody only. This analysis, including additional sites of expression not described here, is summarised in **Table 5**.

### *In situ hybridisation analysis*

An additional choroid plexus epithelial marker, *Foxj1*, was analysed by *in situ* hybridisation. *Foxj1* encodes a winged helix domain-containing transcription factor, which is required for left-right axis specification and ciliogenesis (Brody 2000). *Foxj1* is expressed in the developing choroid plexus epithelium from e10.5 of mouse development and continues to mark this tissue thereafter (Lim 1997). *In vitro* work implicates *Foxj1* as a regulator of *Igf2* expression in the choroid plexus epithelium (Lim 1997). Moreover, *Foxj1* expression is highly variegated in the bronchial epithelium of the developing lung (Brody 2000). *Foxj1* was therefore considered a good candidate for showing variegated expression in the choroid plexus epithelium. Antisense and sense DIG-labelled RNA probes were obtained for *Foxj1* and hybridised with WT e14.5 embryo sections (see Chapter 2 section describing slide mRNA *in situ* hybridisation). *Foxj1* expression (**Figure 14**) was evident in the choroid plexus epithelium and was uniformly distributed. Expression was also seen in the nasal epithelium and clear evidence of variegated expression was apparent in the bronchial epithelium, both sites consistent with previous work (Brody 2000). Control hybridisations with a sense probe did not produce signals. This analysis is summarised in **Table 5**.

**Figure 13. Immunohistochemistry analysis of differentiation markers in the choroid plexus epithelium.** Histological sections containing the choroid plexus were prepared and stained for the presence of various differentiation markers and the distribution of staining (brown precipitate) in the choroid plexus epithelium visualised with brightfield microscopy. **A** Transthyretin (TTR), positive staining was seen in a uniform distribution ; **B** Transferrin (TFN), staining as seen for TTR; **C** Albumin, staining as seen for TTR; **D** Fgfr3, staining as seen for TTR; **E** Igf1r, staining as seen for TTR; **F,G** negative controls; **F** section (containing the choroid plexus) incubated with a biotin labelled  $\alpha$ -rabbit IgG secondary antibody; **G** Insulin, no staining was observed in the choroid plexus epithelium; **H** Insulin, positive staining was observed in differentiating pancreatic  $\beta$ -cells. Sections were counterstained with Mayers haematoxylin (blue). All magnifications are  $\times 200$ ; *Abbreviations*: ep, epithelium; s, stroma.



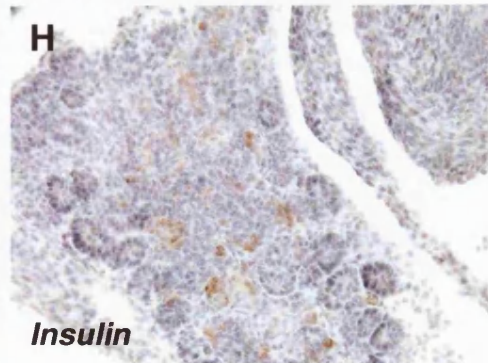
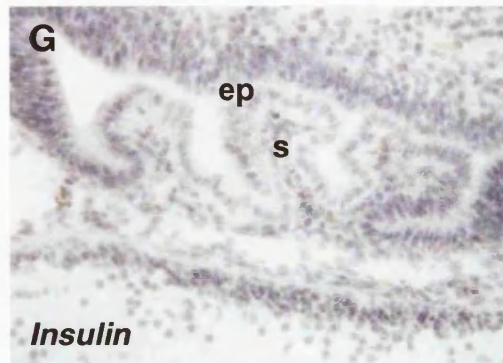
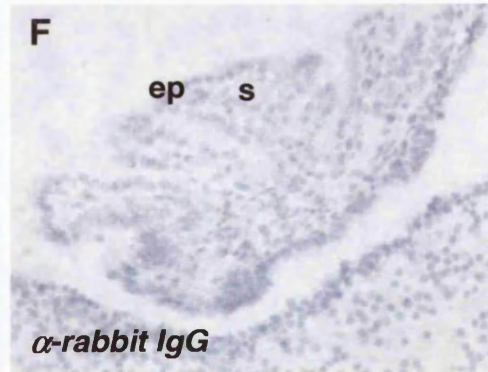
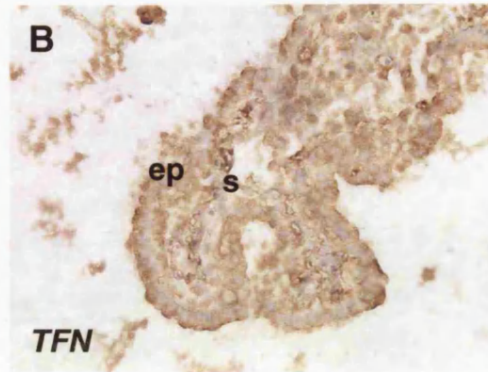
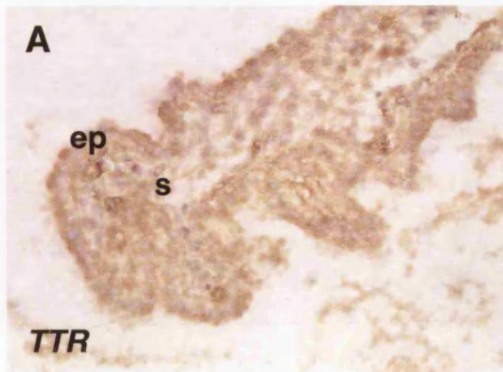
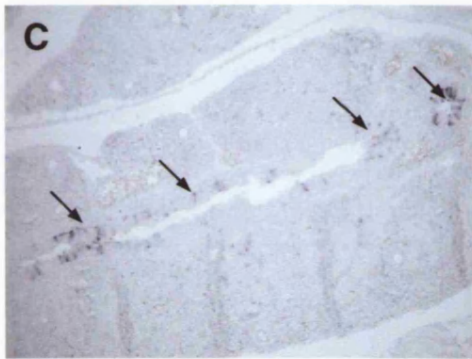


**Figure 14. *In situ* hybridisation analysis of *FoxJ1* expression in the choroid plexus epithelium.** Histological sections containing the choroid plexus at e14.5 were prepared and hybridised with antisense and sense probes to *Foxj1* and the distribution of hybridisation signals (purple staining) visualised with brightfield microscopy. *The in situ* hybridisation revealed a highly discrete expression pattern consistent with that reported for *FoxJ1*. **A** expression in the choroid plexus epithelium, staining was seen in a uniform distribution; **C** expression in the lung, staining was seen in a subpopulation of bronchial epithelial cells, but not the squamous lung epithelium; **E** expression in the nasal epithelium, strong uniform staining was seen. **B,D,F** Control sections hybridised with a sense probe. All magnifications are ×200.

***Foxj1* antisense**

***Foxj1* sense**



<i>Gene/Marker</i>	<i>Method</i>	<i>Expression in CP epithelium</i>	<i>Expression at other sites</i>
<i>TTR</i>	IHC	Uniform	Leptomeninges (pia and arachnoid mater including interconnecting trabecular processes), parenchyma of the brain and spinal cord. Liver, gut epithelium, primordia of vertebrae, squamous epithelium of the lung.
<i>TFN</i>	IHC	Uniform	Essentially as described for <i>TTR</i> .
<i>Alb</i>	IHC	Uniform	Essentially as described for <i>TTR</i> .
<i>Foxj1</i>	ISH	Uniform	Epithelium of nasal passages and ear canal, columnar epithelium of the lung.
<i>Igf1r</i>	IHC	Uniform	Leptomeninges (pia and arachnoid mater) and neurons present in marginal regions of cerebral hemispheres and midbrain. Weaker staining upon neurons in the vicinity of the hypothalamus, in the pons, cerebellar primordium and medulla oblongata.
<i>Fgfr3</i>	IHC	Uniform	Leptomeninges (Pia and arachnoid mater) neurons in marginal regions of cerebral hemispheres. Fairly ubiquitous in peripheral tissues.
<i>Ins</i>	IHC	No expression	Differentiating $\beta$ -cells in pancreatic islets.

**Table 5. Summary of differentiation marker expression analysis.** The markers analysed, the method employed and distribution of expression in the choroid plexus epithelium, is indicated. Other sites of expression are also described. *Abbreviations:* IHC, immunohistochemistry; ISH, *in situ* hybridisation.

## **A potential involvement of Notch signalling in regulating variegated *Igf2* expression**

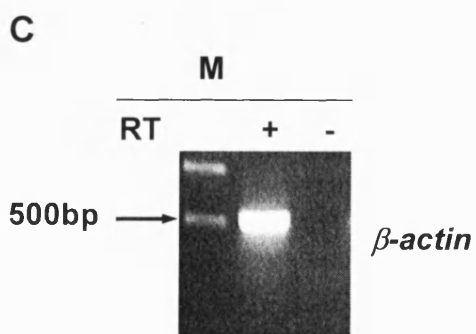
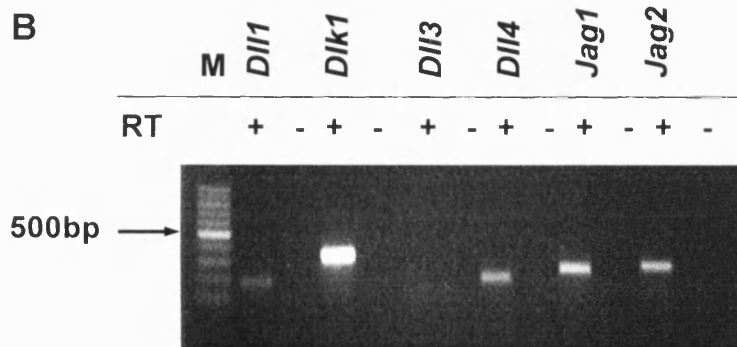
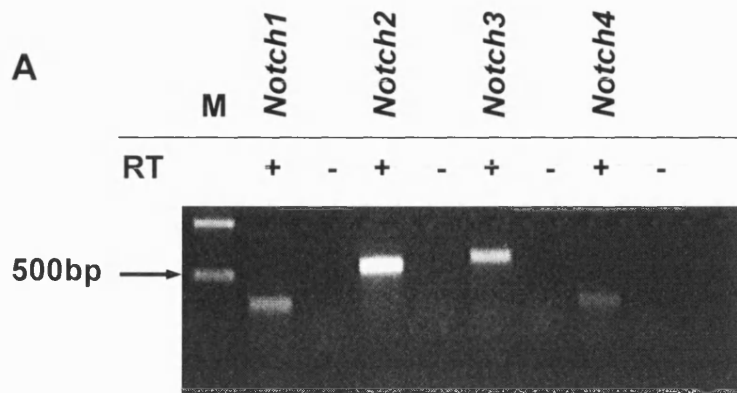
### *RT-PCR analysis*

As discussed in the Introduction to this chapter, the existence of *Igf2* positive and negative subpopulations in the choroid plexus epithelium suggested the possible involvement of Notch signalling. RT-PCR analysis was carried out to ask whether expression of *Notch* genes, and their ligands encoded by the *Delta* and *Jagged* genes, are generally represented in whole choroid plexus mRNA. Total RNA was prepared from choroid plexi (see Chapter 2 section describing preparation of total RNA) dissected from neonatal F<sub>1</sub> mice, complementary DNA (cDNA) was prepared and PCR-amplified (see Chapter 2 section describing RT-PCR) using primers specific to known murine *Notch*, *Delta* and *Jagged* genes (see **Table 3** and **Figure 15**). In the *Notch* assay, expression of *Notch2* and *Notch3* was detected, with basal levels seen for *Notch1* and *Notch4*. In the *Delta/Jagged* experiment, *Dlk1*, *Dll4*, *Jagged1* and *Jagged2* were clearly expressed, with basal levels seen for *Dll1*. *Dll3* expression was not detected, though PCR-analysis of genomic DNA confirmed that this observation was due to absence of *Dll3* expression rather than failure of the PCR (not shown). This analysis therefore demonstrated the expression of all known *Notch*, *Delta* and *Jagged* genes, except *Dll3*, in the neonate choroid plexus.

### *In situ hybridisation analysis*

The lateral inhibition model (Lewis 1998), predicts that distinct cell fates will arise within a field of identical cells as a consequence of Notch receptor activity, with receptor activation mediated by interaction with Delta ligands present on a subset of these cells. Therefore, if Notch signalling is required to specify different *Igf2* phenotypes within the choroid plexus epithelium, uniform Notch expression and variegated *Delta/Jagged* expression might be predicted in this tissue. RT-PCR analysis (above) demonstrated the expression of many *Notch*, *Delta* and *Jagged* genes in whole choroid plexus tissue. *In situ* hybridisation was performed next, to ask if the expression of these genes is localised to the choroid plexus epithelium, and if so, is the distribution of expression consistent with a mechanism of active lateral inhibition, that potentially regulates *Igf2* expression?

**Figure 15. RT-PCR analysis of *Notch*, *Delta* and *Jagged* gene expression in the choroid plexus.** Complementary DNA (cDNA) was prepared from neonate choroid plexus tissue and analysed by PCR using primers specific to the *Notch*, *Delta* and *Jagged* genes (see **Table 3**). **A** *Notch* gene expression; **B** *Delta* and *Jagged* gene expression; **C**  $\beta$ -*actin* expression (lower panel) shows the successful conversion of RNA to cDNA. Samples treated with and without reverse transcriptase are indicated as + and – RT. The molecular weight marker (M) is a 100bp DNA ladder where the lower of the two bright bands represents 500bp.





Probes for the *in situ* hybridisation, corresponding to mouse *Notch*, *Delta* and *Jagged* genes, were generated from IMAGE consortium cDNA clones obtained from the HGMP, UK. The *Notch1* probe was a 1kb cDNA clone. The *Notch2* probe was a 1.8kb cDNA clone. The *Notch3* probe was a 4kb cDNA clone. The *Notch4* probe was a 1.3kb cDNA clone. The *Dlk1* probe was a 1.5kb cDNA clone. The *Dll1* probe was a 1kb cDNA clone. The *Dll3* probe was a 2kb cDNA clone. *Dll4* was a 700bp cDNA clone. The *Jagged1* probe was a 3kb cDNA clone. The *Jagged2* probe was a 1kb cDNA clone. The clones were sequenced in both directions to confirm the identity of the cDNA inserts and determine their orientation in relation to the flanking phage promoter sites. Several clones were found to contain large tracts of polyadenylation in the intervening sequence between the phage promoter sites and the 3' end of the cDNA inserts. An antisense probe generated by transcribing across these regions could potentially generate non-specific signals during an *in situ* hybridisation, thus complicating interpretation of the results. The affected clones (those carrying *Notch2*, *Notch4*, *Dlk1* and *Dll3* sequences) were modified to remove polyadenylation sequences, as described below.

The *Notch2* cDNA was purified away from its parent vector on a 1.8kb *SalI*-*NsiI* fragment and ligated into the *SalI* and *PstI* (*NsiI* compatible) sites of Bluescript to create the pBS-*Notch2* plasmid.

The *Notch4* cDNA was purified away from its parent vector on a 0.7kb *EcoRI*-*FspI* fragment and ligated into the *EcoRI* and *SmaI* (*FspI* compatible) sites of Bluescript to create the pBS-*Notch4* plasmid.

The *Dlk1* cDNA was purified away from its parent vector on a 1.3kb *EcoRI*-*NsiI* fragment and ligated into the *EcoRI* and *PstI* sites of Bluescript to create the pBS-*Dlk1* plasmid.

The *Dll3* cDNA was purified away from its parent vector on a 2kb *EcoRI*-*PsiI* fragment and ligated into the *EcoRI* and *EcoRV* (*PsiI* compatible) sites of Bluescript to create the pBS-*Dll3* plasmid. The identity and orientation of the modified insert DNA was verified by sequencing in each case.



The cDNA clones were linearised by digestion with restriction enzymes and the linearised fragments used in transcription reactions to synthesise DIG-labelled antisense and sense RNA probes. The restriction enzymes and polymerases used to make each probe are listed in **Table 1**. *In situ* hybridisation expression data was generated for the *Notch*, *Delta* and *Jagged* genes in whole mount embryos at e10.5 (not shown) and in sections of e14.5 embryos (**Figure 16**). The analysis at both stages is summarised in **Table 6**.

#### *Notch* expression at e10.5

*Notch3* and *Notch4* probes did not produce clear signals. *Notch1* expression (not shown) was distributed as typically described previously (Higuchi 1995) with moderate staining generally seen in the somites, though very strong staining was seen in the mesoderm of the posteriormost somite pair in the tail. *Notch1* expression was also evident in first and second branchial arches, the telencephalic vesicles and the mesencephalon. No evidence of staining was seen in the presumptive choroid plexus epithelium. *Notch2* expression (not shown) was similar to that of *Notch1*, with particular reference to the somitic expression and was also absent from regions that give rise to the choroid plexus epithelium (Higuchi 1995; Hamada *et al.* 1999).

#### *Delta* and *Jagged* expression at e10.5

*Dll3*, *Dll4* and both *Jagged* probes did not produce clear signals. *Dll1* expression (not shown) was highly discrete with intense staining confined to the ventricular regions of the brain and the penultimate and posteriormost somite pairs in the tail, consistent with previous observations for this gene (Bettenhausen *et al.* 1995; Beckers 1999) and the localisation of *Notch* gene expression described above. In contrast, *Dlk1* expression (not shown) was widespread with strong staining seen in the somites, in subdomains of the limb buds, branchial arches, liver bud and ventricular regions of the brain. Neither *Dll1*, nor *Dlk1* appeared to be expressed in the presumptive choroid plexus epithelium.

#### *Notch* expression at e14.5

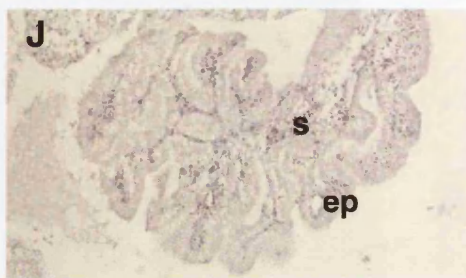
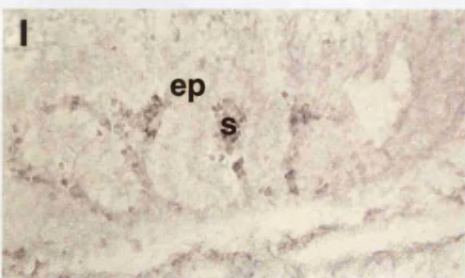
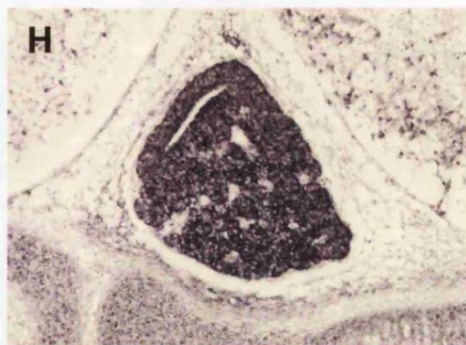
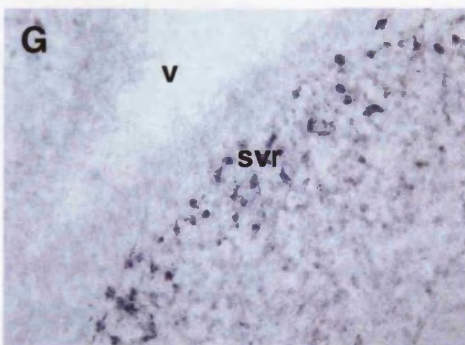
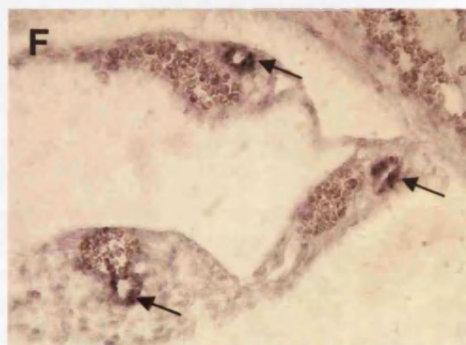
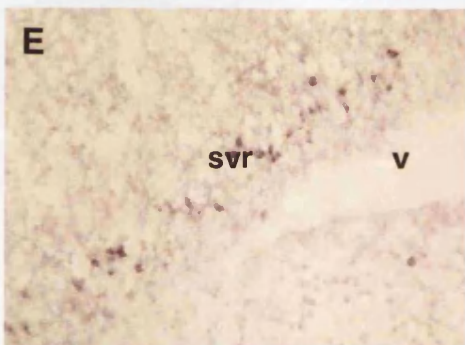
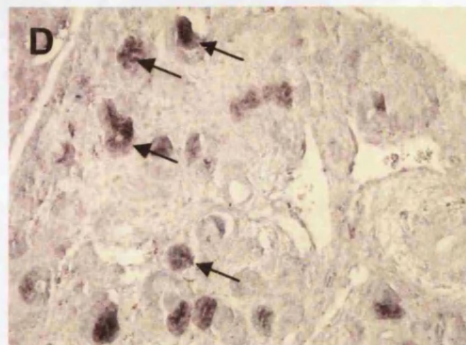
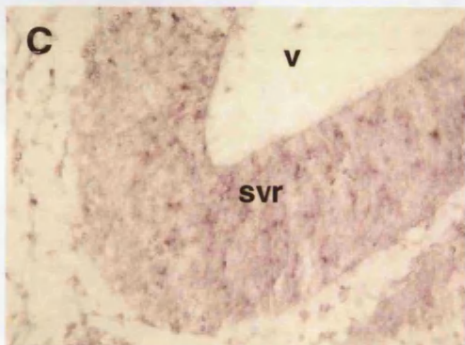
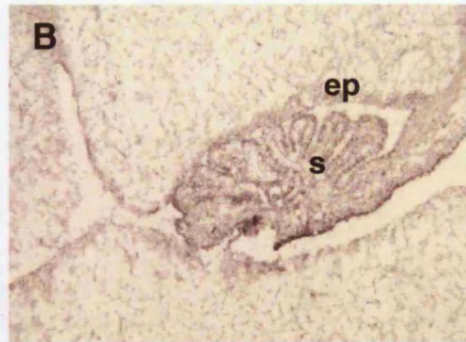
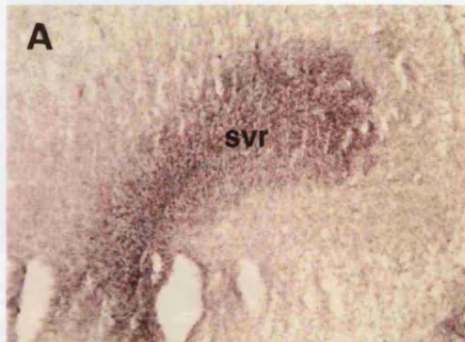
*Notch1*, *Notch3* and *Notch4* probes did not produce clear signals despite repeated attempts to optimise the hybridisation conditions. *Notch2* was clearly expressed in the choroid plexus epithelium (**Figure 16**) with uniform staining seen throughout this

tissue, but was absent from the stroma. *Notch2* expression was also detected in neurons occupying the subventricular zones surrounding the lateral ventricles and the mesencephalon, consistent with earlier work (Higuchi 1995; Hamada *et al.* 1999).

#### *Delta* and *Jagged* expression at e14.5

*Dll3* and *Dll4* probes did not produce clear signals. *Dll1* expression (**Figure 16**) was not seen in the choroid plexus, contrary to that described in earlier studies (Beckers 1999). Staining of moderate intensity was observed in a subset of neuronal cells that occupied the ependymal and subventricular layers of the brain and in the columnar epithelium of the comma- and s-shaped bodies of the developing kidney, as seen previously (Bettenhausen *et al.* 1995; Beckers 1999; McCright *et al.* 2001). *Dlk1* expression (**Figure 16**) was not seen in the choroid plexus epithelium, though some staining was evident in the stromal mesenchyme, possibly corresponding to the abundant expression of this gene shown by earlier RT-PCR analysis of whole choroid plexus tissue. *Dlk1* was widely expressed in peripheral tissues, with strong signals evident in the liver, the pancreatic islets, skeletal muscle including that of the tongue, squamous epithelium of the lung and the pericardium of the heart, but not cardiac muscle (not shown). High levels of expression were seen in glandular cells of the anterior pituitary and in a subpopulation of neuronal cells surrounding the hypothalamus and the subventricular regions of the lateral ventricles. Expression was also evident in what appeared to be smooth muscle cells surrounding cerebral blood vessels, though the vessel endothelium itself was not stained (not shown). *Jagged1* expression (**Figure 16**) was not observed in the choroid plexus epithelium or stroma, and was otherwise restricted to blood vessels throughout peripheral tissues, consistent with previous observations (Loomes 1999; Irvin 2004). Expression was evident in a subpopulation of neuronal cells that occupied subventricular regions surrounding the lateral ventricles, but was not detected in the brain capillary endothelium. *Jagged2* expression was absent from the choroid plexus epithelium and stroma, with expression at other sites as described for *Jagged1* (not shown).

**Figure 16. *In situ* hybridisation analysis of *Notch*, *Delta* and *Jagged* gene expression in the choroid plexus.** Histological sections containing the choroid plexus at e14.5 were prepared and hybridised with antisense and sense probes (refer to **Table 1**) and the distribution of hybridisation signals (purple staining) visualised with brightfield microscopy. **A,B** *Notch2* expression; **A** in brain subventricular regions, staining was seen in neurons surrounding the lateral ventricle; **B** in the choroid plexus epithelium, staining was seen in a uniform distribution, but was absent from the stroma. **C,D,J** *Dll1* expression; **C** in brain subventricular regions, staining was seen in a subset of neurons surrounding the lateral ventricles ( $\times 400$ ); **D** in the kidney, staining (arrows) was seen in condensing epithelium of comma- and s-shaped bodies; **J** staining was absent from the choroid plexus. **E,F** *Jagged1* expression, **E** in brain subventricular regions, staining was similar to that described for *Dll1* ( $\times 400$ ); **F** in peripheral blood vessels, those associated with mesenchyme of the developing hind gut are shown (arrows). Staining was absent from the choroid plexus (not shown). **G,H,I** *Dkl1* expression, **G** in brain subventricular regions, staining was similar to that described for *Dll1* ( $\times 400$ ); **H** glandular cells of the anterior pituitary; **I** staining was absent from the choroid plexus epithelium, but weak staining was seen in the stroma. No signals were seen in sections hybridised with sense control probes (not shown). Unless otherwise stated magnifications are  $\times 200$ . *Abbreviations* svr, subventricular region; v, ventricle; ep, choroid plexus epithelium; s, stroma.



<i>Gene</i>	<i>Stage</i>	<i>Sites of expression</i>
<b><i>Notch1</i></b>	e10.5	Neuroepithelium of telencephalon and mesencephalon, mesoderm of penultimate somite pair (not shown)
	e14.5	Not detected
<b><i>Notch2</i></b>	e10.5	Neuroepithelium of telencephalon and mesencephalon, mesoderm of penultimate somite pair (not shown)
	e14.5	<b>Choroid plexus epithelium</b> , subventricular regions surrounding lateral ventricles ( <b>Figure 16</b> )
<b><i>Notch3</i></b>	e10.5	Not detected
	e14.5	Not detected
<b><i>Notch4</i></b>	e10.5	Not detected
	e14.5	Not detected
<b><i>Dlk1</i></b>	e10.5	Widespread in embryonic mesoderm and endoderm, limb buds, somites, liver bud, branchial arches, nasal recesses, neuroepithelium of telencephalon and mesencephalon (not shown)
	e14.5	Subventricular regions of the brain, anterior pituitary ( <b>Figure16</b> ) hypothalamus, tongue, liver, smooth muscle surrounding the gut and blood vessels, lung epithelium, pancreatic islets, pericardium of the heart (not shown)
<b><i>Dll1</i></b>	e10.5	Neuroepithelium of telencephalon and mesencephalon, mesoderm of penultimate and posteriormost somite pairs (not shown)
	e14.5	Subventricular regions surrounding lateral and fourth ventricles of the brain, condensing epithelium of the kidney ( <b>Figure 16</b> )
<b><i>Dll3</i></b>	e10.5	Not detected
	e14.5	Not detected
<b><i>Dll4</i></b>	e10.5	Not detected
	e14.5	Not detected
<b><i>Jagged1</i></b>	e10.5	Not detected
	e14.5	Endothelium of peripheral blood vessels, subventricular regions surrounding lateral ventricles of the brain ( <b>Figure 16</b> )
<b><i>Jagged2</i></b>	e10.5	Not detected
	e14.5	Endothelium of peripheral blood vessels (not shown)

**Table 6. Summary of *Notch*, *Delta* and *Jagged in situ* hybridisation analysis.**

## Conclusions

A principal aim of this chapter was to examine spatio-temporal features of biallelic *Igf2* expression in the developing brain with emphasis upon the choroid plexus. This was addressed by examining the developmental expression profile for *Igf2* in the brain at several embryonic stages using an *Igf2* (*lacZDMR2<sup>-</sup>*) reporter gene insertional mutant and *Igf2* *in situ* hybridisation.

The *lacZDMR2<sup>-</sup>* reporter gene assays revealed the first evidence of biallelic *Igf2* expression at e10.5, in a subset of neuroepithelial cells that occupied areas destined to form the choroid plexus at later stages. The identity of these cells as precursors for choroid plexus epithelium was confirmed by their expression of the diagnostic marker, TTR (Murakami 1987) in equivalent regions of WT embryos. Unsurprisingly, biallelic expression was also demonstrated at later stages in the differentiated choroid plexus epithelium, consistent with previous work (DeChiara *et al.* 1991). However, in the choroid plexus stroma, reporter gene expression was only seen after paternal transmission in all stages examined, thus providing evidence that *Igf2* is imprinted at this site and not biallelically expressed as previously thought (DeChiara *et al.* 1991; Svensson 1995). It is concluded that the expression of *Igf2* in the presumptive choroid plexus epithelium is initiated between e9.5 and e10.5 of development and that this expression occurs from both alleles from its onset. Prior to this only paternal-specific expression could be detected at any site in the embryo, with both alleles silent in the neuroepithelium.

Although not formally described in mice to date, evidence from the *lacZDMR2<sup>-</sup>* reporter assays indicated that *Igf2* expression occurs in the capillary endothelium of the embryonic brain. This manifested paternal-specific reporter expression at early stages, with expression from both parental alleles evident by e14.5. That is, *Igf2* expression in the capillary endothelium is initially imprinted and becomes biallelic later in gestation. This expression continued from both alleles in the brain of adult mice. Evidence in support of this data comes from studies in the adult rat brain. First, *Igf2* expression was identified in the capillary endothelium associated with the choroid plexus stroma and (Stylianopoulou *et al.* 1988b) and more widely in the brain parenchyma (Logan 1994). More recently, a microarray screen identified an enrichment of *Igf2* expression in isolated capillary endothelium tissue against a

comparison with whole brain tissue. Subsequent experiments in the same study revealed high levels of *Igf2* expression in capillary endothelium *in situ* (Li 2001a). Given the widespread extent of the capillary endothelium (which forms an integral component of the blood brain barrier) it seems likely that, in addition to the choroid plexus and leptomeninges, this is likely to represent a third major source of biologically available IGFII peptide in the CNS. Although a definitive function has yet to be ascribed to *Igf2* in these tissues, it is perhaps noteworthy that the major sites of its brain expression occur in those tissues with exchange or barrier function.

The sites of expression marked by the *lacZDMR2<sup>-</sup>* allele were largely consistent with the *Igf2* mRNA *in situ* data. One exception was found in the anterior lobe of the pituitary at e14.5, where abundant reporter gene expression was seen. Although expression of the reporter in Rathkes pouch, the precursor of the anterior pituitary, correlates well with *Igf2* mRNA expression at earlier stages, *Igf2* mRNA was generally not found in the pituitary at e14.5. The e14.5 anterior pituitary is therefore considered an ectopic site for *lacZDMR2<sup>-</sup>* expression, suggesting that the removal of DMR2 in this mutant may have revealed a cryptic silencer element not identified in the original analysis of this mutant (Murrell *et al.* 2001). Elsewhere in the brain, maternal-specific *lacZDMR2<sup>-</sup>* expression was seen in the neuroepithelium lining the dorsal midline of the mesencephalon. That is, evidence was found for imprinted expression of *Igf2* that is derived from the opposite allele to that seen at most other sites. Whether or not this reflects a genuine feature of *Igf2* expression and imprinting awaits allele-specific whole mount *Igf2 in situ* analysis. Until this data is available, a causal effect of the DMR2 deletion in this expression cannot be excluded. In summary, data from the present study indicates that *Igf2* expression is much more widespread in the developing and mature brain than previously thought. However, this expression is not uniformly distributed as has been implied by some studies (Yang 2003), but rather as illustrated by the data for capillary endothelium, it is concentrated in discrete tissues amongst a much greater volume of neuronal tissue, which generally lacks expression.

*H19* and *Igf2* exhibit overlapping spatio-temporal expression in imprinted peripheral tissues, thus it was of interest to ask whether the co-ordinate expression and imprinting of *Igf2/H19* is preserved in the brain. In mice, whilst it has been shown that

*H19* maintains imprinted expression in the embryonic choroid plexus the cell-type distribution of *H19* RNA in its epithelial and stromal compartments has not been clearly resolved (Svensson 1995). In this study *H19* expression, analysed at e14.5, was detected in the choroid plexus stroma and leptomeninges of WT embryos, but not in embryos carrying a maternal deletion of the *H19* gene. *H19* is therefore imprinted at these sites. *H19* expression was not detected in the choroid plexus epithelium or in the capillary endothelium, sites where biallelic expression of *Igf2* was found. Conversely, *H19* expression was found in subventricular neurons, a site not marked by *Igf2* expression at this stage. This expression was shown to be imprinted as evidenced by its absence in the maternal deletion tissue and may correspond to neuronal expression seen previously (Svensson 1995). Consistent with previous work where paternal-specific expression of *H19* could not be found at any site in embryos staged between e8-17, evidence arguing for biallelic expression of *H19* was not found in any tissue in the present study (Svensson 1998). It is therefore concluded that *H19* expression is stringently imprinted and does not fully coincide with *Igf2* expression (subventricular neurons) in the developing brain, at least at the stage examined.

Therefore, in the choroid plexus epithelium (and brain capillary endothelium) *Igf2* is biallelically expressed and *H19* silenced upon both alleles. In contrast, data for the stroma argues that both genes remain imprinted at this site. These findings apparently contradict the claim of another study, which argued that in the choroid plexus, the co-expression of *Igf2* and *H19* occurs from the same chromosome (Svensson 1995). It should be noted that this conclusion was drawn from a similar observation that imprinted *H19* expression occurs in stromal cells, but was also based upon the incorrect assumption that *Igf2* is biallelically expressed in the same stromal cells. Therefore in both compartments of the choroid plexus, the expression of both genes is mutually exclusive *in cis*, as is the case in peripheral tissues.

Silencing of *H19* and biallelic expression of *Igf2* is particularly striking and suggests that the maternal chromosome has assumed paternal characteristics in the choroid plexus epithelium. Imprinting of both genes in many tissues is dependent upon differential methylation at the DMD (Thorvaldsen *et al.* 1998; Kaffer 2000; Srivastava 2000; Holmgren 2001). Could atypical *Igf2/H19* imprinting in the choroid plexus epithelium be mediated by epigenetic changes within the DMD itself and/or



the hierarchy of DMRs that fall under its control? (Lopes *et al.* 2003; Srivastava 2003). The developmental timing of these proposed events is unknown, although the onset of biallelic *Igf2* expression in choroid plexus epithelial precursors at e10.5, as indicated by *lacZ*<sup>DMR2</sup> reporter gene expression, suggests that such modifications must be initiated prior to, or concomitant with, this stage.

Evidence that methylation is required for maintenance of imprinting is unequivocal, as shown by *trans*-manipulation studies in mice. In embryos experimentally deficient in the maintenance methyltransferase protein, *Dnmt1*, *Igf2* was biallelically silenced and *H19* biallelically expressed (Li 1993). Therefore, in the absence of genome methylation the mono-allelic expression of both genes was disrupted, and it is interesting to note, in the opposite direction to that observed in the choroid plexus epithelium. Implicit in this last point, is the question of whether the reciprocal situation, that is hypermethylation of both alleles of *Igf2* and *H19* can provide a mechanistic basis for deregulation of imprinting in a manner consistent with that observed in the choroid plexus epithelium?

Two lines of evidence suggest that this may be the case. Overexpression of *Dnmt1* in differentiated ES-cell lines was demonstrated sufficient to bring about biallelic expression of *Igf2* and a decrease in expression of *H19* (Biniszkiewicz 2002). Methylation analysis in the same study revealed that the DMD had become highly methylated upon both alleles in these cell lines, although the authors did not report methylation data for DMRs proximal to *Igf2*. Although by no means conclusive, genomic hypermethylation by *Dnmt1* overexpression reveals a possible mechanism by which atypical *Igf2/H19* imprinting may arise in the choroid plexus epithelium.

As discussed in Chapter 1, in the choroid plexus of adult mice (and in contrast to imprinted tissues where differential methylation is seen), the maternal allele of DMRs proximal to *Igf2* and the structural *H19* gene adopt a paternal epigenotype, such that both alleles are hypermethylated, concordant with biallelic *Igf2* expression and *H19* silencing in this tissue (Feil *et al.* 1994). Methylation at the DMD was not examined in this study, but interestingly a scan of the adjacent *H19* promoter proximal region revealed evidence of differential methylation Consistent with this methylation

analysis, a recent study has provided evidence that the DMD is differentially methylated in whole brain tissue (Yang 2003).

The studies of Feil *et al.* (Feil *et al.* 1994) and Yang *et al.* (Yang 2003) appear to describe an asymmetric methylation pattern at the *Igf2/H19* locus, such that methylation in *Igf2* proximal DMRs is acquired independently of the DMD. However, firm conclusions cannot be drawn from either of these studies as comparable tissues and developmental stages were not used. A further criticism of these studies concerns the use of dissected choroid plexus tissue (that would have included both the epithelial and stromal compartments) and whole brain tissue, in which DNA methylation analysis is unlikely to be representative as the brain-specific expression and imprinting of *Igf2* is highly discrete. Clearly *Igf2* expressing tissue would be underrepresented in this type of analysis, with genuine methylation profiles potentially masked by non-expressing tissue. The present study therefore provides a caveat for this type of analysis, suggesting that experiments should instead be conducted in a system where sites of expression are enriched, or isolated, from other tissues. These points are addressed later in the present study by experiments in choroid plexus epithelial cell lines (refer to Chapter 5).

The escape from imprinted expression of *Igf2* together with silencing of *H19*, a second imprinted gene, could suggest that a more pervasive deregulation of imprinted genes occurs in the choroid plexus epithelium and at other sites in the brain. There is some, albeit circumstantial, evidence in support of this as other imprinted genes are similarly affected. The mouse *Grb10* gene, although maternally expressed in many peripheral tissues, is biallelically expressed in the choroid plexus epithelium (Charalambous *et al.* 2003). Similarly, in the present study, expression of the otherwise paternally expressed *Dlk1* gene was not detected in the embryonic choroid plexus epithelium, although its expression was evident in adjacent tissues. Therefore, at least two further imprinted genes show either biallelic expression or silencing in the choroid plexus epithelium.

With the deregulation of multiple and unlinked imprinted loci, it could be argued that a critical *trans*-imprinting factor is either downregulated or functionally repressed upon differentiation of choroid plexus epithelial cells. This hypothesis was tested with

an *in situ* hybridisation approach to ask whether the *Igf2/H19* regulator, *CTCF*, is expressed in the choroid plexus epithelium? In this instance technical problems with the *in situ* hybridisation prevented a proper evaluation of this issue.

Two other studies suggest that further investigation is warranted. First, disruption of *CTCF* binding by mutation of its consensus sequences within the DMD led to uncharacteristic increases in post-zygotic methylation upon the maternal allele of the DMD, with concomitant reactivation of maternal *Igf2* and decreased expression of *H19* in several tissues. Interestingly, the mutated DMD remained devoid of methylation in oocytes, suggesting that *CTCF* is not required to initiate imprinting, but rather acts as a post-zygotic maintenance factor (Schoenherr *et al.* 2003). More recent work, that utilised an RNA interference (RNAi)-mediated knockdown of *CTCF* expression in oocytes, demonstrated increased methylation of the maternal DMD at subsequent post-zygotic stages (Fedoriw *et al.* 2004). These experiments suggest a role for *CTCF* in protecting the DMD (and therefore DMRs proximal to *Igf2*) from the acquisition of abnormal methylation patterns during post-zygotic development. The issue of *CTCF* expression in the choroid plexus epithelium is addressed later in the present study by Northern analysis in immortal cell lines (refer to Chapter 5).

Besides methyltransferases (Li 1993; Biniszkiwicz 2002) and insulator proteins (Schoenherr *et al.* 2003; Fedoriw *et al.* 2004) other proteins with *trans*-imprinting function have been identified (reviewed in (Bird 1999)). Polycomb group (PcG) proteins have well-established roles in the stable transcriptional repression of developmentally regulated genes via interactions with chromatin and are discussed in Chapter 1. Targeted deletion of the PcG gene, *Eed*, in mice led to the reactivation of normally repressed alleles at several imprinted loci, providing genetic proof of an essential role for PcG genes in imprinting (Mager 2003). *Igf2/H19* expression was not informative at the developmental stages examined by Mager *et al.* (2003), thus a role for *Eed* in the regulation of *Igf2* imprinting has yet to be substantiated. It may be relevant that the expression of *Grb10*, which similar to *Igf2* is biallelic in the choroid plexus epithelium, was clearly disrupted in *Eed* knockouts with expression of both parental alleles. Interestingly, in another study, a regulatory element from the mouse *Igf2* locus, the CCD, was shown to confer silencing upon *lacZ* and *miniwhite* reporter genes in transgenic *Drosophila*, with silencing mediated by two PcG proteins,

*Enhancer of zeste (E[z])* and *Posterior sex combs (Psc)* (Erhardt *et al.* 2003). Given the evolutionarily conserved nature of this effect, it might be predicted that mammalian PcG homologues mediate the silencing function reported for this element in mice (Ainscough *et al.* 2000b). Future work should attempt to address potential roles of PcG proteins as *trans*-imprinting factors in the context of the choroid plexus epithelium. It might be possible to manipulate mechanisms that initiate biallelic *Igf2* expression upon its differentiation *in vivo* by overexpression of PcG genes under early choroid plexus or neuroepithelial promoters.

Although not previously reported, the *lacZ*DMR2<sup>-</sup> assays revealed evidence that only a subset of the cells in the choroid plexus epithelium expressed *Igf2*. *In situ* hybridisation data corroborated this finding, thereby excluding an involvement of the DMR2 deletion in the manifestation of this feature. Additional evidence is provided by recent work in transgenic mice where a transgene containing regulatory elements from the *Igf2/H19* locus, *Igf2* promoter 3 (P3) and the CCD, reproducibly conferred variegated expression upon a *lacZ* reporter gene in the choroid plexus epithelium (Charalambous *et al.* 2004). Interestingly, the CCD alone was shown to confer variegated silencing upon the *miniwhite* reporter gene in transgenic *Drosophila*, providing evidence that this element might be at least partially responsible for the effect in the murine choroid plexus (Erhardt *et al.* 2003). Therefore the CCD (and possibly P3) contains the sequences sufficient to impose variegated expression upon *Igf2*. The *Drosophila* experiments implicate the involvement of a conserved silencing mechanism in this process, possibly mediated by PcG proteins.

The absence of a prior report describing variegated *Igf2* expression in the choroid plexus suggests that other studies may have overlooked this unusual feature (Stylianopoulou *et al.* 1988b; DeChiara *et al.* 1991; Svensson 1995; Hemberger 1998). Since these studies employed radioactive detection methods, a technique of relatively lower resolution, variegated expression may not have been apparent, in contrast with the higher resolution techniques of non-radioactive *in situ* hybridisation or *lacZ* reporter gene assays, as used in the present study.

Variegated expression is evident from the onset of expression in the lineage of neuroepithelial cells that give rise to the choroid plexus epithelium and is maintained

throughout development and into the adult. The *lacZ*<sup>DMR2</sup> expression data provided evidence that transcription from both parental alleles is subject to variegation, although the ratio of positive to negative cells appears to be greater when examining expression from the maternal allele, although quantitative cell counting experiments were not done to corroborate these observations. Furthermore, whether the expression from the respective alleles coincides in the same cell or whether they are expressed in distinct non-overlapping cell populations was not addressed in this study. Future experiments involving co-localisation of the *lacZ* gene product with endogenous *Igf2* transcripts or protein in mice heterozygous for the *lacZ*<sup>DMR2</sup> allele is one approach that could address these points.

The possibility that the variegation was a consequence of temporal variation in initiation of the differentiated choroid plexus phenotype was excluded by evidence that expression of TTR, a diagnostic marker, is present in all cells of the developing choroid plexus epithelium. Therefore it is likely that cells both positive and negative for *Igf2* expression have otherwise correctly assumed the choroid plexus phenotype. Conversely, the presence or absence of *Igf2* expression could be said to define two subtypes of choroid plexus epithelial cell. The biochemical analysis was extended to ask whether variable gene expression reflects a more general property of the choroid plexus epithelium. Primary antibodies and *in situ* probes corresponding to several other markers were tested for variegated staining in sections of embryonic choroid plexus epithelium, although none revealed variegated expression. This analysis, although by no means exhaustive, suggests that restriction of gene expression to a subset of cells is not likely to be a general feature of genes expressed in the choroid plexus epithelium.

In support of the data presented in this study, there are precedents for variable phenotypes amongst choroid plexus epithelial cells. Most notably, electron lucent and dense, or light and dark cells have been described in the choroid plexus epithelium of rats, mice and humans (Dohrmann 1970; Sturrock 1979). Sturrock (1979) provided quantitative evidence that light cells predominate with the number of dark cells comprising approximately 11% of the total cell number and proposed that dark cells might contain a greater number of mitochondria and ribosomes, with the implication that these cells are engaged in distinct metabolic activities.

The biological significance of light and dark cells within the choroid plexus epithelium is unclear although evidence from mutant studies suggests that the ratio of light to dark cells is linked to CSF secretion and/or homeostasis. Mice homozygous for the Hydrocephalus and Polydactyl (*Hpy/Hpy*) mutation develop hydrocephalus early in the postnatal period. The condition develops in the apparent absence of any obvious obstruction in the CSF drainage system, suggesting a constitutive, inappropriate, secretion of CSF (Bryan 1977). Further work has shown that the choroid plexus epithelium of these mice contains an elevated number of dark cells, compared with WT animals and it was also shown that a quantitatively equivalent induction of dark cells occurs in WT animals deprived of drinking water (Shuman 1991).

Signalling mediated by arginine vasopressin (AVP), a neuropeptide, has an established role in regulating extracellular fluid balance in the CNS of mammals (Nilsson 1992). AVP has been shown to curtail CSF secretion from the isolated rat choroid plexus *in vitro* (Liszczyk 1986). Therefore AVP negatively regulates CSF secretion by the choroid plexus. Consistent with a role for dark cells in water balance, this and other studies have shown that AVP mediated decreases in CSF secretion are accompanied by an increase in dark cell number (Liszczyk 1986; Johanson 1999a). A similar effect has been shown to occur following treatment with Fibroblast growth factor 2 (FGF2), a protein postulated to act in the same axis as AVP in the central regulation of CSF synthesis (Johanson 1999b; Johanson 2001). This data therefore suggests that dark cells are an important feature of the response to water imbalance in the CNS.

Other reported biochemical differences amongst choroid plexus epithelial cells, aside from the example given by *Igf2*, appear to involve the expression of AVP, components of FGF signalling and other molecules previously linked to CSF secretion/homeostasis. As such, clusters of cells in the rat choroid plexus epithelium demonstrated immunoreactivity to both AVP and FGF receptor antibodies. Therefore a subpopulation of cells in the choroid plexus epithelium is marked by the co-expression of AVP and FGF receptors (Szmydynger-Chodobska 2002). Interestingly, the cystic fibrosis gene product, the cystic fibrosis transmembrane conductance regulator (CFTR), which is known to regulate water flux across many important

epithelia, by functioning as a cyclic AMP-dependent chloride ion channel, also shows variegated expression in the choroid plexus epithelium (Welsh 1992; Hincke 1995). It is difficult to reconcile this data with known functions of *Igf2*, however an important conclusion of this discussion is that, similar to *Igf2*, other phenotypic (and possibly functional) differences are likely to exist amongst subpopulations of choroid plexus epithelial cells. That these differences appear to be linked to a major function of the choroid plexus, that is the secretion of CSF (and fluid homeostasis) underlines the importance of such subpopulations in this tissue, suggesting that a functional role for variegated *Igf2* expression in the choroid plexus epithelium may yet be established.

A further aim of this study was to understand how such a cell subpopulation expressing *Igf2* might be established in the choroid plexus epithelium. The role of Notch signalling in the specification of asymmetric cell fates is well documented and discussed in the Introduction to this chapter. It was postulated that Notch signalling might be involved in the initiation and/or maintenance of variegated expression of *Igf2*. To this end an investigation of *Delta*, *Jagged* and *Notch* gene expression was carried out in the developing choroid plexus in an attempt to identify candidate genes for subsequent functional analysis. RT-PCR analysis, although admittedly crude, was performed in the isolated choroid plexus of neonate mice as a rapid means to ask whether these genes are indeed expressed in this tissue, and revealed the expression of all *Notch*, *Delta* and *Jagged* genes except *Dll3*. Subsequent *in situ* hybridisation analysis was performed at two further developmental stages spanning the duration of choroid plexus morphogenesis, in whole mount preparations at e10.5 and in sections of e14.5 embryos, to examine the distribution of expression between the two major compartments of the choroid plexus.

The literature suggests that the expression of *Notch* and *Delta* genes occurs in a range of tissues and spanning several developmental stages, however *in situ* hybridisation analysis in the present study was limited in its ability to uncover many of these sites of expression. Whilst probes for *Notch2*, *Dll1*, *Dlk1*, *Jagged1* and *Jagged2* produced moderate to strong hybridisation signals in patterns generally consistent with those previously reported (Bettenhausen *et al.* 1995; Higuchi 1995; Hrabe de Angelis *et al.* 1997; Beckers 1999; Hamada *et al.* 1999; McCright *et al.* 2001; Irvin 2004), with use of probes to *Notch1*, *Notch3*, *Notch4*, *Dll3* and *Dll4* signals were either diffuse or

absent. Further attempts to optimise the hybridisation conditions were unsuccessful, suggesting that probe dependent problems were the cause of failure in these examples.

It should be noted that, aside from *Dlk1*, even those probes deemed to have worked well, did not produce a particularly clear or strong response. An inherent problem of *in situ* hybridisation is that it can be very probe dependent and an explanation for the poor performance of *in situ* probes involves the nucleotide sequence. *Notch*, *Delta* and *Jagged* genes contain sequences encoding reiterated conserved motifs, including EGF-like repeats and in the case of *Notch* genes, multiple ankyrin repeats (Lewis 1998). It is possible that, given their repetitive nature, regions of the probes encoding these domains are prone to a degree of secondary structure formation not amenable to hybridisation. For the purposes of this study, an involvement of *Notch3*, *Notch4*, *Dll3* and *Dll4*, cannot be properly evaluated, as expression of these genes could not be clearly demonstrated.

Is there sufficient data to support a role for Notch signalling in the specification variegated *Igf2* expression the choroid plexus epithelium? *Notch1* and *Notch2* expression was evident at e10.5 in subventricular regions of the brain, and the mesoderm of the posteriormost somite pair as previously described (Higuchi 1995). However, neither of these genes appeared to be expressed in the vicinity of the presumptive choroid plexus epithelium, although expression of *Notch2* has been reported in neuroepithelial structures at this stage (Hamada *et al.* 1999). At e14.5, expression of *Notch2*, but not of *Notch1*, was observed in the choroid plexus epithelium, consistent with the RT-PCR data and with earlier reports of its expression in this tissue (Higuchi 1995) and appeared to be uniformly distributed. That *Notch1* expression was not found at any site at e14.5, again implicates probe dependent issues, although previous work provides evidence that *Notch1* is not expressed in the choroid plexus at any stage (Higuchi 1995). Therefore, uniform expression of *Notch2* occurs in choroid plexus epithelium at e14.5, although its expression in choroid plexus epithelial precursors at earlier stages remains unresolved.

Of the various *Delta* and *Jagged* ligands analysed, none were found to be expressed in either the choroid plexus epithelium or stroma, although expression of *Dll1*, and both *Jagged* genes has been described in the choroid plexus at comparable stages (Hrabe



de Angelis *et al.* 1997; Beckers 1999) (Irvin 2004). Further inconsistencies were found, in the tissue-specific expression of *Dll1*, suggesting that the probe used did not detect expression in all tissues. As expected *Dll1* expression was seen in the subventricular neurons of the brain and in the condensing epithelial structures of the kidney at e14.5, but in contrast to published expression patterns, was not present in epithelial structures lining the pancreas and lung, or in muscle lineages (Beckers 1999; McCright *et al.* 2001). It is unlikely that these differences are explained by the existence of tissue specific transcripts not detected by the probe used here, as only a single 3.8kb transcript has been described for this gene (Bettenhausen *et al.* 1995). It is therefore more likely that these inconsistencies result from differences in overall expression levels, or probe dependent penetration between tissues. Given the highly discrete localisation of transcripts reported for this and other Notch ligands, it is conceivable that these negative factors could decrease hybridisation signals to levels below detection thresholds. The use of different probes might improve the detection of gene expression, although it is perhaps significant that an initial set of Notch probes, not described in this study, also failed to give reproducible hybridisation signals. Primary antibodies are commercially available for all mammalian Notch, Delta and Jagged proteins, thus an immunohistochemistry approach could provide an alternative means by which to further investigate a role for Notch signalling.

In summary, expression of a single *Notch* gene, *Notch2*, was demonstrated in the mature choroid plexus epithelium. None of the genes encoding its potential ligands, *Delta* or *Jagged*, were shown to be expressed in an overlapping manner that would be consistent with a receptor-ligand interaction in this tissue. On the basis of this and previous expression data, a role for Notch signalling in the specification or maintenance of subpopulations in the choroid plexus epithelium, positive and negative for *Igf2* expression, is neither supported nor excluded. Further work should attempt to elucidate the role of *Notch2* in a loss-of-function system. This analysis would, however, be largely dependent upon availability of hypomorphic *Notch2* mutant strains (*Notch2* null embryos die prior to the formation of the choroid plexus (Hamada *et al.* 1999)) or tissues and might be better suited to an *in vitro* approach. Immortal choroid plexus epithelial cell lines created in the present study (refer to Chapter 5) appear to have retained variegated *Igf2* expression and could provide a resource to systematically test the function of *Notch2* and other candidates using the RNAi

technique. However, recent evidence perhaps favours a polycomb-based mechanism over Notch-signalling in mediating variegated *Igf2* expression in the choroid plexus epithelium (Erhardt *et al.* 2003; Charalambous *et al.*2004), therefore future RNAi studies of *Notch* function should be extended to include the PcG genes also implicated in this activity.

## CHAPTER 4: *IN VITRO* INVESTIGATION OF CHOROID PLEXUS *CIS* REGULATORY ELEMENTS

### ***Introduction***

The developmental expression analysis identified the choroid plexus epithelium as a site of both biallelic and variegated *Igf2* expression (Chapter 3). An important step toward a complete understanding of mechanisms involved in regulating this pattern of expression requires that the necessary *cis*-regulatory elements are mapped and characterised. Transient expression assays in cultured mammalian cells provide a rapid and sensitive means to investigate the role of regulatory elements isolated from endogenous genes. This approach has been employed to define enhancers (Yoo-Warren *et al.* 1988; Kaffer 2000; Drewell *et al.* 2002a) and dissect boundary or silencing functions in imprinting control regions at the *Igf2/H19* locus (Bell 2000; Hark *et al.* 2000; Kanduri 2000a; Holmgren 2001; Ginjala 2002). In the present study transient expression assays were employed as a means to analyse genomic regions for choroid plexus enhancer activity.

Transgenic experiments have shown that at least one enhancer element driving expression in the choroid plexus epithelium must reside within the 2kb CCD region (discussed in Chapter 1)(Ward *et al.* 1997; Charalambous *et al.* 2004). The function of this region has also been tested within the context of a 12kb germline deletion where consistent with the loss of an enhancer, decreased *Igf2* expression was seen specifically in the choroid plexus and leptomeninges (Jones *et al.* 2001). Importantly, this deletion did not result in complete loss of *Igf2* expression, suggesting the existence of a second enhancer region situated outside of the deletion. The precise location of the enhancer within the CCD is not known, although it presumably lies within one of the two stretches of conserved sequence identified within this region (Ainscough *et al.* 2000b). Transgenic experiments have shown the deletion of the first of these, CCD region 1, within the context of a YAC transgene had no apparent impact on the expression of a *lacZ* reporter gene in the brain, suggesting that the enhancer lies outside of this region. The CCD region 2 is therefore a strong candidate for the enhancer.

Where might additional enhancer elements be located? The insulator model has established a widely accepted paradigm for *Igf2/H19* imprinting and is discussed at length in Chapter 1. A major prediction of this model is that enhancers driving imprinted expression will be situated 3' of the chromatin boundary at the DMD, whilst those driving biallelic expression will be situated 5' of this region. Consistent with this, known choroid plexus enhancers are located 5' of the DMD in the intergenic region between *Igf2* and *H19* (Ward *et al.* 1997; Jones *et al.* 2001; Charalambous *et al.* 2004). Relocation of the *H19* endoderm-specific enhancer region to the intergenic region resulted in biallelic *Igf2* expression in tissues where these enhancers are normally active and imprinted expression occurs (Webber *et al.* 1998). Moreover, when the DMD was moved to a position between the endodermal and skeletal muscle enhancers, *H19* became biallelically expressed in endodermal tissues but was silent in muscle (Kaffer 2000). Enhancer location relative to the DMD is therefore a determinant of imprinted expression at the *Igf2/H19* locus.

Sequence comparisons of the *Igf2/H19* locus in human and mouse have revealed the presence of five conserved non-coding regions, each 120-150bp in length, situated in the intergenic region (Onyango *et al.* 2000). Because of their location, these regions might be predicted to act as choroid plexus-specific enhancers and drive biallelic expression in this tissue. The aims of this chapter were to firstly further delineate the choroid plexus enhancers within the CCD, by separately testing the function of regions 1 and 2 in deletion constructs, and secondly to investigate the function of conserved intergenic sequences in an attempt to locate and characterise the additional choroid plexus enhancer activity implicated in previous work (Jones *et al.* 2001).

Continuous cell lines derived from the choroid plexus epithelium were not available at the onset although two lines have been established from the rat during the course of this work (Kitazawa 2001; Zheng 2002). Primary cultures of choroid plexus epithelium have been successfully established from a range of mammalian species (Crook 1981; Thomas 1992; Holm 1994; Ramanathan 1996; Villalobos *et al.* 1997). Although more difficult to manipulate when compared with continuous cell lines, primary cultures offer the advantage of closely resembling the parent tissue from which they are derived, whereas cell lines have in many cases lost aspects of the differentiated phenotype. Therefore to generate a suitable system for use in transient

expression assays, primary cultures of choroid plexus epithelium were derived from mice.

## **Materials and Methods**

### **Probes**

The *Igf2* probe is described in the Materials and Methods section at the beginning of Chapter 3. The *TTR* probe was derived from the pTTR7kbexV3 plasmid (Prof R.H. Costa unpublished work) and was a 1kb *NruI-StuI* DNA fragment spanning exons 1-2 of the mouse *TTR* gene. For Northern analysis probes were isolated from their parent vectors by digestion with restriction enzymes and purification from agarose gels (see the relevant Chapter 2 sections). Probes were radioactively labelled prior to use (see Chapter 2 section describing synthesis of  $\alpha$ -<sup>32</sup>P(dCTP)-labelled DNA probes).

### **Antibodies**

Primary antibodies to TTR and E-cadherin for immunofluorescence cytochemistry are described in the Materials and Methods section at the beginning of Chapter 5.

### **Plasmids**

*Igf2-Luciferase* constructs, which contained various regulatory regions from the *Igf2/H19* region were previously described (Ward *et al.* 1997). The **M** construct contained the *Igf2* Promoter 3 (P3) linked to the *Luciferase* reporter gene in the Bluescript SK+ vector (Stratagene). The constructs **A** and **H** were generated by the respective insertion of the H19 endoderm-specific enhancer region and the CCD into **M**. Two CCD deletion constructs based upon the **H** construct, **pCCD4** and **pCCD11** contained the CCD with region 1 and region 2 deleted respectively, were obtained from Dr. Marika Charalambous.

### **PCR Primers**

The primer sequences used to amplify conserved elements from the *Igf2/H19* intergenic region were designed from genomic sequence obtained from the National Centre for Biotechnology Information (NCBI) *Nucleotide* database. Genetool primer design software (Biotools, UK) was used to select the primers from these sequences.

<b>Primer pair</b>	<b>Direction</b>	<b>Sequence</b>
Conserved 1	forward	5'CCC CTC ACC CGG CTA CAT CTA CAT-3'
	reverse	5'AGG CCA GAC TTC CCC AGG TAT TGA-3'
Conserved 2	forward	5'GGC CCT TTC CCT GTT CCC TAG AGA-3'
	reverse	5'GCA AGA GCA AGT GGG AAC CCT GTC-3'
Conserved 3-5	forward	5'GCT GGC TTG GCT GGG TGG GAT TAG-3'
	reverse	5'GGA CGC TGG CTT GGC ATG GAT TG-3'

**Table 7. Primers used to PCR-amplify conserved elements from the *Igf2/H19* intergenic region.**

## **Results**

### **Primary culture of choroid plexus epithelial cells**

Primary choroid plexus epithelial cells were prepared as described (see Chapter 2 section describing preparation of primary choroid plexus epithelial cells). This method was based upon an existing protocol (Hoffmann 1996) and was subject to further modifications which involved plating the recovered cells onto dishes pre-coated with fibroblast extracellular matrix (Charalambous 2000). Two additional modifications appeared to improve cell viability sufficiently (not quantified) to allow omission of the fibroblast ECM, such that isolated cells could be plated directly onto tissue culture plastic. First the pronase concentration in HBSS buffer was reduced from 4 to 2mg ml<sup>-1</sup> and second, dissected brains were held in complete growth medium rather than PBS prior to the removal of choroid plexus tissue. These changes appeared to increase the number of small cell aggregates recovered (as opposed to single cells) which are likely to plate more efficiently than single cells. To obtain sufficient cell numbers for subsequent transfection or gene expression experiments, choroid plexi were dissected from the lateral and fourth ventricle of approximately 20 animals (or 2 litters) and disaggregated in the presence of pronase as described. Recovered cells were plated directly into tissue culture treated plastic dishes and left undisturbed overnight to allow for cell attachment, after which unattached cells and debris were removed by changing the medium.

### **Morphology**

Cultured cells originating from the choroid plexus epithelium would be expected to display a diagnostic epithelial morphology. The cultures were examined by light microscopy approximately 48 hours after plating, which revealed that numerous colonies of epithelial-like cells had formed with a characteristic closely opposed cobblestone morphology (**Figure 17a**). These cells displayed a granular appearance, which is suggestive of either secretory activity or the presence of apical microvilli. All of these features were consistent with an origin from the choroid plexus epithelium. A population of fibroblast-like cells, possibly having originated from the choroid plexus stroma, were dispersed between the epithelial colonies. Excessive fibroblastic proliferation could be prevented by the inclusion of cytosine  $\beta$ -D-arabinofuranoside (CAF), a selective DNA synthesis inhibitor, in the growth medium. Choroid plexus

epithelial cells have been reported to lack transport mechanisms for arabinose sugars and were thus insensitive to the action of this drug (Hoffmann 1996). In this manner, confluent cultures enriched for the epithelial colonies were produced a week after plating (**Figure 17b**). However, for the purposes of the transient assays, where additional reagents might interfere with transfection or reporter gene expression, the CAF treatment was omitted. It was not possible to passage the cultures into finite cell lines as the cells were so strongly adherent that their detachment only occurred after prolonged incubation with dissociation reagents and any cells that could be persuaded to detach exhibited poor plating efficiency upon subsequent passage. Thus experimentation with this system was limited to freshly explanted cultures only.

### *Gene expression*

To confirm the origin of the cultures from choroid plexus epithelium, the expression of two genes was examined. As already discussed, the *Transthyretin (TTR)* gene, is a robust marker for choroid plexus epithelial cells (Murakami 1987). *Igf2* expression is another marker of choroid plexus epithelium that is expressed from the earliest stages of choroid plexus differentiation (see Chapter 3). Additionally, as this study involved the dissection of *Igf2* regulatory elements, it was necessary to confirm the expression of this gene in the cultures. RNA was isolated from the primary cultures and from dissected choroid plexus tissue, which would be expected to abundantly express both *Igf2* and *TTR*, thus acting as a positive control for the experiment. RNA was isolated from brain tissue depleted of the choroid plexi and meninges, which would not be expected to express detectable levels of either gene, and served as a negative control. The RNA was analysed by Northern analysis (see Chapter 2 section describing Northern analysis). Hybridisations were performed with DNA probes corresponding to exon 6 of the *Igf2* gene and exons 1-2 of *TTR*. The Northern analysis (**Figure 18**) showed that abundant transcripts for *Igf2* and *TTR* were present in the primary cultures and in the positive control tissue. No hybridisation signals were seen in the negative controls.

To examine gene expression *in situ*, the primary choroid plexus cultures were fixed and stained with an  $\alpha$ -TTR antibody and the antibody visualised with a fluorescein-conjugated secondary antibody (see Chapter 2 section describing immunofluorescence



cytochemistry). High levels of the TTR protein were observed in the majority of epithelial cells in a pericytoplasmic distribution (**Figure 19**). Staining with this antibody was absent from the fibroblastic component. E-Cadherin is a sensitive marker for all epithelial cells, including those of the choroid plexus. The cultures were also stained with an  $\alpha$ -E-Cadherin antibody as described for TTR. E-Cadherin protein was exclusively localised to the plasma membranes of the cells in the epithelial colonies as would be expected for epithelial cells (**Figure 19**). Staining was not seen within the fibroblast component of the cultures (not shown). The primary cultures therefore present morphological and biochemical properties of differentiated choroid plexus epithelial cells.

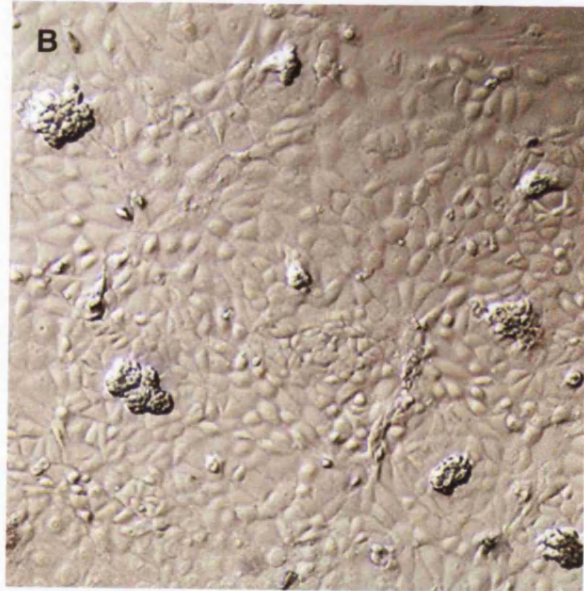
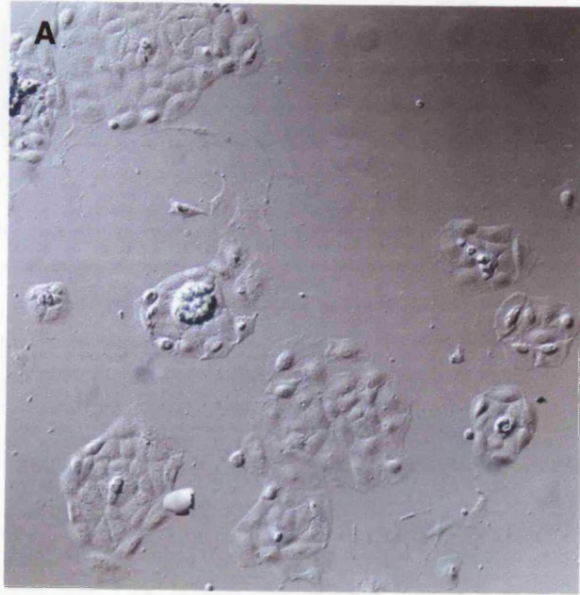
### **PCR-amplification of Intergenic conserved elements**

To address the role of the intergenic conserved elements (Onyango *et al.* 2000), a strategy was devised to examine their activity in the context of *Luciferase* reporter constructs. For the purposes of this study these elements were termed C1-C5. **Figure 20a** shows their genomic location relative to the *Igf2* and *H19* genes. A PCR-based approach was employed to isolate these elements from genomic DNA. It was apparent that the close proximity of C3, C4 and C5, with all three elements occupying a 4kb region in mice, might have some functional significance, as this arrangement is conserved in humans (Onyango *et al.* 2000). It was envisaged that these elements should be assayed as a functional unit initially and then the function of each element could be separately tested in deletion constructs. With this in mind, a long template PCR strategy was devised to isolate all three elements on a single 5kb genomic fragment. Ultimately time constraints prevented the individual analysis of these regions. The C1 and C2 elements were amplified on shorter genomic fragments with a conventional PCR approach. The primers sequences designed to amplify these elements together with some flanking DNA, are listed in the Materials and Methods section at the beginning of this chapter. **Figure 20b** shows the expected sizes of PCR products and the approximate position of the conserved elements within these products for each primer pair.

PCR-amplifications were performed as described (see Chapter 2 section describing PCR). The primer pair for the C2 region amplified the target sequence efficiently

**Figure 17. Primary choroid plexus cultures, morphological analysis**

Primary choroid plexus cultures were examined by light microscopy. Epithelial-like colonies with a characteristic closely-opposed cobblestone morphology were observed at 48 hours (A) after plating. These colonies expanded to cover large areas after 1 week in culture (B). Magnifications  $\times 200$ .



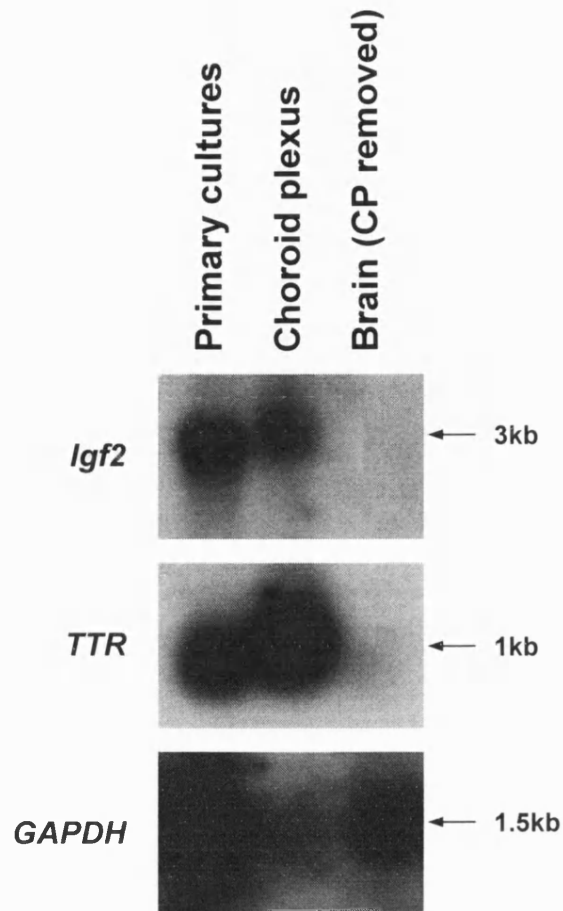


**Figure 18. Primary choroid plexus cultures, Northern analysis of *Igf2* and *TTR* expression.** Total RNA was extracted from the primary choroid plexus cultures, from dissected neonate choroid plexus tissue and from brain tissue with choroid plexi removed, blotted and hybridised with *Igf2* and *TTR* probes. The two upper panels show Northern analysis of primary choroid plexus RNA for *Igf2* and *TTR* mRNA expression. A band corresponding to the 3kb *Igf2* transcript was seen in the primary cultures and dissected choroid plexus, but not in the brain tissue. *TTR* expression was similarly distributed with a 1kb transcript present in the primary cultures and dissected choroid plexus tissue, but not in brain. Hybridisation with a *GAPDH* probe to show equal loading of total RNA in all lanes is shown in the lowermost panel.

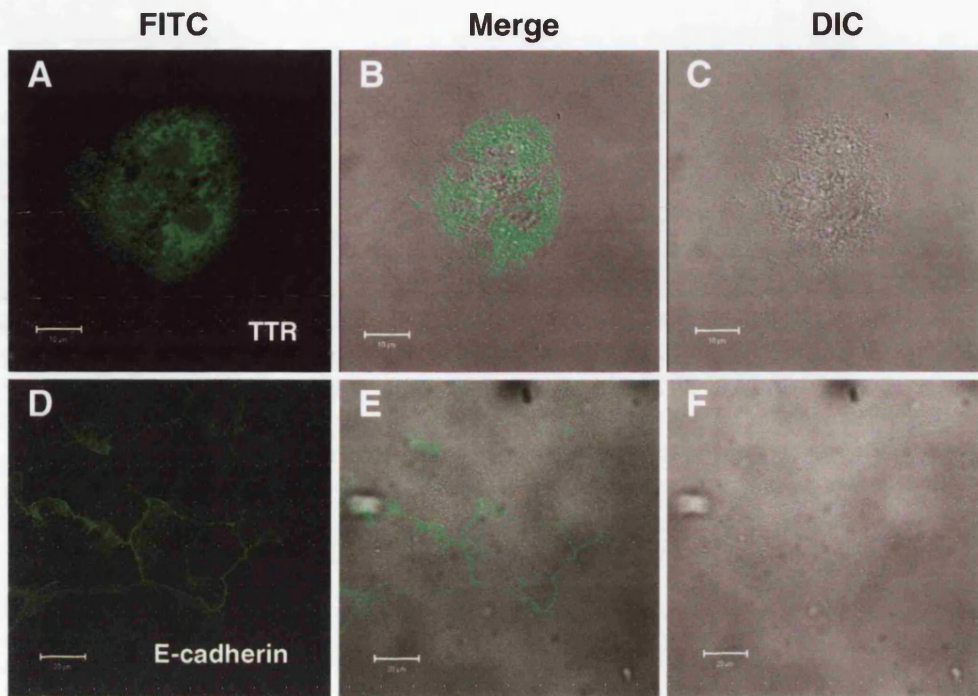


**Figure 19. Primary choroid plexus cultures, immunofluorescence analysis of TTR and E-cadherin expression** Primary cultures were fixed and stained for the presence of TTR and E-cadherin. Images under both FITC and DIC conditions were collected by laser scanning confocal microscopy (left and right columns respectively). These images were overlaid as shown in merge (middle column). **A-B** show the presence of TTR protein in a perinuclear cytoplasmic distribution within a small colony of epithelial cells; **C** DIC image of the same field of cells. **D-E** show E-cadherin staining localised to the plasma membranes surrounding several epithelial cells. **F** DIC image of the same field of cells. Neither protein was detected within the fibroblastic component of the cultures. Scale bars show either 10  $\mu\text{m}$  (**A-C**) or 20  $\mu\text{m}$  (**D-F**)

whereas those for C1 and C3-5 regions did not amplify the expected products and thus required optimisation. Conditions that allowed efficient amplification with these primer pairs were determined empirically in a series of 12 optimisation reactions (see Chapter 2 section describing PCR optimisation and **Figure 21**). The amplified fragments were purified (see Chapter 2 section describing purification of DNA from solutions and agarose gels) and ligated into the pGEM-T-easy vector to create the plasmids pGEM-T-C1, pGEM-T-C2 and pGEM-T-C3-5.

### **Generation of *Igf2*-Luciferase reporter constructs**

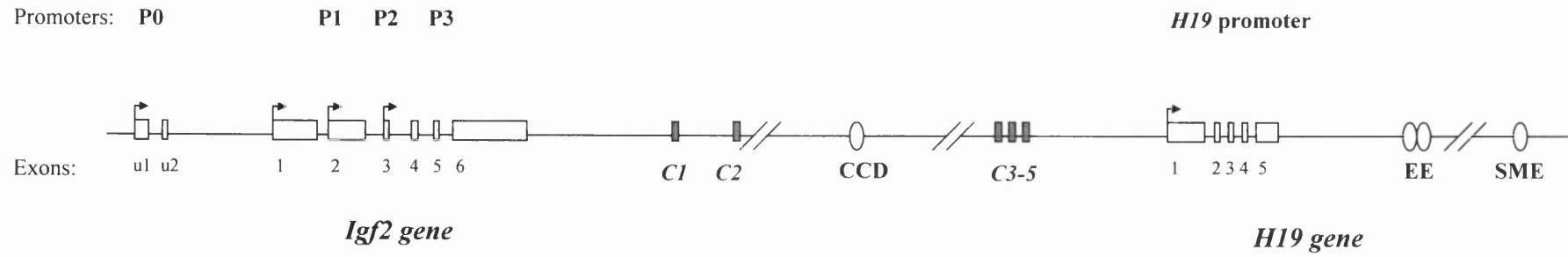
All *Luciferase* reporter constructs were derived from the **M** (*P3-Luciferase*) construct and were created as described below. **M** was linearised at a unique *NotI* site situated immediately 3' of the *Luciferase* sequences and treated with phosphatase (see Chapter 2 section describing dephosphorylation of plasmid ends) to prevent self-ligation. This fragment, designated **M-NotI** was used to derive all *Luciferase* constructs by insertion of the candidate regulatory regions, isolated by PCR and cloned as described above into the *NotI* sites. To create the C1 construct, a 1.2kb *NotI* fragment containing the C1 element was purified away from the pGEM-T-C1 plasmid and ligated into **M-NotI**. To create the C2 construct, a 0.75kb *NotI* fragment containing the C2 element was purified away from the pGEM-T-C2 plasmid and ligated into **M-NotI**. To create the C3-5 construct, a 5.1kb *NotI* fragment containing the C3, C4 and C5 elements was purified away from the pGEM-T-C1 plasmid and ligated into **M-NotI**.

A further set of four constructs was created to investigate potential synergistic interactions between the C1 and C2 intergenic elements and the CCD. The *P3-Luciferase-C1-CCD* construct was created as follows: a 2kb *EcoRI* fragment containing the CCD region was purified from its parent vector and ligated into the *EcoRI* site of the pBS II KS+ vector to create the pBS-CCD plasmid. A 1.2kb *NotI* fragment containing the C1 element was purified away from the pGEM-T-C1 plasmid, the ends filled in by treatment with T4 DNA polymerase (see Chapter 2 section describing conversion of 5' and 3' recessed ends to blunt ends) and ligated into the filled-in *HindIII* site of the pBS-CCD plasmid to create the pBS-C1-CCD plasmid. An additional *NotI* site for subsequent manipulations was created within an existing *KpnI* site at the 5' end of the multiple cloning site, by insertion of a short linker fragment (see Chapter 2 section describing oligonucleotide linker synthesis)..

**Figure 20. Genomic location of *Igf2/H19* intergenic conserved regions.**

**A** The *Igf2/H19* genomic region (not to scale) is shown with the position of conserved regions C1, C2, and C3-5 (shaded boxes) shown relative to the *Igf2* and *H19* genes. Exons (open boxes) and characterised enhancers (ovals) are also shown. **B** Predicted sizes of the PCR products (open boxes) on which the conserved regions (shaded boxes) were isolated are described.

**A**



**B**

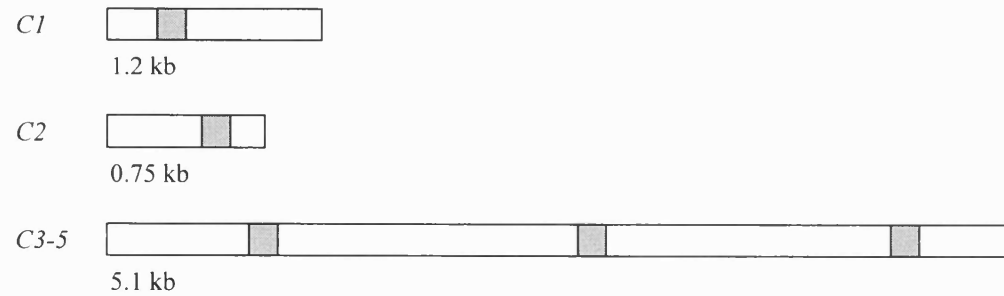
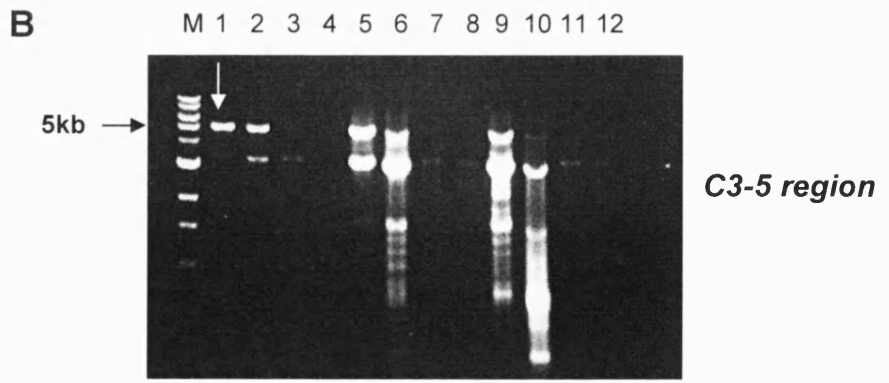
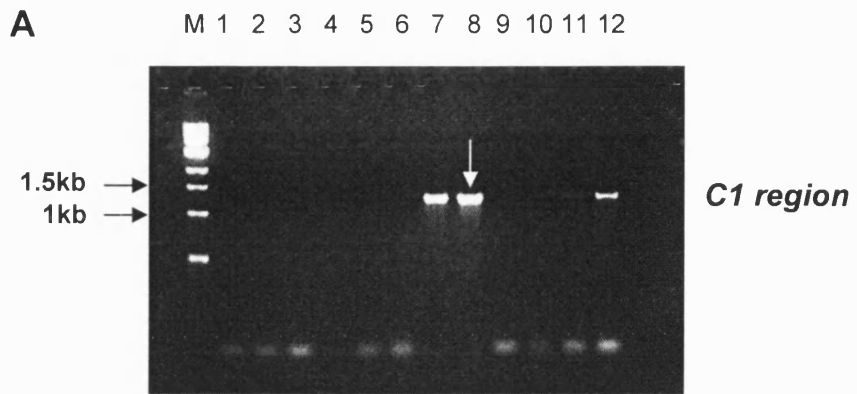


**Figure 20. Intergenic conserved regions at the *Igf2/H19* locus**



**Figure 21. PCR-amplification of *Igf2/H19* intergenic conserved regions.** Optimal PCR conditions were determined empirically by varying the concentration of reaction components ( $Mg^{2+}$ , dNTPs and primers) across lanes 1-12 (for details of this optimisation see Chapter 2 section describing PCR). **A.** Optimal amplification of the C1 region fragment, with a 1.2kb band, occurred in reaction 8 (white arrow) with 1.5mM  $Mg^{2+}$ , 4.5mM dNTPs and 2 $\mu$ M primers. **B.** Optimal amplification of the C3-5 region fragment, with a 5.1kb band, occurred in reaction 1 (white arrow) with 1mM  $Mg^{2+}$ , 0.45mM dNTPs and 0.2 $\mu$ M primers. PCR amplification of the C2 region did not require optimisation (not shown). The molecular weight marker (M) is a 1kb DNA ladder with bands of relevant molecular weight indicated.



The linker was a homodimer generated by the pairwise-annealing of the oligonucleotide sequence 5'CGCGGCCGCGGTAC-3' where the *NotI* site is underlined. Finally, a 3.2kb *NotI* fragment containing the fused C1-CCD regions was purified away from the pBS-C1-CCD plasmid and ligated into **M-NotI**.

The **P3-Luciferase-C2-CCD** construct was created as follows: a 2kb *SpeI-NheI* fragment containing the CCD region was purified from its parent vector and ligated into the *SpeI* site of the pGEM-T-C2 plasmid described above to create the pGEM-T-C2-CCD plasmid. Finally, a 2.8kb *NotI* fragment containing the fused C2-CCD regions was purified away from the pGEM-T-C2-CCD plasmid and ligated into **M-NotI**.

The **P3-Luciferase-C1-C2** construct was created as follows: A 1.2kb *NotI* fragment containing the C1 element was purified away from the pGEM-T-C1 plasmid, filled-in by treatment with T4 DNA polymerase (see Chapter section describing conversion of 5' and 3' ends to blunt ends) ligated into the filled-in *NotI* site of the pBS II KS+ vector to create the pBS-C1 plasmid. The C1 region was purified away from this plasmid within a 1.2kb *SacII* fragment and ligated into the *SacII* site of the pGEM-T-C2 plasmid described above to create the pGEM-T-C1-C2 plasmid. Finally, a 2kb *NotI* fragment containing the fused C1-C2 regions was purified away from the pGEM-T-C1-C2 plasmid and ligated into **M-NotI**.

The **P3-Luciferase-C1-C2-CCD** construct was created as follows: a 1.2kb *SacII* fragment containing the C1 region, the origin of which is described above and ligated into the *SacII* site of the pGEM-T-C2-CCD plasmid also described above, to create the pGEM-T-C1-C2-CCD plasmid. Finally, a 4kb *NotI* fragment containing the fused C1-C2-CCD regions was purified away from the pGEM-T-C1-C2-CCD plasmid and ligated into **M-NotI**. All constructs were sequenced across the cloning junctions at each stage to confirm the correct identity and orientation of the inserted fragments.

### **Transient expression assays**

It has been found that greater transfection efficiencies may be achieved in epithelial cells by performing transfections whilst the cells are in suspension as opposed to the conventional transfection of cells after they have formed an adherent monolayer

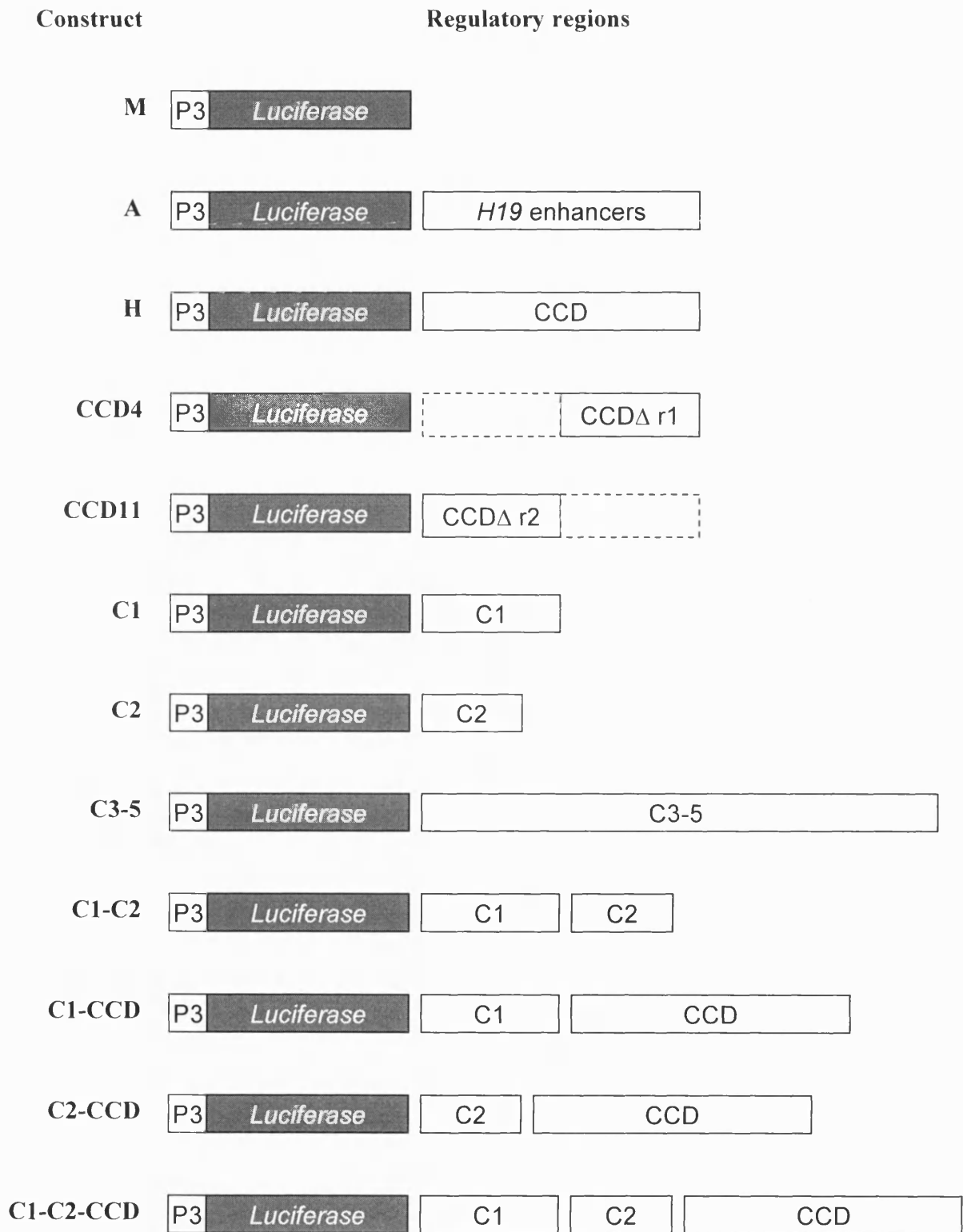
(Sambrook 1989). In the present study, pilot experiments revealed an approximate 2-3-fold increase (not quantified) in the number of transfected cells following transfection with a constitutive SV40-*lacZ* plasmid in suspension cells compared with an adherent cell transfection (data not shown). Primary choroid plexus cultures were transfected immediately following their plating and before attachment had occurred.

*Igf2-Luciferase* reporter constructs (shown in **Figure 22**) were transfected into primary choroid plexus epithelial cells and HepG2 cells (see Chapter 2 sections describing transfection of plasmid DNA into primary choroid plexus cultures and continuous cell lines) for the purposes of three different experiments and *Luciferase* reporter gene measurements were made as described (see Chapter 2 section describing transient expression assays). *Luciferase* measurements were normalised against protein levels to control for cell number. In all cases an SV40-*lacZ* reporter plasmid was co-transfected to allow *Luciferase* measurements to be normalised for transfection efficiency. *Luciferase* expression data was tested for overall significance with one-way analysis of variance (ANOVA). Mean expression levels for each construct were then tested using Bonferroni's multiple comparison test. All tests were performed at the 5% significance level.

### *CCD deletion*

To further delineate enhancers within the CCD region, *Luciferase* expression levels were determined following the transfection of the **H** construct and two CCD deletion constructs, **pCCD4** and **pCCD11**, into primary choroid plexus cultures. The **A** construct contains the *H19* endoderm-specific enhancer region and was transfected as a negative control. The results are expressed in **Table 8** as ratios of the test constructs to the basal expression level provided by the **M** construct. Mean *Luciferase* expression levels for each construct are summarised in **Figure 23**. The CCD demonstrated silencer activity when *in cis* to P3 with a  $0.243 \pm 0.022$  level of *Luciferase* reporter gene expression from **H** compared to basal levels provided by **M** ( $p < 0.001$ ). Neither of the deletion constructs showed significant differences in *Luciferase* expression when compared against that of **H** or with one another.

**Figure 22. *Igf2* promoter 3 (P3) *Luciferase* reporter constructs used in transient expression assays.** All constructs are derived from the M construct (P3-*Luciferase*). Construct names are shown on the left and regulatory regions ligated *in cis* to P3-*Luciferase* are shown as open boxes on the right. These regulatory regions are contained within the following fragments: ***H19* enhancers** (2.7kb *SpeI*-*BglII* fragment); ***CCD*** (2kb *EcoRI* fragment); ***CCDA r1*** (0.9kb *PstI*-*EcoRI* fragment containing CCD region 2); ***CCDA r2*** (1.1kb *EcoRI*-*PstI* fragment containing CCD region 1); ***C1*** (1.2kb *NotI* fragment); ***C2*** (0.75kb *NotI* fragment); ***C3-5*** (5kb *NotI* fragment containing intergenic conserved elements 3,4 and 5).



The experiment was repeated in HepG2 cells. The results are expressed in **Table 9** as ratios of the test constructs to the basal expression level provided by the **M** construct. Mean *Luciferase* expression levels for each construct are summarised in **Figure 24**. No significant differences were observed in *Luciferase* reporter gene expression from **H** compared to the basal levels provided by **M**. in HepG2 cells. Although unresponsive in the primary choroid plexus cultures, the **A** construct containing the *H19* liver-specific enhancer region mediated a highly significant  $11 \pm 0.022$  fold increase ( $p < 0.001$ ) in *Luciferase* reporter gene expression over basal levels, confirming that the assay was able to discriminate tissue-specific responses of the constructs. In summary, silencing activity from the CCD (**H** construct) was only observed in primary choroid plexus epithelial cells but not HepG2 cells. Enhancer activity from the *H19* endoderm-specific enhancer region was observed in HepG2 cells consistent with previous work (Yoo-Warren *et al.* 1988; Leighton *et al.* 1995; Ward *et al.* 1997) but not in primary choroid plexus cultures.

#### *Intergenic conserved regions*

To determine whether any of the conserved intergenic regions could function as enhancers when *in cis* to P3, *Luciferase* expression levels were measured following transfection of the intergenic region constructs **C1**, **C2** and **C3-5** constructs into primary choroid plexus epithelial cells. The results are expressed in **Table 10** as ratios of the test constructs to the basal expression level provided by the **M** construct. Mean *Luciferase* expression levels for each construct are summarised in **Figure 25**. None of the conserved regions significantly increased *Luciferase* reporter gene expression over basal levels provided by **M**. The **C3-5** construct exhibited a  $0.436 \pm 0.058$  level of *Luciferase* expression compared with basal levels ( $p < 0.05$ ) suggesting the presence of silencer activity.

The experiment was repeated in HepG2 cells. The results are expressed in **Table 11** as ratios of the test constructs to the basal expression level provided by the **M** construct. Mean *Luciferase* expression levels for each construct are summarised in **Figure 26**. The **C2** construct exhibited a  $1.94 \pm 0.058$  fold increase in *Luciferase* expression compared with basal levels provided by **M** ( $p < 0.05$ ) suggesting the presence of enhancer activity. As before, the **A** construct produced a highly significant response.

Silencer activity from the C3-5 construct observed in choroid plexus cultures was not seen in HepG2 cells, in contrast to choroid plexus cultures.

*Intergenic conserved region/ CCD synergism*

To ask whether the intergenic conserved regions can function as enhancers in combination with the CCD when placed together *in cis* to P3, a series of synergism constructs containing various combinations of the C1 and C2 elements with the CCD were transfected into primary choroid plexus cultures. The results are expressed in **Table 12** as ratios of the test constructs to the basal expression level provided by the **M** construct. Mean *Luciferase* expression levels for each construct are summarised in **Figure 27**. None of the constructs exhibited expression levels over basal levels. Furthermore no significant differences in expression levels were observed between the constructs, indicating that synergistic interactions between the elements tested are unlikely. This experiment was not done in HepG2 cells.



**Table 8. Summary of transient expression data for CCD deletion constructs, primary choroid plexus cells.** The **M** construct provides the basal expression level for this assay, to which the test constructs are compared. Normalised expression levels are expressed as construct expression divided by the basal expression level for each replicate (n=5). The mean, standard deviation (S.D.) and the standard error of the mean (S.E.M.) are presented for each test construct.

**Figure 23. Luciferase expression levels following transfection of CCD deletion constructs, primary choroid plexus cells.** Mean normalised expression levels are shown for all test constructs. The mean basal expression level provided by the **M** construct is given as 1. Error bars show the standard error of the mean. There were significant differences between **M** and all test constructs ( $p < 0.001$ \*\*\*)

Replicate	Normalised expression levels: ratio/control				
	A	H	CCD4a	CCD11a	pBS
1	0.6	0.174	0.278	0.261	0.017
2	0.6	0.269	0.346	0.231	0.000
3	0.9	0.309	0.515	0.221	0.000
4	0.6	0.230	0.396	0.395	0.020
5	0.5	0.235	0.395	0.519	0.020
<b>Mean</b>	<b>0.639</b>	<b>0.243</b>	<b>0.386</b>	<b>0.325</b>	<b>0.011</b>
<b>S.D.</b>	<b>0.174</b>	<b>0.050</b>	<b>0.087</b>	<b>0.129</b>	<b>0.010</b>
<b>S.E.M.</b>	<b>0.078</b>	<b>0.022</b>	<b>0.039</b>	<b>0.058</b>	<b>0.004</b>

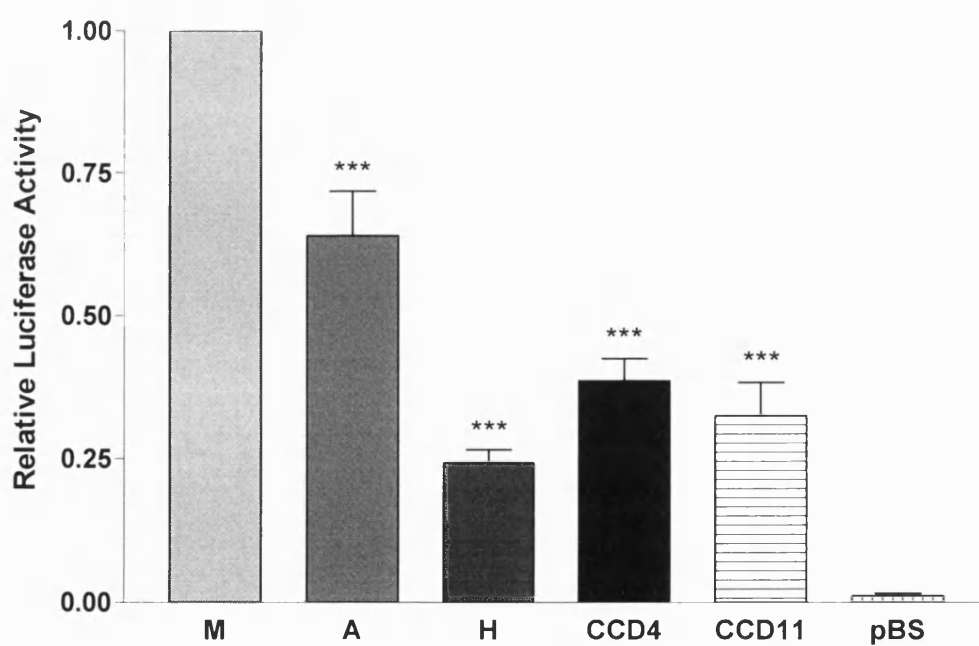


Figure 23. CCD deletion constructs, primary choroid plexus cells.

**Table 9. Summary of transient expression data for CCD deletion constructs, HepG2 cells.** The **M** construct provides the basal expression level for this assay, to which the test constructs are compared. Normalised expression levels are expressed as construct expression divided by the basal expression level for each replicate (n=3). The mean, standard deviation (S.D.) and the standard error of the mean (S.E.M.) are presented for each test construct.

**Figure 24. Luciferase expression levels following transfection of CCD deletion constructs, HepG2 cells.** Mean normalised expression levels are shown for all test constructs. The mean basal expression level provided by the **M** construct is given as 1. Error bars show the standard error of the mean. There were significant differences between **M** and **A** ( $p = <0.001^{***}$ ).

Replicate	Normalised expression levels: ratio/control				
	A	H	CCD4	CCD11	pBS
1	8.8	0.52	0.59	0.59	0.000
2	12.9	0.56	1.000	0.65	0.000
3	11.3	0.52	0.82	0.73	0.000
<b>Mean</b>	<b>11.0</b>	<b>0.533</b>	<b>0.803</b>	<b>0.657</b>	<b>0.000</b>
<b>S.D.</b>	<b>2.061</b>	<b>0.023</b>	<b>0.206</b>	<b>0.070</b>	<b>0.000</b>
<b>S.E.M.</b>	<b>1.190</b>	<b>0.013</b>	<b>0.119</b>	<b>0.041</b>	<b>0.000</b>

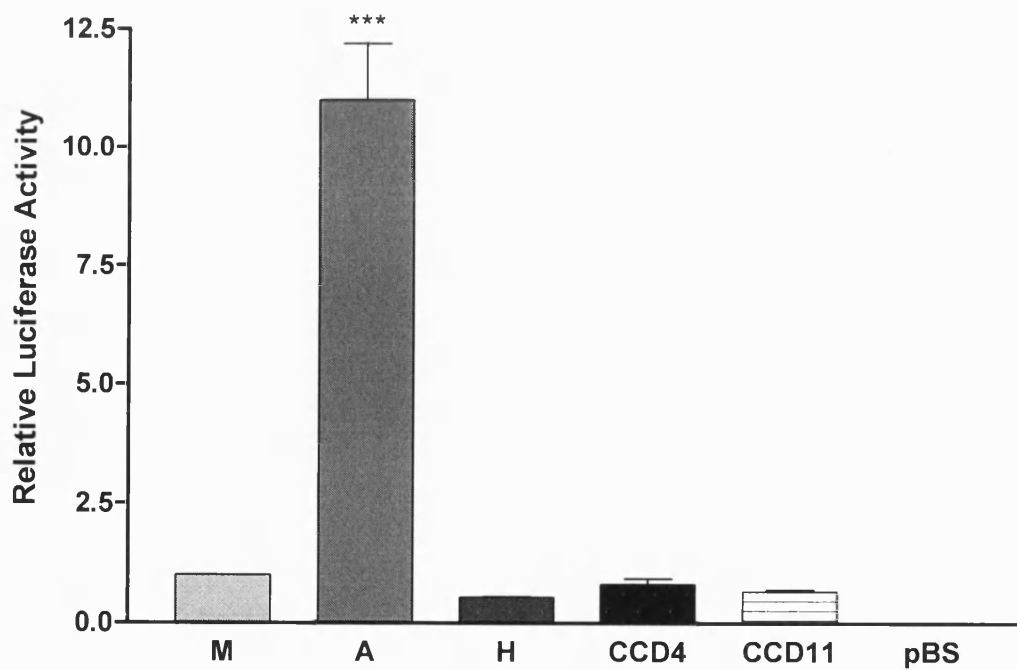


Figure 24. CCD deletion constructs, HepG2 cells.

**Table 10. Summary of transient expression data for intergenic conserved region constructs, primary choroid plexus cells.** The **M** construct provides the basal expression level for this assay, to which the test constructs are compared. Normalised expression levels are expressed as construct expression divided by the basal expression level for each replicate (n=5). The mean, standard deviation (S.D.) and the standard error of the mean (S.E.M.) are presented for each test construct.

**Figure 25. Luciferase expression levels following transfection of intergenic conserved region constructs, primary choroid plexus cells.** Mean normalised expression levels are shown for all test constructs. The mean basal expression level provided by the **M** construct is given as 1. Error bars show the standard error of the mean. There was a significant difference between **M** and **C3** ( $p < 0.05^*$ ).

Replicate	Normalised expression levels: ratio/control				
	A	C1	C2	C3	pBS
1	0.880	1.35	1.610	0.450	0.010
2	0.750	1.290	1.440	0.540	0.010
3	0.530	0.680	1.190	0.330	0.010
4	0.920	0.460	1.800	0.580	0.000
5	0.350	0.620	0.960	0.280	0.000
<b>Mean</b>	<b>0.686</b>	<b>0.880</b>	<b>1.400</b>	<b>0.436</b>	<b>0.006</b>
<b>S.D.</b>	<b>0.242</b>	<b>0.410</b>	<b>0.333</b>	<b>0.130</b>	<b>0.005</b>
<b>S.E.M.</b>	<b>0.108</b>	<b>0.183</b>	<b>0.149</b>	<b>0.058</b>	<b>0.002</b>

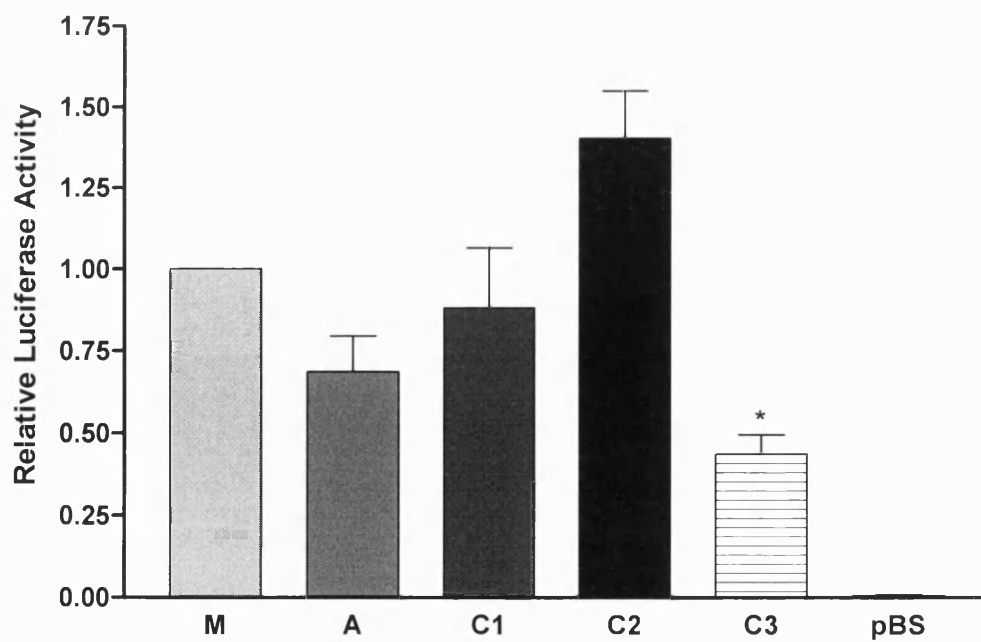


Figure 25. Intergenic conserved region constructs, primary choroid plexus cells.

**Table 11. Summary of transient expression data for intergenic conserved region constructs, HepG2 cells.** The **M** construct provides the basal expression level for this assay, to which the test constructs are compared. Normalised expression levels are expressed as construct expression divided by the basal expression level for each replicate (n=3). The mean, standard deviation (S.D.) and the standard error of the mean (S.E.M.) are presented for each test construct.

**Figure 26. Luciferase expression levels following transfection of intergenic conserved region constructs, HepG2 cells.** Mean normalised expression levels are shown for all test constructs. The mean basal expression level provided by the **M** construct is given as 1. Error bars show the standard error of the mean. There were significant differences between **M** and **A** ( $p = <0.001^{***}$ ) between **M** and **C2** ( $p = <0.05^*$ ).

Replicate	Normalised expression levels: ratio/control				
	A	C1	C2	C3	pBS
1	5.709	0.86	2.174	0.511	0.000
2	5.336	0.63	1.605	0.303	0.000
3	6.377	0.82	2.045	0.400	0.000
<b>Mean</b>	<b>5.807</b>	<b>0.770</b>	<b>1.941</b>	<b>0.404</b>	<b>0.000</b>
<b>S.D.</b>	<b>0.527</b>	<b>0.122</b>	<b>0.298</b>	<b>0.104</b>	<b>0.000</b>
<b>S.E.M.</b>	<b>0.304</b>	<b>0.070</b>	<b>0.172</b>	<b>0.060</b>	<b>0.000</b>

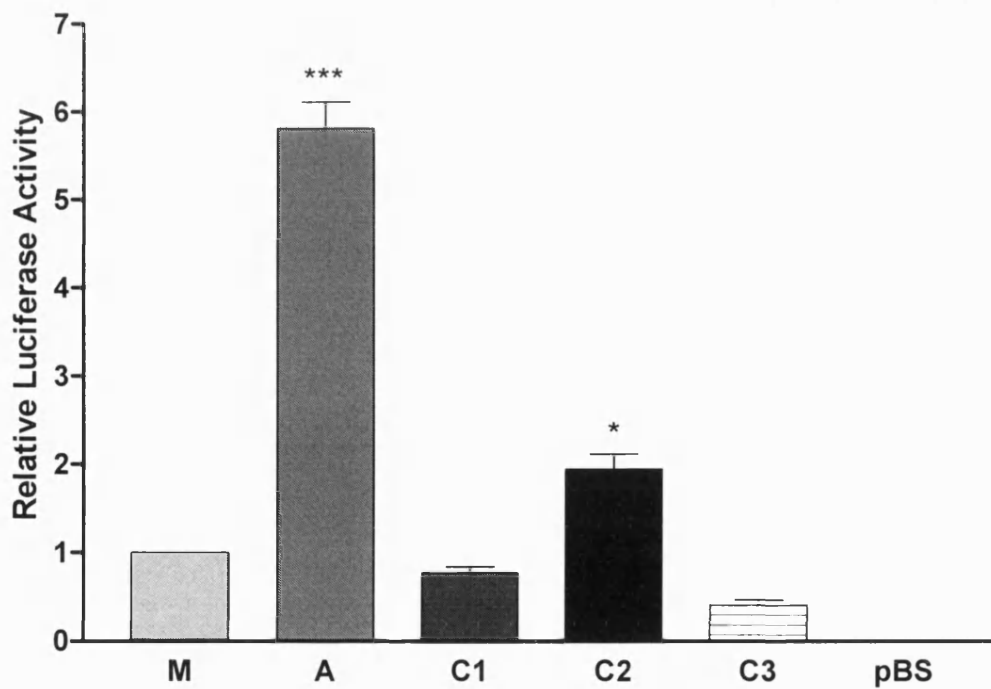


Figure 26. *Luciferase* expression levels of intergenic conserved region constructs, HepG2 cells.



**Table 12. Summary of transient expression data for enhancer synergism constructs, primary choroid plexus cells.** The **M** construct provides the basal expression level for this assay, to which the test constructs are compared. Normalised expression levels are expressed as construct expression divided by the basal expression level for each replicate (n=5). The mean, standard deviation (S.D.) and the standard error of the mean (S.E.M.) are presented for each test construct.

**Figure 27. Luciferase expression levels following transfection of enhancer synergism constructs, primary choroid plexus cells.** Mean normalised expression levels are shown for all test constructs. The mean basal expression level provided by the **M** construct is given as 1. Error bars show the standard error of the mean. There were no significant differences between any of the test constructs.

Replicate	Normalised expression levels: ratio/control							
	H	C1	C2	C1-C2	C1- CCD	C2- CCD	C1-C2 CCD	pBS
1	0.6	2.180	2.450	4.630	2.270	3.450	3.540	0.000
2	1.3	1.250	1.750	2.530	1.000	1.430	1.860	0.000
3	1.0	1.040	1.214	1.350	0.860	0.960	0.820	0.000
4	0.3	0.670	1.170	0.950	0.880	0.710	1.330	0.000
5	0.4	0.690	2.440	2.310	0.500	0.940	1.000	0.000
<b>Mean</b>	<b>0.754</b>	<b>1.166</b>	<b>1.805</b>	<b>2.354</b>	<b>1.102</b>	<b>1.498</b>	<b>1.710</b>	<b>0.000</b>
<b>S.D.</b>	<b>0.416</b>	<b>0.617</b>	<b>0.628</b>	<b>1.431</b>	<b>0.679</b>	<b>1.122</b>	<b>1.097</b>	<b>0.000</b>
<b>S.E.M.</b>	<b>0.186</b>	<b>0.276</b>	<b>0.281</b>	<b>0.640</b>	<b>0.304</b>	<b>0.502</b>	<b>0.491</b>	<b>0.000</b>

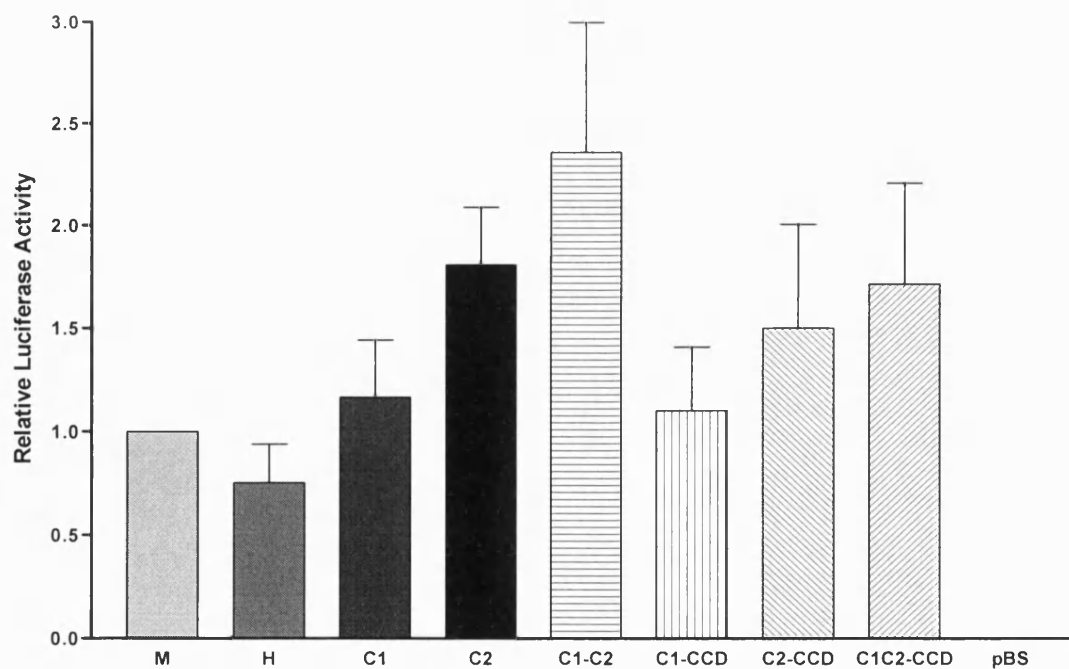


Figure 27. Enhancer synergism constructs, primary choroid plexus cells.

## **Conclusions**

Choroid plexus-specific expression of *Igf2* is likely to be controlled by at least two distinct regulatory regions. One region with this function has been identified, the CCD (Ward *et al.* 1997; Jones *et al.* 2001; Charalambous *et al.* 2004). Two small blocks of conserved sequence located within this region, the first of which contains two sites of strong DNase I hypersensitivity, are candidate *cis*-regulatory elements for choroid plexus gene expression. This hypothesis was tested here by analysis of CCD deletion *Luciferase* reporter constructs in transient assays. The existence of additional regulatory regions distinct from the CCD has been implicated by transgenic experiments, however their location is unknown (Jones *et al.* 2001). In this chapter, *Luciferase* reporter constructs containing conserved *Igf2/H19* intergenic sequences, placed *in cis* to P3, were analysed in transient assays in an attempt to elucidate the role of these sequences as additional choroid plexus-specific enhancers.

To test the function of these elements a primary choroid plexus culture system was set up. Primary cultures of choroid plexus epithelium have been successfully established from a range of mammalian species (Crook 1981; Thomas 1992; Holm 1994; Ramanathan 1996; Villalobos *et al.* 1997). In the present study, primary cultures were established from the mouse using a protocol developed previously (Charalambous 2000). Two further modifications to this protocol, the incubation of tissue in complete pre-warmed growth medium as opposed to PBS and a reduction in pronase concentration by 50%, appeared to increase the plating efficiency. It was not clear why these treatments were effective although it seems likely that cell survival is generally enhanced. Brains are held for periods exceeding 1 hour after animals are sacrificed while dissection takes place, thus incubation in growth medium creates a far better approximation of the natural tissue environment than PBS. As such the serum component of the medium provides an abundance of growth and attachment factors, thus enhancing both cell viability and plating. The reduction in pronase concentration may also have positively affected cell survival. During the disaggregation process it is possible that pronase activity renders a proportion of cells unable to attach, perhaps by destruction of surface adhesion molecules. It is also possible that pronase digestion at lower concentrations generates larger aggregates of epithelial cells that attach more effectively than smaller aggregates or single cells.

The origin of the cultured cells was confirmed with analyses of morphology and gene expression. Two principal cell-types were seen in the cultures. The first of these formed tight colonies and exhibited a polygonal, closely opposed ‘cobblestone’ morphology, all of which are characteristic features of epithelial cells in culture. The remaining cell-types were dispersed amongst the epithelial colonies and were fibroblastic in nature. Gene expression analysis revealed that the cultures abundantly expressed *Igf2* and *TTR* mRNA, both of which are diagnostic biochemical markers for the choroid plexus epithelium. It was also demonstrated that TTR protein was located only in the epithelial cells. A substantial component of the primary culture was likely to have originated from the choroid plexus epithelium. Cells of a fibroblastic morphology were also seen in the cultures. These cells did not express E-cadherin or TTR protein by immunofluorescence and were therefore unlikely to be derivatives of the choroid plexus epithelium. It seems more likely that these cells originated from the choroid plexus stroma.

Most of the cells presented morphological and biochemical properties of the choroid plexus epithelial tissue, however a number of stromal cells were also present. The type of culture system used in this study therefore cannot be considered homogeneous for the epithelial component. As has been shown in Chapter 3, the imprinting status of *Igf2* is not continuous across the epithelial and stromal components of the choroid plexus. The regulatory elements involved might be predicted to behave differently dependent upon the cell-type. Such cell-type specific effects would not have been distinguished in this system therefore conclusions drawn from the transient assays cannot necessarily be directly extrapolated to the choroid plexus epithelium *in vivo*.

Various *Luciferase* reporter constructs were transiently expressed in the cultures to examine any tissue-specific enhancer activity that might be present within conserved sequences from the *Igf2/H19* intergenic region. Surprisingly, rather than acting as an enhancer, the CCD conferred a reproducible and highly significant degree of silencing upon P3 *in cis* with *Luciferase* reporter gene expression ratio of  $0.243 \pm 0.022$  ( $p < 0.001$ ) from the **H** construct compared to basal levels provided P3 alone from the **M** construct. The silencing effect was not observed in HepG2 cells, therefore indicating that this activity may be restricted in a tissue-specific manner, although

because of the low number of replicates (n=3) this conclusion should be treated with caution.

Two previous studies have described a tissue-specific silencing function within region 1 of the CCD, which is active in skeletal muscle (Ainscough *et al.* 2000b; Jones *et al.* 2001). In the present study, reporter gene expression levels were consistently higher following transfection of the **pCCD4** construct, which carried the region 1 deletion, compared with that of the **H** construct containing the non-deleted CCD, although this effect was not significant. Notwithstanding, this observation could be consistent with the silencing activity observed within region 1 *in vivo* (Ainscough *et al.* 2000b).

Despite muscle-specific activity, a silencing function within the CCD active in choroid plexus tissue, as implicated by the present study is nonetheless surprising given the findings of two other transgenic studies where this region in fact conferred enhancer activity upon reporter genes in the choroid plexus (Ward *et al.* 1997; Charalambous *et al.* 2004). In the former study, the constructs **H** and **M** produced opposite responses when integrated as transgenes to that observed in transient assays in the present study. *Luciferase* expression levels measured in choroid plexus tissue dissected from **H**-construct bearing lines were approximately 50-fold greater than basal levels provided by **M**-construct bearing lines (Ward *et al.* 1997). Taken with this evidence, data from the present study may indicate that the CCD can behave as an enhancer within an integrated context, but not upon extra-chromosomal plasmids.

Does CCD enhancer activity require a chromatin environment in order to function? Previous studies have demonstrated that transiently transfected plasmids become chromatinized to a certain extent and that histones can assemble on them. At the same time this acquisition of chromatin was incomplete and did not fully recapitulate the *in vivo* structure (Reeves 1985; Jeong 1994). The function of many *cis*-acting elements involves complex interactions with higher order chromatin structure and it could be argued that chromatin organisation at the plasmid level may not fully support these functions in some cases. It is perhaps noteworthy that two sites of strong hypersensitivity to DNase I have been identified within CCD region 1 (Koide 1994). That is, sequences within this region are able to locally affect the higher-order structure of chromatin. It is possible that enhancer activity at the CCD is dependent

upon interactions with a defined chromatin structure that cannot properly condense upon extra-chromosomal plasmids.

The apparent requirement for integration into a chromosomal context, as transgenic studies seem to suggest, might indicate that the circular arrangement of the plasmid environment (as opposed to the linear conformation of transgenes) generates interference between opposing regulatory activities at the CCD. That is, enhancer activity may have been subject to artifactual suppression by a silencer function in the transient assays, although how this would occur mechanistically is unclear. One explanation is that the close proximity of the CCD to P3 within the plasmid context, compared with their more distant separation at the endogenous locus, may have imposed an artificial silencing effect. Interestingly, the DMD (which also functions as a silencer at its endogenous locus) was found to impose such distance-dependent silencing upon the *H19* promoter in transient expression assays (Drewell *et al.* 2000) (Ginjala 2002). That is, the DMD conferred a second cryptic silencing activity. At present, such an effect cannot be excluded from the experiments in this study, although this could be addressed empirically by the creation of further constructs that contain various spacer fragments to increase the separation between P3 and the CCD.

The analysis described above and the findings of previous studies (Ward *et al.* 1997; Ainscough *et al.* 2000b; Jones *et al.* 2001)(Charalambous *et al.*2004) support an argument that both positive and negative regulatory functions reside within the CCD region. The significance of two opposing activities within this region is unclear. However, given the evidence that the CCD contains sequences sufficient to direct variegated expression (Charalambous *et al.* 2004)(Erhardt *et al.* 2003), it could be argued that these features are consistent with an involvement in regulating variegated *Igf2* activation and/ or silencing in the choroid plexus epithelium. Indeed the apparent silencing imposed by the CCD upon P3 *in cis* could have reflected a CCD-mediated restriction in reporter gene expression to a fraction of the total number of cells transfected, i.e. to those that express *Igf2*. That is, the reporter gene was silenced in a subset of the cells transfected whilst in another subset its expression was activated.

Five conserved intergenic regions provided candidates for additional choroid plexus-specific enhancers at the *Igf2/H19* locus. As such *Luciferase* reporter constructs

containing these regions were transfected into primary choroid plexus cells although none elicited a significant enhancement of reporter gene expression over basal levels. Despite the small number of replicates it was concluded that none of these elements were able to drive reporter gene expression in the primary cultures. In HepG2 cells the C2 construct produced a *Luciferase* expression ratio of  $1.94 \pm 0.172$  ( $p < 0.05$ ) against basal levels (**Figure 26**). By contrast, in primary choroid plexus cells, although this construct consistently expressed at higher levels than basal, the data was not significant (**Figures 25 and 27**). This region may possess intrinsic enhancer activity, however the low number of replicates in each experiment means that any conclusion drawn from this data should be treated with caution.

In isolation neither the CCD, nor any of the conserved intergenic regions were able to reproducibly drive reporter gene expression in primary choroid plexus epithelial cells. To examine potential synergistic enhancer activity between these regions, constructs containing various combinations of the CCD with C1 and C2 regions were transfected into primary choroid plexus cells. Synergistic interactions of statistical significance were not observed for any combination of the three fragments tested. Although not significant, the largest mean *Luciferase* expression ratio of  $2.35 \pm 0.64$  compared with basal levels was observed for the C1-C2 construct, suggesting that at least one or both of these regions may possess enhancer activity. Again, the replicate number was low. The C3-5 region was not analysed, as its conserved sub-regions had not been tested in isolation at this stage. A role for any of the conserved intergenic regions as choroid plexus-specific enhancers cannot be excluded at present, in particular given evidence that the CCD, which exhibits enhancer activity *in vivo*, is also unable to drive reporter gene expression in primary choroid plexus cells.

A formal possibility not considered by the experiments in this study is that additional choroid plexus enhancer activity lies within the *Igf2* promoter 3 (P3) region. The transient expression data is consistent with this argument given that none of the constructs tested in primary choroid plexus cells demonstrated a significant increase in reporter gene expression (and in many cases showed a significant decrease) in comparison with the M construct containing P3 alone. Transgenes containing P3 are consistently expressed in the choroid plexus of transgenic mice and moreover a

germline deletion that encompassed the CCD, but not P3, reduced but did not completely ablate *Igf2* expression in this tissue (Ward *et al.* 1997; Jones *et al.* 2001; Charalambous *et al.* 2004; Kelly 2004). This hypothesis could be rapidly tested by analysis of additional constructs in which P3 is substituted for a heterologous promoter not normally active in the choroid plexus epithelium. The expression data presented in Chapter 3 suggests that the *H19* promoter would be suitable for this purpose. Prospectively, the generation of further transgenic lines bearing P3-*lacZ* reporter constructs could also clarify the role of P3.

Developmentally, the choroid plexus epithelium and hepatocytes of the liver arise from separate embryonic lineages, but intriguingly, are linked in the expression of many genes, particularly those with known roles in serum transport and in metabolism (Thomas 1989; Catala 1998; Chodobski 2001). Studies of the *Transthyretin* (*TTR*) gene have shown that expression from this locus in choroid plexus and liver utilises distinct regulatory regions (Yan 1990). With this in mind, two enhancer regions, the CCD and *H19* endoderm enhancer region that respectively confer *Igf2* expression in the choroid plexus and liver were investigated. Reporter gene expression levels from the **A** construct, containing the *H19* endoderm enhancer region, did not differ significantly from basal levels following transfection into the primary choroid plexus cultures although consistent with previous work, this construct was highly expressed in the liver-derived HepG2 cell line (Yoo-Warren *et al.* 1988; Leighton *et al.* 1995; Ward *et al.* 1997). *H19* transgenes that included this region were reproducibly expressed in the choroid plexus, yet no decrease in *H19* (or *Igf2*) expression was reported in the choroid plexus following deletion of this region (Brunkow 1991; Leighton *et al.* 1995). These results indicate that, similar to *TTR*, mechanisms governing *Igf2* expression in choroid plexus and liver are separable.

In summary, and in agreement with data from transgenic studies (Ainscough *et al.* 2000b; Erhardt *et al.* 2003) where the CCD was shown to act as a silencer in muscle lineages, this region also appeared to exert silencer activity upon P3 in a primary choroid plexus transient expression system (with caveats discussed). Potential roles for such silencer activity in this tissue are unclear, but might pertain to an involvement in variegated expression. Attempts to dissect this and other activities within the CCD using a transient system were unsuccessful. With this in mind, future work might



involve a transgenic approach to address this issue. Ainscough *et al.* did not uncover any choroid plexus-specific enhancer activity following deletion of a 1kb segment containing CCD region 1 (Ainscough *et al.* 2000b). Therefore, the second 1kb segment containing region 2 is a strong candidate for the choroid plexus enhancer region. Prospectively, the creation of a small germline deletion encompassing this region would be the most stringent means to test this proposal.

None of the conserved intergenic regions demonstrated clear enhancer activity in primary choroid plexus cells, suggesting either that they do not function as choroid plexus enhancers *in vivo*, or as has been shown for the CCD, a transient system is not a suitable means to investigate their activity. A transgenic approach should therefore be employed to test the function of these elements within the context of transgenes. The use of the *lacZ* reporter gene would allow any tissue-specific activity to be resolved at many different developmental stages, thus providing a more comprehensive analysis of these elements than was provided here by the transient assays. Additionally, the derivation of immortal choroid plexus epithelial cell lines (described in Chapter 5) may provide an alternative resource in which the function of these regions could be tested within stably integrated transgenes. Given its modest response in the transient assays, the C2 region would be a good candidate for this analysis. This region is highly conserved in mammals with a sequence identity of 98% in human and mouse comparisons, suggesting that it will prove functionally significant.

## CHAPTER 5: GENERATION AND CHARACTERISATION OF IMMORTAL CHOROID PLEXUS EPITHELIAL CELL LINES

### *Introduction*

Transgenic studies provide evidence that enhancer location plays a significant role in biallelic *Igf2* expression in the choroid plexus (Ward *et al.* 1997; Jones *et al.* 2001; Charalambous *et al.* 2004). Epigenetic studies show that the differentially methylated regions located proximal to the *Igf2* gene, DMR1 and DMR2, which confer methylation-dependent gene silencing or activation (Constancia *et al.* 2000; Eden *et al.* 2001; Murrell *et al.* 2001), are biallelically hypermethylated in the choroid plexus, suggesting that additional mechanisms are also important (Feil *et al.* 1994). The developmental expression analysis presented in Chapter 3 demonstrates that biallelic *Igf2* expression does not occur throughout the choroid plexus, but is restricted to the epithelial compartment of this tissue, whilst imprinted expression occurs in the stroma. To date, no attempt has been made to analyse epigenetic modifications in isolated choroid plexus epithelium. The creation of a culture system for choroid plexus epithelial cells would therefore assist in the identification of *cis*- and *trans*-imprinting factors that mediate biallelic *Igf2* expression in this tissue.

A method for culturing primary choroid plexus epithelial cells, described in Chapter 4 of this work, was developed as a means to analyse the function of putative regulatory elements. It was also hoped that this method could be used to address the impact of DNA methylation and chromatin structure upon *Igf2* transcription by treatment of the cultures with inhibitors of DNA methyl-transferase (Dnmt) and histone de-acetylase (HDAC) activity. However, these techniques require cells to be in an active state of proliferation, whereas the primary cultures do not proliferate and cannot be subcultured once plated. Moreover, these experiments would need extensive optimisation, requiring the sacrifice of large numbers of animals. The primary culture method was considered unsuitable for these reasons.

As discussed in Chapters 1 and 4, immortal choroid plexus epithelial cell lines have been established. However, such cell lines are scarce, with only three examples reported to date, one derived from the sheep and two from the rat (Torchio 1977; Kitazawa 2001; Zheng 2002). These cell lines are a superior choice as they are free

from the many limitations of primary culture. First, they would be expected to proliferate rapidly in culture and may be routinely subcultured. Moreover, all were isolated via a cell cloning approach and are therefore assumed to represent homogeneous culture systems. Although not demonstrated formally, these cell lines would also be expected to express *Igf2*, reflecting that of the choroid plexus epithelium *in vivo* (Stylianopoulou *et al.* 1988b; DeChiara *et al.* 1991) and in primary choroid plexus cultures derived from these species (Holm 1994; Nilsson 1996). For numerous reasons, these cell lines were not used in the present study. The sheep cell line is known to be infected with the Maedi-Visna virus, its potential use therefore raising containment issues. Furthermore, this cell line has a fibroblastic phenotype, suggesting that it has undergone a degree of de-differentiation whilst in culture or was in fact derived from stromal cells (Torchio 1977). One of the rat cell lines was conditionally immortalised by a temperature sensitive (ts) allele of SV40 T-antigen and must be cultured at 33°C (Kitazawa 2001). This physiological condition would cast doubt over any extrapolation of results to the *in vivo* environment. Finally, the locus under investigation in the present study originates from the mouse, whereas all available cell lines were derived from other species. Given that the genomic organisation and regulation of the *Igf2/H19* locus exhibits a degree of divergence between mammalian species (Schofield and Tate 1987; Overall 1997; Charalambous 2000; Onyango *et al.* 2000; Jones *et al.* 2002; Ulaner 2003) it would be prudent to conduct any investigation within the context of a mouse system. Therefore, the principal aim of the work described in this chapter was to establish an immortal choroid plexus epithelial cell line from the mouse as an *in vitro* model for biallelic *Igf2* expression.

A principal route to cell immortality involves the respective gain or loss-of-function in key cell cycle regulators encoded by proto-oncogenes and tumour suppressor genes. The *p53* gene encodes a transcription factor that regulates progression through the G1/S phase cell cycle checkpoint and has been dubbed the 'guardian of the cell'. Mice that are homozygous for a *p53* null mutation (*p53*<sup>-/-</sup>) display an increased susceptibility to tissue sarcomas in particular those affecting the lymphoid tissues (Clarke 1993). The *p53* gene therefore functions as a tumour suppressor, by conferring cell growth restraint in a lineage specific manner. Consistent with this function,

primary mouse embryonic fibroblasts (PMEFs) derived from  $p53^{-/-}$  null mice are immortal and may be propagated into continuous cell lines (Kuerbitz 1992). Preliminary work done previously in the laboratory, suggests that in contrast to the observations in fibroblasts, primary choroid plexus epithelial cells carrying a  $p53^{-/-}$  null mutation may possess some survival advantage compared with WT cells of this type, but are not fully immortalised in culture (Charalambous 2000). Therefore, whilst loss of  $p53$  function provides a direct route to immortalisation in some cell types, it appears to be insufficient for immortalisation of choroid plexus epithelial cells.

T-antigens are produced by a number of mammalian tumour-inducing viruses and are thought to act by binding and subverting the function of host cell tumour suppressor genes. In this manner, T-antigens force terminally differentiated (and hence quiescent) host cells to express DNA replication proteins that the virus requires for its replication. In its natural host, the simian virus 40 (SV40) infects and perpetuates itself in differentiated kidney tissue. Upon infection the SV40 early promoter, which confers a high level of gene expression in a broad range of cell types, directs the synthesis of three proteins, a large T-antigen (hereafter referred to as T-antigen) of 708 amino acids and two small t-antigens (smt) of 175 and 135 amino acids, the function of which will not be discussed further. T-antigen is often sufficient for transformation in a large number of different cell types (Pipas 2001)(and references therein).

The principal transforming activity of T-antigen is bipartite, located between amino acids 350-450 and 525-625, and governs interaction with the tumour suppressor protein, p53. Mutants within this region of T-antigen that abrogate p53-binding are transformation defective in many cell types (Peden 1998). Genetic studies have shown that two additional transformation-related functions map to the amino-terminal 121 amino acids of T-antigen. The first of these corresponds to amino acids 105-114, which contains an LXCXE motif required for interaction with *Retinoblastoma* family tumour suppressor proteins (DeCaprio 1988; Ewen 1989). Another transforming activity is located between amino acids 1-82 and corresponds to a J-domain, a feature that is functionally conserved and indeed originally identified within the Hsp40 family of chaperone proteins. This domain directs interaction with the Hsp70 chaperones, which have known roles in protein refolding and stability (Helmbrecht 2000; Garrido

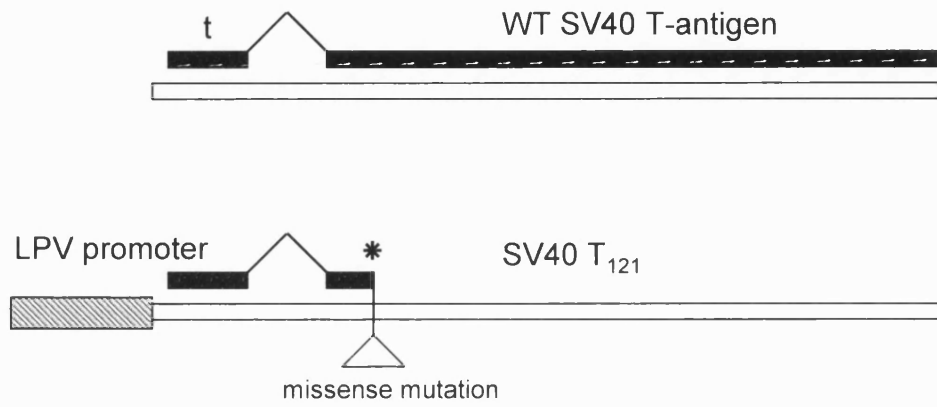
2003)(and references therein). Deletions within the J-domain of T-antigen are transformation defective (Peden 1992). Interestingly, there is evidence that the J-domain may co-operate with the *Retinoblastoma*-interacting domain in an Hsp70-dependent manner to disrupt interactions between *Retinoblastoma* proteins and E2F transcription factors, although the precise mode of action is unclear (Stubdal 1997)[Sullivan *et al.* 2000]. Three independent domains of T-antigen are therefore required for transformation in most cell types.

T-antigen overexpression has been used to immortalise continuous cell lines, indeed both of the existing rat choroid plexus cell lines were established using this approach (Kitazawa 2001; Zheng 2002) suggesting that it could also be successful in the mouse. The rat cell lines were induced to proliferate aberrantly and could be passaged indefinitely yet retained morphological and biochemical features consistent with their origin from the choroid plexus epithelium. Therefore T-antigen mediated immortalisation does not appear to unduly perturb the differentiated functions of this cell type. With this in mind a line of transgenic mice, the T<sub>121</sub> strain, which over-express a T-antigen variant were obtained (Saenz Robles *et al.* 1994). This variant known as T<sub>121</sub> was created by introduction of an 11 amino acid missense mutation after codon 121 in the wild-type T-antigen coding sequence, such that the protein is truncated at this point. The resulting T<sub>121</sub> protein therefore lacks the p53-binding domain, but retains the binding domain for *Retinoblastoma* proteins and the J-domain. The transgene is driven by the B-Lymphotropic papovavirus early promoter, which directs T<sub>121</sub> expression exclusively to the choroid plexus epithelium and lymphocytes ((Chen 1989) **Figure 28**). In this manner, T<sub>121</sub> selectively inactivates the function of *Retinoblastoma* proteins, but not *p53* in the choroid plexus epithelium.

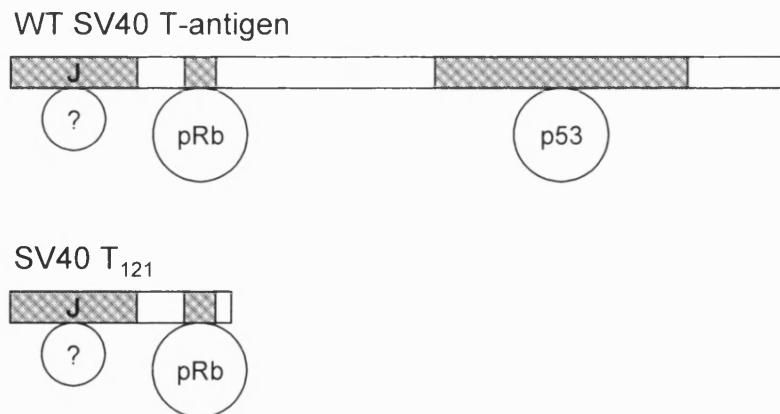
Studies utilising the T<sub>121</sub> line have elucidated the roles of T-antigen binding activities in cellular transformation. In mice, the choroid plexus epithelium normally exits from the cell cycle and becomes mitotically quiescent shortly after birth and remains so thereafter. Inactivation of *Retinoblastoma* proteins by T<sub>121</sub> induced aberrant cell proliferation and was sufficient for uniform tumourigenesis of the choroid plexus epithelium, without a requirement for *p53* mutations. Tumours induced in this manner

**Figure 28. Structure of the SV40 T<sub>121</sub> transgene.** **A** Structure of the wild type Sv40 large T-antigen gene is shown; the splice site that generates the small t-antigens is indicated. The structure of the *LPV-SV40 T<sub>121</sub>* transgene is also shown. The LPV early promoter which confers expression to the choroid plexus epithelium is shown as a shaded box. The insertion of 11 missense codons (\*) following codon 121 truncates the T-antigen protein at this position. **B** Structures of the WT and T<sub>121</sub> proteins; the binding domains for Retinoblastoma proteins and for p53 are shown; the J-domain (interacting factors are unknown and are denoted with a question mark) is also indicated. T<sub>121</sub> lacks the p53 binding domain, but retains the amino terminal J-domain and the binding domain for Retinoblastoma proteins (pRb).

## A Transgene



## B Protein



however were apoptotic and developed slowly, with death occurring at approximately 8 months of age (Saenz Robles *et al.* 1994). Suppressed tumour progression in these animals was attributed to *p53* function, as crossing the T<sub>121</sub> mice onto a *p53*<sup>-/-</sup> null background, thereby inactivating both *p53* and *Retinoblastoma*, lead to significantly more rapid uniform tumourigenesis of the choroid plexus epithelium, with death occurring at around 4 weeks of age. Interestingly, when crossed onto a *p53*<sup>+/-</sup> heterozygous background, T<sub>121</sub> induced phenotypically distinct focal tumourigenesis with an intermediate the end point, death occurring at approximately 8 weeks of age (Symonds 1994). Tumour progression was thought to be dependent upon *p53* in both cases, although its apparent latency in the latter instance probably reflecting the stochastic acquisition of mutations in the remaining functional *p53* allele. That is, in T<sub>121</sub> *p53*<sup>+/-</sup> animals, the tumour foci are presumed to have arisen from individual progenitor cells in which *p53* function had been completely lost. Taken together these experiments demonstrate that, while tumourigenesis of the choroid plexus epithelium can be induced following inactivation of *Retinoblastoma*, tumour progression is significantly accelerated following the combined inactivation of both *Retinoblastoma* and *p53*. Within this framework, it appeared that choroid plexus epithelial cells expressing T<sub>121</sub> in the presence of a *p53*-null mutation would provide suitable material from which to attempt derivation of a cell line.

To address imprinting mechanisms in a prospective choroid plexus epithelial cell line, a means to discriminate the parental alleles at *Igf2* would be essential. This is conventionally achieved by deriving the cells from the progeny of a cross between parents that exhibit DNA polymorphisms between the alleles. Two mouse strains were particularly suited to this purpose. The first of these, the *lacZ*DMR2<sup>-</sup> strain (described in detail in Chapter 3) carries a *lacZ* reporter gene, prospectively allowing either quantitative or *in situ* gene expression analysis within an immortal culture system. Whilst providing an excellent visual marker for *Igf2* expression, this strain would not provide a means for allele-specific epigenetic studies to be conducted in DMRs surrounding the *Igf2/H19* locus. The use of the second strain, the *spretus* upon distal chromosome 7, or SD7 strain was thought more suitable for this purpose. SD7 mice are derived from an original *Mus musculus* versus *Mus spretus* outcross, with the progeny then repeatedly backcrossed onto the *musculus* background such that only the distal region of chromosome 7 (containing the *Igf2/H19* locus) from *spretus* has been



retained. DNA polymorphisms specific to the *spretus* region have been described in *Igf2* and *H19* coding sequences and in the regulatory regions surrounding both genes (Forne *et al.* 1997; Hemberger 1998; Lopes *et al.* 2003). Both allele-specific expression and DNA methylation assays would therefore be possible in a cell line heterozygous for the SD7 chromosome.

The aim of the work in this chapter was therefore to derive a cell line from the choroid plexus epithelium, using the T<sub>121</sub> transgene as an immortalising agent and incorporating either the *lacZDMR2*<sup>-</sup> or SD7 alleles to permit allele discrimination. Prospectively, a cell line of this description would provide a resource for the *in vitro* evaluation and manipulation of epigenetic marks that regulate *Igf2* expression in the choroid plexus epithelium.

## **Materials and Methods**

### **Probes**

The *Igf2*, *H19* and *Foxj1* probes are described in Chapter 3. The *TTR* and *GAPDH* probes are described in Chapter 4. The *CTCF* probe is described in Chapter 3. The *Msx1* probe was described previously (Furuta 1997). The DMR1 probe was a 2.8kb *EcoR1*-*BamHI* fragment isolated from the G-construct plasmid described previously (Ward *et al.* 1997). The DMD probe was a 3.3kb *KpnI*-*ScaI* fragment isolated from the pICR plasmid described previously (Holmgren 2001). All probes for Northern and Southern analysis were isolated from their parent vectors by digestion with restriction enzymes and purification from agarose gels (see the relevant Chapter 2 sections). Probes were radioactively labelled prior to use (see Chapter 2 section describing synthesis of  $\alpha$ -<sup>32</sup>P(dCTP)-labelled DNA probes). The use of the *Igf2* probe for the purposes of *in situ* hybridisation is described in **Table 1**.

### **Plasmids**

Transferrin (*TFN*)-*DsRed* reporter constructs were created as follows. The TF-CAT and pBS-TF plasmids were the respective sources of the 0.6kb and 3kb TFN promoters (Chaudhary 1998). The reporter constructs were based upon the p*DsRed1*-N1 plasmid (Clontech) which contains the *DsRed* reporter gene driven by the Cytomegalovirus (CMV) promoter. p*DsRed1*-N1 was digested with *VspI* and *NheI* to excise the CMV promoter, the 3'recessed ends of the plasmid were removed by treatment with T4 DNA polymerase (see Chapter 2 section describing conversion of 5' and 3' recessed ends to blunt ends) and then re-ligated to create the p*DsRed* plasmid.

To create the -3kb*TFN*-*DsRed* construct, a 3kb *EcoRI*-*BamHI* fragment containing the 3kb *TFN* promoter from plasmid pBS-Tf was purified from an agarose gel and ligated into the *EcoRI* and *BamHI* sites of p*DsRed*.

To create the -0.6kb*TFN*-*DsRed* construct, a 0.75 kb *HindIII*-*XhoI* fragment containing the 0.6kb TFN promoter from plasmid Tf-CAT was similarly purified and ligated directionally into the *HindIII* and *SalI* sites of p*DsRed*. The constructs were sequenced to confirm the order and orientation of ligated fragments prior to use.

### Antibodies

Transthyretin (TTR), Transferrin, pan-cytokeratin and E-cadherin antibodies used for immunofluorescence cytochemistry are listed in **Table 13**.

Antibody	Source	Manufacturer	Dilution	Fixation
Transthyretin (TTR) $\alpha$ -human	rabbit	DAKO	1:100	4% (w/v) PFA
Transferrin (TFN) $\alpha$ -human	rabbit	DAKO	1:300	4% (w/v) PFA
Pan-cytokeratin $\alpha$ -mouse	mouse	Santa Cruz Biotechnologies	1:100	1:1 (v/v) acetone: methanol
E-cadherin $\alpha$ -mouse	mouse	Signal Transduction Laboratories	1:100	1:1 (v/v) acetone: methanol

**Table 13. Primary antibodies used for immunofluorescence cytochemistry.** The primary antibodies are shown in the far left column. The source species in which the antibodies were raised, the manufacturer, the dilutions at which they were applied and tissue fixation method employed are also shown.

### PCR Primers

Primer pairs specific to *Igf2* (exon3-4 containing transcripts) and to *E-cadherin* cDNA sequences, used for RT-PCR expression analysis are shown in **Table 14**. A primer pair to *lacZ*, used to detect transcripts from the *lacZDMR2* allele is described (refer to Chapter 2 section describing PCR genotyping of transgenic mice). All primers were designed from published cDNA sequences obtained from the National Centre for Biotechnology Information (NCBI) *Nucleotide* database. Genetool primer design software (Biotools, UK) was used to select primer pairs from these sequences.

Primer	Direction	Sequence
<i>Igf2</i> (ex3-4)	forward	5'- CCCCTCCCCACCAAAAAG -3'
	reverse	5'- GCCAAAGAGATGAGAAGCACCAAC -3'
<i>E-cadherin</i>	forward	5'GGC CCT TTC CCT GTT CCC TAG AGA-3'
	reverse	5'GCA AGA GCA AGT GGG AAC CCT GTC-3'

**Table 14. Primers used for RT-PCR expression analysis.**

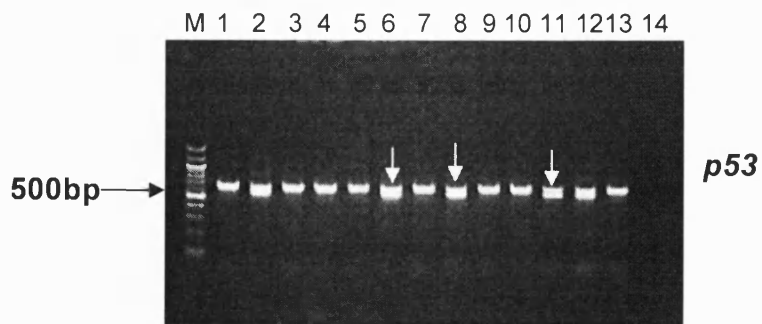
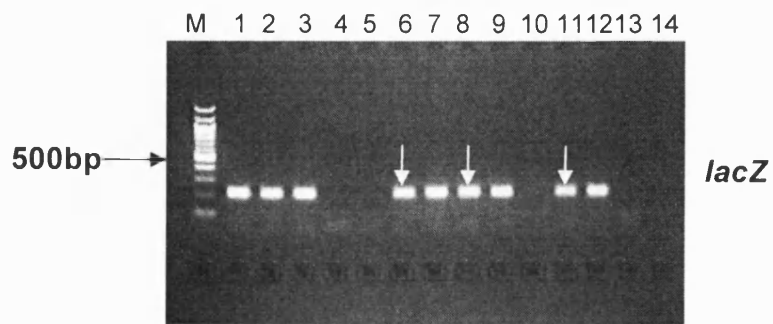
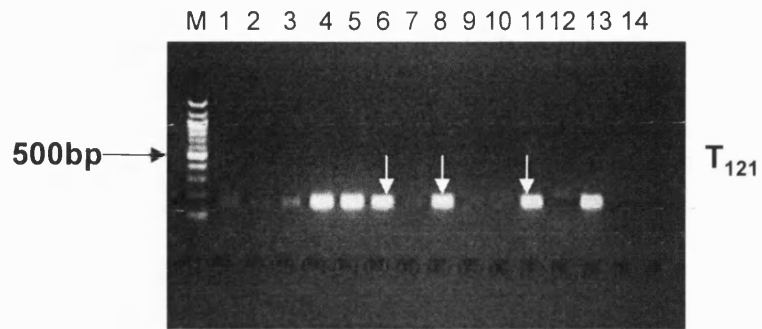
## Results

### Generation of immortal choroid plexus epithelial cell lines

#### *T-antigen mediated tumour induction*

Tumours were induced in mice genetically by crossing T<sub>121</sub> homozygous mice with *p53*<sup>-/-</sup> knockout homozygous mice such that all progeny carried the genotype T<sub>121</sub> *p53*<sup>+/-</sup>. For allele discrimination at *Igf2*, further crosses were done to introduce either the *lacZDMR2*<sup>-</sup> or SD7 allele as discussed in the Introduction to this chapter. In the case of *lacZDMR2*<sup>-</sup>, paternal transmission results in severe intra-uterine growth retardation with frequent neonatal death, whereas its maternal transmission produces no apparent phenotype, both of which are consistent with observations in *Igf2*-knockout mice (DeChiara *et al.* 1991; Murrell *et al.* 2001). To avoid complex phenotypes arising in the offspring, it was decided to transmit the *lacZDMR2*<sup>-</sup> mutation via the maternal germline. Therefore, to create T<sub>121</sub>:*p53*<sup>+/-</sup>:*lacZDMR2*<sup>-</sup> triple mutant mice, matings were set up between *lacZDMR2*<sup>-</sup> heterozygous females and T<sub>121</sub> homozygous males. Double mutant T<sub>121</sub>:*lacZDMR2*<sup>+/mat</sup> female animals were identified amongst the resulting progeny by PCR genotyping analysis (not shown, but see Chapter 2 section describing PCR genotyping). T<sub>121</sub>:*lacZDMR2*<sup>+/mat</sup> females were crossed with *p53*<sup>-/-</sup> males, and T<sub>121</sub>:*p53*<sup>+/-</sup>:*lacZDMR2*<sup>+/mat</sup> triple mutants identified amongst the progeny by PCR genotyping (**Figure 29**). From a litter of 13 animals, 3 triple mutants were identified. To create the T<sub>121</sub>:*p53*<sup>+/-</sup>:SD7 mice, an identical protocol was followed with SD7 homozygous females substituted for those carrying *lacZDMR2*<sup>-</sup>. Time constraints prevented the derivation of cell lines from the T<sub>121</sub>:*p53*<sup>+/-</sup>:SD7 mice, however tumours were induced in these animals, cells were isolated from them and frozen for future use. The experiment was continued with the triple mutant T<sub>121</sub>:*p53*<sup>+/-</sup>:*lacZDMR2*<sup>+/mat</sup> animals. These were monitored daily and those showing evidence of choroid plexus tumour development (as judged by the appearance of a bulged cranium) were sacrificed and tumours removed by dissection. Tumours were observed to have arisen at multiple foci within the choroid plexus of the lateral ventricle in all cases, consistent with previous observations for the T<sub>121</sub>:*p53*<sup>+/-</sup> genotype (Symonds 1994). These tumours were disaggregated to release the cells for culture (see Chapter 2 section describing isolation and culture of choroid plexus tumour tissue).

**Figure 29. PCR genotyping analysis, identification of  $T_{121}$ :  $p53^{+/-}$ :  $lacZDMR2^{+/mat}$  mutants.** Crude tissue lysates were made from a 4-week old litter derived from a  $p53^{-/-} \times T_{121}:lacZDMR2^{+/mat}$  cross and analysed by PCR using primers specific to the  $T_{121}$  transgene, to *lacZ* (*lacZDMR2*<sup>-</sup> allele) and to the *p53* locus. PCR reactions were analysed by gel electrophoresis where the presence of the  $T_{121}$  transgene, was indicated by a 170bp band (upper panel); the presence of the *lacZDMR2*<sup>-</sup> allele was indicated by a 206bp band (middle panel); in the *p53* assay, wild-type and knockout alleles were discriminated by 600bp and 500bp bands respectively (lower panel) such that the presence of both bands denotes the  $p53^{+/-}$  genotype. The analysis identified animals 6, 8 and 11 as triple mutants (indicated by vertical arrows). The molecular weight marker (M) is a 100bp DNA ladder where the lower of the two bright bands represents 500bp.



### *Isolation of clones by limiting dilution*

Disaggregated tumour tissue was cultured for 5 days after which two cell types predominated, colonies of epithelial morphology, which were presumed to have originated from the choroid plexus epithelium, and extensive colonies of rapidly proliferating fibroblastic cells, presumed to be of stromal origin. The epithelial colonies were isolated from the cultures with the use of cloning rings (see Chapter 2 section describing the cloning of cell lines by limiting dilution). In total, 4 colonies were successfully isolated in this manner and each distributed between 8 wells of a 96-well plate, thus establishing 32 subclones. These were cultured for an additional two weeks, after which only 2 subclones had yielded homogeneous populations of well-differentiated cells of epithelial morphology. The remaining 30 clones had become variably populated with fibroblastic growth and were discarded.

To derive clonal cell populations for expansion into cell lines, the limiting dilution method was employed (see Chapter 2 section describing the cloning of cell lines by limiting dilution). In theory, this involves the culture of single isolated cells such that all cells derived from them can be considered identical. Single cell suspensions were prepared from homogeneous subclones isolated in the previous stage, their cell concentrations were estimated by counting small aliquots on a haemocytometer, then these were serially diluted to an appropriate concentration and dispensed into 96-well plates. The plates were inspected to identify those wells that contained 1 cell (all other wells were then excluded from the experiment) and were incubated under standard culture conditions. Inspection of the plates after 5 days revealed that cell growth had not occurred in any of the wells and in many cases the cells had not even attached to the plate. Further incubation of these plates for periods of 3 weeks or longer and repeated attempts did not reveal any evidence of cell growth.

Given the epithelial nature of cells under study, it was postulated that contacts between adjacent cells perform an important cell viability function thus isolated cells might be compromised in their ability to divide in culture. With this in mind, further limiting dilution experiments were done as described above, but using suspensions of small cell aggregates rather than single cells, where it was hoped that minimal cell-cell contacts within aggregates could restore cell viability. A single 96-well plate was set up as before, but such that each well contained 1 cell aggregate. Inspection of the



plate after 5 days revealed expanding subclones in 14 wells. These subclones continued to expand with a further week in culture. As these subclones had not been established from single cells, the possibility remained that they were not clonal. Two of these subclones were therefore subjected to a second round of limiting dilution cloning from which a total of ten further subclones, termed CPlacZ1-10 were derived. Four of these subclones CPlacZ1, 2, 3 and 6 were successfully expanded into cell lines during a six-week period by successive passage through 96-well, 24-well and 6-well plates, then transferred into 25cm<sup>2</sup> flasks and finally expanded into 75cm<sup>2</sup> flasks. During the expansion process, aliquots of each cell line were cryopreserved at each passage.

## **Characterisation of immortal choroid plexus epithelial cell lines**

### *Morphology*

Closely opposed membrane junctions and ‘cobblestone’ morphology are differentiated features of the choroid plexus epithelial cells in culture (see Chapter 4). Examination of the cell lines by light microscopy revealed that this most important feature and been retained, thus suggesting that they originated from the choroid plexus epithelium. **Figure 30** shows a field of live cells from the CPlacZ6 line, where the morphological features described above are evident. A view of live primary choroid plexus epithelial cells (originally presented in Chapter 4) is shown for comparison.

### *Genotype analysis*

The genotype of each cell line was confirmed by PCR. Genomic DNA was prepared from all cell lines (see Chapter 2 section describing isolation of high-purity genomic DNA from mouse tissues). 1µl aliquots of the genomic DNA samples were amplified by PCR essentially as detailed earlier (see Chapter 2 section describing polymerase chain reaction) using primer pairs that allow discrimination of the T<sub>121</sub>, *p53* and (*Igf2*) *lacZDMR2*<sup>-</sup> mutations (see Chapter 2 section that describes genotyping transgenic mice by PCR). Completed PCR reactions were analysed by gel electrophoresis (**Figure 31**). As expected all cell lines were found to be positive for the T<sub>121</sub> transgene and heterozygous for the *lacZDMR2*<sup>-</sup> allele. Interestingly, all of the cell lines were found to carry the *p53*<sup>-/-</sup> genotype despite their original derivation from an animal that was heterozygous (*p53*<sup>+/-</sup>) for the *p53* knockout allele (see **Figure 29** for comparison).

Therefore the choroid plexus cell lines (and presumably the tumour from which they were derived) appear to have undergone loss of heterozygosity at *p53*.

### *Growth*

Successfully immortalised cell lines would be expected to proliferate at a greater rate than primary cells of the same origin when placed in culture. The growth of CPlacZ2 cells was compared against primary choroid plexus cultures derived from mice of the following genotypes; WT; T<sub>121</sub>, *p53*<sup>+/-</sup>; T<sub>121</sub> *p53*<sup>+/-</sup>. To generate mice of the T<sub>121</sub> genotype, T<sub>121</sub> homozygous males were mated with F<sub>1</sub> females. To generate mice of the *p53*<sup>+/-</sup> genotype, *p53*<sup>-/-</sup> homozygous males were mated with F<sub>1</sub> females. To generate mice of the T<sub>121</sub> *p53*<sup>+/-</sup> genotype, T<sub>121</sub> homozygous males were mated with *p53*<sup>-/-</sup> females. Litters of neonate mice born from each cross were sacrificed and primary choroid plexus cultures prepared (see Chapter 2 section describing primary culture of choroid plexus epithelial cells). Viable cell number counts (see Chapter 2 section describing growth curves) were collected daily over a 6 day period for the CPlacZ2 cells, which proliferate rapidly in culture and at 2-day intervals over a 12 day period for the primary choroid plexus cultures, which show a markedly lower rate of proliferation (**Figure 32a**). CPlacZ2 cells (which carried the T<sub>121</sub> *p53*<sup>-/-</sup> genotype) proliferated at a significantly greater rate than primary choroid plexus cultures prepared from T<sub>121</sub> *p53*<sup>+/-</sup> or T<sub>121</sub> mice, providing evidence that inactivation of *p53* dramatically enhances the growth effects of T<sub>121</sub>, consistent with observations *in vivo* (Symonds 1994). Non-linear regression analysis was used to calculate the mean doubling time of CPlacZ cells (**Figure 32b**). This was done by fitting an exponential curve to the viable cell count data, with a mean doubling time of 2.58 days calculated. Interestingly, the T<sub>121</sub> *p53*<sup>+/-</sup> primary cultures proliferated at a significantly greater rate than cultures that carried either the T<sub>121</sub> or *p53*<sup>+/-</sup> genotypes alone suggesting an additive effect upon growth. In addition, T<sub>121</sub> cultures displayed rate of proliferation significantly greater than wild type cultures, consistent with *in vivo* observations.

**Figure 30. Comparison of CPlacZ cell lines and primary choroid plexus cultures, morphological analysis.** The CPlacZ cell lines were examined by light microscopy. **A** CPlacZ6 cells exhibited a characteristic closely-opposed cobblestone morphology that is typically observed for epithelial cells in culture. The other cell lines derived following limiting dilution displayed an identical morphology (not shown). **B** A field of primary choroid plexus epithelial cells (previously shown in **Figure 11**) is shown for comparison. Magnifications  $\times 200$ .

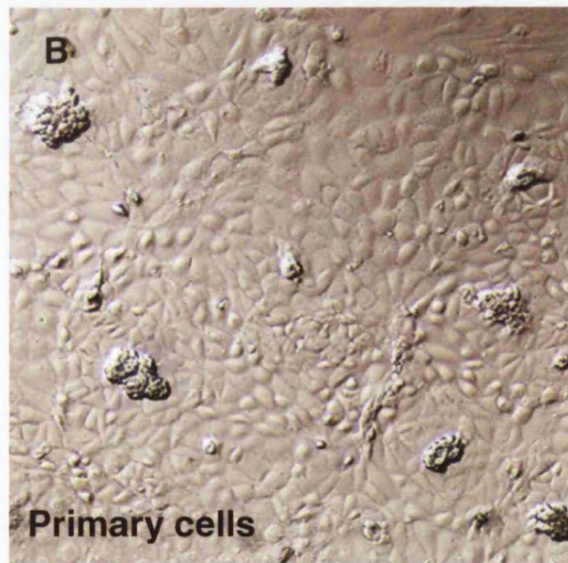
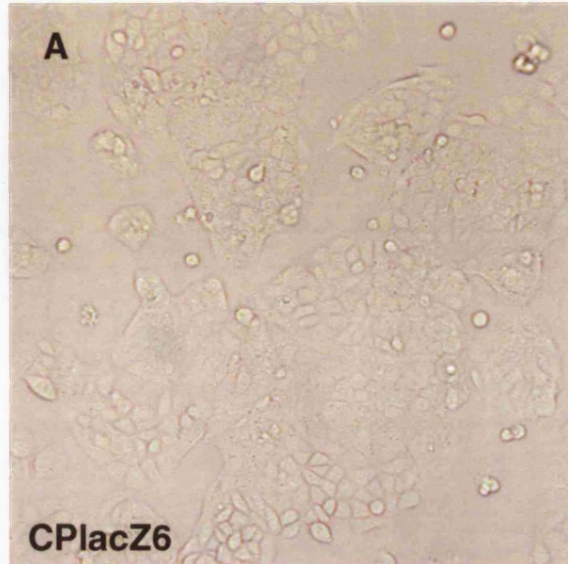
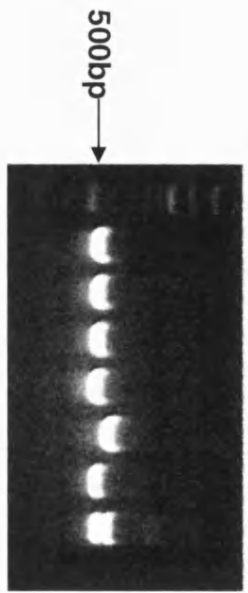
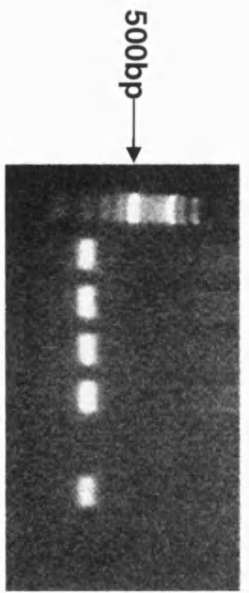


**Figure 31. PCR genotyping analysis, CPlacZ cell lines.** Genomic DNA was prepared from the cell lines and analysed by PCR using primers specific to the  $T_{121}$  transgene, *Igf2* intron 3/exon 4, to *lacZ* (*lacZDMR2<sup>-</sup>* allele) and to the *p53* locus (primer sequences are listed in the Chapter 2 section that describes genotyping transgenic mice by PCR). PCR reactions were analysed by gel electrophoresis; in the  $T_{121}$  assay, the presence of the  $T_{121}$  transgene is indicated by a 170bp band; in the *Igf2* assay, the presence of the endogenous *Igf2* allele is indicated by the presence of a 206bp band; in the *lacZ* assay the presence of the *lacZDMR2<sup>-</sup>* allele is indicated by a 206bp band; in the *p53* assay, wild-type and mutant alleles are discriminated by 600bp and 500bp bands respectively (lower panel) such that presence of both bands indicates the *p53<sup>+/-</sup>* genotype. The analysis showed that all cell lines are positive for  $T_{121}$  are heterozygous for the *lacZDMR2<sup>-</sup>* allele and have undergone loss of heterozygosity at the *p53* locus to become *p53<sup>-/-</sup>*. The molecular weight marker (M) is a 100bp DNA ladder where the lower of the two bright bands represents 500bp.



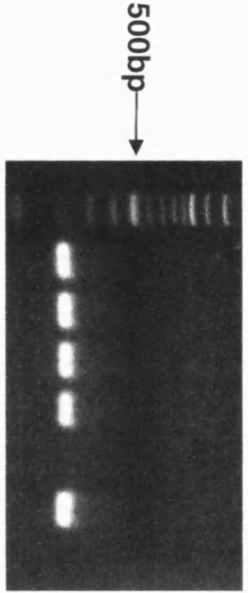
*p53*

M  
 C*PlacZ*1  
 C*PlacZ*2  
 C*PlacZ*3  
 C*PlacZ*6  
 WT  
 p53<sup>-/-</sup>  
 p53<sup>+/-</sup>



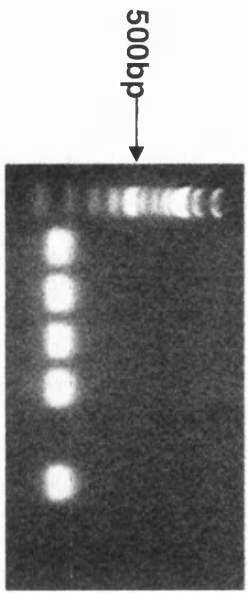
*lacZ*

M  
 C*PlacZ*1  
 C*PlacZ*2  
 C*PlacZ*3  
 C*PlacZ*6  
 WT (-ve)  
*lacZ* (+ve)



*Igf2*

M  
 C*PlacZ*1  
 C*PlacZ*2  
 C*PlacZ*3  
 C*PlacZ*6  
 Water (-ve)  
 WT (+ve)

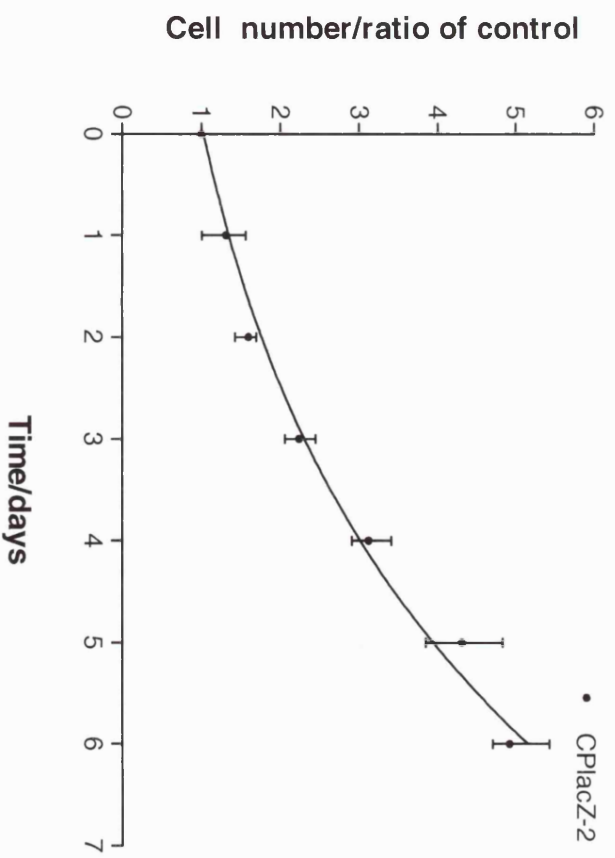
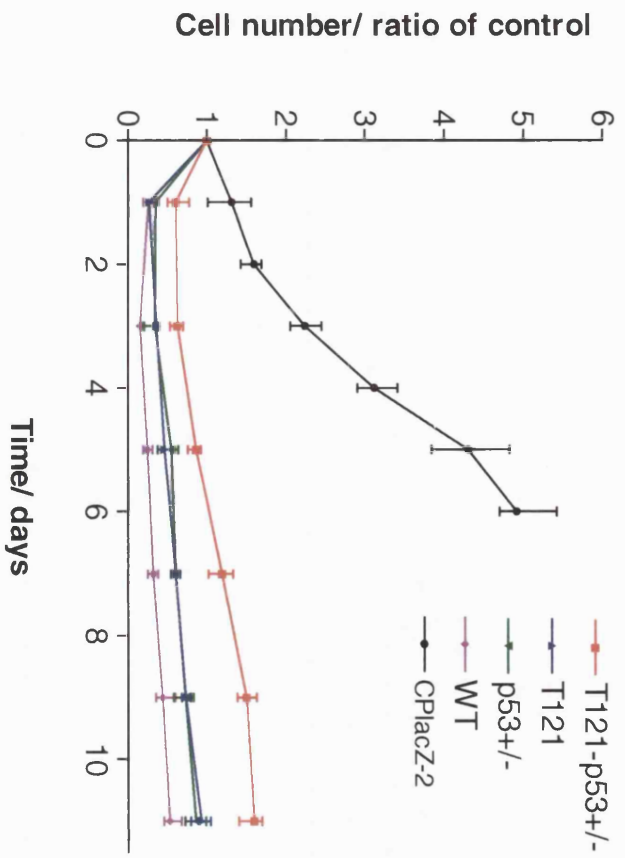


*T<sub>121</sub>*

M  
 C*PlacZ*1  
 C*PlacZ*2  
 C*PlacZ*3  
 C*PlacZ*6  
 WT (-ve)  
 T<sup>121</sup> (+ve)

**Figure 32a. Comparison of CPlacZ cell lines and primary choroid plexus cultures, cell growth in relation to  $T_{121}$  expression and  $p53$  function.** The growth of CPlacZ2 cells ( $T_{121} p53^{-/-}$ ) was compared against that of primary choroid plexus cultures carrying either the wild type (WT),  $T_{121}$ ,  $p53^{+/-}$  or  $T_{121}p53^{+/-}$  genotypes by counting the viable cell number. Cell number is shown as the ratio of the control (cell number at time 0). Each data point is the mean of 4 independent replicates with each replicate counted twice. Error bars show the standard error of the mean (S.E.M.). The combination of  $T_{121}$  activity and loss of  $p53$  function in CPlacZ2 cells leads to an increased rate of growth compared with  $T_{121}$  alone, which imparts a modest increase in growth compared with wild-type cells (compare error bars).

**Figure 32b. Quantitative growth of CPlacZ2 cells in culture.** An exponential curve was fitted to the viable cell number data for CPlacZ2 ( $R^2 = 0.9592$ ). A mean doubling time of 2.58 days was predicted by non-linear regression upon this curve. Cell number is shown as the ratio of the control (cell number at time 0). Each data point is the mean of 4 independent replicates with each replicate counted twice. Error bars show the S.E.M.

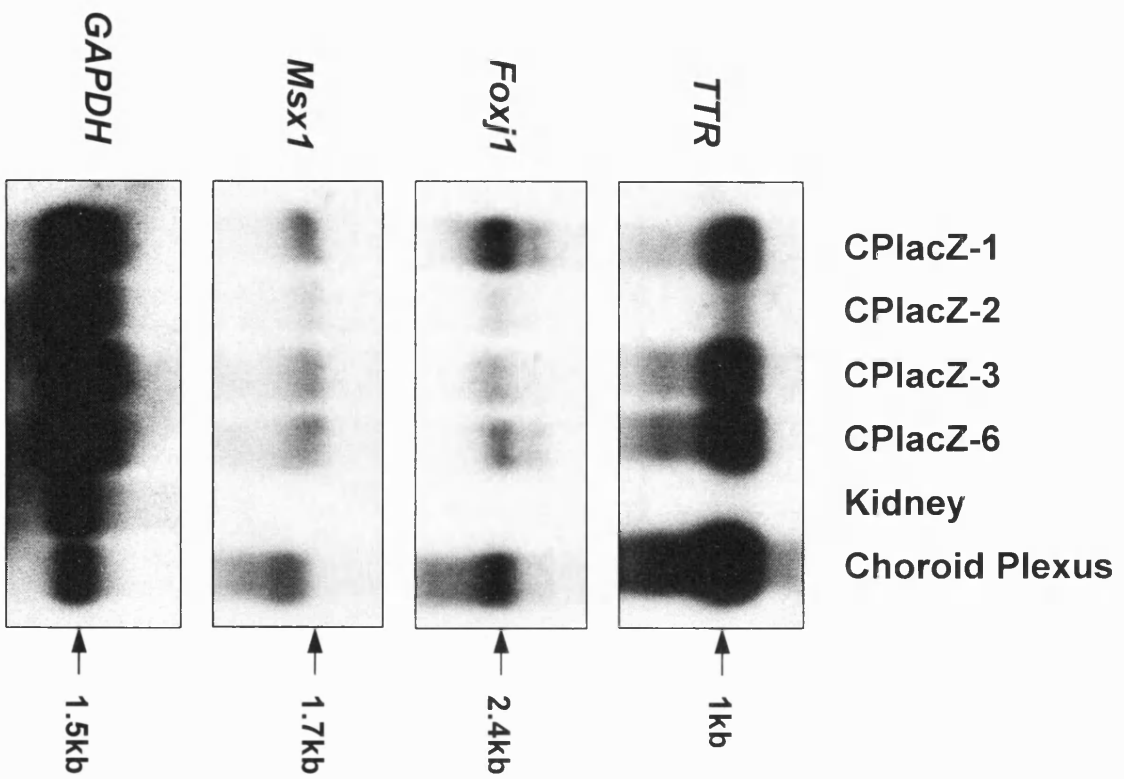




### *Gene expression - Northern analysis*

The expression of three genes, Transthyretin (*TTR*) *Foxj1* and *Msx1*, were analysed to confirm the identity of the cell lines. The function and expression of *TTR* is described in Chapters 3 and 4. *Foxj1* encodes a winged helix domain-containing transcription factor, which is required to correctly specify the left-right body axis and for formation of ciliated epithelia (Brody 2000). *Foxj1* is expressed in the developing choroid plexus epithelium from e10.5 of mouse development and continues to mark choroid plexus epithelial cells thereafter (Lim 1997). *Foxj1* therefore provided a good marker of differentiated choroid plexus epithelium. *Msx1* encodes a homeodomain protein with a prominent role in craniofacial development (Houzelstein 1997). *Msx1* expression occurs at several discrete sites in the developing brain including the choroid plexus epithelium and leptomeninges, Rathkes pouch, nasal recesses and streams of migrating cranial neural crest. In the presumptive choroid plexus epithelium, *Msx1* expression commences at e11.5 and is maintained as the choroid plexus matures (MacKenzie 1991). *Msx1* therefore provided a third marker for this gene expression analysis. RNA was isolated from the 4 cell lines and from neonate choroid plexus tissue, which acted as a positive control (see Chapter 2 section describing isolation of total RNA). Total RNA isolated from kidney at 3 weeks of age, a tissue in which neither *TTR*, *Foxj1* or *Msx1* expression would be expected, served as a negative control. The RNA samples were blotted and sequentially hybridised with probes to *TTR*, *Foxj1* and *Msx1* (**Figure 33**). Abundant expression of *TTR* was seen in all cell lines except CPlacZ-2, which only showed a weak signal. Two *TTR* transcripts were observed, a 1kb choroid plexus-specific transcript and 0.7kb transcript. *Foxj1* expression was variable between the cell lines with high levels of a 2.4kb transcript in CPlacZ-1, and slightly lower levels in all other lines with expression in CPlacZ-2 almost absent. *Msx1* expression followed a similar trend with abundant expression of a 1.7kb transcript clearly visible in CPlacZ-1, lower levels in the other cell lines and expression again almost absent in CPlacZ-2. Hybridisation with a *GAPDH* probe demonstrated approximately equal loading of RNA in each of the cell lines. With the exception of CPlacZ2 where marker expression was either weak or absent, the cell lines have retained the expression of three choroid plexus epithelial markers, *TTR*, *Foxj1* and *Msx1*.

**Figure 33. Northern analysis of *TTR*, *Foxj1* and *Msx1* expression in CPlacZ cell lines.** Total RNA prepared from the cell lines was blotted and successively hybridised with probes to the mouse *TTR*, *Foxj1* and *Msx1* genes. Total RNAs from week 3 kidney and from choroid plexus tissue were included as negative and positive controls for *TTR* expression respectively. Also shown is a separate probing for *GAPDH* which demonstrates equivalent loading of total RNA from each cell line.



### *Gene expression - Immunofluorescence*

Gene expression was also examined at the protein level by immunofluorescence (see Chapter 2 section describing immunofluorescence cytochemistry) using antibodies to TTR and to three additional markers, Transferrin (TFN), Pan-cytokeratin and epithelial (E-) cadherin. TFN, a major serum protein, performs an important function in the serum transport of iron and its major sites of expression in rodents and humans are liver hepatocytes, choroid plexus epithelium, oligodendrocytes of the brain and Sertoli cells of the testis. TFN is thought to be expressed in the developing and mature choroid plexus epithelium in mice and therefore provides an additional marker for this tissue (Tu 1991; Chaudhary 1998)(and references therein). Cytokeratins form an integral component of intermediate filaments in all epithelia and occur in obligate heterodimeric pairs. Simple secretory epithelia, within which the choroid plexus epithelium is classified, are primarily characterised by the expression of the cytokeratin 8/cytokeratin 18 pair, but often acquire cytokeratin 7, 19 and 20 expression as differentiation proceeds (Fuchs 1988; Owens 2003). The pan-cytokeratin antibody used here recognises all cytokeratins and would therefore be expected to positively stain choroid plexus epithelial cells. E-cadherin is found in all epithelia, including that of the choroid plexus, where it mediates homophilic cell-cell adhesion within specific membrane interfaces known as adherens junctions (Takeichi 1991). Both cadherins and cytokeratins participate in the provision of mechanical support that protects epithelial cells from external stress (Perez-Moreno 2003).

The CPlacZ cell lines were analysed using the same panel of primary antibodies. Results for the CPlacZ6 line, which were representative of observations made in the other cell lines, are shown. Primary choroid plexus epithelial cells analysed in parallel provided positive controls in all cases. **Figure 34** shows cells that have been stained with  $\alpha$ -TTR and  $\alpha$ -TFN primary antibodies and the staining pattern visualised with a fluorescein-labelled secondary antibody. TTR protein was present at high levels in a perinuclear distribution in both the cell line and primary cells. TFN protein was detected in an uncharacteristic submembrane distribution (a perinuclear distribution is typical for TFN, as seen in the HepG2 cells shown in **Figure 36**) in CPlacZ cells and all other CPlacZ cell lines tested. Surprisingly, TFN was not detected in the primary cells although some positive staining was expected on the basis of earlier work

(Tsutsumi 1989; Tu 1991) and also the strong immunoreactivity seen with the same  $\alpha$ -TFN antibody in sections of choroid plexus tissue presented in Chapter 3. **Figure 35** shows cells that have been stained with  $\alpha$ -pan-cytokeratin and  $\alpha$ -E-cadherin primary antibodies and the staining pattern visualised with a fluorescein-labelled secondary antibody. Neither of these proteins were obviously present in any of the cell lines, yet both were clearly present in primary choroid plexus epithelial cells with pan-cytokeratin staining localised to the cytoplasm of primary cells in a filamentous distribution, consistent with the distribution of intermediate filaments and with E-cadherin localised almost exclusively to the plasma membrane, consistent with its known activity at cellular adherens junctions (Fuchs 1988; Takeichi 1991; Owens 2003). Some evidence of E-cadherin immunoreactivity was seen in the perinuclear region of both CPlacZ cells and primary choroid plexus epithelial cells, possibly indicative of *de novo* synthesis of this protein.

In summary, the immunofluorescence analysis of the CPlacZ cell lines clearly demonstrated the expression of TTR and possibly TFN, but did not provide convincing evidence for the expression of the epithelial cell markers, E-cadherin or cytokeratins. An additional positive control for this analysis was provided by comparison of the choroid plexus cell lines and primary culture data with hepatocytes, an epithelial cell type that is known to highly express the markers used in this analysis (Tosh 2002b; Tosh 2002a). The hepatocyte-derived HepG2 cell line was exploited for this purpose and stained with the same panel of primary antibodies as before. The staining patterns were visualised with a fluorescein-labelled secondary antibody as before (**Figure 36**). As expected all of the markers were strongly expressed in HepG2 cells, confirming the sensitivity of the primary antibodies used in this analysis.

**Figure 34. Immunofluorescence: comparison of CPlacZ cell lines and primary choroid plexus cultures, hepatocyte/choroid plexus differentiation markers.** Cells were fixed and stained for the presence of two serum proteins, Transthyretin (TTR) and Transferrin (TFN). Images under both FITC and DIC conditions were collected by laser scanning confocal microscopy (left and right columns respectively). These images were overlaid as shown in merge (middle column). **A-F** TTR expression, **A-C** CPlacZ6 line, strong positive staining was observed in a perinuclear distribution; **D-F** Primary choroid plexus cultures, strong positive staining was observed as in the cell lines. **G-L** TFN expression, **G-I** CPlacZ6 line, uncharacteristic staining was observed in membranes and in a diffuse pattern throughout the cells. **J-L** Primary choroid plexus cultures, no positive staining was observed. **M-O** Negative control, CPlacZ6 cells incubated with fluorescein-labelled  $\alpha$ -mouse IgG secondary antibody. Scale bars show 10  $\mu$ m.

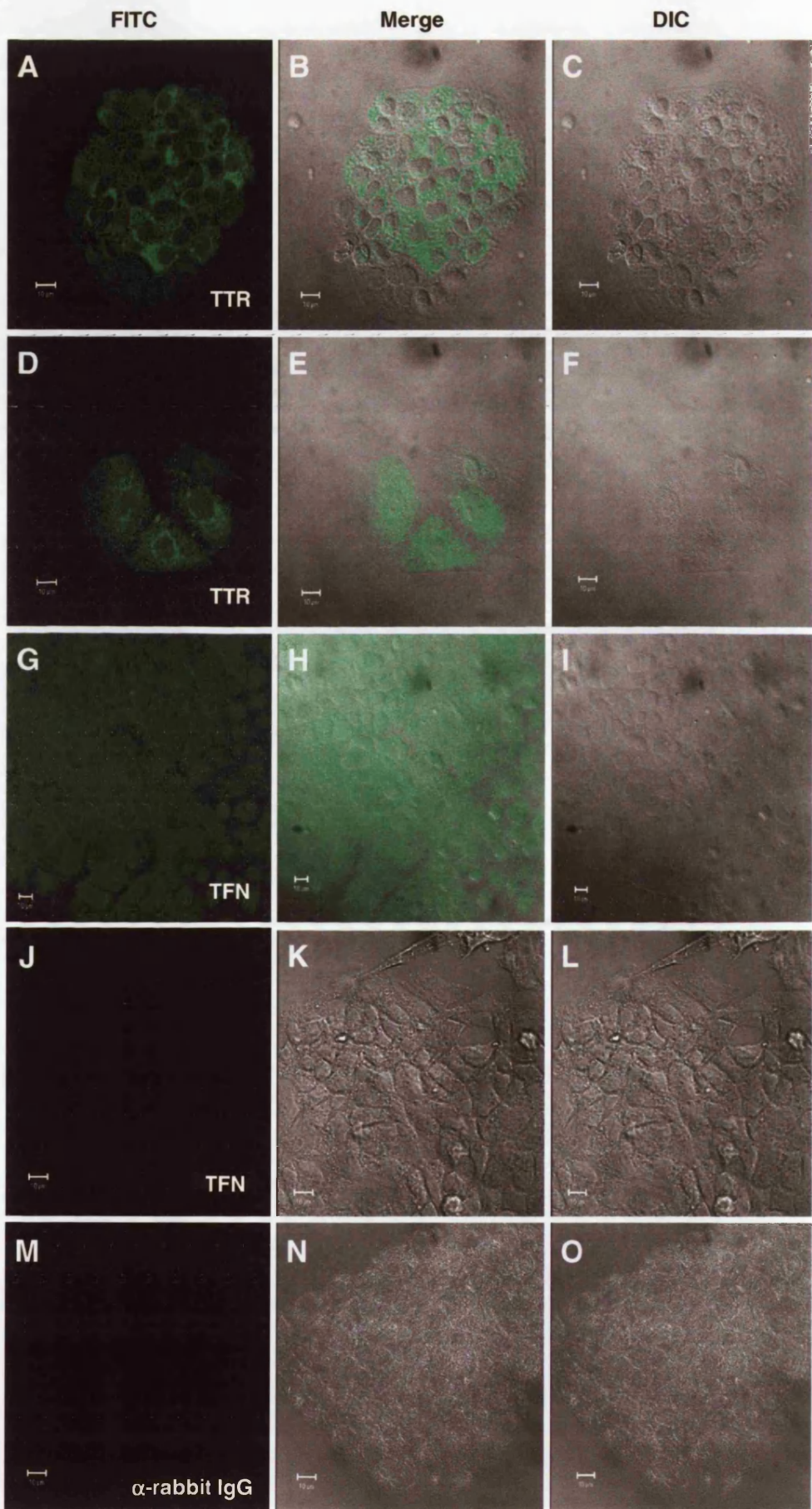


**Figure 35. Immunofluorescence: comparison of CPlacZ cell lines and primary choroid plexus cultures, epithelial cell differentiation markers.** Cells were fixed and stained for the presence of two generic epithelial cell proteins, Pan-cytokeratin and E-cadherin. Images under both FITC and DIC conditions were collected by laser scanning confocal microscopy (left and right columns respectively). These images were overlaid as shown in merge (middle column). **A-F** Pan-cytokeratin expression; **A-C** CPlacZ-6 line, no positive staining was observed; **D-F** Primary choroid plexus cultures, strong positive staining was observed in a filamentous cytoplasmic distribution. **G-L** E-cadherin expression; **G-I** CPlacZ-6 line; no staining was observed in a pattern consistent with the known membrane localisation of E-cadherin (see staining in primary cultures), but some faint perinuclear staining was visible. **J-L** Primary choroid plexus cultures, strong positive staining was observed in a plasma membrane distribution with clear perinuclear staining apparent in many cells (arrows). **M-O** Negative control, CPlacZ-6 cells incubated with fluorescein labelled  $\alpha$ -mouse IgG secondary antibody. Scale bars show 10  $\mu$ m.



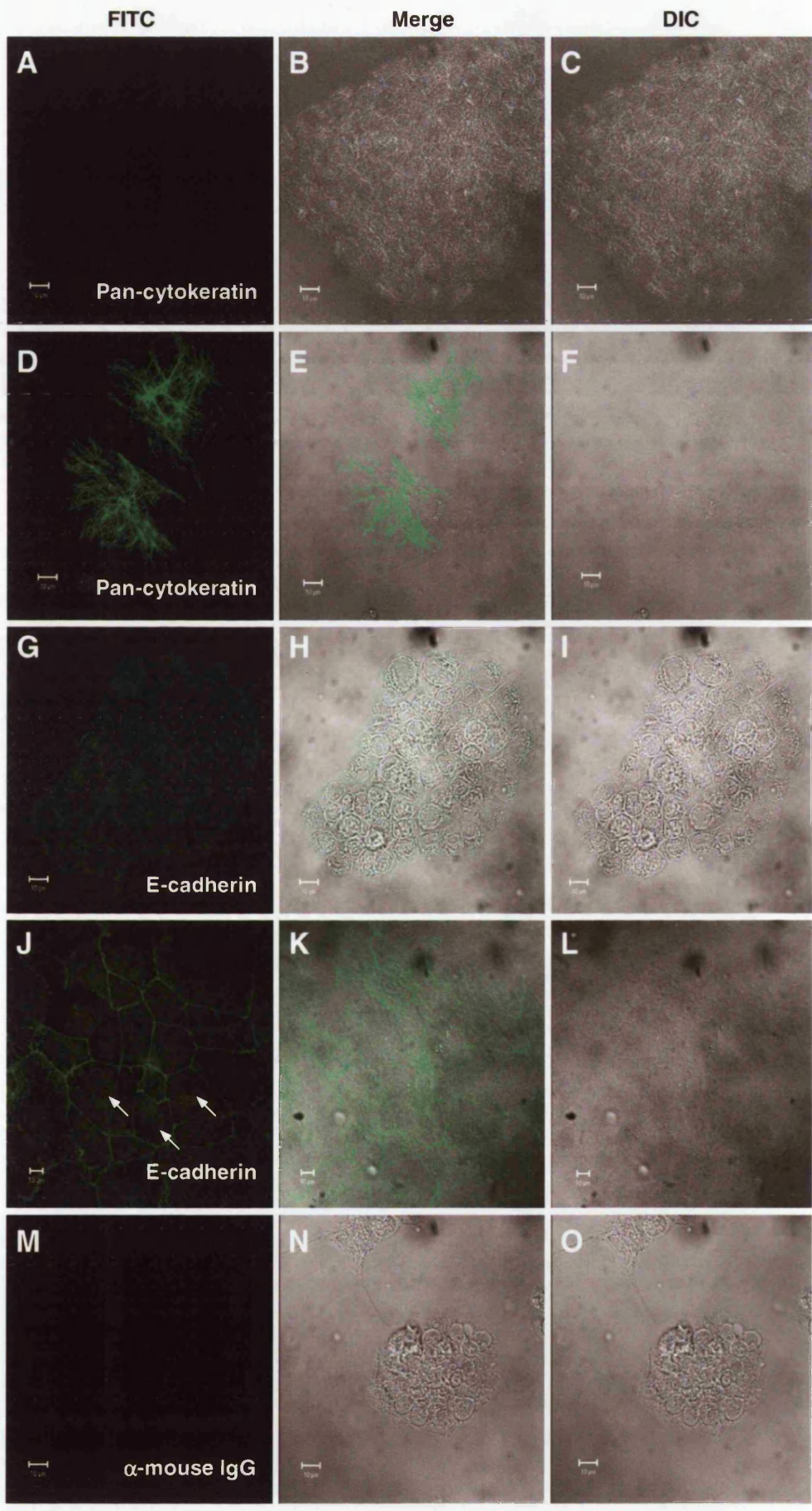
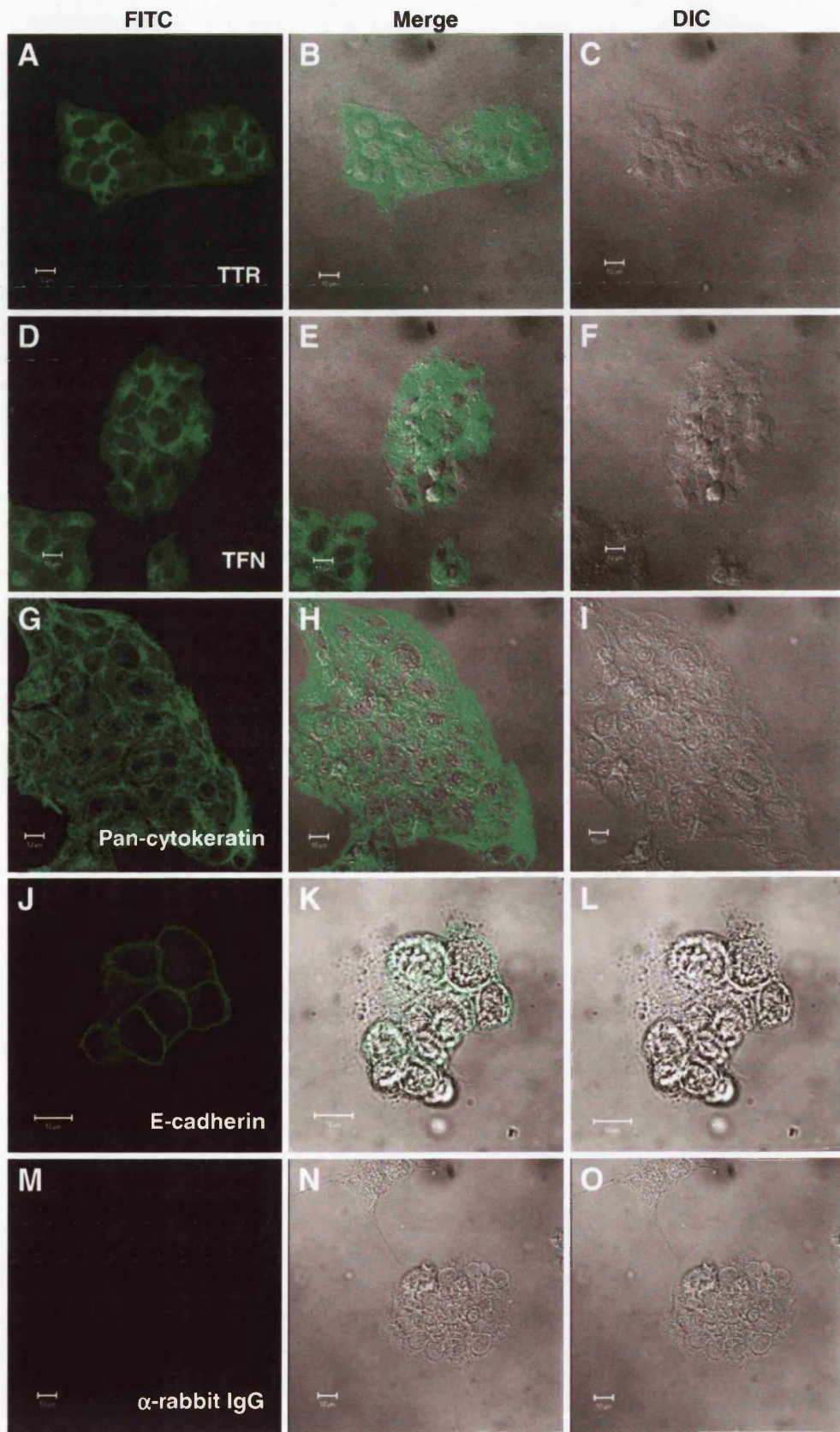


**Figure 36. Immunofluorescence: analysis of HepG2 cells, hepatocyte/choroid plexus differentiation markers.** HepG2 cells were fixed and stained for the presence of four biochemical markers common to both differentiated hepatocytes and choroid plexus epithelial cells, TTR, TFN, Pan-cytokeratin and E-cadherin. Images under both FITC and DIC conditions were collected by laser scanning confocal microscopy (left and right columns respectively). These images were overlaid as shown in merge (middle column). **A-C** TTR expression, staining was observed in a perinuclear distribution. **D-F** TFN expression, staining was as seen for TTR. **G-I** Pan-cytokeratin expression, positive staining was seen in the cytoplasm in a filamentous distribution. **J-L** E-cadherin expression, positive staining was observed in the plasma membrane. **M-O** Negative control, HepG2 cells incubated with fluorescein labelled  $\alpha$ -mouse IgG secondary antibody. Scale bars show 10  $\mu$ m.



### *Gene expression -RT-PCR analysis*

The failure to uncover immunoreactive E-cadherin and pan-cytokeratin in the CPlacZ cell lines was inconsistent both with the strong epithelial morphology and expression of numerous differentiation markers displayed by these cells, which otherwise supported an origin from choroid plexus epithelium. Downregulation of *E-cadherin* expression is frequently observed in tumours and correlates with the invasive or metastatic state (reviewed in (Hazan 2004)). To ask whether aberrant silencing of *E-cadherin* gene expression could explain the apparent absence of E-cadherin protein in the CPlacZ cell lines, an RT-PCR approach was adopted to examine gene expression at the mRNA level. Complementary DNA (cDNA) was prepared from the CPlacZ cell lines and from neonate choroid plexus tissue, which acted as a positive control, then PCR amplified (see Chapter 2 section describing RT-PCR) using primers specific to a portion of the mouse *E-cadherin* cDNA sequence (see **Table 14**). This analysis (**Figure 37**) showed abundant expression of *E-cadherin* mRNA in two of the cell lines, CPlacZ1 and CPlacZ6, with much lower levels seen in CPlacZ2 and CPlacZ3 cells. This finding was surprising given that immunoreactive E-cadherin could not be detected in any of these cell lines, suggesting a discrepancy between gene expression at the mRNA and protein level. The absence of E-cadherin protein, at least in CPlacZ1 and CPlacZ6 cells, is therefore unlikely to be a consequence of gene silencing, instead implicating posttranslational factors in these observations.

### *TFN promoter trans-activation assays*

TFN protein was seen in an uncharacteristic sub-membrane distribution in the CPlacZ cell lines and could not be found at all in primary choroid plexus epithelial cells when assayed by immunofluorescence. A cell transfection approach using *TFN*-promoter reporter gene constructs was used previously to map *cis*-elements involved in the tissue-specific expression of this gene (Chaudhary 1998). In an attempt to qualitatively demonstrate *TFN* gene expression in the CPlacZ cell lines, constructs containing either -0.6kb or -3kb *TFN* promoter regions fused to the *DsRed* reporter gene (see Materials and Methods section at the beginning of this chapter) were transfected into CPlacZ6 cells (see Chapter 2 section describing transient transfection of choroid plexus epithelial cells). A CMV-promoter *DsRed* construct was transfected as a positive transfection control. To confirm an appropriate tissue-specific activation of these constructs, two control cell lines were included in this analysis. The liver-



derived HepG2 cell line, in which high levels of TFN protein are expressed (as demonstrated by immunofluorescence in this chapter) and primary choroid plexus epithelial cells provided positive controls. Mouse NIH:3T3 fibroblasts should not express TFN and were included as negative controls. **Figure 38** shows reporter gene expression visualised under red fluorescence approximately 48 hours after transfection. Reporter gene expression was seen in CPlacZ6 cells and both control cell lines following transfection with the CMV-*DsRed*, indicating that the transfection had been successful. Reporter gene expression was seen from both the -0.6kb and -3kb *TFN-DsRed* constructs in the CPlacZ6 cells and in HepG2 cells although both constructs appeared to be expressed in a greater number of cells and at higher levels in the HepG2 transfection. No evidence of reporter gene expression was seen following transfection of either construct into primary choroid plexus epithelial cells or NIH:3T3 cells (not shown).

**Figure 37. RT-PCR analysis of *E-cadherin* expression in CPlacZ cell lines.** Complementary DNA (cDNA) was prepared from the cell lines and from neonate choroid plexus tissue and analysed by PCR using primers corresponding to a portion of the mouse *E-cadherin* cDNA. PCR reactions were analysed by gel electrophoresis. In the *E-cadherin* assay (upper panel), gene expression is indicated by a 520bp band. Analysis of  $\beta$ -actin expression (lower panel) in the same samples shows the successful conversion of RNA to cDNA. Samples treated with and without reverse transcriptase are indicated as + and – RT. The molecular weight marker (M) is a 100bp DNA ladder where the lower of the two bright bands represents 500bp.

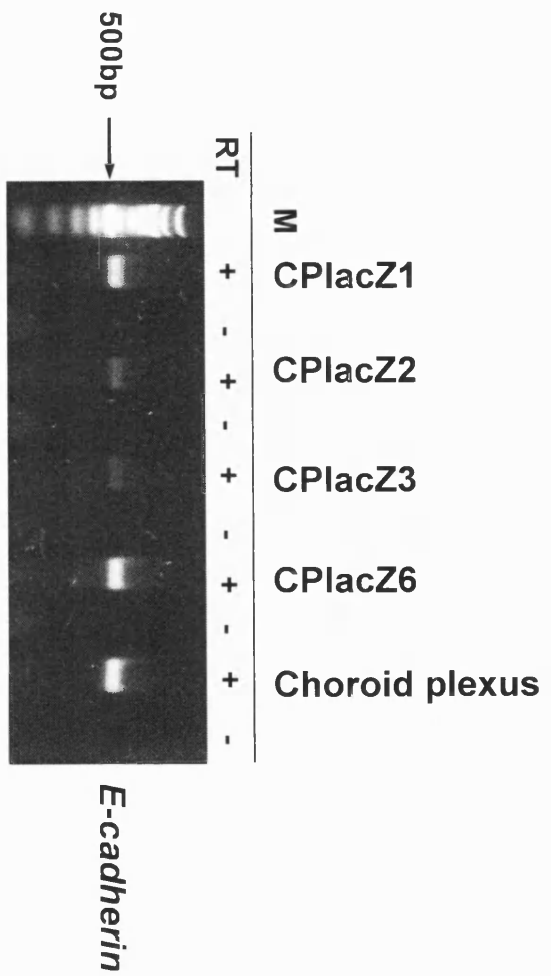
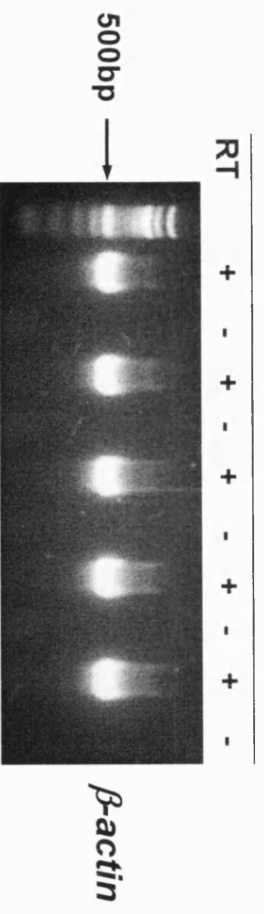
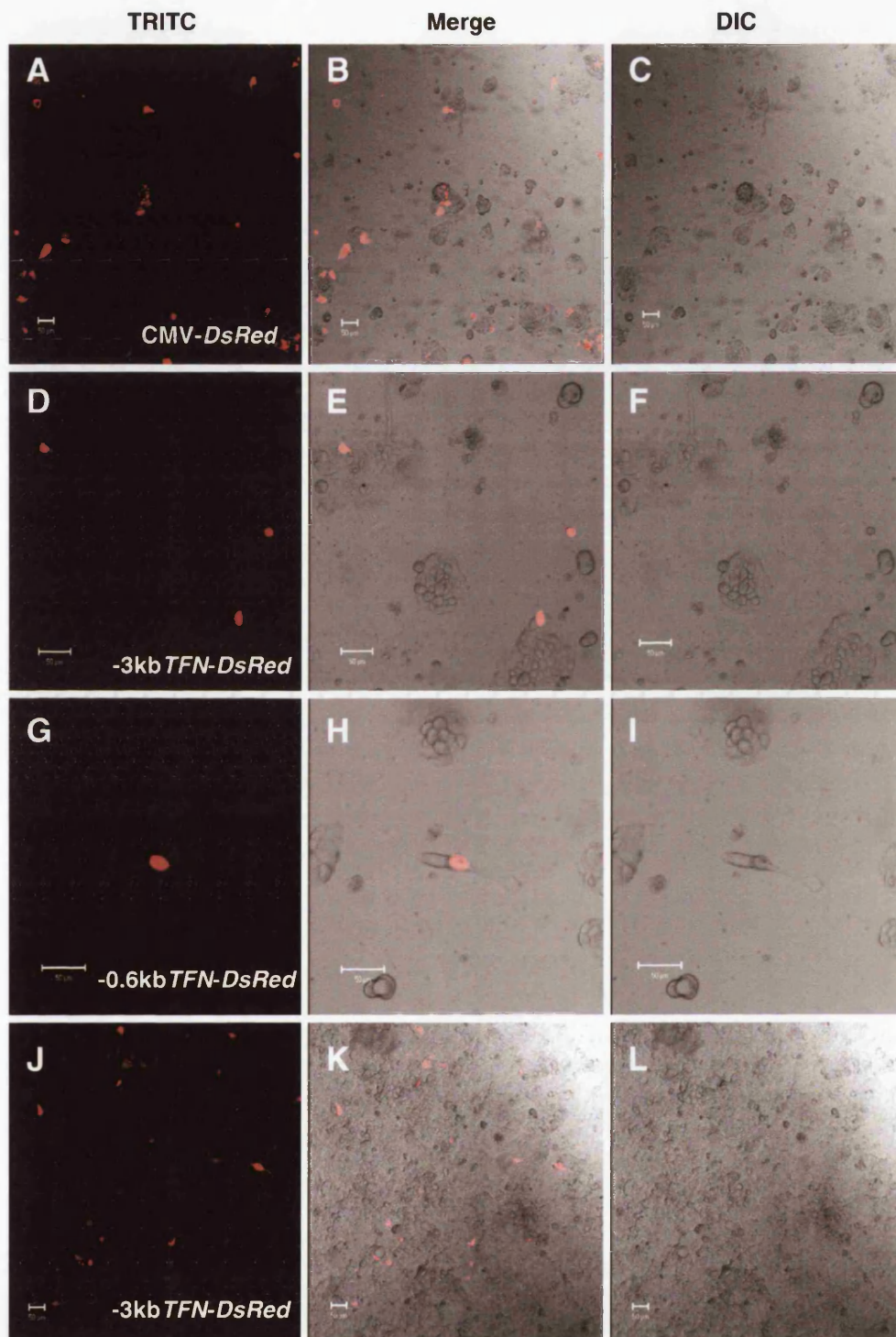


**Figure 38. *TFN* promoter *trans*-activation assays: comparison of CPlacZ cell lines and HepG2 cells.** Two *DsRed* reporter constructs respectively containing -3kb and -0.6 kb upstream regions of the mouse *TFN* gene were transfected into CPlacZ6 cells. In addition, transfection of a CMV-*DsRed* construct provided a positive control. Images under both TRITC and DIC conditions were collected by laser scanning confocal microscopy (left and right columns respectively). These images were overlaid as shown in merge (middle column). **A-I** CPlacZ6 transfection; **A-C** -3kb *TFN-DsRed* construct; **D-F** -0.6kb *TFN-DsRed* construct; **G-I** CMV-*DsRed*. **J-L** HepG2 cells transfected with the 3kb *TFN-DsRed* construct. Neither of the *TFN-DsRed* constructs were expressed following transfection into primary choroid plexus epithelial cells or the fibroblast NIH:3T3 cell line (not shown). Scale bars show 50  $\mu$ m.





## Gene expression at the *Igf2/H19* locus

### Northern analysis

*Igf2* expression would be predicted in the CPlacZ cell lines given their probable origin from the choroid plexus epithelium (DeChiara *et al.* 1991; Svensson 1995)(and see Chapter 3), on the other hand *H19* expression would not be expected given its absence from the embryonic choroid plexus epithelium (see Chapter 3). *Igf2/H19* expression was next examined by Northern analysis. RNA was isolated from the 4 cell lines and from e12.5 embryos, which acted as a positive control for *Igf2* expression (see Chapter 2 section describing isolation of total RNA). RNA extracted from kidney tissue at 3 weeks of age provided a negative control. Although highly expressed in the embryonic kidney, both *Igf2* and *H19* expression are sharply downregulated postnatally and were expected to be absent from this tissue at this stage (Weber 2001). The RNA samples were blotted and sequentially hybridised with cDNA probes corresponding to *Igf2* exon 6 and to *H19* (**Figure 39**). Surprisingly, *Igf2* mRNA was not detected in any of the cell lines, though several transcripts were present in the positive control. This was surprising given work presented in Chapter 4, which showed abundant *Igf2* expression in primary choroid plexus cultures. Low levels of transcript were unexpectedly observed in the negative control, suggesting residual expression in this tissue. *H19* RNA was not detected in any of the cell lines, although an abundant 2.5kb transcript was seen in the positive control. As seen for the *Igf2* hybridisation, low levels of *H19* RNA were present in the kidney sample expected to act as a negative control. *GAPDH* expression levels were similar in all lanes thereby excluding major differences in RNA loading as an influence upon the levels of *Igf2* and *H19*.

The question of whether *CTCF*, a critical regulator of *Igf2/H19* imprinting, is expressed in the choroid plexus epithelium was unsuccessfully addressed using an *in situ* hybridisation approach in Chapter 3. The derivation of CPlacZ cell lines provided a opportunity to readdress this question. The *Igf2/H19* blot was stripped and hybridised with a probe to *CTCF* (**Figure 39**) and revealed abundant expression of *CTCF* mRNA in all CPlacZ cell lines with comparable levels of a 3.8kb transcript visible in each case. *CTCF* expression is therefore likely to occur in the choroid plexus epithelium.

**Figure 39. Northern analysis of *Igf2*, *H19* and *CTCF* expression in CPlacZ cell lines.** Total RNA prepared from the cell lines were blotted and successively hybridised with probes to the mouse *Igf2*, *H19* and *CTCF* genes. Total RNAs from week 3 kidney and from e12.5 embryos were included as negative and positive controls for *Igf2* and *H19* expression respectively. Also shown is a separate probing for *GAPDH* which demonstrates similar loading of total RNA in each of the cell lines and controls.



### *RT-PCR analysis*

Northern analysis failed to detect *Igf2* expression in the CPlacZ cell lines, suggesting that expression was either below the detection threshold of this technique or absent, and since these lines carry a maternally inherited *lacZDMR2*<sup>-</sup> allele, that this could reflect specific silencing of the paternal allele. Allele-specific RT-PCR analysis was performed next to determine the imprinting status of *Igf2* in the cell lines using primer pairs specific to either the WT or *lacZDMR2*<sup>-</sup> alleles (see Materials and Methods section at the beginning of this chapter), thus discriminating transcripts of paternal and maternal origin. cDNA was prepared from the cell lines, and also from e10.5 WT and paternal transmission *lacZDMR2*<sup>-</sup>heterozygous embryos, which provided controls for the analysis, then PCR amplified (see Chapter 2 section describing RT-PCR) using primer pairs described (see **Table 14**). This analysis (**Figure 40**) showed transcripts from both WT and *lacZDMR2*<sup>-</sup> alleles to be present at low levels in all of the cell lines.

### **Allele-specific *Igf2* expression *in situ***

The expression data in Chapter 3 demonstrated that *Igf2* expression is restricted to a subset of choroid plexus epithelial cells. Could the absence of *Igf2* expression seen in the majority of the CPlacZ cell lines, following Northern and RT-PCR analysis, be explained by variegated *Igf2* expression in these cells? An *in situ* approach seemed the most appropriate means to elucidate this question. This was done by separate analysis of expression from each of the parental alleles using the *lacZDMR2*<sup>-</sup> allele to discriminate maternal from paternal expression.

### *Igf2* mRNA *in situ* hybridisation (paternal-specific expression)

To examine paternal-specific *Igf2* expression *in situ*, CPlacZ6 cells were fixed and hybridised with antisense and sense DIG-labelled RNA probes corresponding to exon 6 of the *Igf2* gene (see Chapter 2 section describing mRNA *in situ* hybridisation in cultured cells) with primary choroid plexus cultures analysed in parallel as positive controls for *Igf2* expression (**Figure 41**). No evidence of *Igf2* expression was seen in CPlacZ cells, either in a cell subset or otherwise. By contrast, high levels of *Igf2* expression were seen in the primary choroid plexus cultures, which assumed a clear perinuclear staining pattern in the epithelial cells and staining also evident in cells of non-epithelial morphology, presumed to have originated from the stromal

mesenchyme. The *in situ* hybridisation analysis together with the Northern and RT-PCR data suggest that paternal *Igf2* expression is either weak or absent in the CPlacZ cell lines.

*lacZDMR2<sup>-</sup> expression in situ (maternal-specific expression)*

To examine any transcriptional activity originating from the *lacZDMR2<sup>-</sup>* reporter gene (maternal *Igf2* expression) *in situ*, CPlacZ6 cells were fixed and stained for  $\beta$ -galactosidase activity (see Chapter 2 section describing the detection of  $\beta$ -galactosidase activity *in situ* in cultured cells). Reporter gene expression was highly variegated, with stained cells evidently fewer in number than unstained cells (**Figure 41**). This analysis demonstrated transcriptional activity from the mutant *Igf2* maternal allele in the cell lines, which occurs in a variegated manner.

**Figure 40. Allele-specific RT-PCR analysis of *Igf2* (*lacZDMR2*<sup>-</sup>) expression in CPlacZ cell lines.** Complementary DNA (cDNA) was prepared from the cell lines, and from e10.5 WT and *lacZDMR2*<sup>pat/+</sup> heterozygous embryos, which acted as controls then analysed by PCR for expression of the WT allele using primers spanning exons 3-4 of the *Igf2* gene, and for expression of the *lacZDMR2*<sup>-</sup> allele using primers to *lacZ*. PCR reactions were analysed by gel electrophoresis. Expression of the wild-type *Igf2* allele (upper panel) is indicated by a 170bp band. Expression of the *lacZDMR2*<sup>-</sup> allele (middle panel) is indicated by a 206bp band (middle panel). The RT-PCR shows that low levels of transcript from both alleles are present in the cell lines. Analysis of  $\beta$ -*actin* expression (lower panel) in the same samples shows the successful conversion of RNA to cDNA in all cases. Samples treated with and without reverse transcriptase are indicated as + and – RT. The molecular weight marker (M) is a 100bp DNA ladder where the lower of the two bright bands represents 500bp.

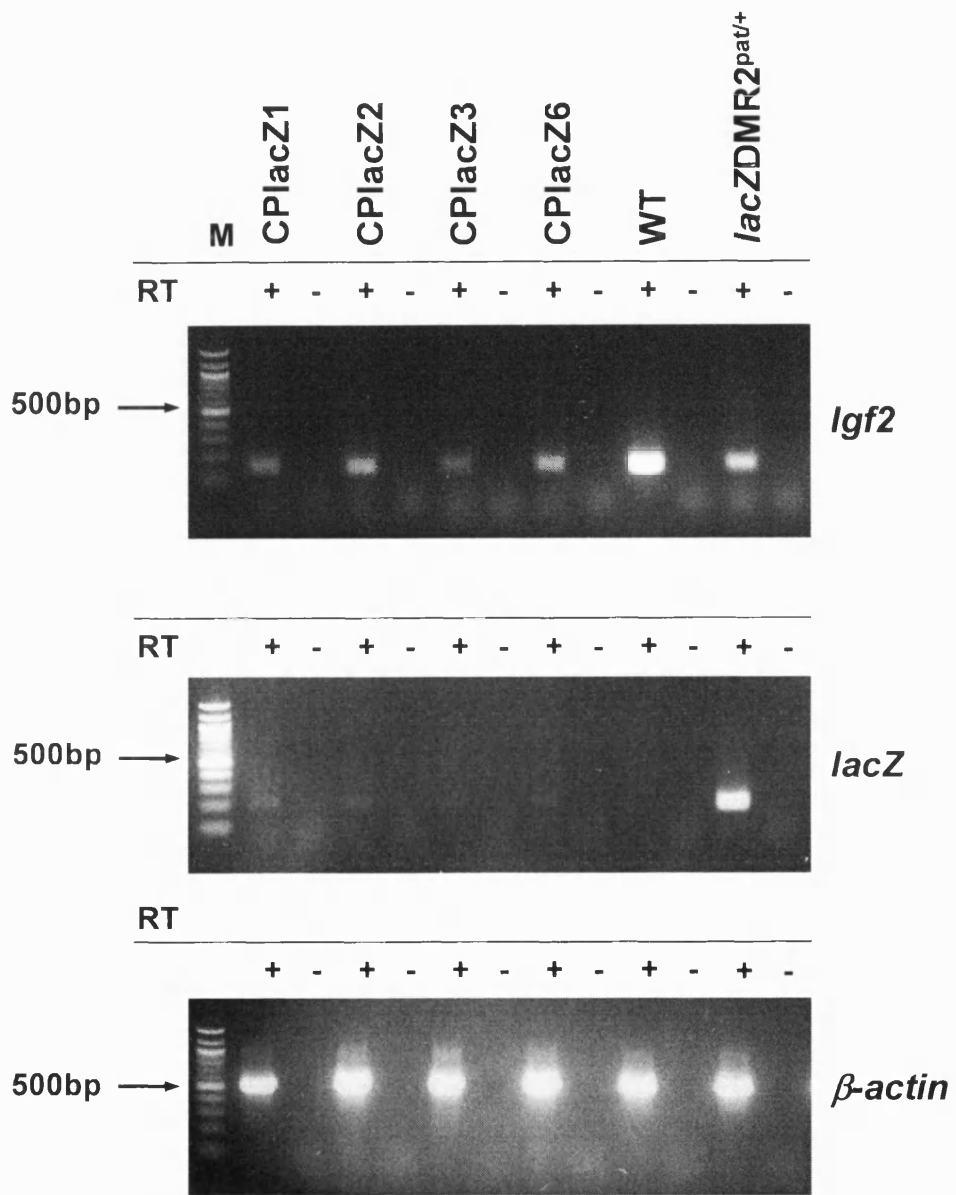
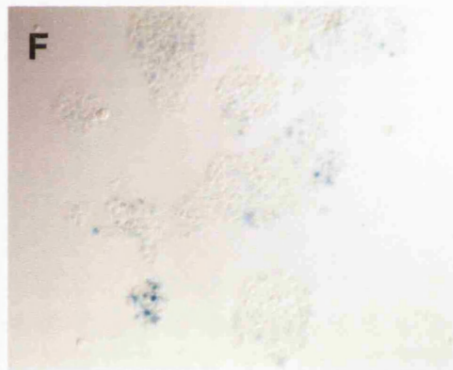
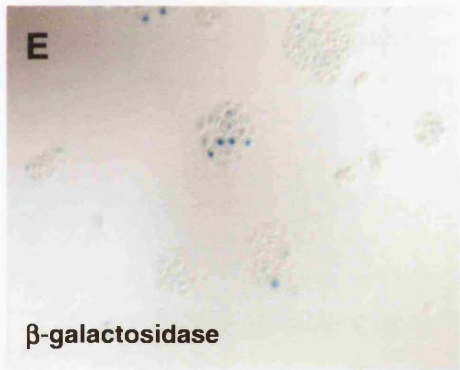
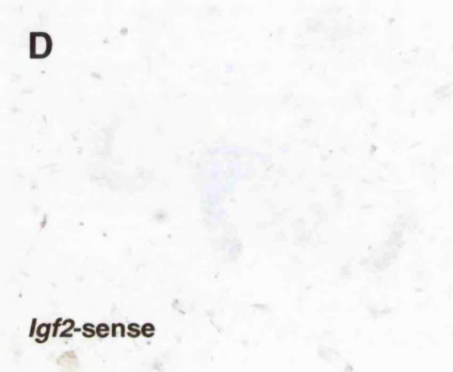
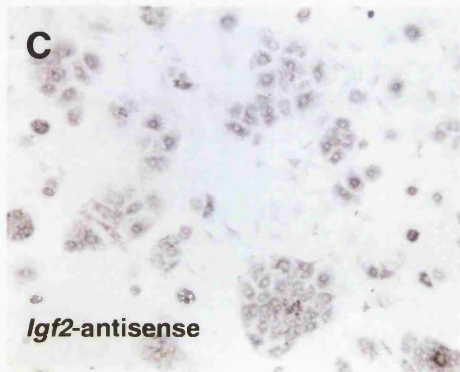
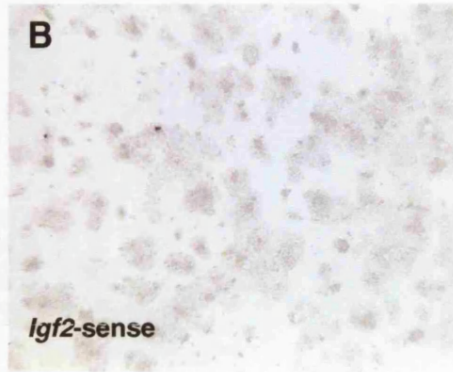
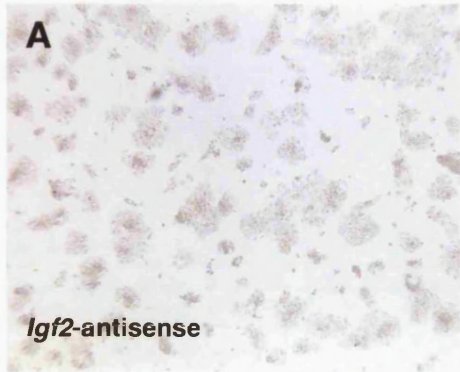




**Figure 41. Allele-specific analysis of *Igf2* (*lacZDMR2*<sup>-</sup>) expression *in situ*, CPlacZ cell lines. A-D** Paternal-specific expression was analysed by *Igf2 in situ* hybridisation. CPlacZ6 cells were hybridised with antisense (A) or sense (B) probes. Primary choroid plexus cultures provided positive controls for *Igf2* expression and are shown after hybridisation with antisense (C) or sense (D) probes. E-F Maternal-specific expression (*lacZDMR2*<sup>-</sup> reporter gene) was analysed by staining for  $\beta$ -galactosidase activity *in situ*. Cells from two independent fields of view are shown. All magnifications are  $\times 200$ .





## DNA methylation at the *Igf2/H19* locus

The developmental expression analysis described in Chapter 3 has shown that biallelic *Igf2* expression is confined to the choroid plexus epithelium. Could this escape from imprinted expression be explained by disruption of allele-specific methylation patterns within *Igf2/H19* DMRs within this tissue? Loss of differential methylation has been previously observed in *Igf2* proximal DMRs both in the choroid plexus and in mutant mice that express *Igf2* biallelically (Feil *et al.* 1994; Lopes *et al.* 2003). This question was indirectly addressed by examination of methylation at two regions, the DMD and *Igf2* DMR1 in the CPlacZ cell lines. Genomic DNA was prepared from the cell lines (see Chapter 2 section describing genomic DNA extraction from tissue) and digested with *Bam*HI/*Bgl*II. The DNA was further digested with the isoschizomer pair *Hpa*II and *Msp*I where both enzymes cut within the same recognition sequence (CCGG). *Hpa*II activity is blocked by CpG methylation whereas *Msp*I is insensitive, thus the methylation status of CpG dinucleotides within these sites will determine the pattern of restriction fragments on a Southern blot dependent upon the enzyme used. Restriction maps of the *H19* DMD and *Igf2* DMR1 genomic regions including the sites relevant to this study are respectively shown in **Figures 42** and **43**. *Hpa*II/*Msp*I was predicted to cut at 5 sites within the DMD fragment, at 6 sites within the *H19* promoter-proximal fragment (**Figure 42**) and at 13 sites within the DMR1 fragment (**Figure 43**). Digested DNA samples were blotted and hybridised either with a probe encompassing the DMD and *H19* promoter proximal region or a probe corresponding to DMR1 (see Chapter 2 section describing Southern analysis).

### *Methylation at the DMD and H19 promoter proximal region*

The cell lines displayed intermediate methylation of the DMD (**Figure 44**) as shown by a partial resistance to digestion by *Hpa*II. A similar profile was observed in liver, where paternal-specific hypermethylation of the DMD has been reported previously (Weber 2001), brain and choroid plexus controls. The *H19* promoter proximal region was also intermediately methylated in all of the cell lines and control tissues. However, in the cell lines a slightly greater proportion of both regions appeared to be methylated compared with the liver control as exhibited by the levels of the unmethylated 1kb fragments. Interestingly, in the cell lines the DMD appeared more highly methylated than the *H19* promoter proximal region relative to control tissues, where this pattern was in fact reversed (compare relative levels of the 2.5kb and

2.38kb bands). Whether these patterns actually represent higher methylation levels at the DMD, or indeed lower methylation at the *H19* promoter proximal region in the cell lines compared with the control tissues cannot be judged, as the DNA was not equivalently loaded in all cases.

### ***Methylation at DMR1***

The cell lines displayed almost complete methylation of DMR1 (**Figure 45**) as shown by a high level of resistance to digestion by *HpaII*. Indeed a large proportion of the DMR1 fragments were methylated at all 13 *HpaII/MspI* sites covered by the probe (see restriction map shown in **Figure 43**), although the presence a faint band at 4.6 kb in all of the cell lines indicated that a small fraction were unmethylated at a single site. By comparison, DMR1 was intermediately methylated in liver, a site where paternal hypermethylation of this region has been reported previously (Weber 2001) and in brain with a range of lower molecular weight fragments produced by digestion with *HpaII*. Choroid plexus DNA appeared to be highly methylated at DMR1 as shown by resistance to *HpaII* digestion, although unequal loading of this sample prevents a comprehensive evaluation of this data.

**Figure 42. Restriction map of the *H19* locus.** Restriction map of the 10kb genomic region containing the *H19* gene and proximal sequences. *H19* exons are shown as shaded boxes; open boxes show other features; hypersensitive sites 1 (HS1) and 2 (HS2); GC-rich repeat element (GCR). Arrows indicate positions of the DMD, the H19 promoter proximal region and the DMD probe. Restriction sites relevant to the methylation analysis are shown, *Bgl*II, *Bam*HI; lollipops represent sites of potential CpG methylation within *Hpa*II/*Msp*I restriction sites. Digestion with *Bgl*II/*Bam*HI will produce 2.3 and 2.5kb fragments containing the DMD and promoter proximal region respectively, both of which are predicted to hybridise to the DMD probe.

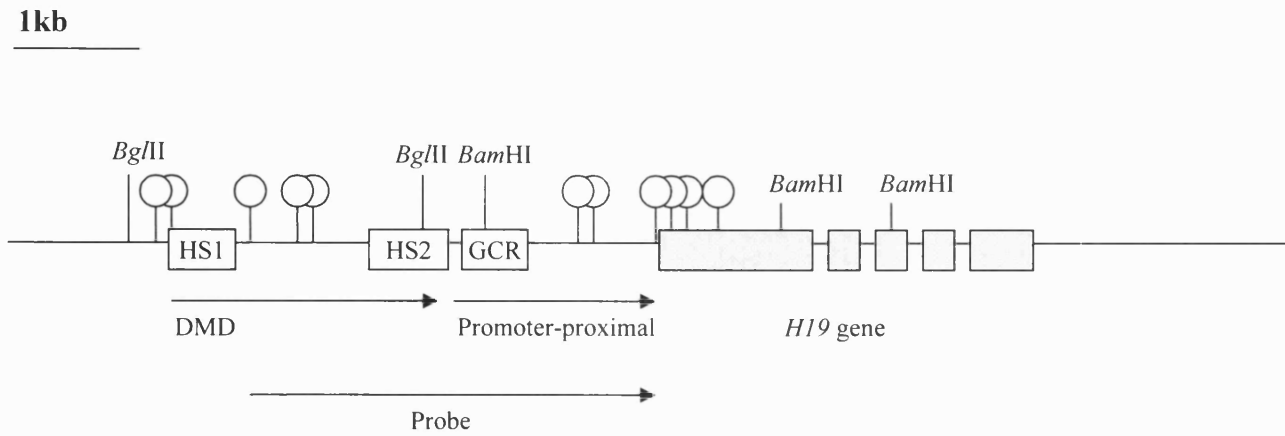


**Figure 42.** The *H19* genomic region

**Figure 43. Restriction map of the *Igf2* locus.** Restriction map of the 18kb genomic region containing the *Igf2* gene and proximal sequences. *Igf2* exons are shown as shaded boxes; other features include the *Igf2*-proximal differentially methylated regions, DMR0 and DMR1. Restriction sites pertinent to the methylation analysis are shown, *Bgl*II, *Bam*HI; lollipops represent sites of potential CpG methylation within *Hpa*II/*Msp*I restriction sites. Digestion with *Bgl*II/*Bam*HI will produce a 4.8kb fragment containing the DMR1 region which is predicted to hybridise to the DMR1 probe (indicated by lower arrow).



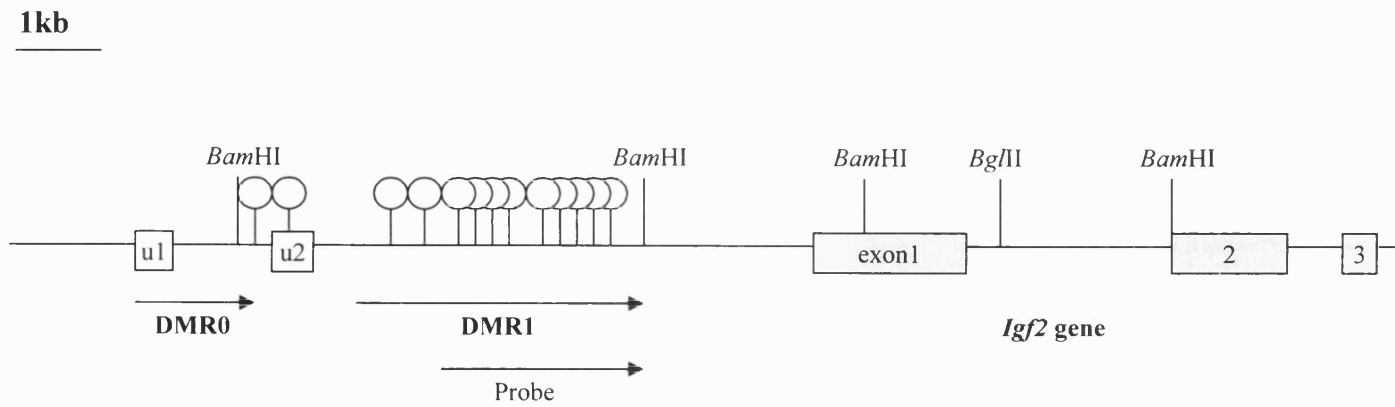


**Figure 43.** The *Igf2* proximal genomic region

**Figure 44. Methylation analysis of the DMD and *H19* promoter-proximal region in CPlacZ cell lines.** The cell lines and three control tissues, neonate liver, brain and choroid plexus were analysed. Genomic DNA samples from each tissue were digested with *Bam*HI-*Bgl*III, *Bam*HI-*Bgl*III-*Hpa*II or *Bam*HI-*Bgl*III-*Msp*I. Digested DNA samples were blotted and hybridised with a probe spanning the DMD and promoter proximal region. The predicted sizes of fragments resulting from these digests are represented in **Figure 42**. The DMD displayed intermediate (50%) methylation in all cell lines and controls, with a proportion of the total 2.38kb fragment content protected in the *Hpa*II digests. The *H19* promoter proximal region (*H19*) was also intermediately methylated in all cell lines and controls with a proportion of the 2.5kb fragment protected in the *Hpa*II digests in all cases. Levels of the 2.38kb DMD fragment predominated over the 2.5kb *H19* fragment in the cell lines compared to liver, brain and choroid plexus controls where this pattern was reversed. The ratio of *Hpa*II to *Msp*I digested fragments of lower molecular weight was slightly greater in the cell lines, except CplacZ6, compared with liver and brain controls (compare levels of the 1kb DMD and *H19* promoter proximal bands).

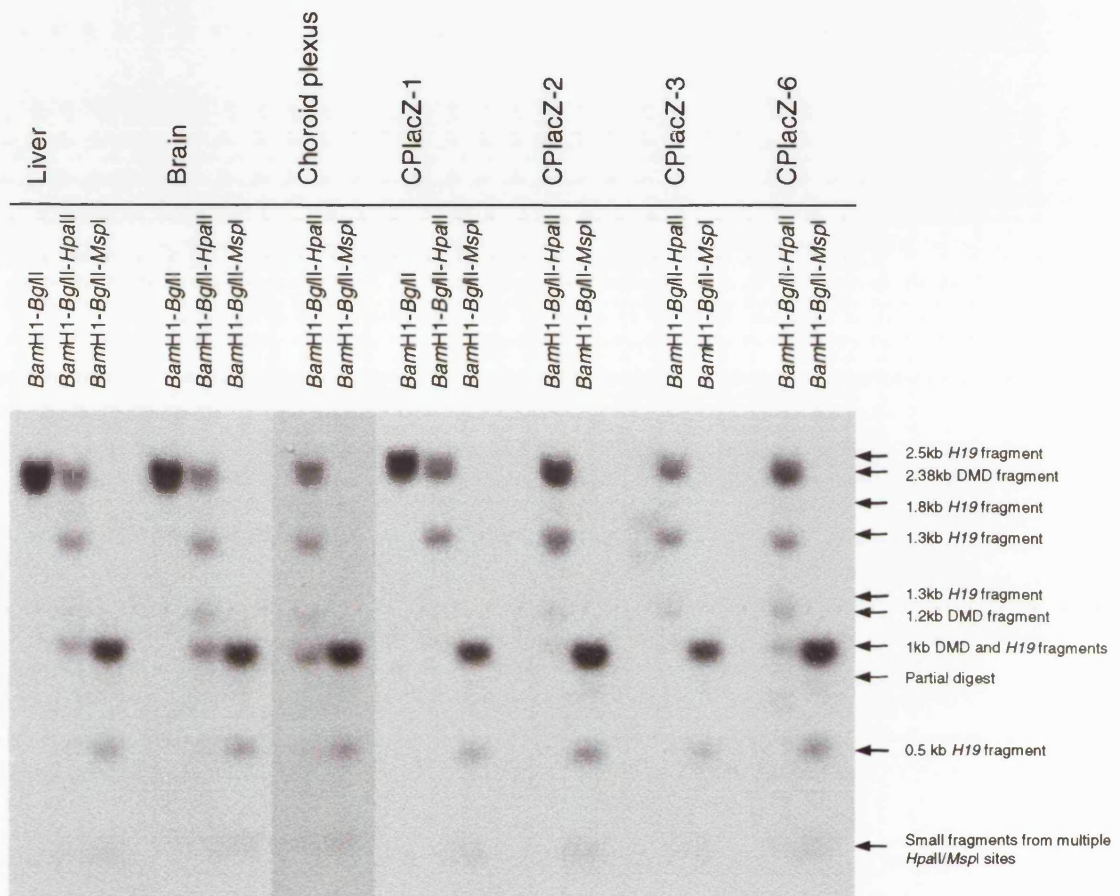
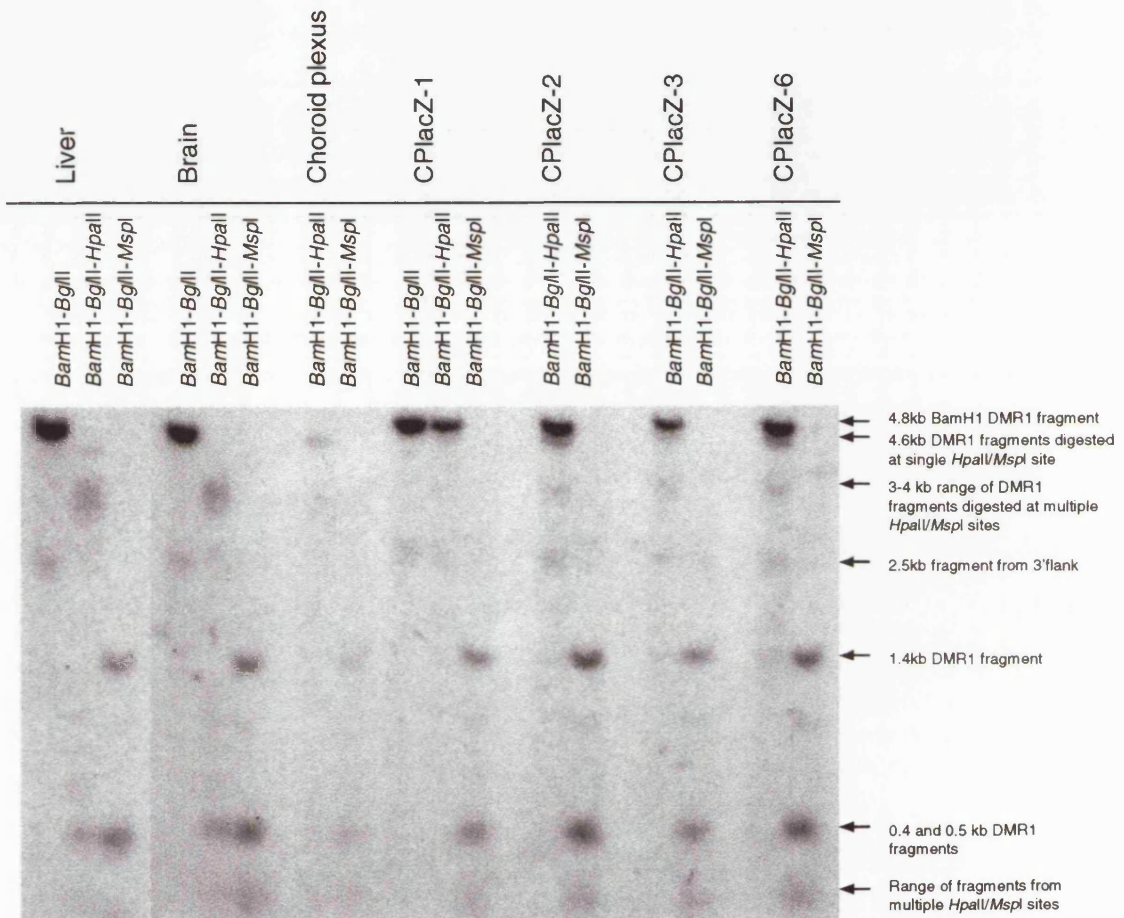


**Figure 45. Methylation analysis of *Igf2* DMR1 in CPlacZ cell lines.**

The cell lines and three control tissues, neonate liver, brain and choroid plexus were analysed. Genomic DNA samples from each tissue were digested with *Bam*HI-*Bgl*III, *Bam*HI-*Bgl*III-*Hpa*II or *Bam*HI-*Bgl*III-*Msp*I. Digested DNA samples were blotted and hybridised with a probe corresponding to DMR1. The predicted sizes of fragments resulting from these digests are represented in **Figure 43**. DMR1 appeared to be highly (near 100%) methylated in all of the cell lines with a large proportion of the total 4.8kb fragment content protected in the *Hpa*II digests. A small proportion of the total 4.8kb fragment content had been digested at a single site to give a 4.6kb fragment and at additional sites to give a range of 3-4kb fragments in all of the cell lines. DMR1 displayed intermediate (>50%) methylation levels in liver and brain controls, where the 4.8kb fragment had been completely digested by *Hpa*II to give a range of fragments of 3-4kb and much lower molecular weight fragments of 0.5kb and 0.4kb. In the choroid plexus control, DMR1 appeared highly methylated, with a clear 4.6kb fragment and much fainter 3-4kb fragments visible in the *Hpa*II digest, although unequal loading of this sample confounds comparison with the cell lines and controls.



## Conclusions

The primary aim of the work in this chapter was to establish an immortal cell line from the choroid plexus epithelium of the mouse as a means to investigate how the *Igf2* gene escapes imprinting in this tissue. This was achieved by a genetic approach in which overexpression of the T-antigen-derived T<sub>121</sub> protein was used to inactivate *Retinoblastoma* family proteins and bring about tumourigenesis of the choroid plexus epithelium. Tumour tissue was isolated and ultimately four independent cell lines were successfully derived.

Successful derivation of the cell lines appeared to be dependent upon inactivation of both *Retinoblastoma* and *p53* gene products. The CPlacZ cell lines were ultimately derived from tumour foci induced in one T<sub>121</sub> *p53*<sup>+/-</sup> *lacZDMR2*<sup>+mat-</sup> animal. Subsequent PCR analyses showed that whilst the founder animal was indeed heterozygous for the *p53* knockout allele prior to tumour development, the cell lines (which were all derived from this animal) were *p53* null. Consistent with previous observations (Symonds 1994), these results argue that the loss of *p53* in this case is both the consequence of a secondary somatic mutation and the underlying cause of the tumour focus. Examination of the *p53* status in non-transformed choroid plexus tissue adjoining the tumours, where preservation of a single wild type *p53* allele would have been predicted, would have substantiated these conclusions but was not done. Interestingly, the additional loss of *p53* was reflected in the growth rate of the cells, which was significantly higher than that observed for any of the primary cultures expressing T<sub>121</sub> in the presence of functional *p53*. In conclusion, inactivation of both *Retinoblastoma* and *p53* was required for the successful derivation of the CPlacZ cell lines.

This observation is interesting, particularly given the study by Saenz Robles *et al.* who reported that inactivation of *Retinoblastoma* proteins by T<sub>121</sub> was, in the absence of *p53* mutations, sufficient for uniform tumourigenesis of the choroid plexus epithelium *in vivo* (Saenz Robles *et al.* 1994). In the present study, attempts to derive cell lines from cultured choroid plexus tissue dissected from neonatal mice of this genotype were unsuccessful as the epithelial cell fraction did not survive beyond a few passages and could not be cloned. Taken together, these observations argue that whilst T<sub>121</sub> is capable of transformation *in vivo*, it is not able to immortalise choroid

plexus epithelial cells *in vitro*. Could this discrepancy have been a consequence of *p53*-dependent apoptosis? Observations made *in vivo* show that tumours induced by T<sub>121</sub> develop slowly and are highly apoptotic, yet upon a *p53*<sup>-/-</sup> null background, where *p53* dependent apoptosis is absent, this tumour induction is significantly accelerated (Saenz Robles *et al.* 1994; Symonds 1994). It is conceivable that the T<sub>121</sub>-expressing choroid plexus epithelial cells lacked the growth potential required to properly establish and immortalise *in vitro*.

This issue was explored at the *in vitro* level by comparison of the relative growth rates of primary choroid plexus cultures carrying T<sub>121</sub> in the presence or absence of a *p53*<sup>+/-</sup> knockout mutation (with the T<sub>121</sub> *p53*<sup>-/-</sup> genotype provided by the CPlacZ2 cell line) with wild type controls. This analysis revealed that in isolation, T<sub>121</sub> was able to induce a modest increase in cell proliferation compared with wild type controls *in vitro*. Interestingly, the *p53*<sup>+/-</sup> mutation mediated a quantitatively similar increase in the overall proliferation rate compared with wild type controls. However, cultures carrying both mutations proliferated at a greater rate than those derived from either mutation alone, suggestive of an additive growth effect. Significantly, the proliferation rate of CPlacZ2 cells, which carried the T<sub>121</sub> *p53*<sup>-/-</sup> genotype, was many times greater than that conferred upon primary cultures by T<sub>121</sub> alone, suggestive of a synergistic growth effect. Conclusions drawn from this data should be treated with caution as several factors complicate its interpretation. CPlacZ2 cells represent a homogenous population of epithelial cells whereas the primary cultures would have contained both epithelial and mesenchymal cell types, which the growth assay did not discriminate. In the primary cultures, growth effects may not have manifested uniformly (at least in some of the genotypes) and could equally be ascribed to disproportionate effects of each mutation within these two cell types.

For example, in consideration of the T<sub>121</sub> and *p53*<sup>+/-</sup> genotypes, different outcomes might be predicted. In T<sub>121</sub> mice, the LPV promoter directs T<sub>121</sub> expression specifically to the choroid plexus epithelium and lymphoid cells. The proliferation increase conferred upon the primary cultures by T<sub>121</sub> was therefore likely to be specific to the epithelial cell fraction. The same conclusion cannot be drawn for the *p53*<sup>+/-</sup> genotype, as both cell types would be affected by this mutation. Moreover, fibroblasts of this genotype are reported to share some characteristics of *p53*<sup>-/-</sup>

knockout fibroblasts, which are immortal. That is,  $p53^{+/-}$  fibroblasts are 'semi-immortal' and possess an increased capacity for proliferation compared with the wild type. It seems possible therefore, that the growth rate of the  $p53^{+/-}$  choroid plexus cultures could be explained by a similar effect in the mesenchymal fraction. By the same argument, the increased growth rate of T<sub>121</sub>  $p53^{+/-}$  cells compared with cells carrying either mutation alone cannot necessarily be explained by an interaction between both mutations within the same nucleus, as it could equally be due separate effects in the epithelial and mesenchymal fractions. Moreover, the observation that T<sub>121</sub> and  $p53^{+/-}$  mutations manifest an additive effect in double mutant (T<sub>121</sub>  $p53^{+/-}$ ) cells is consistent with the latter hypothesis. Perhaps more meaningful interpretations could have been made with the inclusion of cultures derived from T<sub>121</sub>  $p53^{-/-}$  mice, however ethical considerations prohibited the creation of such animals and hence, derivation of cells from them. To summarise, potentially independent effects in the epithelial and mesenchymal cell fractions prevent a clear conclusion, but the growth assay data suggests that, a finding that is consistent with observations *in vivo*, the  $p53$  null genotype significantly enhanced growth effects of T<sub>121</sub> conferred upon choroid plexus epithelial cells *in vitro*.

Clonality is an important feature of continuous cell lines and aims to provide reproducibility across multiple experiments. This is conventionally achieved by cloning a single progenitor cell such that a population of genetically identical cells are generated. In this instance, clones could not be derived from single cells with poor cell viability a probable determinant in this issue. Ultimately a compromise was sought where clones were eventually derived from small cell aggregates (containing 20 cells or less) as opposed to single cells that are the convention. The cloning process was repeated to minimise the probability of variation within the clones prior to their expansion into the CPlacZ cell lines. Although unlikely, it remains a formal possibility that the cell lines contain two or more distinct lineages.

The limiting dilution method used in the present study has been successfully used to derive single cell clones from many tissues (Freshney 1987). It is conceivable that the failure to derive single clones from the choroid plexus epithelium reflects an intrinsic property of this tissue. Reasons for the differences in cloning potential between single and aggregated cells were not obvious but suggest an involvement of cell-cell contact.



The epithelial nature of these cells would favour maximal contact of plasma membranes with adjacent cells, a situation that isolated cells clearly would not achieve. Density dependent influences such as growth factor availability should also be considered. For similar reasons, many cell lines cease to proliferate when plated at low densities, growth signals produced by a dense population of cells will rapidly equilibrate with the environment whereas those from a single isolated cells never will. By judicious application of exogenous growth factors and thus mimicking a cell-dense environment, it is often possible to 'deceive' cells into mitosis (Freshney 1987). Although not described in the results section of this chapter, alternative attempts were made to address this issue and involved the use of elevated serum concentrations, epidermal growth factor supplementation, fibroblast growth-conditioned medium and mitomycin-C inactivated fibroblasts in feeder layers. However none of these alternative protocols proved successful. A point of possible relevance is that the *lacZDMR2* mutation carried by the cell lines may have compromised their viability in some way. Additionally, *Igf2* transcripts could not be detected from the non-disrupted paternal allele in any of the CPlacZ cell lines, when assayed by Northern analysis. Could an IGFII deficiency explain the poor cloning potential of single cells? In the future this could be investigated by supplementation of the cloning plates with exogenous IGFII. Prospectively, the derivation of a cell line that carries a copy of the *Mus spretus*-derived SD7 region, which is functionally wild type at *Igf2*, would also address this question.

During embryogenesis, differentiation of the choroid plexus epithelium from the embryonic neuroepithelium is signified by characteristic changes in cell morphology and the expression of specific genes (Catala 1998). The identity of the CPlacZ cell lines was investigated by asking whether their morphology and gene expression profile was consistent with the phenotype of the differentiated choroid plexus epithelium. The cell lines displayed the characteristic cobblestone morphology that typifies epithelial cells although these cells presented a smaller apical surface area than their primary counterparts possibly suggesting a less intimate association with the culture vessel. Gene expression was analysed both at the mRNA and protein level. The cell lines were shown to express many but not all of the markers analysed, suggesting that a partial loss of the choroid plexus phenotype might have occurred. Northern analysis demonstrated the expression of three genes, *TTR*, *FoxJ1* and *Msx1*

in three of the four cell lines. These genes are robust markers for the choroid plexus epithelium and discriminate this layer from surrounding tissues *in vivo* (Murakami 1987; MacKenzie 1991; Lim 1997). Expression of all three markers was severely reduced in CPlacZ2 cells compared with the other cell lines, suggesting that this cell line in particular had lost differentiated properties or perhaps reverted to a choroid plexus precursor phenotype.

To further characterise the cell lines, the expression of TTR and that of three additional markers TFN, E-cadherin and Pan-cytokeratin, was examined at the protein level by immunofluorescence. Surprisingly, of these markers, only the presence of TTR was clearly demonstrated. Of the other markers, TFN was unexpectedly, yet consistently observed in an uncharacteristic sub-plasma membrane distribution, as opposed to the perinuclear distribution normally observed for this protein, as seen in the HepG2 cells here and previously (Tosh 2002b). Why TFN should be membrane localised, is unclear but could reflect the transformed state of the cell lines in some manner. Staining artefacts cannot be excluded from these observations, but are an unlikely cause given that the protocol used was identical to that successfully used to uncover immunoreactive TFN in HepG2 cells. Despite repeated attempts, TFN was never detected in primary choroid plexus controls, although its expression was expected on the premise of TFN immunoreactivity, revealed with the same primary antiserum batch in the choroid plexus epithelium at e14.5 (see Chapter 3) and by Northern blot analysis *in vivo* and *in vitro* (Tsutsumi 1989; Tu 1991). The former of these studies demonstrated the presence of a 2.3kb choroid plexus-specific *TFN* transcript, in addition to the 2.5kb transcript found at all other sites of expression. Distinct protein isoforms potentially encoded by this transcript might not have been detected by the primary antiserum used here and could explain the discrepancy between the cell lines and primary choroid plexus epithelial cells. A transfection approach involving *TFN* promoter-*DsRed* constructs was attempted to resolve the issue of *TFN* expression. Both *TFN* promoters tested in this assay were activated in CPlacZ6 cells and HepG2 cells but not in primary choroid plexus epithelial cells thus corroborating the immunofluorescence data.

E-cadherin and cytokeratins, both of which are excellent differentiation markers for epithelial cells (Fuchs 1988; Takeichi 1991) did not appear to be expressed at the

protein level in any of the cell lines, although both were abundant in primary choroid plexus epithelial cells and HepG2 cells. This was particularly surprising, given the well-differentiated epithelial morphology of the cell lines and also other clear indications of choroid plexus epithelium origin. The normal expression of these markers in the primary choroid plexus epithelial cells eliminates failure of the protocol and instead suggests an involvement of the transformed state. Loss of function in the *E-cadherin* gene is well documented in cell transformation and tumour progression (Hazan 2004). Generally, cadherins mediate cell adhesion at adherens junctions via interactions with the actin-based cytoskeleton. Mutations in *E-cadherin*, by both genetic and epigenetic pathways, which downregulate or extinguish its expression, lead to the disruption of cell-cell adhesion. Within this framework, loss of *E-cadherin* expression is frequently correlated with the invasive or metastatic state in many instances of cancer (Hirohashi 2003; Hazan 2004)(and references therein). Therefore, inactivation of *E-cadherin* function plays a significant role during tumourigenesis. RT-PCR analysis was performed to ask whether the absence of E-cadherin protein reflected a general downregulation of *E-cadherin* gene expression in the CPlacZ cell lines and revealed that whilst this was likely to be the case for two of the cell lines in which little or no expression could be detected, relatively high levels of *E-cadherin* mRNA were found in the two remaining cell lines, thus implicating posttranslational factors in the absence of the protein in these examples. It is conceivable that changes in *E-cadherin* expression at the mRNA and protein levels could reflect, or might have been required for acquisition of the transformed state by the cell lines.

Could a similar argument be put forward to account for the loss of pan-cytokeratin expression? Clinical studies provide evidence that cytokeratin expression is in fact maintained virtually all human choroid plexus tumours (Rickert 2001). Nonetheless, the absence of this important marker suggests that the cell lines have lost a specific differentiated function. Interestingly, normal epithelial cells show transient disassembly of cytokeratin-based intermediate filaments during mitosis (Lane 1982). Therefore, with a very high proportion of cells undergoing mitosis almost continuously, it could be argued that the cytokeratin-based intermediate filament network is established only transiently, or not at all in the cell lines. Although speculative at present, an involvement of cytokeratins (and possibly E-cadherin) in

cytoskeletal reorganisation would be consistent with the altered morphology of the cell lines, where the cells appeared much smaller and less flattened compared with primary choroid plexus epithelial cells. It is also possible that cytokeratin gene expression has been affected specifically at the protein level, as seems to be the case for *E-cadherin*, at least in some of the cell lines. Though not done in the present study, RT-PCR or Northern analysis of cytokeratin genes known to be expressed in the choroid plexus epithelium could resolve this question.

Mitotic quiescence is a major differentiated feature of the choroid plexus epithelium *in vivo* (Saenz Robles *et al.* 1994), therefore by forcing these cells into proliferation by the genetic inactivation of tumour suppressor genes, it is perhaps unsurprising that normal gene expression patterns have been disrupted. Similar findings have been reported in another example of T-antigen mediated immortalisation, where dedifferentiation of a rat hepatocyte cell line was observed (Kim 2000). This loss of phenotype was correlated with a high passage number (>50), which the authors attributed to the acquisition of secondary somatic mutations during this extended culture period. However, the CPlacZ cell lines were kept within a maximum of 10-15 passages for all experiments described, thus it seems less likely that passage number would have substantially influenced differentiation markers in this case. Examination of the parent tumour tissue, from which the cell lines originate, using the same panel of markers might have elucidated this point, however this was not done.

Interestingly, in neither of the two previous descriptions of choroid plexus epithelial cell lines, both immortalised with T-antigen, do the authors report dedifferentiation even at greater than 100 passages (Kitazawa 2001; Zheng 2002). It should be noted however that in these studies, the expression of only a single marker, TTR, was examined, whereas in the present analysis, a broader panel of markers was assessed. Indeed in the present study, TTR was one of the markers analysed whose expression had been retained by the cell lines. Although speculative, it is possible that the partial loss of phenotype in the cell lines represents a default state imposed by the compulsive cell proliferation induced by T<sub>121</sub> activity. The domain structure of T-antigen is discussed in the Introduction to this chapter. The J-domain, which is retained by the T<sub>121</sub> protein, is known to mediate interactions with the Hsp70 chaperones, which have well-established roles in protein refolding and stability

(Helmbrecht 2000; Garrido 2003)(and references therein). The apparent absence of protein expression (E-cadherin and pan-cytokeratin) and altered subcellular localisation (TFN) of some of the markers in the cell lines could potentially be a consequence of T<sub>121</sub> J-domain activity, by interference with chaperone function. Though speculative, J-domain activity could explain the discrepancy between gene expression at the mRNA and protein level observed for E-cadherin and possibly pan-cytokeratin. It is concluded that three of the four CPlacZ cell lines have retained many aspects of the choroid plexus epithelial phenotype and provide useful *in vitro* models for this tissue. By contrast, the almost complete absence of marker gene expression in the CPlacZ2 cell line, suggests a more global loss of phenotype is likely to have occurred in this example.

As discussed in Chapter 1, recent genetic evidence has established a pivotal role for BMP-signalling in the specification and differentiation of the choroid plexus epithelium (Bulchand 2001; Hebert 2002; Hebert 2003). In this work embryos carrying a telencephalon-specific deletion within the *Bmpr-1a* gene, which encodes the BMP-type IA receptor, fail to develop the choroid plexus in the lateral ventricles of the brain (Hebert 2002). In these mutants, choroid plexus epithelial precursors lacked the expression of tissue-specific markers, showed reduced expression of *Msx1*, a BMP-responsive dorsal midline marker and remained in a proliferative state. BMP signalling is therefore required to correctly specify and differentiate the choroid plexus. Interestingly, in the present study, Northern analysis revealed that expression of *Msx1* though present, was somewhat reduced in some of the CPlacZ cell lines compared with wild-type choroid plexus tissue, thus suggesting that BMP signalling may be compromised. With this in mind, it would be interesting to ask whether augmentation of BMP-signalling could promote differentiation and re-establish the choroid plexus phenotype in the CPlacZ cell lines? An earlier study has demonstrated that either BMP2 or BMP4 protein soaked beads were able to promote expression of *Msx1* and inhibit cell proliferation in cultured telencephalon explants (Furuta 1997). This work suggests the exogenous delivery of BMP proteins as a potential method by which BMP-signalling could be stimulated in the cell lines. With the goal of a robustly differentiated *in vitro* model for choroid plexus epithelium in mind, experiments of this nature should be pursued in future work.

The principal aim of this chapter was to establish choroid plexus epithelial cell lines as *in vitro* models for biallelic *Igf2* expression. Indeed, biallelic *Igf2* expression would be predicted in cell lines derived from the choroid plexus epithelium, upon the basis of observations made *in vivo* (DeChiara *et al.*, 1991) therefore it was necessary to demonstrate this important criterion in the CPlacZ cell lines. Unexpectedly, Northern analysis failed to detect *Igf2* expression from the non-disrupted paternal allele, suggesting either that expression levels were below the detection threshold of this technique, or since the cells carried a maternally inherited *lacZDMR2*<sup>-</sup> allele, that the paternal allele had been silenced by an unknown mechanism. Allele-specific RT-PCR analysis, using primers that discriminate the wild type and *lacZDMR2*<sup>-</sup> sequences revealed evidence of weak expression from both paternal and maternal alleles. That is, biallelic *Igf2* expression, albeit at low levels, was observed in the cell lines.

Allele-specific analysis of *Igf2* expression *in situ* demonstrated transcription of the maternally inherited *lacZDMR2*<sup>-</sup> reporter gene allele, as evidenced by *in situ* staining for  $\beta$ -galactosidase activity. Remarkably, reporter gene activity was clearly restricted to a scattered cell population in all of the cell lines, thus mimicking the variegated expression profile of the choroid plexus epithelium *in vivo* (Charalambous *et al.* 2004). *In situ* hybridisation using an *Igf2* probe, to examine transcriptional activity from the paternal allele did not uncover any clear expression in a cell subset or otherwise, though abundant *Igf2* expression was seen in primary choroid plexus epithelial cells analysed in parallel. Whilst the RT-PCR analysis provided evidence of biallelic *Igf2* expression in the cell lines, the *in situ* analysis superficially describes monoallelic expression occurring specifically from the maternal allele. However the absolute gene expression levels from each allele cannot be formally related, as the various methods used to interrogate these factors are not directly comparative.

Interestingly, this data could reflect an unconfirmed observation made in the developmental expression assays (see Chapter 3), where a greater proportion of choroid plexus epithelial cells were seen to express the *lacZDMR2*<sup>-</sup> reporter gene upon maternal transmission. Expression of the paternal allele in a very small number of cells, as appears to be the case in the choroid plexus epithelium *in vivo*, could have been missed, even with the *in situ* approach used here. The issue of whether *Igf2*

expression predominating from the maternal allele actually occurs in the choroid plexus epithelium could be stringently addressed in the future by examination of expressed polymorphisms in similar cell lines carrying the *Mus spretus*-derived SD7 chromosome. *H19* expression was not detected in the cell lines by Northern analysis, a finding that was expected given the absence of *H19* expression from the choroid plexus epithelium *in vivo* (Charalambous *et al.* 2004)(and Chapter 3), though sensitive RT-PCR analysis that would have confirmed this observation was not done. As already discussed, the cell lines showed clear evidence of variegated reporter gene expression as observed *in vivo* (Charalambous *et al.* 2004)(and Chapter 3). Whether this variegated expression pattern has arisen as consequence of clonal heterogeneity within the cell lines or whether a cell autonomous mechanism is involved remains unanswered. Time constraints prevented further work on this very interesting feature, but potentially the conservation of variegated *Igf2* expression in the CPlacZ cell lines would provide a useful system for further analysis. The investigation of candidate genes in the Notch signalling pathway (see Chapter 3) could be extended to the cell lines. As such an RNA interference (RNAi) approach could be employed *in vitro* to assess the function of these molecules in the context of variegated expression.

Differential methylation upon CpG dinucleotides at imprinted loci is widely documented and discussed at length in Chapter 1. Primary imprinting control of the *Igf2/H19* locus is centred upon a differentially methylated domain (DMD) that lies in the 5' flank of the *H19* gene and in the unmethylated state, functions as an insulator to prevent activation of *Igf2* by distal enhancers. The insulator function of the DMD is dependent upon the zinc-finger protein CTCF, which binds to specific sites within this region in a methylation-sensitive manner (Thorvaldsen *et al.* 1998; Bell 2000; Hark *et al.* 2000; Kaffer 2000; Kanduri 2000a). Recent genetic evidence demonstrates that CTCF binding is required to maintain the unmethylated state of the DMD during development (Schoenherr *et al.* 2003; Fedoriw *et al.* 2004; Pant 2004).

One of the most significant questions posed by the present study was to ask whether epigenetic modifications at the DMD underlie the deregulation imprinting at *Igf2/H19* in the choroid plexus epithelium? That is, could aberrant methylation of the maternal DMD allele and/or the absence of CTCF protein explain biallelic *Igf2* expression (and biallelic *H19* silencing) in this tissue? These questions were tackled indirectly by

analysis of the CPlacZ cell lines. Northern analysis revealed the abundant expression of *CTCF* mRNA in all of the cell lines suggesting that the protein would also be present. Time constraints prevented Western blot analysis that would have corroborated the Northern analysis. Prospectively, the examination of allele-specific CTCF binding at the DMD within the context of the cell lines could better define the role of this protein as an epigenetic regulator in the choroid plexus epithelium.

CpG methylation was examined at several *HpaII/MspI* sites within the DMD and also in the associated *H19* promoter proximal region, in the cell lines using a methylation-sensitive Southern blotting approach. Both regions were partially (approximately 50%) methylated in all of the cell lines with this pattern assumed to represent differential methylation. Two lines of evidence support this assumption. First, paternal-specific hypermethylation of the DMD is consistently observed throughout development in a wide range of tissues (Tremblay *et al.* 1997; Weber 2001). Secondly, a similar degree of partial methylation was observed at the DMD in the neonate liver controls, a tissue where its robust differential methylation has been previously shown (Weber 2001). Though allele-specific analysis would be required to formally exclude other possibilities, the present data argue that the DMD is differentially methylated in a tissue where non-imprinted expression occurs, the choroid plexus epithelium.

In addition to the DMD, other regions of differential methylation, DMR1 and DMR2, have been identified proximal to *Igf2* that display hypermethylation upon the predominantly expressed paternal *Igf2* allele in many mesodermal and endodermal tissues (Sasaki *et al.* 1992; Weber 2001). These regions possess methylation-dependent silencing or activating functions respectively (Constancia *et al.* 2000; Eden *et al.* 2001; Murrell *et al.* 2001) and therefore provide the basis of secondary imprinting controls that act upon *Igf2*. More recent work has shown that methylation within these regions is dependent upon and acquired in a manner consistent with that of the DMD lying *in cis*, and has led to the proposal that these DMRs fall under the control of the DMD in a hierarchical manner (Lopes *et al.* 2003).

Earlier work demonstrated that *Igf2* proximal DMRs are highly methylated upon both parental alleles in the choroid plexus providing evidence of an epigenetic basis to



biallelic *Igf2* expression in this tissue (Feil *et al.* 1994). Strikingly, almost complete methylation of DMR1 was observed in the cell lines, thus indicating almost absolute hypermethylation of both alleles in a manner consistent with this work (Feil *et al.* 1994). At the same time, measurements made in intact choroid plexus tissue (which would have contained both epithelium and stroma) observed somewhat lower methylation levels within this region suggesting that its hypermethylation is likely to be specific to the choroid plexus epithelium, but not the stroma. These observations are consistent with the developmental expression analysis (see Chapter 3) where *Igf2* expression was found to be biallelic in the choroid plexus epithelium, but imprinted in the stroma. The cell line methylation data provides compelling evidence that epigenetic modification (the acquisition of maternal hypermethylation) of DMR1 is associated with biallelic *Igf2* expression in this tissue. Importantly, when considered with the analysis of the DMD, which appeared to be differentially methylated in the cell lines, it seems likely that this modification of DMR1 occurs by a DMD-independent mechanism.

In consideration of the DMR1 methylation data, a surprising outcome was the lack of concordance between the parental-origin specific expression and methylation of *Igf2* in the cell lines. Hypermethylation within the DMR1 region is usually associated with the transcriptionally active *Igf2* allele and its hypomethylation with silencing (Sasaki *et al.* 1992; Constancia *et al.* 2000; Eden *et al.* 2001; Weber 2001). In the cell lines DMR1 appeared to be highly methylated upon both alleles, yet only low levels of expression could be detected from either allele. That is, DMR1 methylation and *Igf2* expression are negatively correlated in the cell lines. Examination of methylation at other sites within the *Igf2* gene might further elucidate this discrepancy and exclude other possibilities such as linear spreading of methylation into adjacent regulatory elements. DMR2 or the promoter regions would be good candidates for this analysis. A concern is that the partial loss of phenotype in the cell lines, as indicated by gene expression analysis, has also impacted upon transcriptional regulation and/or epigenetic modifications at the *Igf2/H19* locus, although that methylation patterns observed within DMR1 and the DMD are consistent with those seen previously is encouraging (Feil *et al.* 1994; Yang 2003). Nonetheless, in general terms aberrant epigenetic modifications leading to the inappropriate expression or silencing of genes are frequent events *in vitro*. Similar effects in the CPlacZ cell lines cannot be

excluded at present, which means that any extrapolation of the methylation data should be made with caution.

The DMR hierarchy proposal asserts that the DMD protects *Igf2* proximal DMRs lying *in cis*, from *de novo* methylation and thus maintains their maternal hypomethylated state (Lopes *et al.* 2003). While this is likely to be the case in the majority of tissues, the findings of the present study and of earlier work (Feil *et al.* 1994) argue against such DMD-centred control in the choroid plexus epithelium. In the wake of the DMR hierarchy proposal, it could be argued that mechanisms conferring DMD-mediated protection are either absent, or in some way surmounted in the choroid plexus epithelium. Lopes *et al.* posit the involvement of regional chromatin dynamics in mediating DMR interactions and propose a chromatin-looping model by which the DMD and *Igf2* proximal DMRs might associate, via the vertebrate insulator CTCF and other proteins, to form a single nucleo-protein complex. Future work might attempt to address the possibility of such interactions by performing chromatin immuno-precipitation (ChIP) assays in choroid plexus epithelial tissue. The choroid plexus epithelial cell lines created in the present study would provide a good resource for this analysis. Comparative ChIP analysis using the choroid plexus cell lines against a second cell line in which imprinted *Igf2* expression is maintained, could reveal much about potential mechanisms that regulate DMR interactions. Along these lines, it might also be interesting to ask whether DMD-independent controls operate within additional sites of biallelic *Igf2* expression in the brain, the capillary endothelium and leptomeninges. Indeed, a method for isolating capillary endothelium from rat brain parenchymal tissue has been described (Li 2001a). This technique could be adapted to isolate brain endothelial tissue for methylation and ChIP analysis.

A criticism of the methylation analysis presented in this study is that it lacks allele-specificity; instead gross methylation levels from both alleles were measured inclusively. This is particularly relevant to the DMD analysis, where partial methylation was interpreted as differential- and hence, paternal-specific methylation for reasons discussed. Although unlikely, these findings could represent mosaic methylation patterns upon both alleles. In this instance, allele-specific methylation assays were not possible in the CPlacZ cell lines as there was no means of

discriminating the alleles at either DMR1 or the DMD. Nonetheless, such assays should be done to corroborate the conclusions of this chapter. This awaits the derivation of further choroid plexus epithelial cell lines carrying the *Mus spretus* derived SD7 chromosome. In this system, restriction fragment length polymorphisms that exist between the *Mus musculus* and *Mus spretus* alleles will be identified and used to interrogate parental-origin specific methylation marks both at DMD and the DMR1. A further limitation of the analysis here is that it only considered methylation at CpG dinucleotides within *HpaII/MspI* sites, with the status of these sites assumed representative of other CpG sites in the surrounding genomic DNA. This is particularly relevant to DMR1, where the magnitude of differential methylation has been shown to vary between specific CpG sites within this region (Forne *et al.* 1997; Weber 2001). Further work utilising a bisulphite mutagenesis approach, which can determine methylation frequencies within all CpG dinucleotides of a given genomic region, might further elucidate findings of this study.

In summary, immortal cell lines have been successfully established from the choroid plexus epithelium of the mouse. Three of the four cell lines established bear a close resemblance to the parent tissue by criteria of morphology and the expression of marker genes, though the expression of epithelial cell markers E-cadherin, cytokeratins and possibly other genes may have been perturbed in response to the transformed state of the cells. Biallelic *Igf2* expression was not clearly demonstrated in the cells though, encouragingly, other hallmarks of *Igf2/H19* expression described within the choroid plexus epithelium *in vivo*, that is, variegated reporter gene expression and biallelic silencing of *H19* appear to have been conserved. Asymmetrical methylation patterns were observed at *Igf2/H19*, where biallelic hypermethylation of DMR1 was seen in the presence of differential methylation at the DMD *in cis*. This epigenotype suggests that a DMD-independent modification of the *Igf2* proximal DMRs may, in part, provide the basis of biallelic *Igf2* expression in the choroid plexus epithelium.

## CHAPTER 6: CONCLUSIONS

### ***Developmental expression analysis***

The *Igf2* and *H19* genes are expressed in multiple tissues during embryonic development and are subject to genomic imprinting. Both genes are regulated by an imprinting control region (ICR) that is situated within a differentially methylated domain (DMD) 2-4kb 5' of *H19* (Tremblay *et al.* 1997; Thorvaldsen *et al.* 1998). The DMD exists in two epigenetic states, dependent upon its parental origin. Following transmission through the paternal germline, it is hypermethylated, adopts a closed chromatin conformation and is required to initiate but not maintain silencing of the *H19* gene. After maternal transmission, it is almost entirely devoid of methylation, exists in an open chromatin conformation and is required to both initiate and maintain silencing of *Igf2 in cis* (Tremblay *et al.* 1997; Thorvaldsen *et al.* 1998; Drewell *et al.* 2000; Srivastava 2000). The DMD contains a chromatin boundary or insulator element that acts to block the interaction of *Igf2* promoters with enhancers that lie 3' of this region with insulator activity dependent upon the protein CTCF, which binds in a methylation-sensitive manner (Bell 2000; Hark *et al.* 2000; Holmgren 2001; Schoenherr *et al.* 2003; Fedoriw *et al.* 2004; Pant 2004). Consistent with the insulator model, which predicts that enhancers active in imprinted tissues will be situated 3' of the DMD, both endoderm and mesoderm-specific enhancer regions have been identified 3' of *H19* (Leighton *et al.* 1995; Ishihara and Jinno 2000; Kaffer 2000; Davies *et al.* 2002).

*Igf2* escapes imprinted regulation and is biallelically expressed in the exchange tissues of the brain, the choroid plexus and leptomeninges, in mice and humans (DeChiara *et al.* 1991; Ohlsson *et al.* 1994; Svensson 1995). A greater understanding of the molecular mechanisms involved in this mode of expression has been sought, as *Igf2* frequently undergoes loss of imprinting in human overgrowth disorders and cancer. Regulatory elements that confer *Igf2* expression in these tissues would be predicted to lie 5' of the DMD and therefore not be affected by insulator activity. Consistent with this expectation, at least one enhancer driving expression in the choroid plexus and leptomeninges is located within the *Igf2/H19* centrally conserved domain (CCD) situated approximately 32kb 5' of the DMD (Ward *et al.* 1997; Jones *et al.* 2001; Charalambous *et al.* 2004). Importantly, the CCD can also drive expression in a subset

of tissues where *Igf2* is imprinted suggesting that enhancer location alone cannot fully explain biallelic *Igf2* expression in the exchange tissues of the brain (Charalambous *et al.* 2004). Differentially methylated regions situated proximal to *Igf2* are hypermethylated upon both alleles in the choroid plexus, suggestive of an additional mechanism that could mediate biallelic expression in this tissue (Feil *et al.* 1994; Constanica *et al.* 2000; Eden *et al.* 2001).

The choroid plexus arises from two distinct embryonic lineages. The epithelium originates from the neural tube, whereas the stroma is derived from cephalic mesoderm (Catala 1998). In the present study, allele-specific analysis to determine the imprinting status of *Igf2 in situ*, which made use of the *lacZDMR2*<sup>-</sup> reporter gene knock-in mutant, revealed strikingly different expression profiles between the epithelial and stromal components of this tissue. *Igf2 (lacZDMR2*<sup>-</sup>) expression was initiated in the presumptive choroid plexus epithelium between e9.5 and e10.5 of development and was biallelic from its onset. Biallelic expression continued in the mature choroid plexus epithelium consistent with previous work, though in the stroma *Igf2* was imprinted, with expression from the paternal allele at all stages examined, contrary to earlier reports of biallelic expression in this component (DeChiara *et al.* 1991; Svensson 1995). *Igf2 in situ* hybridisation experiments verified these observations. *H19* was biallelically silenced in the choroid plexus epithelium, but maintained imprinting in the stroma with exclusive maternal expression. In the adult brain, biallelic *Igf2* expression was observed in the choroid plexus epithelium, although the stromal expression had almost completely disappeared, possibly reflecting the situation in other imprinted tissues, where expression of this gene is downregulated after birth. These observations appear to reflect the dual embryonic origin of the choroid plexus and strengthen the argument that *Igf2/H19* expression is governed by distinct mechanisms in the two components of this tissue.

Regulatory elements that confer expression in the choroid plexus epithelium are situated 5' to the DMD, within the CCD region and provide the basis of biallelic *Igf2* expression at this site (Jones *et al.* 2001; Charalambous *et al.* 2004). Silencing of the *H19* gene in this tissue could also be consistent with its location on the opposite side of the DMD (to *Igf2*), where the insulator potentially blocks an interaction between the *H19* promoter and the CCD. In support of this proposal, no change in the level of

*H19* RNA was reported in the choroid plexus following deletion of the CCD (Jones *et al.* 2001). Imprinted expression of both genes in the stroma invokes elements situated 3' to the DMD. Consistent with this expectation, mesodermal enhancers (that would be predicted to confer expression in the stroma), are located 3' of the *H19* gene (Ainscough *et al.* 1997; Ishihara and Jinno 2000; Kaffer 2000; Davies *et al.* 2002). In apparent contradiction to the insulator model, the CCD has also been shown to drive reporter gene expression in a subset of mesodermal tissues that includes the choroid plexus stroma (Charalambous *et al.* 2004). Transgenic experiments indicate that this activity may be specific to *Igf2* as no change in *H19* expression was reported in the choroid plexus following deletion of the CCD, again possibly reflecting the presence of the insulator within the intervening region (Jones *et al.* 2001). The CCD therefore drives *Igf2*, but probably not *H19* expression, in both the stroma (imprinted) and epithelium (non-imprinted).

Other sites of biallelic *Igf2* expression were identified in the brain, most notably the capillary endothelium. Expression in this tissue was imprinted at early stages with expression from both parental alleles evident later in gestation, which continued in the adult brain. Regulatory elements driving *Igf2* expression in capillary endothelium have not been formally defined, although the mesodermal origin of this tissue implicates enhancers situated 3' of the DMD, or possibly the restricted mesoderm-specific activity observed at the CCD (Charalambous *et al.* 2004). Speculatively, the transition from imprinted to non-imprinted expression observed in developing capillaries, is suggestive of a switch between regulatory mechanisms involving distinct enhancer regions.

Given the extensive network of brain capillary endothelium, it seems likely that this tissue provides a third major source of biologically available IGFII peptide in the brain, complementing that provided by the choroid plexus and leptomeninges. A definitive function has yet to be ascribed to *Igf2* in the CNS and with this in mind it may be no coincidence that the major sites of its brain expression are in tissues with exchange or barrier function.

*Igf2* (*lacZDMR2'*) expression was observed in a finely scattered distribution in the choroid plexus epithelium. This variegated pattern was seen at the onset of *Igf2*

expression in the presumptive choroid plexus epithelium at e10.5 and at all other stages examined. By contrast, uniform expression of Transthyretin (TTR) and several other differentiated markers was observed throughout this tissue. Therefore, two cell-subpopulations respectively defined by the presence or absence of *Igf2* expression exist in the choroid plexus epithelium.

It would be of interest to identify *cis*-elements and the associated *trans*-factors controlling this mode of expression. Recent studies suggest the participation of the CCD in this role. In transgenic mice, the CCD reproducibly conferred variegated expression upon *Igf2* Promoter3 (P3)-*lacZ* reporter genes in the choroid plexus epithelium, thus reflecting that of the endogenous *Igf2* gene (Charalambous *et al.* 2004). Remarkably, analysis of the mouse CCD in transgenic *Drosophila* demonstrated that the variegation/silencing functions of this region are conserved, with the polycomb group (PcG) genes *Enhancer of zeste* (*E[z]*) and *Posterior sex combs* (*Psc*) involved in mediating this activity (Erhardt *et al.* 2003). The CCD (and possibly P3) must therefore contain the sequences sufficient to direct this pattern of expression within the choroid plexus epithelium *in vivo*. It would be interesting to ask if mammalian *E[z]* and *Psc* homologues perform analogous roles in the mouse, by mediating the variegation and silencing functions of the CCD at the *Igf2/H19* locus. Indeed the absence of genome methylation in *Drosophila* and the hypomethylated state of the CCD reported previously in the mouse, suggests that repression conferred by this region in both species may be mediated by a conserved, methylation-independent mechanism (Koide 1994; Lyko *et al.* 1999).

There was good reason to suspect an involvement of *Delta* and *Notch* genes in the specification of putative subpopulations within the choroid plexus epithelium. Notch signalling has an established role in generating asymmetric cell fates within lineages of identical cells during embryogenesis (discussed in the Introduction to Chapter 3). Mammalian *Notch* receptors and the cognate ligands encoded by *Delta* genes are widely expressed in the primitive neuroectoderm layer from which the CNS and associated structures, including the choroid plexi later arise. RT-PCR analysis showed expression of all *Notch* and most *Delta* genes in whole neonate choroid plexus tissue. *In situ* hybridisation analysis was performed to examine the distribution of *Delta/Notch* expression in the embryonic choroid plexus epithelium, but technical

difficulties prevented a comprehensive evaluation of these genes in this tissue. At present, the role of Notch signalling in the choroid plexus epithelium remains unresolved.

### ***Transient expression assays***

It was of interest to define the minimal sequences within the CCD that confer biallelic expression in the choroid plexus epithelium. One approach to the localisation of functional elements is to search for conserved sequences between divergent species. Earlier work that utilised this approach identified two stretches of conserved sequence, region 1 and region 2, within the 2kb CCD region, where region 1 coincides with three sites of strong DNaseI hypersensitivity (Koide 1994). Deletion of the 5' most 1kb of the CCD, which removed region 1 and the hypersensitive sites had no apparent effect upon *Igf2* expression in the brain, but resulted in reactivation of the maternal *Igf2* allele in tissues with a significant skeletal muscle component after e17.5 of development (Ainscough *et al.* 2000b). That is, region 1 contains a muscle-specific silencer element that is active in late embryogenesis. A function for the second 1kb of the CCD containing region 2 has not been described, but could possibly contain the elusive choroid plexus enhancer element.

An *in vitro* approach was taken to further delineate regulatory elements controlling *Igf2* expression. Primary choroid plexus cultures were established and shown to present appropriate morphological features and express diagnostic marker genes. These cultures were subsequently used in transient expression assays to analyse *Igf2* P3-*Luciferase* constructs, which either carried the full length CCD or smaller fragments from which region 1 or region 2 had been deleted. Consistent with previous work where the CCD could not drive reporter gene expression above the level of a control construct *in vitro*, no tissue-specific enhancer activity was seen in the primary cultures (Charalambous 2000). Instead the CCD conferred a large and significant silencing effect upon P3. Although not statistically significant, deletion of region 1 from this construct resulted in a partial but reproducible loss of this silencing, possibly consistent with the silencer activity reported previously for region 1 *in vivo* (Ainscough *et al.* 2000b; Jones *et al.* 2001). Taken together with previous transgenic and transient analyses of the CCD, data from the present study argues that this region can behave as an enhancer when integrated into the genomic environment, but not in



the extra-chromosomal context (Ward *et al.* 1997; Charalambous 2000; Jones *et al.* 2001; Charalambous *et al.* 2004). This hypothesis remains to be tested in the *in vitro* cell culture system (CPlacZ cells) by analysis of stably integrated transgenes.

Does region 2 of the CCD contain the choroid plexus enhancer? Given the failure of the transient system to dissect activities within the CCD, future studies should involve a transgenic approach. The creation of a small germline deletion encompassing region 2 would be the most stringent means to address this issue.

Are other elements besides the CCD required for *Igf2* expression in the choroid plexus? Deletion of the CCD led to a reduction in *Igf2* mRNA levels, but did not eliminate expression from the choroid plexus, which argues for the existence of at least one additional regulatory region with activity in this tissue (Jones *et al.* 2001). The present study made use of comparative sequence analysis of a 1Mb region encompassing the *Igf2/H19* locus in human and mouse, which identified a number of conserved non-coding sequences, five of which were located within the *Igf2/H19* intergenic region and did not correspond to known elements (Onyango *et al.* 2000). These sequences, C1-C5, were inserted into P3-*Luciferase* reporter constructs and transfected into primary choroid plexus cultures to examine any tissue-specific enhancer activity, although none were found to drive reporter gene expression above the levels of the **M** construct, containing *Igf2* P3 alone.

Could cryptic enhancer activity implicated in the study by Jones *et al.* reside at P3? Transgenes containing P3 consistently confer expression in the choroid plexus, providing evidence in support of this proposal (Ward *et al.* 1997; Charalambous 2000; Charalambous *et al.* 2004; Kelly 2004). Transient expression data from the present study could also be consistent with this hypothesis as none of the constructs tested significantly increased reporter gene expression levels above that of the **M** construct, containing P3 alone. However it is unclear whether silencing conferred by the CCD upon P3 *in vitro* genuinely represents that observed *in vivo* (Ainscough *et al.* 2000b) or a second aberrant activity, thus complicating any interpretation of the transient data. Prospectively, the generation of further transgenic lines bearing P3-*lacZ* reporter constructs would provide a more appropriate means to clarify the role of P3. In

conclusion, the CCD represents the only brain/choroid plexus enhancer element formally identified at the *Igf2/H19* locus to date.

### ***Immortal choroid plexus epithelial cell lines***

*Igf2* expression is biallelic in the choroid plexus epithelium and imprinted in the stroma. This may reflect the distinct embryonic origin of the two tissues and suggests that epigenetic marks may be differently established in these cell types (Catala 1998). Indeed biallelic hypermethylation of the differentially methylated regions proximal to *Igf2*, DMR1 and DMR2, has been described previously following analysis of whole choroid plexus, yet the same study provided evidence that the *H19* promoter-proximal region is only 50% methylated, consistent with a profile of differential (paternal-specific) methylation similar to that normally observed in imprinted tissues (Feil *et al.* 1994). Feil *et al.* did not address the methylation status of the DMD in the choroid plexus, raising the question of whether differential methylation of this region is maintained in this tissue.

It was therefore of interest to separately examine epigenetic modifications in the choroid plexus epithelium. Primary choroid plexus cultures were not suited to this analysis, as they contained both epithelial and stromal cell types. In addition these cells did not proliferate once explanted in culture and could not be passaged, thus further limiting their use. Therefore a strategy was devised to derive an immortal cell line from the choroid plexus epithelium. Transgenic mice of the T<sub>121</sub> strain were obtained, which over-express a T-antigen variant. This T<sub>121</sub> protein binds and inactivates Retinoblastoma but not p53 such that its expression in these animals induces aberrant cell proliferation and tumourigenesis of the choroid plexus epithelium (Saenz Robles *et al.* 1994). However, this activity alone was not sufficient to allow derivation of cell lines, therefore the absence of p53 binding activity in T<sub>121</sub> was *trans*-complemented by crossing the mice onto a *p53*<sup>+/-</sup> knockout background, creating T<sub>121</sub>:*p53*<sup>+/-</sup> mice, which have a significantly increased rate of choroid plexus tumour development. Tumour tissue taken from these animals was the source from which four choroid plexus epithelial cell lines were derived.

Genetic analysis showed these cell lines to be *p53* null, consistent with loss of the single wild-type *p53* copy carried by the founder animal. This was reflected in the

growth rate of the cell lines (essentially of the  $T_{121}p53^{-/-}$  genotype), which proliferated at a significantly greater rate than primary cultures expressing  $T_{121}$  in the presence of functional  $p53$ . The cell growth data thus indicates that combined inactivation of both *Retinoblastoma* and  $p53$  are required to fully immortalise the choroid plexus epithelium *in vitro*.

The identity of the cell lines was confirmed by analysis of morphology and gene expression. All of the cell lines presented the polygonal closely opposed morphology that is characteristic of epithelial cells, consistent with their origin from the choroid plexus epithelium. Three out of four cell lines expressed marker genes consistent with their origin from the choroid plexus epithelium but none of the cell lines appeared to express the epithelial cell markers E-cadherin and pan-cytokeratin at the protein level, possibly indicating the downregulation of these genes in response to the transformed state induced in these cells. One of the cell lines, CPlacZ2, exhibited a marked reduction in the expression of all genes analysed indicating that a global loss of phenotype had occurred in this case. Biallelic *Igf2* expression could not be clearly demonstrated in the cell lines though, biallelic silencing of *H19* appears to have been maintained. Good evidence for expression of the maternal *Igf2* allele was found *in situ* as judged by staining for activity of the lacZDMR2<sup>-</sup> reporter gene allele. This expression was variegated and thus reflected the pattern of expression seen in the choroid plexus epithelium *in vivo* (Charalambous *et al.* 2004).

Once the identity of the cell lines had been examined and largely confirmed, DNA methylation analysis was performed as an indirect means to assess epigenotypes at the *Igf2/H19* locus in the choroid plexus epithelium. The DMD and *H19* promoter-proximal region were found to be approximately 50% methylated in the cell lines and in whole choroid plexus consistent with the previous analysis of the *H19* promoter (Feil *et al.* 1994). These observations indicate that differential methylation of the alleles occurs at the DMD in both components of the choroid plexus. The protein CTCF is essential for the maintenance of differential methylation at the DMD postzygotically, where binding of this protein prevents *de novo* methylation of the maternal allele (Schoenherr *et al.* 2003; Fedoriw *et al.* 2004; Pant 2004). In agreement with these studies, abundant *CTCF* mRNA expression was demonstrated in all of the cell lines. By contrast, DMR1 was almost 100% methylated in the cell lines,

consistent with biallelic hypermethylation of this region. Methylation levels were significantly lower at this region in whole choroid plexus. Together these results suggest that DMR1 acquires distinct epigenotypes in the epithelial and stromal components of the choroid plexus, with biallelic hypermethylation of DMR1 predominating in the epithelium.

In imprinted tissues, differential marking within *Igf2* proximal DMRs is dependent upon and acquired in a manner consistent with that of the DMD lying *in cis*, and has led to the proposal that these DMRs fall under the control of the DMD in a hierarchical manner (Lopes *et al.* 2003). The DMD therefore protects *Igf2* proximal DMRs from *de novo* methylation on the maternal allele. Recent evidence suggests that the mechanism conferring this protection may involve the physical association of the DMD and DMR1 on the maternal chromosome via a chromatin loop, with the protein CTCF implicated in mediating this interaction (Murrell 2004). *In vitro* analysis of the choroid plexus epithelium (CPlacZ cell lines) in the present study showed that the maternal allele is hypermethylated at DMR1 in the presence of the DMD in the hypomethylated state lying *in cis*. That is, parental-origin specific methylation at these DMRs is dissociated in the choroid plexus epithelium. In the wake of the chromatin-looping proposal, it could be argued that interactions normally existing between these regions at imprinted sites may be decoupled in this tissue (Murrell 2004). How this might occur mechanistically is unclear, but it is possible that the local chromatin environment in differentiated choroid plexus epithelial cells is not permissive for DMR interactions at *Igf2/H19*.

In summary, two mechanisms are proposed to mediate biallelic *Igf2* expression in the choroid plexus epithelium (**Figure 46**). First, the identification of at least one enhancer within the CCD region that drives expression in the choroid plexus epithelium provides a fundamental mechanism for biallelic *Igf2* expression in this tissue (Ward *et al.* 1997; Jones *et al.* 2001; Charalambous *et al.* 2004). Enhancers governing expression in imprinted tissues are located 3' of the DMD and access *Igf2* exclusively on the paternal allele as a consequence of insulator activity. The CCD is located 5' to DMD and therefore gains access to *Igf2* promoters upon both alleles, as presumably the insulator does not affect it. Second, biallelic hypermethylation of *Igf2* proximal DMRs may be permissive for biallelic expression, presumably by excluding

**Figure 46. Proposed mechanisms of biallelic *Igf2* expression in the choroid plexus epithelium.** The *Igf2* and *H19* genes are shown as open boxes (not to scale), regions of differential methylation between the parental alleles are shown as filled boxes, from left to right, DMR1, DMR2, DMD, *H19* promoter proximal region; lollipops above these regions indicate hypermethylation. Enhancers are shown as ovals, from left to right, the CCD, endoderm enhancers, mesoderm enhancers. Where present the curved arrows indicate interactions between enhancers and promoters; curved flat-ended lines indicate silencing or enhancer blocking activity. **A** *Igf2* expression in the choroid plexus epithelium is mediated by enhancers at the CCD and by biallelic methylation of proximal DMRs which abrogates binding of repressor proteins such as GCF2. *H19* is silenced in this tissue by hypermethylation of the DMD and promoter proximal region on the paternal allele and by insulator activity (associated with hypomethylation of the DMD) which may block an interaction with the CCD on the maternal allele. **B** In the choroid plexus stroma and a subset of mesodermal tissues the CCD drives *Igf2* expression as the proximal DMRs are paternally methylated. Hypomethylation of these DMRs on the maternal allele allows repressor proteins to bind and prevent activation of *Igf2* by the CCD. Maternal-specific *H19* expression in the stroma may not be mediated by the CCD but instead governed by the distal enhancers.



protein factors with a silencing function (DMR1) or recruiting those that activate gene expression (DMR2) respectively (Eden *et al.* 2001; Murrell *et al.* 2001). Hypomethylation of maternal allele at these DMRs is probably required in a subset of mesodermal tissues to prevent activation of *Igf2* by the CCD (Charalambous *et al.* 2004). Biallelic silencing of *H19* in the epithelium is consistent with paternal-specific methylation of its promoter region and by maternal-specific insulator activity both of which could prevent its activation by the CCD.

### **Future work**

Choroid plexus epithelial cells provide the structural basis of the blood-cerebrospinal fluid (CSF) barrier and play important roles in regulating the delivery of biologically important molecules, including therapeutic compounds, to the brain. *In vitro* models that mimic the barrier and transport properties of this tissue are widely sought as a means to assess the delivery of novel drug compounds to the CNS, potentially lessening the need for laboratory animals (Gherzi-Egea 2001; Haselbach *et al.* 2001; Speake 2001)(and references therein). Morphological and biochemical analyses performed in the present study suggest that the CPlacZ cell lines could provide such *in vitro* models for the characterization of choroid plexus function. It would be necessary to determine whether cultured CPlacZ cells can reproduce functional properties of the choroid plexus epithelium, for example the polarized ion fluxes associated with CSF secretion. A preliminary means to address this question would be to culture CPlacZ cells in specialized trans-well apparatus and look for any directional fluid movement across the cell monolayer that would be indicative of functional CSF production. This approach has been successfully used in both primary and immortal choroid plexus epithelial culture systems (Haselbach *et al.* 2001; Zheng 2002). Analysis of such functional markers of the choroid plexus phenotype, it is envisaged, could further confirm the identity of the CPlacZ cells, thus complementing the morphological and biochemical data already described in this study.

Biallelic methylation of the *Igf2* proximal DMRs is observed in association with biallelic *Igf2* expression in the choroid plexus epithelium. Whether these epigenetic marks are the determinant factors or the consequence of biallelic expression in this tissue remains unanswered. Could the imprinting of *Igf2* be manipulated by experimentally removing CpG methylation at this locus? This could be addressed in

the CPlacZ cell lines by treatment with the DNA methyltransferase inhibitor, 5'-aza-2'-deoxycytidine (aza-C) and the lacZDMR2<sup>-</sup> reporter gene used to differentiate the parental origin of transcripts. However, as there would be no means of discriminating the alleles for the purposes of methylation analysis, this would be better suited to a similar cell line carrying one copy of the *Mus spretus*-derived SD7 chromosome. DNA polymorphisms that exist between the *musculus* and *spretus* sub-species have been described in *Igf2* and *H19* coding sequences and in the DMRs surrounding both genes (Forne *et al.* 1997; Hemberger 1998; Lopes *et al.* 2003; Murrell 2004). Both allele-specific expression and DNA methylation assays would therefore be possible in such a cell line following global demethylation with aza-C treatment. Live tumour tissue has been successfully explanted from a single T<sub>121</sub>:p53<sup>+/-</sup>:SD7<sup>+/-</sup> animal and cryopreserved. The derivation of cell lines carrying the SD7 region awaits cloning of the epithelial cell fraction from this tissue.

Biallelic *Igf2* expression commences at an early stage in the specification of the choroid plexus epithelium (see Chapter 3). Are the epigenetic marks associated with this mode of expression established in a synchronistic manner? The CPlacZ cell lines created in this study represent the choroid plexus epithelium at a postnatal stage of development. Whilst it is likely that the methylation patterns observed in these cell lines reflect those present in the mature tissue, they do not describe the ontogeny of epigenetic marks during the formation of the choroid plexus epithelium or indeed within the lineage of neuroepithelial cells that generate this tissue. This could be investigated by the derivation of further cell lines using presumptive and differentiating choroid plexus epithelial tissue explanted from different embryonic stages. Lines of T<sub>121</sub>:p53<sup>+/-</sup>:SD7<sup>+/-</sup> mice would provide a useful resource for this purpose. Examination of the epigenetic modifications at *Igf2/H19* in this context could further elucidate the mechanisms by which the DMD-centred control at this locus is surmounted in the choroid plexus epithelium. The pursuit of studies utilising this approach may provide a greater understanding of the molecular events that lead to loss of imprinting mutations in overgrowth and cancer.



## REFERENCES

- Aden, D.P., Fogel, A., Plotkin, S., Damjanov, I. and Knowles, B.B. (1979). "Controlled synthesis of HBsAg in a differentiated human liver carcinoma-derived cell line." Nature **282**: 615-6.
- Ainscough, J.F., Dandolo, L. and Surani, M.A. (2000a). "Appropriate expression of the mouse H19 gene utilises three or more distinct enhancer regions spread over more than 130 kb." Mech Dev **91**(1-2): 365-8.
- Ainscough, J.F., John, R.M., Barton, S.C. and Surani, M.A. (2000b). "A skeletal muscle-specific mouse Igf2 repressor lies 40 kb downstream of the gene." Development **127**(18): 3923-30.
- Ainscough, J.F., Koide, T., Tada, M., Barton, S. and Surani, M.A. (1997). "Imprinting of Igf2 and H19 from a 130 kb YAC transgene." Development **124**(18): 3621-32.
- Alam, J. and Cook, J.L. (1990). "Reporter Genes: Application to the Study of Mammalian Gene Transcription." Analytical Biochemistry **188**: 245-254.
- Arney, K.L. (2003). "H19 and Igf2--enhancing the confusion?" Trends Genet **19**(1): 17-23.
- Barlow, D.P. (1997). "Competition - a common motif for the imprinting mechanism." Embo J **16**(23): 6899-905.
- Barlow, D.P., Stoger, R., Herrmann, B.G., Saito, K. and Schweifer, N. (1991). "The mouse insulin-like growth factor type-2 receptor is imprinted and closely linked to the Tme locus." Nature **349**(6304): 84-7.
- Bartolomei, M.S., Webber, A.L., Brunkow, M.E. and Tilghman, S.M. (1993). "Epigenetic mechanisms underlying the imprinting of the mouse H19 gene." Genes Dev **7**(9): 1663-73.
- Bartolomei, M.S., Zemel, S. and Tilghman, S.M. (1991). "Parental imprinting of the mouse H19 gene." Nature **351**(6322): 153-5.
- Barton, S.C., Adams, C.A., Norris, M.L., Surani, M.A. (1985). "Development of gynogenetic and parthenogenetic inner cell mass and trophectoderm tissues in reconstituted blastocysts in the mouse." J Embryol Exp Morphol **90**: 267-85.
- Barton, S.C., Surani, M.A., Norris, M.L. (1984). "Role of paternal and maternal genomes in mouse development." Nature **311**(5984): 374-6.
- Beck, F., Samani, N.J., Penschow, J.D., Thorley, B., Tregear, G.W., Coghlan, J.P. (1987). "Histochemical localization of IGF-I and -II mRNA in the developing rat embryo." Development **101**(1): 175-84.
- Beckers, J., Clark, A., Wunsch, K., Hrabe De Angelis, M., Gossler, A. (1999). "Expression of the mouse Delta1 gene during organogenesis and fetal development." Mech Dev **84**(1-2): 165-8.

- Beechey, C.V., Cattanaach, B.M., Blake, A., Peters, J. (2003). Genetic and Physical Imprinting Map of the Mouse., MRC Mammalian Genetics Unit, Harwell, Oxfordshire.
- Bell, A.C., Felsenfeld, G. (1999a). "Stopped at the border: boundaries and insulators." Curr Opin Genet Dev 9(2): 191-8.
- Bell, A.C., Felsenfeld, G. (2000). "Methylation of a CTCF-dependent boundary controls imprinted expression of the Igf2 gene." Nature 405(6785): 482-5.
- Bell, A.C., West, A.G., Felsenfeld, G. (1999b). "The protein CTCF is required for the enhancer blocking activity of vertebrate insulators." Cell 98(3): 387-96.
- Bestor, T.H. (2000). "The DNA methyltransferases of mammals." Hum Mol Genet 9(16): 2395-402.
- Bettenhausen, B., Hrabe de Angelis, M., Simon, D., Guenet, J.L. and Gossler, A. (1995). "Transient and restricted expression during mouse embryogenesis of Dll1, a murine gene closely related to Drosophila Delta." Development 121(8): 2407-18.
- Bhattacharya, S.K., Ramchandani, S., Cervoni, N. and Szyf, M. (1999). "A mammalian protein with specific demethylase activity for mCpG DNA." Nature 397(6720): 579-583.
- Bickmore, W.C., A.D. (1995). "Factors affecting the timing and imprinting of replication on a mammalian chromosome." J Cell Sci 108: 2801-09.
- Biniszkiewicz, D., Gribnau, J., Ramsahoye, B., Gaudet, F., Eggan, K., Humpherys, D., Mastrangelo, M.A., Jun, Z., Walter, J., Jaenisch, R. (2002). "Dnmt1 overexpression causes genomic hypermethylation, loss of imprinting, and embryonic lethality." Mol Cell Biol 22(7): 2124-35.
- Bird, A.P., Wolffe, A.P. (1999). "Methylation-induced repression--belts, braces, and chromatin." Cell 99(5): 451-4.
- Boissinot, S., Entezam, A., Furano, A.V. (2001). "Selection against deleterious LINE-1-containing loci in the human lineage." Mol Biol Evol 18(6): 926-35.
- Bourc'his, D. and Bestor, T.H. (2004). "Meiotic catastrophe and retrotransposon reactivation in male germ cells lacking Dnmt3L." Nature.
- Bourc'his, D., Xu, G.L., Lin, C.S., Bollman, B. and Bestor, T.H. (2001). "Dnmt3L and the establishment of maternal genomic imprints." Science 294(5551): 2536-9.
- Bradford, M.M. (1976). "A rapid and sensitive method for the quantitation of nanogram quantities of protein utilising the principle of protein dye binding." Analytical Biochemistry 72: 248-254.
- Brandeis, M., Kafri, T., Ariel, M., Chaillet, J.R., McCarrey, J., Razin, A. and Cedar, H. (1993). "The ontogeny of allele-specific methylation associated with imprinted genes in the mouse." Embo J 12(9): 3669-77.

- Brannan, C.I., Dees, E.C., Ingram, R.S., Tilghman, S.M. (1990). "The product of the H19 gene may function as an RNA." Mol Cell Biol **10**(1): 28-36.
- Brenton, J.D., Drewell, R.A., Viville, S., Hilton, K.J., Barton, S.C., Ainscough, J.F. and Surani, M.A. (1999). "A silencer element identified in *Drosophila* is required for imprinting of H19 reporter transgenes in mice." Proc Natl Acad Sci U S A **96**(16): 9242-7.
- Brightman, M.W. and Reese, T.S. (1969). "Junctions between intimately apposed cell membranes in the vertebrate brain." J. Cell Biol. **40**(3): 648-677.
- Brody, S.L., Yan, X.H., Wuerffel, M.K., Song, S.K., Shapiro, S.D.. (2000). "Ciliogenesis and left-right axis defects in forkhead factor HFH-4-null mice." Am J Respir Cell Mol Biol **23**(1): 45-51.
- Brunkow, M.E.a.T. (1991). "Ectopic expression of the H19 gene in mice causes prenatal lethality." Genes Dev **5**: 1092-101.
- Bryan, J.H., Hughes, R.L., Bates, T.J. (1977). "Brain development in hydrocephalic-polydactyl, a recessive pleiotropic mutant in the mouse." Virchows Arch A Pathol Anat Histopathol **374**(3): 205-14.
- Buiting, K., Lich, C., Cottrell, S., Barnicoat, A. and Horsthemke, B. (1999). "A 5-kb imprinting center deletion in a family with Angelman syndrome reduces the shortest region of deletion overlap to 880 bp." Hum Genet **105**(6): 665-6.
- Bulchand, S., Grove, E.A., Porter, F.D., Tole, S. (2001). "LIM-homeodomain gene *Lhx2* regulates the formation of the cortical hem." Mech Dev **100**(2): 165-75.
- Caspary, T., Cleary, M.A., Baker, C.C., Guan, X.J. and Tilghman, S.M. (1998). "Multiple mechanisms regulate imprinting of the mouse distal chromosome 7 gene cluster." Mol Cell Biol **18**(6): 3466-74.
- Caspary, T., Cleary, M.A., Perlman, E.J., Zhang, P., Elledge, S.J. and Tilghman, S.M. (1999). "Oppositely imprinted genes *p57*(*Kip2*) and *igf2* interact in a mouse model for Beckwith-Wiedemann syndrome." Genes Dev **13**(23): 3115-24.
- Catala, M. (1998). "Embryonic and fetal development of structures associated with the cerebro-spinal fluid in man and other species. Part I: The ventricular system, meninges and choroid plexuses." Arch Anat Cytol Pathol **46**(3): 153-69.
- Catchpoole, D., Lam, W.W., Valler, D., Temple, I.K., Joyce, J.A., Reik, W., Schofield, P.N. and Maher, E.R. (1997). "Epigenetic modification and uniparental inheritance of H19 in Beckwith-Wiedemann syndrome." J Med Genet **34**(5): 353-9.
- Cattanach, B.M., Kirk, M. (1985). "Differential activity of maternally and paternally derived chromosome regions in mice." Nature **315**(6019): 496-8.

- Cerrato, F., Dean, W., Davies, K., Kagotani, K., Mitsuya, K., Okumura, K., Riccio, A. and Reik, W. (2003). "Paternal imprints can be established on the maternal Igf2-H19 locus without altering replication timing of DNA." Hum Mol Genet **12**(23): 3123-32.
- Charalambous, M. (2000). Characterisation of a putative control element which lies between the imprinted Igf2 and H19 genes in the mouse. Biology and Biochemistry. Bath, University of Bath: 238.
- Charalambous, M., Menheniott, T.R., Bennett, W.R., Kelly, S.M., Dell, G., Dandolo, L., Ward, A. (2004). "An enhancer element at the Igf2/H19 locus drives gene expression in both imprinted and non-imprinted tissues." Dev Biol **271**(2): 488-97.
- Charalambous, M., Smith, F.M., Bennett, W.R., Crew, T.E., Mackenzie, F. and Ward, A. (2003). "Disruption of the imprinted Grb10 gene leads to disproportionate overgrowth by an Igf2-independent mechanism." Proc Natl Acad Sci U S A **100**(14): 8292-7.
- Chaudhary, J., Skinner, M.K. (1998). "Comparative sequence analysis of the mouse and human transferrin promoters: hormonal regulation of the transferrin promoter in Sertoli cells." Mol Reprod Dev **50**(3): 273-83.
- Chen, J.D., Neilson, K., Van Dyke, T. (1989). "Lymphotropic papovavirus early region is specifically regulated transgenic mice and efficiently induces neoplasia." J Virol **63**(5): 2204-14.
- Chess, A., Simon, I., Cedar, H. and Axel, R. (1994). "Allelic inactivation regulates olfactory receptor gene expression." Cell **78**(5): 823-34.
- Chodobski, A.a.S.-C., J. (2001). "Choroid plexus: target for polypeptides and site of synthesis." Microsc Res Tech **52**(1): 65-82.
- Church, G.M.a.G., W. (1984). "Genomic sequencing." Proceedings of the National Academy of Sciences of the United States of America- Biological Sciences **81**: 1991-1995.
- Clarke, A.R., Purdie, C.A., Harrison, D.J., Morris, R.G., Bird, C.C., Hooper, M.L. and Wyllie, A.H. (1993). "Thymocyte apoptosis induced by p53-dependent and independent pathways." Nature **362**: 849-852.
- Constancia, M., Dean, W., Lopes, S., Moore, T., Kelsey, G. and Reik, W. (2000). "Deletion of a silencer element in Igf2 results in loss of imprinting independent of H19." Nat Genet **26**(2): 203-6.
- Constancia, M., Hemberger, M., Hughes, J., Dean, W., Ferguson-Smith, A., Fundele, R., Stewart, F., Kelsey, G., Fowden, A., Sibley, C. and Reik, W. (2002). "Placental-specific IGF-II is a major modulator of placental and fetal growth." Nature **417**(6892): 945-8.
- Crook, R.B., Kasagami, H. and Prusiner, S.B. (1981). "Culture and Characterisation of Epithelial Cells from Bovine Choroid Plexus." Journal of Neurochemistry **37**: 845-854.

- Davies, K., Bowden, L., Smith, P., Dean, W., Hill, D., Furuumi, H., Sasaki, H., Cattanach, B. and Reik, W. (2002). "Disruption of mesodermal enhancers for Igf2 in the minute mutant." Development **129**(7): 1657-68.
- DeCaprio, J.A., Ludlow, J.W., Figge, J., Shew, J.Y., Huang, C.M., Lee, W.H., Marsilio, E., Paucha, E., Livingston, D.M. (1988). "SV40 large tumor antigen forms a specific complex with the product of the retinoblastoma susceptibility gene." Cell **54**(2): 275-83.
- DeChiara, T.M., Efstratiadis, A. and Robertson, E.J. (1990). "A growth-deficiency phenotype in heterozygous mice carrying an insulin-like growth factor II gene disrupted by targeting." Nature **345**(6270): 78-80.
- DeChiara, T.M., Robertson, E.J. and Efstratiadis, A. (1991). "Parental imprinting of the mouse insulin-like growth factor II gene." Cell **64**(4): 849-59.
- Dewulf, N., Verschueren, K., Lonnoy, O., Moren, A., Grimsby, S., Vande Spiegle, K., Miyazono, K., Huylebroeck, D., Ten Dijke, P. (1995). "Distinct spatial and temporal expression patterns of two type I receptors for bone morphogenetic proteins during mouse embryogenesis." Endocrinology **136**(6): 2652-63.
- Dohrmann, G.J. (1970). "Dark and light epithelial cells in the choroid plexus of mammals." J Ultrastruct Res **32**(3): 268-73.
- Drewell, R.A., Arney, K.L., Arima, T., Barton, S.C., Brenton, J.D. and Surani, M.A. (2002a). "Novel conserved elements upstream of the H19 gene are transcribed and act as mesodermal enhancers." Development **129**(5): 1205-13.
- Drewell, R.A., Brenton, J.D., Ainscough, J.F., Barton, S.C., Hilton, K.J., Arney, K.L., Dandolo, L. and Surani, M.A. (2000). "Deletion of a silencer element disrupts H19 imprinting independently of a DNA methylation epigenetic switch." Development **127**(16): 3419-28.
- Drewell, R.A., Goddard, C.J., Thomas, J.O. and Surani, M.A. (2002b). "Methylation-dependent silencing at the H19 imprinting control region by MeCP2." Nucleic Acids Res **30**(5): 1139-44.
- Dziegielewska, K.M., Ek, J., Habgood, M.D., Saunders, N.R. (2001). "Development of the choroid plexus." Microsc Res Tech **52**(1): 5-20.
- Eden, S., Constancia, M., Hashimshony, T., Dean, W., Goldstein, B., Johnson, A.C., Keshet, I., Reik, W. and Cedar, H. (2001). "An upstream repressor element plays a role in Igf2 imprinting." Embo J **20**(13): 3518-25.
- Efstratadis, A. (1998). "Genetics of mouse growth." Int J Dev Biol **42**(7): 955-76.
- Eggenchwiler, J., Ludwig, T., Fisher, P., Leighton, P.A., Tilghman, S.M. and Efstratiadis, A. (1997). "Mouse mutant embryos overexpressing IGF-II exhibit phenotypic features of

- the Beckwith-Wiedemann and Simpson-Golabi-Behmel syndromes." Genes Dev **11**(23): 3128-42.
- Ekstrom, T., Cui, H., Li, X. and Ohlsson, R. (1995). "Promoter-specific IGF2 imprinting status and its plasticity during human liver development." Development **121**(2): 309-316.
- Elson, D. and Bartolomei, M. (1997). "A 5' differentially methylated sequence and the 3'-flanking region are necessary for H19 transgene imprinting." Mol. Cell. Biol. **17**(1): 309-317.
- Engel, J.R., Smallwood, A., Harper, A., Higgins, M.J., Oshimura, M., Reik, W., Schofield, P.N. and Maher, E.R. (2000). "Epigenotype-phenotype correlations in Beckwith-Wiedemann syndrome." J Med Genet **37**(12): 921-6.
- Engemann, S., Stroedicke, M., Paulsen, M., Franck, O., Reinhardt, R., Lane, N., Reik, W., Walter, J. (2000). "Sequence and functional comparison in the Beckwith-Wiedemann region: implications for a novel imprinting centre and extended imprinting." Hum Mol Genet **9**(18): 2691-706.
- Erhardt, S., Lyko, F., Ainscough, J.F., Surani, M.A. and Paro, R. (2003). "Polycomb-group proteins are involved in silencing processes caused by a transgenic element from the murine imprinted H19/Igf2 region in Drosophila." Dev Genes Evol **213**(7): 336-44.
- Ewen, M.E., Ludlow, J.W., Marsilio, E., DeCaprio, J.A., Millikan, R.C., Cheng, S.H., Paucha, E., Livingston, D.M. (1989). "An N-terminal transformation-governing sequence of SV40 large T antigen contributes to the binding of both p110Rb and a second cellular protein, p120." Cell **58**(2): 257-67.
- Falls, J.G., Pulford, D.J., Wylie, A.A., Jirtle, R.L. (1999). "Genomic imprinting: implications for human disease." Am J Pathol **154**(3): 635-47.
- Fedoriw, A.M., Stein, P., Svoboda, P., Schultz, R.M. and Bartolomei, M.S. (2004). "Transgenic RNAi reveals essential function for CTCF in H19 gene imprinting." Science **303**(5655): 238-40.
- Feil, R., Moore, T.F., Oswald, J., Walter, J., Sun, F., Reik, W. (1997). The imprinted insulin-like growth factor 2 gene. Genomic Imprinting. W. Reik, Surani, A. Oxford, New York, Tokyo, Oxford University Press.
- Feil, R., Walter, J., Allen, N.D. and Reik, W. (1994). "Developmental control of allelic methylation in the imprinted mouse Igf2 and H19 genes." Development **120**(10): 2933-43.
- Ferguson-Smith, A.C., Sasaki, H., Cattanach, B.M., Surani, M.A. (1993). "Parental-origin-specific epigenetic modification of the mouse H19 gene." Nature **362**(6422): 751-5.

- Fitzpatrick, G.V., Soloway, P.D., Higgins, M.J. (2002). "Regional loss of imprinting and growth deficiency in mice with a targeted deletion of KvDMR1." Nat Genet **32**(3): 426-431.
- Forne, T., Oswald, J., Dean, W., Saam, J.R., Bailleul, B., Dandolo, L., Tilghman, S.M., Walter, J. and Reik, W. (1997). "Loss of the maternal H19 gene induces changes in Igf2 methylation in both cis and trans." Proc Natl Acad Sci U S A **94**(19): 10243-8.
- Franz, T. (1994). "Extra-toes (Xt) homozygous mice demonstrate a role for the Gli3 gene in the development of the forebrain." Acta Anatomica **150**(1): 38-44.
- Freshney, R.I. (1987). Culture of Animal Cells: A Manual of Basic Technique. New York, Alan R. Liss Inc.
- Fuchs, E. (1988). "Keratins as biochemical markers of epithelial differentiation." Trends Genet **4**(10): 277-81.
- Furuta, Y., Piston, D.W., Hogan, B.L.M. (1997). "Bone morphogenetic proteins (BMPs) as regulators of dorsal forebrain development." Development **124**: 2203-2212.
- Gardiner-Garden, M., Frommer, M. (1987). "CpG islands in vertebrate genomes." J Mol Biol **196**(2): 261-82.
- Garrido, C., Schmitt, E., Cande, C., Vahsen, N., Parcellier, A., Kroemer, G. (2003). "HSP27 and HSP70: potentially oncogenic apoptosis inhibitors." Cell Cycle **2**(6): 579-84.
- Gaston, V., Le Bouc, Y., Soupre, V., Vazquez, M.P., Gicquel, C. (2000). "Assessment of p57(KIP2) gene mutation in Beckwith-Wiedemann syndrome." Horm Res **54**(1): 1-5.
- Gherzi-Egea, J., Strazielle, N. (2001). "Brain drug delivery, drug metabolism, and multidrug resistance at the choroid plexus." Microsc Res Tech **52**(1): 83-8.
- Ginjala, V., Holmgren, C., Ulleras, E., Kanduri, C., Pant, V., Lobanenko, V., Franklin, G., Ohlsson, R. (2002). "Multiple cis elements within the Igf2/H19 insulator domain organize a distance-dependent silencer. A cautionary note." J Biol Chem **277**(8): 5707-10.
- Greally, J.M. (2002). "Short interspersed transposable elements (SINEs) are excluded from imprinted regions in the human genome." Proc Natl Acad Sci U S A **99**(1): 327-32.
- Greally, J.M., Starr, D.J., Hwang, S., Song, L., Jaarola, M., Zemel, S. (1998). "The mouse H19 locus mediates a transition between imprinted and non-imprinted DNA replication patterns." Hum Mol Genet **7**(1): 91-5.
- Gribnau, J., Hochedlinger, K., Hata, K., Li, E., Jaenisch, R. (2003). "Asynchronous replication timing of imprinted loci is independent of DNA methylation, but consistent with differential subnuclear localization." Genes Dev **17**(6): 759-73.

- Grove, E.A., Tole, S., Limon, J., Yip, L., Ragsdale, C.W. (1998). "The hem of the embryonic cerebral cortex is defined by the expression of multiple Wnt genes and is compromised in Gli3-deficient mice." Development **125**(12): 2315-25.
- Guillemot, F., Caspary, T., Tilghman, S.M., Copeland, N.G., Gilbert, D.J., Jenkins, N.A., Anderson, D.J., Joyner, A.L., Rossant, J. and Nagy, A. (1995). "Genomic imprinting of Mash2, a mouse gene required for trophoblast development." Nat Genet **9**(3): 235-42.
- Hamada, Y., Kadokawa, Y., Okabe, M., Ikawa, M., Coleman, J.R. and Tsujimoto, Y. (1999). "Mutation in ankyrin repeats of the mouse Notch2 gene induces early embryonic lethality." Development **126**(15): 3415-24.
- Hao, Y., Crenshaw, T., Moulton, T., Newcomb, E., Tycko, B. (1993). "Tumour-suppressor activity of H19 RNA." Nature **365**(6448): 764-7.
- Hark, A.T., Schoenherr, C.J., Katz, D.J., Ingram, R.S., Levorse, J.M. and Tilghman, S.M. (2000). "CTCF mediates methylation-sensitive enhancer-blocking activity at the H19/Igf2 locus." Nature **405**(6785): 486-9.
- Hark, A.T. and Tilghman, S.M. (1998). "Chromatin conformation of the H19 epigenetic mark." Hum Mol Genet **7**(12): 1979-85.
- Haselbach, M., Wegener, J., Decker, S., Engelbertz, C. and Galla, H.J. (2001). "Porcine Choroid plexus epithelial cells in culture: regulation of barrier properties and transport processes." Microsc Res Tech **52**(1): 137-52.
- Hasse, A., Schulz, W.A. (1994). "Enhancement of reporter gene de novo methylation by DNA fragments from the alpha-fetoprotein control region." J Biol Chem **269**(3): 1821-6.
- Hata, K., Okano, M., Lei, H., Li, E. (2002). "Dnmt3L cooperates with the Dnmt3 family of de novo DNA methyltransferases to establish maternal imprints in mice." Development **129**(8): 1983-93.
- Hazan, R.B., Qiao, R., Keren, R., Badano, I. and Suyama, K. (2004). "Cadherin switch in tumor progression." Ann NY Acad Sci **1014**: 155-63.
- Hebert, J.M., Hayhurst, M., Marks, M.E., Kulesa, H., Hogan, B.L., McConnell, S.K. (2003). "BMP ligands act redundantly to pattern the dorsal telencephalic midline." Genesis **35**(4): 214-9.
- Hebert, J.M., Mishina, Y., McConnell, S.K. (2002). "BMP signaling is required locally to pattern the dorsal telencephalic midline." Neuron **35**(6): 1029-41.
- Helmbrecht, K., Zeise, E., Rensing, L. (2000). "Chaperones in cell cycle regulation and mitogenic signal transduction: a review." Cell Prolif **33**(6): 341-65.



- Hemberger, M., Redies, C., Krause, R., Oswald, J., Walter, J., Fundele, R.H. (1998). "H19 and Igf2 are expressed and differentially imprinted in neuroectoderm-derived cells in the mouse brain." Dev Genes Evol **208**(7): 393-402.
- Hetts, S.W., Rosen, K.M., Dikkes, P., Villa-Komaroff, L., Mozell, R.L. (1997). "Expression and imprinting of the insulin-like growth factor II gene in neonatal mouse cerebellum." J Neurosci Res **50**(6): 958-66.
- Higuchi, M., Kiyama, H., Hayakawa, T., Hamada, Y., Tsujimoto, Y. (1995). "Differential expression of Notch1 and Notch2 in developing and adult mouse brain." Brain Res Mol Brain Res **29**(2): 263-72.
- Hincke, M.T., Nairn, A.C., Staines, W.A. (1995). "Cystic fibrosis transmembrane conductance regulator is found within brain ventricular epithelium and choroid plexus." Neurochem **64**(4): 1662-8.
- Hirohashi, S., Kanai, Y. (2003). "Cell adhesion system and human cancer morphogenesis." Cancer Sci **94**(7): 575-81.
- Hoffmann, A., Gath, U., Gross, G., Lauber, J., Getzlaff, R., Hellwig, S., Galla, H.J. and Conrath, H.S. (1996). "Constitutive secretion of b-trace protein by cultivated porcine choroid plexus epithelial cells: elucidation of its complete amino acid and cDNA sequences." Journal of Cellular Physiology **169**: 235-241.
- Holm, N.R., Hansen, L.B., Nilsson, C., Gammeltoft, S. (1994). "Gene expression and secretion of insulin-like growth factor-II and insulin-like growth factor binding protein-2 from cultured sheep choroid plexus epithelial cells." Brain Res Mol Brain Res **21**(1-2): 67-74.
- Holmgren, C., Kanduri, C., Dell, G., Ward, A., Mukhopadhyaya, R., Kanduri, M., Lobanenkova, V., Ohlsson, R. (2001). "CpG methylation regulates the Igf2/H19 insulator." Curr Biol **11**(14): 1128-30.
- Houzelstein, D., Cohen, A., Buckingham, M.E., Robert, B. (1997). "Insertional mutation of the mouse Msx1 homeobox gene by an nlacZ reporter gene." Mech Dev **65**(1-2): 123-33.
- Howell, C.Y., Bestor, T.H., Ding, F., Latham, K.E., Mertineit, C., Trasler, J.M. and Chaillet, J.R. (2001). "Genomic imprinting disrupted by a maternal effect mutation in the Dnmt1 gene." Cell **104**(6): 829-38.
- Hrabe de Angelis, M., McIntyre, J., 2nd and Gossler, A. (1997). "Maintenance of somite borders in mice requires the Delta homologue DII1." Nature **386**(6626): 717-21.
- Hurst, L.D. (1997). Evolutionary theories of genomic imprinting. in *Genomic Imprinting*. Oxford, New York, Tokyo, Oxford University press.
- Hurst, L.D., Smith, N.G. (1999). "Molecular evolutionary evidence that H19 mRNA is functional." Trends Genet **15**(4): 134-5.

- Irvin, D.K., Nakano, I., Paucar, A., Kornblum, H.I. (2004). "Patterns of Jagged1, Jagged2, Delta-like 1 and Delta-like 3 expression during late embryonic and postnatal brain development suggest multiple functional roles in progenitors and differentiated cells." J Neurosci Res **75**(3): 330-43.
- Ishihara, K., Hatano, N., Furuumi, H., Kato, R., Iwaki, T., Miura, K., and Jinno, Y., Sasaki, H. (2000). "Comparative genomic sequencing identifies novel tissue-specific enhancers and sequence elements for methylation sensitive factors implicated in Igf2/H19 imprinting." Genome Res **10**: 664-71.
- Jarriault, S., Le Bail, O., Hirsinger, E., Pourquie, O., Logeat, F., Strong, C.F., Brou, C., Seidah, N.G., Israel, A.. (1998). "Delta-1 activation of notch-1 signaling results in HES-1 transactivation." Mol Cell Biol **18**(12): 7423-31.
- Jeong, S., Stein, A. (1994). "Micrococcal nuclease digestion of nuclei reveals extended nucleosome ladders having anomalous DNA lengths for chromatin assembled on non-replicating plasmids in transfected cells." Nucleic Acids Res **22**(3): 370-5.
- Jirtle, R.L. (1999). "Genomic imprinting and cancer." Exp Cell Res **248**(1): 18-24.
- Johanson, C.E., Gonzalez, A.M., Stopa, E.G. (2001). "Water-imbalance-induced expression of FGF-2 in fluid-regulatory centers: choroid plexus and neurohypophysis." Eur J Pediatr Surg **11**(11S37-8).
- Johanson, C.E., Preston, J.E., Chodobski, A., Stopa, E.G., Szmydynger-Chodobska, J., McMillan, P.N. (1999a). "AVP V1 receptor-mediated decrease in Cl<sup>-</sup> efflux and increase in dark cell number in choroid plexus epithelium." Am J Physiol **276**(1): C82-90.
- Johanson, C.E., Szmydynger-Chodobska, J., Chodobski, A., Baird, A., McMillan, P., Stopa, E.G. (1999b). "Altered formation and bulk absorption of cerebrospinal fluid in FGF-2-induced hydrocephalus." Am J Physiol **277**(1): 263-71.
- Jones, B.K., Levorse, J. and Tilghman, S.M. (2001). "Deletion of a nuclease-sensitive region between the Igf2 and H19 genes leads to Igf2 misregulation and increased adiposity." Hum Mol Genet **10**(8): 807-14.
- Jones, B.K., Levorse, J. and Tilghman, S.M. (2002). "A human H19 transgene exhibits impaired paternal-specific imprint acquisition and maintenance in mice." Hum Mol Genet **11**(4): 411-8.
- Kaffer, C.R., Grinberg, A. and Pfeifer, K. (2001). "Regulatory Mechanisms at the Mouse Igf2/H19 Locus." Mol. Cell. Biol. **21**(23): 8189-8196.
- Kaffer, C.R., Srivastava, M, Park, K.Y., Ives, E., Hsieh, S., Battle, J., Grinberg, A., Huang, S.P., Pfeifer, K. (2000). "A transcriptional insulator at the imprinted H19/Igf2 locus." Genes Dev **14**(15): 1908-19.

- Kafri, T., Ariel, M., Brandeis, M., Shemer, R., Urven, L., McCarrey, J., Cedar, H., Razin, A. (1992). "Developmental pattern of gene-specific DNA methylation in the mouse embryo and germ line." Genes Dev **6**(5): 705-14.
- Kanduri, C., Fitzpatrick, G., Mukhopadhyay, R., Kanduri, M., Lobanekov, V., Higgins, M., Ohlsson, R. (2002). "A differentially methylated imprinting control region within the *Kcnq1* locus harbors a methylation-sensitive chromatin insulator." J Biol Chem **277**(20): 18106-10.
- Kanduri, C., Holmgren, C., Pilartz, M., Franklin, G., Kanduri, M., Liu, L., Ginja, V., Ulleras, E., Mattsson, R., Ohlsson, R. (2000a). "The 5' flank of mouse H19 in an unusual chromatin conformation unidirectionally blocks enhancer-promoter communication." Curr Biol **10**(8): 449-57.
- Kanduri, C., Pant, V., Loukinov, D., Pugacheva, E., Qi, C.F., Wolffe, A., Ohlsson, R., Lobanekov, V.V. (2000b). "Functional association of CTCF with the insulator upstream of the H19 gene is parent of origin-specific and methylation-sensitive." Curr Biol **10**(14): 853-6.
- Kaneda, M., Okano, M., Hata, K., Sado, T., Tsujimoto, N., Li, E. and Sasaki, H. (2004). "Essential role for de novo DNA methyltransferase Dnmt3a in paternal and maternal imprinting." Nature **429**(6994): 900-903.
- Kantor, B., Makedonski, K., Green-Finberg, Y., Shemer, R., Razin, A. (2004). "Control elements within the PWS/AS imprinting box and their function in the imprinting process." Hum Mol Genet **13**(7): 751-62.
- Kao, H.Y., Ordentlich, P., Koyano-Nakagawa, N., Tang, Z., Downes, M., Kintner, C.R., Evans, R.M., Kadesch, T. (1998). "A histone deacetylase corepressor complex regulates the Notch signal transduction pathway." Genes Dev **12**(15): 2269-77.
- Ke, X., Thomas, N.S., Robinson, D.O., Collins, A. (2002). "The distinguishing sequence characteristics of mouse imprinted genes." Mamm Genome **13**(11): 639-45.
- Kelly, S.M. (2004). The role of the differentially methylated region 1 in regulating the expression of the *Igf2* gene. Biology and Biochemistry. Bath, University of Bath.
- Khosla, S., Aitchison, A., Gregory, R., Allen, N.D. and Feil, R. (1999). "Parental Allele-Specific Chromatin Configuration in a Boundary-Imprinting-Control Element Upstream of the Mouse H19 Gene." Mol. Cell. Biol. **19**(4): 2556-2566.
- Kim, B.H., Sung, S.R., Choi, E.H, Kim, Y.I., Kim, K.J., Dong, S.H., Kim, H.J., Chang, Y.W., Lee, J.I., Chang, R. (2000). "Dedifferentiation of conditionally immortalized hepatocytes with long-term in vitro passage." Exp Mol Med **32**(1): 29-37.
- Kitazawa, T., Hosoya, K., Watanabe, M., Takashima, T., Ohtsuki, S., Takanaga, H., Ueda, M., Yanai, N., Obinata, M., Terasaki, T. (2001). "Characterization of the amino acid transport of new immortalized choroid plexus epithelial cell lines: a novel in vitro

- system for investigating transport functions at the blood-cerebrospinal fluid barrier." Pharm Res **18**(1): 16-22.
- Kitsberg, D., Selig, S. and Cedar, H. (1991). "Chromosome structure and eukaryotic gene organization." Curr Opin Genet Dev **1**(4): 534-7.
- Kitsberg, D., Selig, S., Brandeis, M., Simon, I., Keshet, I., Driscoll, D.J., Nicholls, R.D., Cedar, H. (1993). "Allele-specific replication timing of imprinted gene regions." Nature **364**(6436): 459-63.
- Koide, T., Ainscough, J., Wijgerde, M. and Surani, M.A. (1994). "Comparative analysis of Igf2/H19 imprinted domain: identification of a highly conserved intergenic DNaseI hypersensitive region." Genomics **24**(1): 1-8.
- Krebs, L.T., Xue, Y., Norton, C.R., Shutter, J.R., Maguire, M., Sundberg, J.P., Gallahan, D., Closson, V., Kitajewski, J., Callahan, R., Smith, G.H., Stark, K.L. and Gridley, T. (2000). "Notch signaling is essential for vascular morphogenesis in mice." Genes Dev **14**(11): 1343-52.
- Krebs, L.T., Xue, Y., Norton, C.R., Sundberg, J.P., Beatus, P., Lendahl, U., Joutel, A. and Gridley, T. (2003). "Characterization of Notch3-deficient mice: normal embryonic development and absence of genetic interactions with a Notch1 mutation." Genesis **37**(3): 139-43.
- Kuerbitz, S.J., Plunkett, B.S., Walsh, W.V., and Kastan, M.B. (1992). "Wild-type p53 is a cell cycle checkpoint determinant following irradiation." Proc Natl Acad Sci U S A **89**: 7491-5.
- Kurooka, H., Honjo, T. (2000). "Functional interaction between the mouse notch1 intracellular region and histone acetyltransferases PCAF and GCN5." J Biol Chem **275**(22): 17211-20.
- Lane, E.B., Goodman, S.L., Trejdosiewicz (1982). "Disruption of the keratin filament network during epithelial cell division." Embo J **1**: 1365-72.
- Lau, M.M., Stewart, C.E., Liu, Z., Bhatt, H., Rotwein, P., Stewart, C.L. (1994). "Loss of the imprinted IGF2/cation-independent mannose 6-phosphate receptor results in fetal overgrowth and perinatal lethality." Genes Dev **8**(24): 2953-63.
- Lee, J.T., Davidow, L.S., Warshawsky, D. (1999). "Tsix, a gene antisense to Xist at the X-inactivation centre." Nat Genet **21**(4): 343-4.
- Lee, M.P., DeBaun, M.R., Mitsuya, K., Galonek, H.L., Brandenburg, S., Oshimura, M. and Feinberg, A.P. (1999). "Loss of imprinting of a paternally expressed transcript, with antisense orientation to KVLQT1, occurs frequently in Beckwith-Wiedemann syndrome and is independent of insulin-like growth factor II imprinting." Proc Natl Acad Sci USA **96**(9): 5203-5208.

- Leighton, P.A., Ingram, R.S., Eggenschwiler, J., Efstratiadis, A., Tilghman, S.M. (1995). "Disruption of imprinting caused by deletion of the H19 gene region in mice." Nature **375**(6526): 34-9.
- Leighton, P.A., Saam, J.R., Ingram, R.S., Stewart, C.L. and Tilghman, S.M. (1995). "An enhancer deletion affects both H19 and Igf2 expression." Genes Dev **9**(17): 2079-89.
- Lewis, A., Mitsuya, K., Constancia, M., Reik, W. (2004). "Tandem repeat hypothesis in imprinting: deletion of a conserved direct repeat element upstream of H19 has no effect on imprinting in the Igf2-H19 region." Mol Cell Biol **24**(13): 5650-6.
- Lewis, J. (1998). "Notch signalling and the control of cell fate choices in vertebrates." Semin Cell Dev Biol **9**(6): 583-9.
- Li, E., Beard, C., Jaenisch, R. (1993). "Role for DNA methylation in genomic imprinting." Nature **366**(6453): 302-3.
- Li, E., Bestor, T.H. and Jaenisch, R. (1992). "Targeted mutation of the DNA methyltransferase gene results in embryonic lethality." Cell **69**(6): 915-26.
- Li, J.Y., Boado, R.J., Pardridge, W.M. (2001a). "Blood-brain barrier genomics." J Cereb Blood Flow Metab **21**(1): 61-8.
- Li, M., Squire, J., Shuman, C., Fei, Y.L., Atkin, J., Pauli, R., Smith, A., Nishikawa, J., Chitayat, D., Weksberg, R. (2001b). "Imprinting status of 11p15 genes in Beckwith-Wiedemann syndrome patients with CDKN1C mutations." Genomics **77**(1-2): 115.
- Li, Y.-M., Franklin, G., Cui, H.-M., Svensson, K., He, X.-B., Adam, G., Ohlsson, R. and Pfeifer, S. (1998). "The H19 Transcript Is Associated with Polysomes and May Regulate IGF2 Expression in trans." J. Biol. Chem. **273**(43): 28247-28252.
- Lim, L., Zhou, H., Costa, R.H. (1997). "The winged helix transcription factor HFH-4 is expressed during choroid plexus epithelial development in the mouse embryo." Proc Natl Acad Sci U S A **94**(7): 3094-9.
- Liszcak, T.M., Black, P.M., Foley, L. (1986). "Arginine vasopressin causes morphological changes suggestive of fluid transport in rat choroid plexus epithelium." Cell Tissue Res **246**(2): 379-85.
- Liu, J.P., Baker, J., Perkins, A.S., Robertson, E.J., Efstratiadis, A. (1993). "Mice carrying null mutations of the genes encoding insulin-like growth factor I (Igf-1) and type 1 IGF receptor (Igf1r)." Cell **75**(1): 59-72.
- Lloyd, V. (2000). "Parental imprinting in Drosophila." Genetica **109**(1-2): 35-44.
- Logan, A., Gonzalez, A.M., Hill, D.J., Berry, M., Gregson, N.A., Baird, A. (1994). "Coordinated pattern of expression and localization of insulin-like growth factor-II (IGF-II) and IGF-binding protein-2 in the adult rat brain." Endocrinology **135**(5): 2255-64.

- Loomes, K.M., Underkoffler, L.A., Morabito, J., Gottlieb, S., Piccoli, D.A., Spinner, N.B., Baldwin, H.S., Oakey, R.J. (1999). "The expression of Jagged1 in the developing mammalian heart correlates with cardiovascular disease in Alagille syndrome." Hum Mol Genet **8**(13): 2443-9.
- Lopes, S., Lewis, A., Hajkova, P., Dean, W., Oswald, J., Forne, T., Murrell, A., Constancia, M., Bartolomei, M., Walter, J. and Reik, W. (2003). "Epigenetic modifications in an imprinting cluster are controlled by a hierarchy of DMRs suggesting long-range chromatin interactions." Hum Mol Genet **12**(3): 295-305.
- Louvi, A., Accili, D., Efstratiadis, A. (1997). "Growth-promoting interaction of IGF-II with the insulin receptor during mouse embryonic development." Dev Biol **189**(1): 33-48.
- Lustig, O., Ariel, I., Ilan, J., Lev-Lehman, E., De-Groot, N., Hochberg, A. (1994). "Expression of the imprinted gene H19 in the human fetus." Mol Reprod Dev **38**(3): 239-46.
- Lyko, F., Brenton, J.D., Surani, M.A. and Paro, R. (1997). "An imprinting element from the mouse H19 locus functions as a silencer in Drosophila." Nat Genet **16**(2): 171-3.
- Lyko, F., Ramsahoye, B.H., Kashevsky, H., Tudor, M., Mastrangelo, M.A., Orr-Weaver, T.L. and Jaenisch, R. (1999). "Mammalian (cytosine-5) methyltransferases cause genomic DNA methylation and lethality in Drosophila." Nat Genet **23**(3): 363-6.
- Lyle, R., Watanabe, D., te Vruchte, D., Lerchner, W., Smrzka, O.W., Wutz, A., Schageman, J., Hahner, L., Davies, C. and Barlow, D.P. (2000). "The imprinted antisense RNA at the Igf2r locus overlaps but does not imprint Mas1." Nat Genet **25**(1): 19-21.
- MacKenzie, A., Ferguson, M.W., Sharpe, P.T. (1991). "Hox-7 expression during murine craniofacial development." Development **113**(2): 601-11.
- Mager, J., Montgomery, N.D., de Villena, F.P., Magnuson, T. (2003). "Genome imprinting regulated by the mouse Polycomb group protein Eed." Nat Genet **33**(4): 502-7.
- Maher, E.R., Reik, W. (2000). "Beckwith-Wiedemann syndrome: imprinting in clusters revisited." J Clin Invest **105**(3): 247-52.
- Malcolmson, R.D.G., Clarke, A.R., Peter, A., Coutts, S.B., Howie, S.E.M. and Harrison, D.J. (1997). "Apoptosis induced by g-irradiation, but not CD4 ligation of peripheral T-lymphocytes *in vivo* is p53 dependent." Journal of Pathology **181**: 166-171.
- Malik, K.T., Wallace, J.I., Ivins, S.M., Brown, K.W. (1995). "Identification of an antisense WT1 promoter in intron 1: implications for WT1 gene regulation." Oncogene **11**(8): 1589-95.
- Mann, J.R., Szabo, P.E., Reed, M.R., Singer-Sam, J. (2000). "Methylated DNA sequences in genomic imprinting." Crit Rev Eukaryot Gene Expr **10**(3-4): 241-57.
- McCright, B., Gao, X., Shen, L., Lozier, J., Lan, Y., Maguire, M., Herzlinger, D., Weinmaster, G., Jiang, R. and Gridley, T. (2001). "Defects in development of the

- kidney, heart and eye vasculature in mice homozygous for a hypomorphic Notch2 mutation." Development **128**(4): 491-502.
- McGrath, J., Solter, D. (1984). "Completion of mouse embryogenesis requires both the maternal and paternal genomes." Cell **37**(1): 179-83.
- Milner, R.D., Hill, D.J. (1984). "Fetal growth control: the role of insulin and related peptides." Clin Endocrinol **21**(4): 415-33.
- Monk, M., Boubelik, M., Lehnert, S. (1987). "Temporal and regional changes in DNA methylation in the embryonic, extraembryonic and germ cell lineages during mouse embryo development." Development **99**(3): 371-82.
- Moore, T. (2001). "Genetic conflict, genomic imprinting and establishment of the epigenotype in relation to growth." Reproduction **122**(2): 185-193.
- Moore, T., Constancia, M., Zubair, M., Bailleul, B., Feil, R., Sasaki, H. and Reik, W. (1997). "Multiple imprinted sense and antisense transcripts, differential methylation and tandem repeats in a putative imprinting control region upstream of mouse *Igf2*." Proc Natl Acad Sci U S A **94**(23): 12509-14.
- Moore, T., Haig, D. (1991). "Genomic imprinting in mammalian development: a parental tug-of-war." Trends Genet **7**(2): 45-9.
- Mostoslavsky, R., Singh, N., Tenzen, T., Goldmit, M., Gabay, C., Elizur, S., Qi, P., Reubinoff, B.E., Chess, A., Cedar, H. and Bergman, Y. (2001). "Asynchronous replication and allelic exclusion in the immune system." Nature **414**(6860): 221-5.
- Murakami, T., Yasuda, Y., Mita, S., Maeda, S., Shimada, K., Fujimoto, T., Araki, S. (1987). "Prealbumin gene expression during mouse development studied by in situ hybridization." Cell Differ **22**(1): 1-9.
- Murrell, A., Heeson, S., Bowden, L., Constancia, M., Dean, W., Kelsey, G. and Reik, W. (2001). "An intragenic methylated region in the imprinted *Igf2* gene augments transcription." EMBO Rep **2**(12): 1101-6.
- Murrell, A., Heeson, S., Reik, W. (2004). "Interaction between differentially methylated regions partitions the imprinted genes *Igf2* and *H19* into parent-specific chromatin loops." Nat Genet **36**(8): 889-93.
- Neumann, B., Kubicka, P., Barlow, D.P. (1995). "Characteristics of imprinted genes." Nat Genet **9**(1): 12-3.
- Nicholls, R.D., Saitoh, S., Horsthemke, B. (1998). "Imprinting in Prader-Willi and Angelman syndromes." Trends Genet **14**(5): 194-200.
- Nicholson-Flynn, K., Hitchcock-DeGregori, S.E. and Levitt, P. (1996). "Restricted Expression of the Actin-Regulatory Protein, Tropomyosin, Defines Distinct Boundaries, Evaginating Neuroepithelium, and Choroid Plexus Forerunners during Early CNS Development." J. Neurosci. **16**(21): 6853-6863.

- Niemitz, E.L., DeBaun, M.R., Fallon, J., Murakami, K., Kugoh, H., Oshimura, M., Feinberg, A.P. (2004). "Microdeletion of LIT1 in Familial Beckwith-Wiedemann Syndrome." Am J Hum Genet **75**(5).
- Nilsson, C., Hultberg, B.M., Gammeltoft, S. (1996). "Autocrine role of Insulin-like growth factor II secretion by the rat choroid plexus." Eur J Neurosci **8**(3): 629-35.
- Nilsson, C., M. Lindvall-Axelsson, and C. Owman. (1992). "Neuroendocrine regulatory mechanisms in the choroid plexus-cerebrospinal fluid system." Brain Res Rev **17**: 109-38.
- Nishimura, A., Morita, M., Nishimura, Y. & Sugino, Y. (1990). "A rapid and highly efficient method for preparation of competent Escherichia coli cells." Nucleic Acids Research **18**: 6169.
- Norton, P.A.a.C., S.M. (1985). "Bacterial beta-galactosidase as a marker for Rous Sarcoma Virus gene expression and replication." Molecular and Cellular Biology **5**: 281-290.
- Ohlsson, R., Hedborg, F., Holmgren, L., Walsh, C. and Ekstrom, T. (1994). "Overlapping patterns of IGF2 and H19 expression during human development: biallelic IGF2 expression correlates with a lack of H19 expression." Development **120**(2): 361-368.
- Ohta, T., Buiting, K., Kokkenen, H., McCandless, S., Heeger, S., Driscoll, D.J., Cassidy, S.B., Horsthemke, B., Nicholls, R.D. (1999). "Molecular mechanism of Angelman syndrome in two large families involves an imprinting mutation." Am J Hum Genet **64**: 385-96.
- Okano, M., Bell, D.W., Haber, D.A., Li, E. (1999). "DNA methyltransferases Dnmt3a and Dnmt3b are essential for de novo methylation and mammalian development." Cell **99**(3): 247-57.
- Onyango, P., Miller, W., Lehoczy, J., Leung, C.T., Birren, B., Wheelan, S., Dewar, K. and Feinberg, A.P. (2000). "Sequence and comparative analysis of the mouse 1-megabase region orthologous to the human 11p15 imprinted domain." Genome Res **10**(11): 1697-710.
- Overall, M., Bakker, M., Spencer, J., Parker, N., Smith, P., Dziadek, M. (1997). "Genomic imprinting in the rat: linkage of Igf2 and H19 genes and opposite parental allele-specific expression during embryogenesis." Genomics **45**(2): 416-20.
- Owens, D.W., Lane, E.B. (2003). "The quest for the function of simple epithelial keratins." Bioessays **25**(8): 748-58.
- Pachnis, V., Brannan, C.I. and Tilghman, S.M. (1988). "The structure and expression of a novel gene activated in early mouse embryogenesis." Embo J **7**(3): 673-81.
- Pant, V., Kurukuti, S., Pugacheva, E., Shamsuddin, S., Mariano, P., Renkawitz, R., Klenova, E., Lobanenkova, V., Ohlsson, R. (2004). "Mutation of a Single CTCF Target Site within the H19 Imprinting Control Region Leads to Loss of Igf2 Imprinting and



- Complex Patterns of De Novo Methylation upon Maternal Inheritance." Mol Cell Biol **24**(8): 3497-504.
- Paulsen, M., Davies, K.R., Bowden, L.M., Villar, A.J., Franck, O., Fuermann, M., Dean, W.L., Moore, T.F., Rodrigues, N., Davies, K.E., Hu, R.J., Feinberg, A.P., Maher, E.R., Reik, W., Walter, J. (1998). "Syntenic organization of the mouse distal chromosome 7 imprinting cluster and the Beckwith-Wiedemann syndrome region in chromosome 11p15.5." Hum Mol Genet **7**(7): 1149-59.
- Paulsen, M., El-Maarri, O., Engemann, S., Stroedicke, M., Franck, O., Davies, K., Reinhardt, R., Reik, W., Walter, J. (2000). "Sequence conservation and variability of imprinting in the Beckwith-Wiedemann syndrome gene cluster in human and mouse." Hum Mol Genet **9**(12): 1829-41.
- Peden, K.W., Pipas, J.M. (1992). "Simian virus 40 mutants with amino-acid substitutions near the amino terminus of large T antigen." Virus Genes **6**(2): 107-18.
- Peden, K.W., Srinivasan, A., Vartikar, J.V., Pipas, J.M. (1998). "Effects of mutations within the SV40 large T antigen ATPase/p53 binding domain on viral replication and transformation." Virus Genes **16**(2): 153-65.
- Perez-Moreno, M., Jamora, C., Fuchs, E. (2003). "Sticky business: orchestrating cellular signals at adherens junctions." Cell **112**(4): 535-48.
- Pham, N.V., Nguyen, M.T., Hu, J.F., Vu, T.H., Hoffman, A.R. (1998). "Dissociation of IGF2 and H19 imprinting in human brain." Brain Res **810**(1-2): 1-8.
- Pipas, J.M., Levine, A.J. (2001). "Role of T antigen interactions with p53 in tumourigenesis." Semin Cancer Biol **11**: 23-30.
- Poirier, F., Chan, C.T., Timmons, P.M., Robertson, E.J., Evans, M.J., Rigby, P.W. (1991). "The murine H19 gene is activated during embryonic stem cell differentiation in vitro and at the time of implantation in the developing embryo." Development **113**(4): 1105-14.
- Pulford, D.J., Falls, J.G., Killian, J.K., Jirtle, R.L. (1999). "Polymorphisms, genomic imprinting and cancer susceptibility." Mutat Res **436**(1): 59-67.
- Ramanathan, V.K., Hui, A.C., Brett, C.M., Giacomini, K.M. (1996). "Primary cell culture of the rabbit choroid plexus: an experimental system to investigate membrane transport." Pharm Res **13**(6): 952-6.
- Reeve, A.E. (1996). "Role of genomic imprinting in Wilms' tumour and overgrowth disorders." Med Pediatr Oncol **27**(5): 470-5.
- Reeves, R., Gorman, C.M., Howard, B. (1985). "Minichromosome assembly of non-integrated plasmid DNA transfected into mammalian cells." Nucleic Acids Res **13**(10): 3599-615.

- Reik, W., Brown, K.W., Schneid, H., Le Bouc, Y., Bickmore, W. and Maher, E.R. (1995). "Imprinting mutations in the Beckwith-Wiedemann syndrome suggested by altered imprinting pattern in the IGF2-H19 domain." Hum Mol Genet **4**(12): 2379-85.
- Reik, W., Davies, K., Dean, W., Kelsey, G. and Constancia, M. (2001). "Imprinted genes and the coordination of fetal and postnatal growth in mammals." Novartis Found Symp **237**: 19-31; discussion 31-42.
- Reik, W., Dean, W., Walter, J. (2001a). "Epigenetic reprogramming in mammalian development." Science **293**: 1089-93.
- Reik, W., Walter, J. (2001b). "Genomic imprinting: parental influence on the genome." Nat Rev Genet **2**(1): 21-32.
- Rickert, C.H., Paulus, W. (2001). "Tumors of the choroid plexus." Microsc Res Tech **52**(1): 104-11.
- Ripoche, M.A., Kress, C., Poirier, F. and Dandolo, L. (1997). "Deletion of the H19 transcription unit reveals the existence of a putative imprinting control element." Genes Dev **11**(12): 1596-604.
- Rougeulle, C., Cardoso, C., Fontes, M., Colleaux, L., Lalande, M. (1998). "An imprinted antisense RNA overlaps UBE3A and a second maternally expressed transcript." Nat Genet **19**(1): 15-6.
- Runge, S., Nielsen, F.C., Nielsen, J., Lykke-Andersen, J., Wewer, U.M. and Christiansen, J. (2000). "H19 RNA Binds Four Molecules of Insulin-like Growth Factor II mRNA-binding Protein." J. Biol. Chem. **275**(38): 29562-29569.
- Saenz Robles, M.T., Symonds, H., Chen, J. and Van Dyke, T. (1994). "Induction versus progression of brain tumor development: differential functions for the pRB- and p53-targeting domains of simian virus 40 T antigen." Mol Cell Biol **14**(4): 2686-98.
- Sambrook, F., Maniatis (1989). Molecular Cloning: A Laboratory Manual. New York, Cold Spring Harbor Laboratory Press, USA.
- Santos, F., Hendrich, B., Reik, W., Dean, W. (2002). "Dynamic reprogramming of DNA methylation in the early mouse embryo." Dev Biol **241**(1): 172-82.
- Sasaki, H., Jones, P.A., Chaillet, J.R., Ferguson-Smith, A.C., Barton, S.C., Reik, W. and Surani, M.A. (1992). "Parental imprinting: potentially active chromatin of the repressed maternal allele of the mouse insulin-like growth factor II (Igf2) gene." Genes Dev **6**(10): 1843-56.
- Schmidt, J.V., Levorse, J.M. and Tilghman, S.M. (1999). "Enhancer competition between H19 and Igf2 does not mediate their imprinting." Proc Natl Acad Sci U S A **96**(17): 9733-8.
- Schoenherr, C.J., Levorse, J.M. and Tilghman, S.M. (2003). "CTCF maintains differential methylation at the Igf2/H19 locus." Nat Genet **33**(1): 66-9.

- Schofield, P.N. and Tate, V.E. (1987). "Regulation of human IGFII transcription in fetal and adult tissues." Development **101**: 793-803.
- Segal, M.B. (2001). "Transport of nutrients across the choroid plexus." Microsc Res Tech **52**(1): 38-48.
- Selig, S., Okumura, K., Ward, D.C. and Cedar, H. (1992). "Delineation of DNA replication time zones by fluorescence in situ hybridization." Embo J **11**(3): 1217-25.
- Shuman, C.S.r., Bryan, J.H. (1991). "Comparative quantitative ultrastructural studies of the choroidal epithelium of hydrocephalic (hpy/hpy) and normal mice, and the effect of stress induced by water deprivation." Anat Anz **173**(1): 33-44.
- Simon, I., Tenzen, T., Reubinoff, B.E., Hillman, D., McCarrey J.R., Cedar, H. (1999). "Asynchronous replication of imprinted genes is established in the gametes and maintained during development." Nature **401**(6756): 929-32.
- Sleutels, F., Tjon, G., Ludwig, T., Barlow, D.P. (2003). "Imprinted silencing of Slc22a2 and Slc22a3 does not need transcriptional overlap between Igf2r and Air." Embo J **22**(14): 3696-704.
- Sleutels, F., Zwart, R. and Barlow, D.P. (2002). "The non-coding Air RNA is required for silencing autosomal imprinted genes." Nature **415**(6873): 810-3.
- Smilnich, N.J., Day, C.D., Fitzpatrick, G.V., Caldwell, G.M., Lossie, A.C., Cooper, P.R., Smallwood, A.C., Joyce, J.A., Schofield, P.N., Reik, W., Nicholls, R.D., Weksberg, R., Driscoll, D.J., Maher, E.R., Shows, T.B. and Higgins, M.J. (1999). "A maternally methylated CpG island in KvLQT1 is associated with an antisense paternal transcript and loss of imprinting in Beckwith-Wiedemann syndrome." Proc Natl Acad Sci U S A **96**(14): 8064-9.
- Speake, T., Whitwell, C., Kajita, H., Majid, A., Brown, P.D. (2001). "Mechanisms of CSF secretion by the choroid plexus." Microsc Res Tech **52**(1): 49-59.
- Srivastava, M., Frolova, E., Rottinghaus, B., Boe, S.P., Grinberg, A., Lee, E., Love, P.E., Pfeifer, K. (2003). "Imprint control element-mediated secondary methylation imprints at the Igf2/H19 locus." J Biol Chem **278**(8): 5977-83.
- Srivastava, M., Hsieh, S., Grinberg, A., Williams-Simons, L., Huang, S.P., Pfeifer, K. (2000). "H19 and Igf2 monoallelic expression is regulated in two distinct ways by a shared cis acting regulatory region upstream of H19." Genes Dev **14**(10): 1186-95.
- Strichman-Almashanu, L.Z., Lee, R.S., Onyango, P.O., Perlman, E., Flam, F., Frieman, M.B., Feinberg, A.P. (2002). "A genome-wide screen for normally methylated human CpG islands that can identify novel imprinted genes." Genome Res **12**(4): 543-54.
- Stubdal, H., Zalvide, J., Campbell, K.S., Schweitzer, C., Roberts, T.M., DeCaprio, J.A. (1997). "Inactivation of pRB-related proteins p130 and p107 mediated by the J domain of simian virus 40 large T antigen." Mol Cell Biol **17**(9): 4979-90.

- Sturrock, R.R. (1979). "A morphological study of the development of the mouse choroid plexus." *J Anat* **129**(4): 777-93.
- Stylianopoulou, F., Efstratiadis, A., Herbert, J. and Pintar, J. (1988a). "Pattern of the insulin-like growth factor II gene expression during rat embryogenesis." *Development* **103**(3): 497-506.
- Stylianopoulou, F., Herbert, J., Soares, M.B. and Efstratiadis, A. (1988b). "Expression of the insulin-like growth factor II gene in the choroid plexus and the leptomeninges of the adult rat central nervous system." *Proc Natl Acad Sci U S A* **85**(1): 141-5.
- Sun, F.L., Dean, W.L., Kelsey, G., Allen, N.D. and Reik, W. (1997). "Transactivation of Igf2 in a mouse model of Beckwith-Wiedemann syndrome." *Nature* **389**(6653): 809-15.
- Surani, M.A., Barton, S.C. and Norris, M.L. (1986). "Nuclear transplantation in the mouse: heritable differences between parental genomes after activation of the embryonic genome." *Cell* **45**(1): 127-36.
- Svensson, K., Mattsson, R., James, T.C., Wentzel, P., Pilartz, M., MacLaughlin, J., Miller, S.J., Olsson, T., Eriksson, U.J., Ohlsson, R. (1998). "The paternal allele of the H19 gene is progressively silenced during early mouse development: the acetylation status of histones may be involved in the generation of variegated expression patterns." *Development* **125**(1): 61-9.
- Svensson, K., Walsh, C., Fundele, R., Ohlsson, R. (1995). "H19 is imprinted in the choroid plexus and leptomeninges of the mouse foetus." *Mech Dev* **51**(1): 31-7.
- Swiatek, P.J., Lindsell, C.E., del Amo, F.F., Weinmaster, G. and Gridley, T. (1994). "Notch1 is essential for postimplantation development in mice." *Genes Dev* **8**(6): 707-19.
- Symonds, H., Krall, L., Remington, L., Saenz Robles, M., Jacks, T., Van Dyke, T. (1994). "p53-dependent apoptosis in vivo: impact of p53 inactivation on tumorigenesis." *Cold Spring Harb Symp Quant Biol* **59**: 247-57.
- Szabo, P., Tang, S.H., Rentsendorj, A., Pfeifer, G.P., Mann, J.R. (2000). "Maternal-specific footprints at putative CTCF sites in the H19 imprinting control region give evidence for insulator function." *Curr Biol* **10**(10): 607-10.
- Szebenyi, G., Rotwein, P. (1994). "The mouse insulin-like growth factor II/cation-independent mannose 6-phosphate (IGF-II/MPR) receptor gene: molecular cloning and genomic organization." *Genomics* **19**(1): 120-9.
- Szmydynger-Chodobska, J., Chun, Z.G., Johanson, C.E., Chodobski, A. (2002). "Distribution of fibroblast growth factor receptors and their co-localization with vasopressin in the choroid plexus epithelium." *Neuroreport* **13**(2): 257.
- Takagi, N. (1980). "Primary and secondary nonrandom X chromosome inactivation in early female mouse embryos carrying Searle's translocation T(X; 16)16H." *Chromosoma* **81**(3): 439-59.

- Takano, Y., Shiota, G., Kawasaki, H. (2000). "Analysis of genomic imprinting of insulin-like growth factor 2 in colorectal cancer." Oncology **59**(3): 210-6.
- Takeichi, M. (1991). "Cadherin cell adhesion receptors as a morphogenetic regulator." Science **251**(5000): 1451-5.
- Tanaka, M., Puchyr, M., Gertsenstein, M., Harpal, K., Jaenisch, R., Rossant, J., Nagy, A. (1999). "Parental origin-specific expression of Mash2 is established at the time of implantation with its imprinting mechanism highly resistant to genome-wide demethylation." Mech Dev **87**(1-2): 129-42.
- Thomas, T., Dziadek M. (1993). "Capacity to form choroid plexus-like cells in vitro is restricted to specific regions of the mouse neural ectoderm." Development **117**(1): 253-62.
- Thomas, T., Schreiber, G., Jaworowski, A. (1989). "Developmental patterns of gene expression of secreted proteins in brain and choroid plexus." Dev Biol **143**(1): 38-47.
- Thomas, T., Stadler, E., Dziadek, M. (1992). "Effects of the extracellular matrix on fetal choroid plexus epithelial cells: changes in morphology and multicellular organization do not affect gene expression." Exp Cell Res **203**(1): 198-213.
- Thorvaldsen, J.L., Duran, K.L. and Bartolomei, M.S. (1998). "Deletion of the H19 differentially methylated domain results in loss of imprinted expression of H19 and Igf2." Genes Dev **12**(23): 3693-702.
- Thorvaldsen, J.L., Mann, M.R., Nwoko, O., Duran, K.L. and Bartolomei, M.S. (2002). "Analysis of sequence upstream of the endogenous H19 gene reveals elements both essential and dispensable for imprinting." Mol Cell Biol **22**(8): 2450-62.
- Tole, S., Ragsdale, C.W., Grove, E.A. (2000). "Dorsoventral patterning of the telencephalon is disrupted in the mouse mutant extra-toes." Dev Biol **217**(2): 254-65.
- Torchio, C., Trowbridge, R.S. (1977). "Ovine cells: their long-term cultivation and susceptibility to visna virus." In Vitro **13**(4): 252-9.
- Tosh, D., Shen, C.N., Slack, J.M. (2002a). "Conversion of pancreatic cells to hepatocytes." Biochem Soc Trans **30**(2): 51-5.
- Tosh, D., Shen, C.N., Slack, J.M. (2002b). "Differentiated properties of hepatocytes induced from pancreatic cells." Hepatology **36**(3): 534-43.
- Tremblay, K.D., Duran, K.L. and Bartolomei, M.S. (1997). "A 5' 2-kilobase-pair region of the imprinted mouse H19 gene exhibits exclusive paternal methylation throughout development." Mol Cell Biol **17**(8): 4322-9.
- Tremblay, K.D., Saam, J.R., Ingram, R.S., Tilghman, S.M. and Bartolomei, M.S. (1995). "A paternal-specific methylation imprint marks the alleles of the mouse H19 gene." Nat Genet **9**(4): 407-13.

- Tsutsumi, M., Skinner, M.K., Sanders-Bush, E. (1989). "Transferrin gene expression and synthesis by cultured choroid plexus epithelial cells. Regulation by serotonin and cyclic adenosine 3',5'-monophosphate." J Biol Chem **264**(16): 9626-31.
- Tu, G.F., Achen, M.G., Aldred, A.R., Southwell, B.R., Schreiber, G. (1991). "The distribution of cerebral expression of the transferrin gene is species specific." J Biol Chem **266**(10): 6201-8.
- Uchida, S., Watanabe, S. (1969). "Transformation of mouse 3T3 cells by T antigen-forming defective SV40 virions (T particles)." Virology **39**(4): 721-8.
- Ulaner, G.A., Yang, Y., Hu, J.F., Li, T., Vu, T.H., Hoffman, A.R. (2003). "CTCF binding at the insulin-like growth factor-II (IGF2)/H19 imprinting control region is insufficient to regulate IGF2/H19 expression in human tissues." Endocrinology **144**(10): 4420-6.
- Villalobos, A.R., Parmelee, J.T. and Pritchard, J.B. (1997). "Functional characterization of choroid plexus epithelial cells in primary culture." J Pharmacol Exp Ther **282**(2): 1109-16.
- Von Ohlen, T., Lessing, D., Nusse, R. and Hooper, J.E. (1997). "Hedgehog signalling regulates transcription through cubitus interruptus, a sequence-specific DNA binding protein." Proc Natl Acad Sci U S A **94**(6): 2404-09.
- Walter, J., Paulsen, M. (2003). "Imprinting and Disease." Semin Cell Dev Biol **14**(1): 101-10.
- Wang, Z.Q., Fung, M.R., Barlow, D.P. and Wagner, E.F. (1994). "Regulation of embryonic growth and lysosomal targeting by the imprinted Igf2/Mpr gene." Nature **372**(6505): 464-7.
- Ward, A., Bates, P., Fisher, R., Richardson, L. and Graham, C. (1994). "Disproportionate Growth in Mice with Igf-2 Transgenes." PROC NATL ACAD SCI U S A **91**(22): 10365-10369.
- Ward, A., Fisher, R., Richardson, L., Pooler, J.A., Squire, S., Bates, P., Shaposhnikov, R., Hayward, N., Thurston, M. and Graham, C.F. (1997). "Genomic regions regulating imprinting and insulin-like growth factor-II promoter 3 activity in transgenics: novel enhancer and silencer elements." Genes Funct **1**(1): 25-36.
- Webber, A.L., Ingram, R.S., Levorse, J.M. and Tilghman, S.M. (1998). "Location of enhancers is essential for the imprinting of H19 and Igf2 genes." Nature **391**(6668): 711-5.
- Weber, M., Milligan, L., Delalbre, A., Antoine, E., Brunel, C., Cathala, G., Forne, T. (2001). "Extensive tissue-specific variation of allelic methylation in the Igf2 gene during mouse fetal development: relation to expression and imprinting." Mech Dev **101**(1-2): 133-41.

- Weksberg, R., Shen, D.R., Fei, Y.L., Song, Q.L., Squire, J. (1993). "Disruption of insulin-like growth factor 2 imprinting in Beckwith-Wiedemann syndrome." Nat Genet **5**(2): 143-50.
- Weksberg, R., Squire, J.A. (1996). "Molecular biology of Beckwith-Wiedemann syndrome." Med Pediatr Oncol **27**(5): 462-9.
- Welsh, M.J., Anderson, M.P., Rich, D.P., Berger, H.A., Denning, G.M., Ostedgaard, L.S., Sheppard, D.N., Cheng, S.H., Gregory, R.J., Smith, A.E. (1992). "Cystic fibrosis transmembrane conductance regulator: a chloride channel with novel regulation." Neuron **8**(5): 821-9.
- Wilkinson, D.G., Nieto, M.A. (1992). "Detection of messenger RNA by in situ hybridisation to tissue section and whole mounts." Methods Enzymol **225**: 361-73.
- Wilting, J., Christ, B. (1989). "An experimental and ultrastructural study on the development of the avian choroid plexus." Cell Tissue Res **255**(3): 487-94.
- Wroe, S.F., Kelsey, G., Skinner, J.A., Bodle, D., Ball, S.T., Beechey, C.V., Peters, J., Williamson, C.M. (2000). "An imprinted transcript, antisense to Nesp, adds complexity to the cluster of imprinted genes at the mouse Gnas locus." Proc Natl Acad Sci U S A **97**(7): 3342-6.
- Wutz, A., Smrzka, O.W., Schweifer, N., Schellander, K., Wagner, E.F., Barlow, D.P. (1997). "Imprinted expression of the Igf2r gene depends upon an intronic CpG island." Nature **389**(6652): 669-71.
- Yan, C., Costa, R. H., Darnell, J. E., Jr., Chen, J. D. & Van Dyke, T. A. (1990). "Distinct positive and negative elements control the limited hepatocyte and choroid plexus expression of transthyretin in transgenic mice." Embo J **9**: 869-78.
- Yang, T., Adamson, T.E., Resnick, J.L., Leff, S., Wevrick, R., Francke, U., Jenkins, N.A., Copeland, N.G., Brannan, C.I. (1998). "A mouse model for Prader-Willi syndrome imprinting-centre mutations." Nat Genet **19**(1): 25-31.
- Yang, Y., Hu, J.F., Ulaner, G.A., Li, T., Yao, X., Vu, T.H., Hoffman, A.R. (2003). "Epigenetic regulation of Igf2/H19 imprinting at CTCF insulator binding sites." J Cell Biochem **90**(5): 1038-55.
- Yen, P.H., Patel, P., Chinault, A.C., Mohandas, T., Shapiro, L.J. (1984). "Differential methylation of hypoxanthine phosphoribosyltransferase genes on active and inactive human X chromosomes." Proc Natl Acad Sci U S A **81**(6): 1759-63.
- Yoon, B.J., Herman, H., Sikora, A., Smith, L.T., Plass, C., Soloway, P.D. (2002). "Regulation of DNA methylation of Rasgrf1." Nat Genet **30**(1): 92-6.
- Yoo-Warren, H., Pachnis, V., Ingram, R.S. and Tilghman, S.M. (1988). "Two regulatory domains flank the mouse H19 gene." Mol Cell Biol **8**(11): 4707-15.

- Zemel, S., Bartolomei, M.S. and Tilghman, S.M. (1992). "Physical linkage of two mammalian imprinted genes, H19 and insulin-like growth factor 2." Nat Genet **2**(1): 61-5.
- Zhang, P., Liegeois, N.J., Wong, C., Finegold, M., Hou, H., Thompson, J.C., Silverman, A., Harper, J.W., DePinho, R.A., Elledge, S.J. (1997). "Altered cell differentiation and proliferation in mice lacking p57KIP2 indicates a role in Beckwith-Wiedemann syndrome." Nature **387**(6629): 151-8.
- Zhang, Y., Tycko, B. (1992). "Monoallelic expression of the human H19 gene." Nat Genet **1**(1): 40-4.
- Zheng, W., Zhao, Q. (2002). "Establishment and characterization of an immortalized Z310 choroidal epithelial cell line from murine choroid plexus." Brain Res **958**(2): 371-80.
- Zwart, R., Sleutels, F., Wutz, A., Schinkel, A.H., Barlow, D.P. (2001). "Bidirectional action of the Igf2r imprint control element on upstream and downstream imprinted genes." Genes Dev **15**(18): 2361-6.



## PUBLICATIONS ARISING

**An enhancer element at the *Igf2/H19* locus drives gene expression in imprinted and non-imprinted tissues.**

Marika Charalambous, Trevelyan R. Menheniott, William R. Bennett, Sharon M. Kelly, Ghislaine Dell, Luisa Dandolo and Andrew Ward (2004) *Dev Biol* **271**(2): 488-97



Genomes & Developmental Control

# An enhancer element at the *Igf2/H19* locus drives gene expression in both imprinted and non-imprinted tissues

Marika Charalambous,<sup>a,1</sup> Trevelyan R. Menheniott,<sup>a,4</sup> William R. Bennett,<sup>a,2</sup> Sharon M. Kelly,<sup>a,3</sup> Ghislaine Dell,<sup>a,5</sup> Luisa Dandolo,<sup>b</sup> and Andrew Ward<sup>a,\*</sup>

<sup>a</sup>Developmental Biology Program, Department of Biology and Biochemistry, University of Bath, Bath, BA2 7AY, UK

<sup>b</sup>Department of Development, Genetics and Molecular Pathology, Institut Cochin, Paris 75014, France

Received for publication 16 January 2004, revised 30 March 2004, accepted 1 April 2004  
Available online 28 May 2004

## Abstract

The insulin-like growth factor 2 (*Igf2*) gene encodes a potent growth factor that is expressed in multiple tissues during embryonic development. Expression at this locus is mediated by genomic imprinting. In the developing endodermal tissues, imprinting of *Igf2* is mediated by the interaction of a set of enhancers downstream of the linked *H19* gene with a differentially methylated domain (DMD) that lies approximately 2–4 kb upstream of *H19* that has a boundary or insulator function in the hypomethylated state. In the remainder of tissues that express *Igf2* and *H19*, the *cis* elements that drive their correct expression and imprinting are not well understood. In addition, enhancers driving expression of *Igf2* in the choroid plexus and leptomeninges, tissues where the gene is thought not to be imprinted, have not been isolated. Here we show that biallelic (non-imprinted) expression within the choroid plexus is restricted to the epithelium, and we provide evidence that a conserved intergenic region functions as an enhancer for *Igf2* both in tissues where the gene is imprinted, and where *Igf2* is biallelically expressed. The presence of an enhancer for imprinted tissues in the intergenic region argues for the existence of imprinting controls distinct from the DMD, which may be provided by differential methylation at sites proximal to *Igf2*.

© 2004 Elsevier Inc. All rights reserved.

**Keywords:** Choroid plexus; Genomic imprinting; Insulin-like growth factor; Methylation; Transgenic mice

## Introduction

The centrally conserved domain (CCD) was initially characterized by Koide et al. (1994) as a GC-rich, relatively unmethylated region approximately 32 kb upstream of the mouse *H19* gene. This region was found to contain DNaseI hypersensitive sites (HSS) as well as a high degree of sequence conservation between mammals, a strong indication that this region is functional. Subsequent analysis (Ainscough et al., 2000) showed that this region can be subdivided into two domains based on comparisons with human sequence (see Fig. 1c, shaded areas). Region 1 shares 86% identity between mouse and human sequences over approximately 100 bp and contains the previously mapped HSS. Region 2 displays 87% identity between the two species over approximately 200 bp. Region 1 has been analyzed in the context of a yeast artificial chromosome (YAC) transgene that contains 130 kb of the mouse genomic region spanning from approximately 5 kb upstream of the first exon of insulin-like growth factor 2 (*Igf2*) to approximately 35 kb downstream of

**Abbreviations:** *Igf2*, insulin-like growth factor 2; DMD, differentially methylated domain; CCD, centrally conserved domain; HSS, hypersensitive sites; YAC, yeast artificial chromosome; DMR, differentially methylated region; P3, promoter 3.

\* Corresponding author. Developmental Biology Program, Department of Biology and Biochemistry, University of Bath, Building 4 South, Bath, BA2 7AY, UK. Fax: +44-1225-826779.

E-mail address: [bssaw@bath.ac.uk](mailto:bssaw@bath.ac.uk) (A. Ward).

<sup>1</sup> Present address: Centre for Diabetes and Endocrinology, Division of Medicine, Rayne Building, 5 University Street, London WC1E 6JJ, UK.

<sup>2</sup> Present address: UK Centre for Tissue Engineering, Room 3.446, Stopford Building, Biological Sciences, University of Manchester, Manchester M13 9PT, UK.

<sup>3</sup> Present address: Henry Wellcome Laboratories for Integrative Neuroscience and Endocrinology, Dorothy Hodgkin Building, Whitson Street, Bristol, BS1 3NY, UK.

<sup>4</sup> Present address: Imprinting Group, Division of Genetics, GKT School of Medicine, Guys Tower, London Bridge, London, SE1 9RT, UK.

<sup>5</sup> Present address: Department of Biochemistry, School of Medical Sciences, University of Bristol, University Walk, Bristol, BS8 1TD, UK.

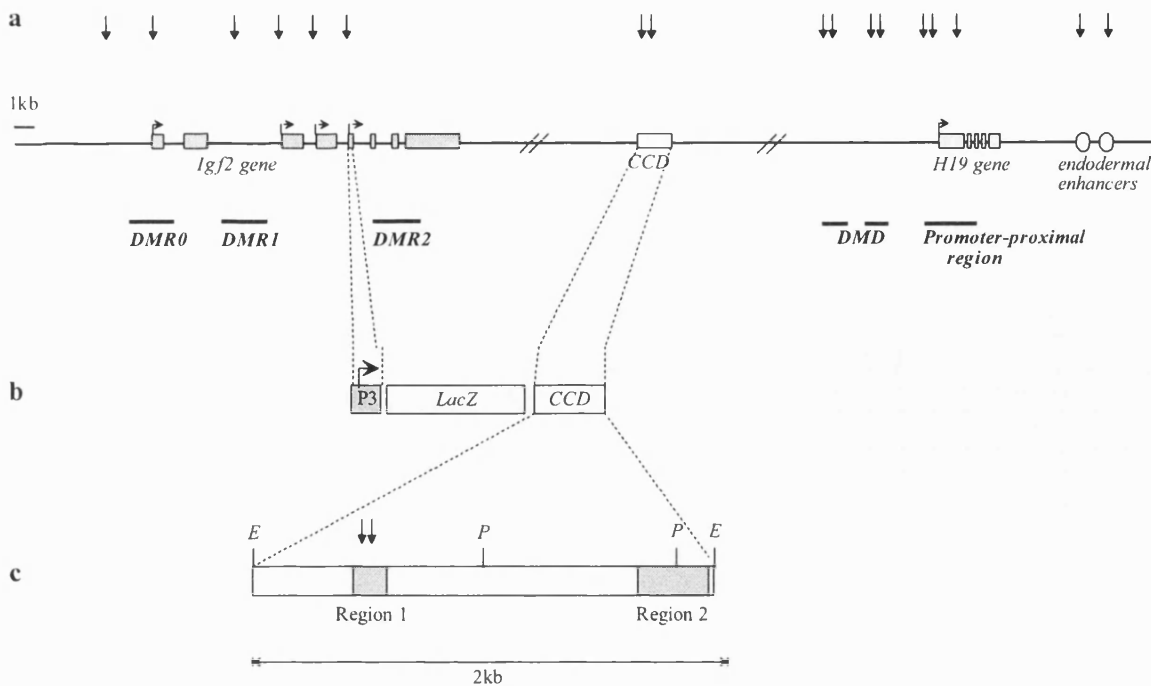


Fig. 1. The *Igf2/H19* gene locus and P3-*LacZ*-CCD transgene construct. (a) The relative positions of the *Igf2* and *H19* genes within the 100 kb genomic region are indicated by their position along the horizontal line. Exons are indicated by filled boxes and regulatory elements by open boxes. Vertical arrows above the line indicate regions of DNaseI hypersensitivity. Horizontal arrows show the direction of transcription from the four *Igf2* promoters (P0, P1, P2, and P3) and the single *H19* promoter. Regions that exhibit differential levels of methylation between parental alleles (DMRs, DMD, and *H19* promoter-proximal region) are indicated by solid horizontal lines. (b) Structure of the P3-*LacZ*-CCD transgene (Construct C). *Igf2* promoter 3 was cloned upstream of the *E. coli LacZ* coding sequence, and the 2 kb CCD region was inserted immediately downstream. (c) The CCD in detail. The 2 kb CCD regions contains two regions of strong sequence conservation with the human locus, Regions 1 and 2 (see text). The CCD deletion in the YAC experiment (Ainscough et al., 2000) referred to in the text is the 5' 1 kb *EcoRI* (E)–*PstI* (P) interval containing Region 1.

the *H19* gene. With the intact YAC transgene, imprinting is maintained of both an *Igf2-LacZ* fusion gene and *H19*, and transgenic mice display expression of both genes in the majority of tissues where *Igf2* and *H19* are normally expressed (Ainscough et al., 1997). In transgenic mice where 1 kb of the intergenic region, including Region 1 but not Region 2, was deleted from the same YAC, the maternal allele of *LacZ* was reactivated in late gestation in a subset of skeletal muscle cells, most notably those of the tongue (Ainscough et al., 2000). Region 1 therefore contains a maternal allele-specific, tissue-specific silencer that is active in late gestation. The role of Region 2 has not been elucidated, though evidence from transgenic and germline knock out experiments suggests that it may contain the exchange tissue enhancers (Jones et al., 2001; Ward et al., 1997).

Imprinting of the *Igf2* gene in endodermal tissues is thought to be mediated by the interaction of tissue-specific enhancer elements with a differentially methylated domain (DMD) 2–4 kb upstream of the *H19* gene (for relative positions, see Fig. 1). On the maternal allele, where the DMD is unmethylated, it functions as a boundary to prevent the access of downstream enhancers to the *Igf2* gene. This boundary function is mediated by the protein CTCF (Bell and Felsenfeld, 2000; Hark et al., 2000; Kanduri et al., 2000; Pant et al., 2003; Szabo et al., 2000). On the paternal allele,

methylation of the DMD prevents CTCF binding; therefore, the *Igf2* promoters and the downstream enhancers are able to interact. If the DMD provides the sole imprinting element for *Igf2*, a prediction would be that the enhancers that drive imprinted *Igf2* expression would lie on the opposite side of the boundary. Indeed, a region that can drive gene expression in skeletal muscle, where *Igf2* is abundantly expressed and imprinted, has recently been mapped as lying approximately 28–30 kb downstream of the *H19* gene, on the predicted side of the boundary (Kaffer et al., 2000), and is one of many putative enhancers in this region (Davies et al., 2002; Ishihara et al., 2000). However, the existence of several regions of differential methylation proximal to *Igf2* (DMR0, DMR1, DMR2, see Fig. 1) that display methylation-dependent, tissue-specific silencer activity (Constancia et al., 2000; Eden et al., 2001; Murrell et al., 2001) argues that the DMD may not directly mediate the imprinting of *Igf2* in all tissues.

The CCD lies between the *Igf2* gene and the DMD and consequently the CCD should not be affected by the boundary element that prevents the interaction of *Igf2* with more distant enhancers. We therefore considered the CCD as a good candidate for driving expression in the tissues where *Igf2* is biallelically expressed, the choroid plexus and leptomeninges. To test this hypothesis, we have created transgenic mice that carry the CCD in the context of a

*LacZ* reporter construct. As expected, these mice express the reporter gene in the exchange tissues of the brain. We show that within the choroid plexus endogenous, *Igf2* expression is imprinted in the stromal compartment (with the paternal allele active) but non-imprinted in the epithelium (both alleles expressed), and that this is opposite to the pattern of *H19* expression (with the maternal allele expressed in the stroma and both alleles silent in epithelium). The CCD was able to drive transgene expression in both stromal and epithelial components of the choroid plexus in a pattern very similar to that of endogenous *Igf2* expression. In addition, the CCD was able to reproducibly drive gene expression in further tissues of mesodermal or neural crest origin that are consistent with the known expression pattern of *Igf2*. The presence of an enhancer for *Igf2* proximal to the boundary, in addition to the existence of tissue-specific silencers upstream of the *Igf2* gene, suggests that a second mechanism acts to imprint this gene in a subset of tissues.

## Methods

### Mice

The *LacZDMR2*<sup>-</sup> mice were maintained on an F<sub>1</sub> (CBA × C57BL/6J) background. To derive embryos for allele-specific expression analysis, male and female mice heterozygous for the *LacZDMR2*<sup>-</sup> mutation were mated with F<sub>1</sub> partners. To distinguish *LacZDMR2*<sup>-</sup> heterozygous embryos from wild-type littermates, yolk sacs were collected and crude lysates were made by heating in 50 mM NaOH at 100°C for 10 min. Lysates were analyzed for the presence of the *LacZ* reporter by PCR using primers internal to the *LacZ* gene: 407, 5' ATG AAC GGT CTG GTC TTT GC-3' and 408, 5' ACA TCC AGA GGC ACT TCA CC-3'. The *H19* knockout strain, designated *H19Δ3*, was previously described, together with methods for distinguishing the wild-type and knockout alleles (Ripoche et al., 1997).

### Transgenesis

The P3-*LacZ*-CCD construct C (see Fig. 1) contained a 3.6 kb coding region of the bacterial β-galactosidase (*LacZ*) gene driven from *Igf2* promoter 3 (*Igf2* P3, as described in Caricasole and Ward, 1993). The CCD fragment, placed immediately 3' to the *LacZ* gene, was a 2 kb *EcoRI* fragment (pA-4, as detailed in Koide et al., 1994). Cloning steps were performed in the Bluescript II SK+ vector, according to standard techniques (Sambrook et al., 1989).

Transgenic mouse lines were constructed as follows: Linear construct DNA (1 μg/ml) was purified from vector sequences and microinjected into one pronucleus of an F1 (C57BL/6J×CBA/Ca) zygote, using standard techniques

(Hogan et al., 1986). Injected embryos were transferred into the oviduct of pseudopregnant MF1 females. Lines were established and maintained by breeding the transgenics with F1 partners.

Founders were identified by PCR of sequences unique to the *Igf2* P3-*LacZ*-CCD transgene (primers *Igf2* P3: 5' CTGTGAGAACCTTCCAGCCTTTTC 3' and *LacZ*: 5' CAAGGCGATTAAGTTGGGTAACGCC 3') and confirmed by Southern blotting of tail genomic DNA with a probe generated from the transgene construct, according to standard techniques. Copy number was estimated on Southern blots by titrating DNA from hemizygous transgenic animals, with reference to an endogenous band detected using CCD sequences within the transgene probe.

### Tissue processing

Embryos and tissues were analyzed for *LacZ* expression according to Ainscough et al. (2000), with the following modifications: Samples were incubated in X-Gal or BLU-GAL (Melford Laboratories Ltd) staining solution for 16–24 h, washed with PBS, then fixed overnight in 4% paraformaldehyde in PBS (PFA) and stored in 70% ethanol. Paraformaldehyde fixed material from both *LacZ* analysis and obtained for in situ hybridization analysis was processed according to standard techniques as described previously (Charalambous et al., 2003).

### Probes and antibodies

The *H19* in situ hybridization probe was a 346 bp fragment spanning exons 3–4 of the mouse *H19* cDNA, amplified by PCR using the following primers: 416; 5'AAT GAG TTT CTA GGG AGG GAG G-3' and 417; 5'GGA AAA GTG AAA GAA CAG ACG G-3', then cloned into the pGEM-T easy vector. Sense and antisense transcripts were obtained for this gene and for *Igf2*, as described previously (Charalambous et al., 2003). Transthyretin (TTR) was detected in tissue sections using a rabbit polyclonal antiserum (DAKO) at a dilution of 1:100. Immunohistochemistry and mRNA in situ hybridizations were performed essentially as detailed in Charalambous et al. (2003).

## Results

### Generation of P3-*LacZ*-CCD transgenic mice

To test the CCD function, we created a transgene construct containing the *LacZ* gene driven by *Igf2* promoter 3 (P3), in *cis* to the CCD (construct C, see Fig. 1). Previous experiments have shown that *Igf2* P3 alone cannot drive reproducible tissue-specific expression of a reporter gene (Ishihara et al., 2000; Ward et al., 1997). Construct C (P3-*LacZ*-CCD) DNA was used to generate five transgenic

founder animals, designated Connie, Columbo, Cornelius, Christian, and Clive, all of which were shown by PCR and Southern blotting to transmit the transgene (data not shown). Founder animals were mated to generate an F1 generation of males and females hemizygous for the transgene, and these animals were backcrossed onto stock (CBA/C57BL6) mice to yield the embryos used in this study. Embryos were assayed for the expression of  $\beta$ -galactosidase by an in situ assay at various embryonic and neonatal stages. Within each line, no differences in spatial patterns of gene expression, or obvious differences in the level of gene expression, were observed following the transmission of the transgene from either males or females at any developmental stage examined (not shown). This is consistent with the absence of parental allele-specific methylation or DNaseI hypersensitivity in the CCD (Koide et al., 1994).

*P3-LacZ-CCD reporter transgenes are expressed in tissues where *Igf2* is biallelically expressed*

Four of five lines demonstrated a detectable level of gene expression from embryonic day 12.5 (e12.5). In the Clive line, the transgene appears to have been silenced by a position effect. As expected, the remaining lines displayed reporter gene expression in the choroid plexus and leptomeninges from their formation at e12.5. Embryos from the Connie line expressed the transgene at very low levels, and not all individuals positive for the transgene demonstrated detectable levels of expression. The Connie line was therefore excluded from further analysis. By e14.5, the Columbo, Cornelius, and Christian lines all expressed the transgene reproducibly in the third, fourth, and lateral ventricle choroid plexus, as well as in the leptomeninges of the brain, and surrounding the spinal cord (Fig. 2a). Expression of the reporter gene in the choroid plexus and leptomeninges was maintained throughout embryonic development and persisted after birth (Figs. 2b–d), consistent with the previously reported endogenous *Igf2* expression pattern (Stylianpoulou et al., 1988b).

The choroid plexus develops from more than one cell population. It is comprised of a stromal stalk that extends into the ventricular cavities of the brain, surrounded by the columnar choroid plexus epithelium. The stroma develops from the same mesenchymal cell population as will form the pia mater of the leptomeninges, some of which may be derived from the neural crest (Catala, 1998; Davson, 1967). At approximately e10.5 in the mouse, mesenchymal cells overlying the neuroepithelium expand and become highly populated with vasculature. This expansion into the ventricles forms a stromal stalk that retains its ependymal lining. The ependyma is the innermost layer of the neuroepithelium that lines the ventricles of the brain and the spinal cord. Concomitant with the expansion and invagination of the stroma, the ependyma in this region also

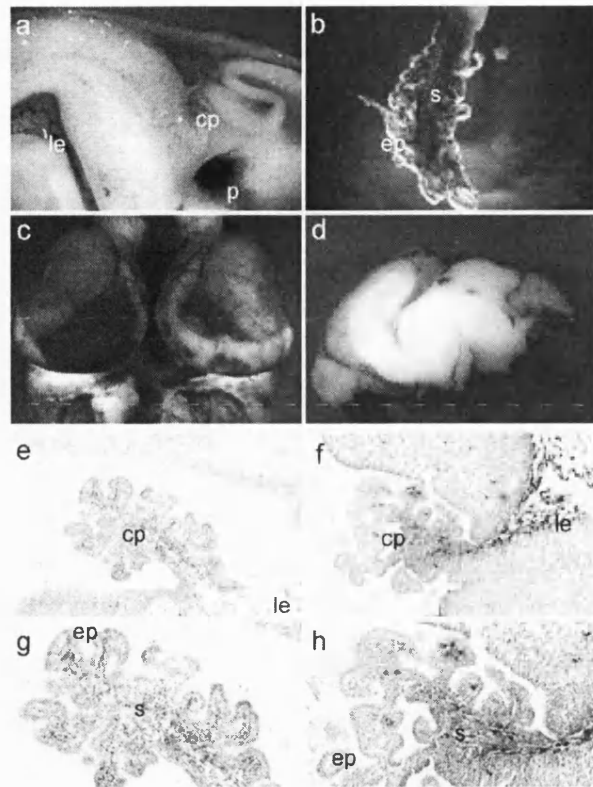


Fig. 2. Expression of the P3-LacZ-CCD transgene construct mirrors that of *Igf2* in the brain. (a) Bisected embryo at e14.5 of the Columbo line, focusing on the area surrounding the fourth ventricle of the brain. The choroid plexus (cp) is expressing the reporter gene, as are the connecting leptomeninges (le) surrounding the brain. The leptomeninges that enclose the neural tube also express the transgene. Some additional gene expression is seen in the pons (p), which is limited to the Columbo line and thought to be due to a position effect of transgene integration. (b) Dissected fourth ventricle choroid plexus at 10 days post-partum from the Columbo line. Gene expression can clearly be seen in the connective stromal tissue (s) as well as in a subset of epithelial (ep) cells. (c and d) Whole brain from the individual shown in b. Gene expression is confined to the meningeal layers surrounding the brain and its cavities. (e–h) A comparison of reporter gene expression from the Columbo line, and *Igf2* mRNA localization at e15.5. (e, g) Show in situ hybridization to the fourth ventricle choroid plexus with an antisense *Igf2* probe at 100 $\times$  and 200 $\times$  magnification, respectively. (f, h) Show reporter gene expression in the fourth ventricle at the same magnification. Both *Igf2* and reporter gene expression is abundant in the stroma and leptomeninges, and is less abundant and mosaic in the choroid plexus epithelium.

expands, becoming highly convoluted by e12.5. The morphology of the cells changes from low cuboidal to a high cylindrical epithelium with an apical brush border (Davson, 1967), the choroid plexus epithelium.

The expression pattern of the reporter gene was compared in detail with that of *Igf2* mRNA at mid-gestation. In the fourth ventricle of the brain, both *Igf2* and the reporter gene were expressed at high levels in the stromal stalk of the choroid plexus, and in the underlying pia mater and arachnoid mater layers of the leptomeninges (Figs. 2c, f). At higher magnification (Figs. 2g, h), a lower level of reporter

gene and *Igf2* expression can be detected in a scattered cell distribution in the outer epithelial layer of the choroid plexus. Therefore, reporter constructs mirror the expression of *Igf2* in both the fine distribution of gene expression within the exchange tissues, and in the maintenance of gene expression in these tissues after birth.

*Igf2* is biallelically expressed in the choroid plexus epithelium, but imprinted in the stroma

Expression of *Igf2* has been previously reported in both the stroma and the choroid plexus epithelium (Stylianiopoulou

et al., 1988b). However, whether the gene is biallelically expressed in both compartments has never been resolved (Svensson et al., 1995). In addition, it is not known whether the expression of the gene is initially parent-of-origin specific in this organ, becoming biallelic as development proceeds, or expressed from both alleles from the onset of development.

To answer these questions, we made use of a previously described allele of *Igf2* in which exons 4–6 (including DMR2) are replaced with a *LacZ* cassette. This *LacZDMR2*<sup>-</sup> allele faithfully recapitulates the expression of *Igf2* (Murrell et al., 2001). We followed the expression of

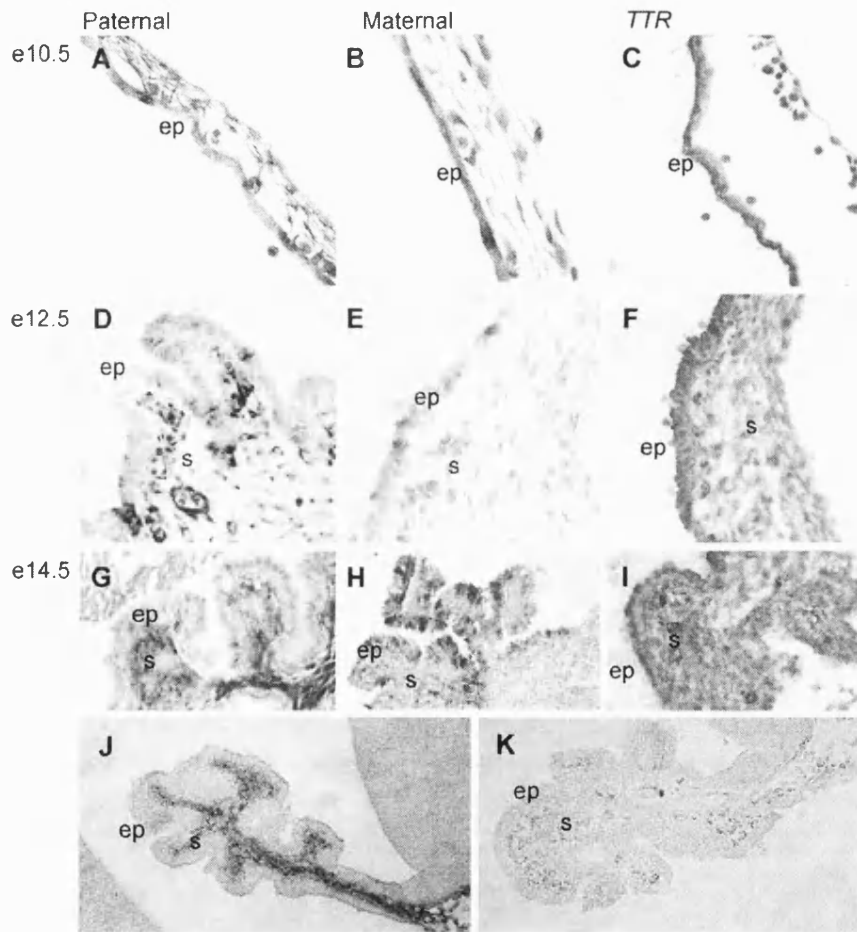


Fig. 3. *Igf2* demonstrates both monoallelic and biallelic expression in the choroid plexus. Reporter gene expression (blue stain) from the *Igf2 LacZDMR2*<sup>-</sup> allele is detectable from both parental alleles at developmental stages spanning the course of choroid plexus development. (A) At e10.5, paternal expression of the reporter is present in both a scattered population of ependymal cells (the presumptive choroid plexus epithelium, ep) and in the overlying mesenchyme (the presumptive choroid plexus stroma, s). (B) At the same stage, reporter gene expression from the maternal allele is present in a similar scattered population of ependymal cells, but absent from the overlying mesenchyme. Expression was not detected before e10.5, either following maternal or paternal transmission of the *Igf2 LacZDMR2*<sup>-</sup> allele. (D, G) At e12.5 to e14.5, reporter gene expression from the paternal allele is detectable in both the epithelium and in the stroma. (E, H) However, following maternal transmission of *LacZDMR2*<sup>-</sup>, reporter gene expression is detected in the epithelium, but never in the stroma. A similar pattern of parental allele-specific gene expression was observed by in situ hybridization for the wild-type *Igf2* allele in *LacZDMR2*<sup>-</sup> heterozygotes (not shown). (C, F, and I) An antibody recognizing transthyretin (TTR) protein was used as a marker of developing choroid plexus tissue and shows uniform expression of TTR (brown stain) throughout the plexus epithelium at all stages examined. (J) *H19* mRNA can be readily detected in the choroid plexus stroma, but not in the epithelium, of a wild-type embryo at e14.5. (K) Following maternal transmission of the *H19A3* allele, *H19* gene expression cannot be detected in either compartment of the choroid plexus. Tissue sections were counter-stained with either nuclear fast red (A, B, D, E, G, and H) or Mayer's hematoxylin (C, F, and I), and images were captured at a magnification of either 400× (A–I) or 200× (J, K).

the reporter in the fourth ventricle choroid plexus of embryos from e9.5 to e14.5 to ask whether *Igf2* is expressed from the earliest formation of the organ in both epithelial and stromal compartments. In addition, we were able to determine the imprinting status of *Igf2* in both compartments by examining embryos that had inherited the *LacZDMR2*<sup>-</sup> allele uniparentally. Before e10.5, we could not detect reporter gene expression in either ependymal cells or in the underlying mesenchyme, following maternal or paternal transmission of *LacZDMR2*<sup>-</sup> (not shown). At e10.5, paternal gene expression was detected in both the mesenchyme and in a subset of the overlying ependymal cells of the presumptive choroid plexus (Fig. 3a). At the same stage, expression from the maternal allele was detectable only in the ependyma (Fig. 3b). Subsequently, paternally derived gene expression was abundant in the developing stroma (Figs. 3d, g), whereas the maternally derived reporter gene expression could not be detected in this region (Figs. 3e, h). Gene expression from both parental alleles was detected in the choroid plexus epithelium. In contrast, *H19* mRNA was detected in the stroma but not the epithelium of a wild-type embryo at e14.5 (Fig. 3j), and was absent from both cell types in embryos with maternal transmission of an *H19A3* knockout allele (Fig. 3k). To confirm that *Igf2* expression is associated with the choroid plexus, particularly at earlier stages when the characteristic-folded morphology of this organ has not been established, we have used an antibody that recognizes transthyretin (TTR). Within the brain, TTR expression was confined to the presumptive and definitive choroid plexus epithelium, with expression commencing at around e10.5 when the plexus epithelial cells differentiate from the neuroepithelium. This expression pattern is consistent with the previous description of TTR as a marker of choroid plexus epithelium (Murakami et al., 1987). It is noted that TTR expression is uniform throughout the epithelium, in contrast with the variegated expression of *Igf2* in this tissue.

We conclude that *Igf2* is expressed in both the epithelial and stromal compartments of the choroid plexus from the onset of its development. *Igf2* is imprinted (paternally expressed) in stromal cells, but biallelically expressed in the choroid plexus epithelium. *H19* has a reciprocal expression pattern in the choroid plexus with expression from the maternally derived allele in the stroma and with both alleles silent in the epithelium. The CCD was thus able to drive reporter gene expression in a region where *Igf2* is biallelically expressed, as predicted, but also in a region where the gene is imprinted.

*P3-LacZ-CCD reporter transgenes are expressed in further tissues where Igf2 is imprinted*

Further examination of CCD-bearing transgenics revealed gene expression in some additional embryonic tissues. The three high expressing lines (Columbo, Cornelius, and Christian) demonstrated reproducible patterns of

gene expression in structures derived from the mesoderm and the neural crest (summarized in Table 1), as well as several line-specific sites of expression that are a presumed consequence of the transgene insertion sites (position effects).

At e9.5, all three lines showed staining in the mesenchyme at the site of the head fold, in the developing eye, and in the branchial arches. A subset of the condensing paraxial mesoderm was stained, as was the urogenital ridge (Fig. 4b). By e10.5, a high level of staining was observed in the somites at their dorsolateral edge, in the mesenchyme surrounding the myelencephalon including that which condenses to form the pia and arachnoid membranes of the leptomeninges (Rugh, 1990; Stylianpoulou et al., 1988a), as well as in the mesenchyme surrounding the neural tube (Fig. 4c). The mesonephros maintained expression of the reporter gene, and the developing eye was clearly stained. At e12.5 (Fig. 4f), expression in the paraxial mesoderm had declined and was present only in the most posterior somites. Gene expression was wide-

Table 1  
Summary of transgene copy number and expression at e14.5 across the P3-*LacZ-CCD* transgenic lines

Line	Copy number	Embryos examined	Position-dependent sites of gene expression at e14.5	Common sites of gene expression at e14.5
Connie	2–4	48	none detected	choroid plexus (fourth ventricle)
Columbo	>20	25	oculomotor nerve, pons, roof of midbrain, abdominal wall muscle, mullerian tubicle, floorplate	leptomeninges (roof of midbrain and surrounding the third ventricle, and surrounding the neural tube), choroid plexus (of the third, fourth, and lateral ventricles), lens of eye, tongue muscle, mesenchyme of the head and neck tubules of the ear (eustacian tubules and lateral and posterior semicircular canal), ureter and degenerating mesonephros
Cornelius	2–4	52	trigeminal and facial ganglia, dorsal root ganglia, and peripheral ganglia (including those of the limbs)	choroid plexus (of the third, fourth, and lateral ventricles), lens of eye, tongue muscle, mesenchyme of the head and neck tubules of the ear (eustacian tubules and lateral and posterior semicircular canal), ureter and degenerating mesonephros
Christian	>20	34	cartilage of the digits, tubules of the kidney, dermis of the skin	mesenchyme of the head and neck tubules of the ear (eustacian tubules and lateral and posterior semicircular canal), ureter and degenerating mesonephros
Clive	1–2	24	none detected	none detected

For each of the P3-*LacZ-CCD* transgenic lines, an estimation of transgene copy is given and also the number of embryos examined for expression of the *LacZ* reporter. Common sites of expression are those regions where the transgenes were expressed in the majority of lines. Position-dependent sites of expression were those unique to a transgenic line.

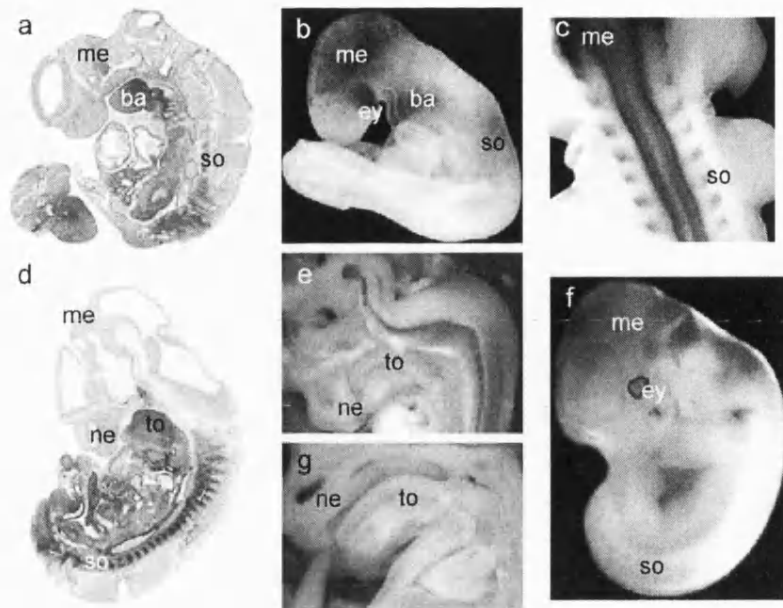


Fig. 4. Expression of the C construct in tissues where *Igf2* is imprinted. Representative embryos from the Columbo line are shown at e9.5 (b), e10.5 (c), e12.5 (e, f), and at e14.5 (g) with reference to *Igf2* expression at e10 (a) and e12.5 (d). In the early embryo (a–c), the transgene is expressed in the head mesenchyme (me), in the branchial arches (ba), in a subset of the somitic mesoderm (so), and in the eye (ey). By e12.5 (d–f), this expression has become refined to the ependyma of the brain (me), the lens of the eye (ey), several regions of facial mesenchyme, to the posterior somites (dm), and the mesonephros (not shown). In later development (g), facial mesenchymal expression is resolved into specific areas including the tongue (to), the nasal epithelium (ne), and the ear (not shown).

spread in the condensing ependyma of the brain and was present in the choroid plexus as it forms in the fourth ventricle. Cranial structures such as the eustachian tubules and semicircular canals of the ear, and the nasal mesenchyme and epithelium began to express the transgene at this stage, as did the intrinsic muscle of the tongue (Fig. 4e). Expression was maintained in the mesonephros and in the eye (not shown). At e14.5, gene expression was lost from the derivatives of the somites. The tongue muscle, nasal epithelium and mesenchyme, ear and neck cartilage expressed the transgene (Fig. 4g). The mesonephros has degenerated at this stage, but one of its derivatives, the ureter, displayed reporter gene expression (not shown). The choroid plexus and meninges surrounding the brain and spinal cord continued to express the transgene, and we note that within the choroid plexus epithelium expression is restricted to a subset of cells, as is expression of endogenous *Igf2* (see Fig. 3). After e14.5, gene expression declined in all tissues except the exchange tissues of the brain (Fig. 2c).

In summary, reproducible expression patterns were seen in three transgenic mouse lines containing the C construct, representing three independent integration events. This expression pattern represents a subset of the tissues in which *Igf2* is expressed during mouse development (see Figs. 4a, d). Furthermore, in all the tissues described above (with the exception of the exchange tissues of the brain), the majority of *Igf2* transcripts are generated from the paternal allele of the gene. The CCD is therefore acting as an enhancer both

in tissues where *Igf2* is imprinted and where it is biallelically expressed.

## Discussion

We have established that *Igf2* expression is biallelic from the earliest stages at which it can be detected (e10.5) in the presumptive choroid plexus epithelium. In contrast, imprinted (paternal-allele) expression is seen from the onset in choroid plexus stroma. We propose that this reflects the different origins of these two tissues (Catala, 1998; Davson, 1967), and that epigenetic marks may be differently established in these lineages (see Fig. 5). Biallelic methylation of the differentially methylated regions proximal to *Igf2* (DMR1 and DMR2) has been reported previously following analysis of whole choroid plexus, and the same report indicated that the *H19* promoter exhibits only 50% methylation, consistent with differential allelic marking of this region (Feil et al., 1994). The methylation status of the DMD in this tissue remains unknown, and no attempt has yet been made to separately analyze methylation in the stromal and epithelial compartments. However, it is possible that within the choroid plexus, biallelic methylation of *Igf2* DMRs is restricted to the epithelium, and that this local hypermethylation is permissive for *Igf2* expression.

The results of our transgenic experiments using the *Igf2* P3-LacZ-CCD construct demonstrate that the CCD can act as a regional enhancer of a reporter gene during mouse devel-



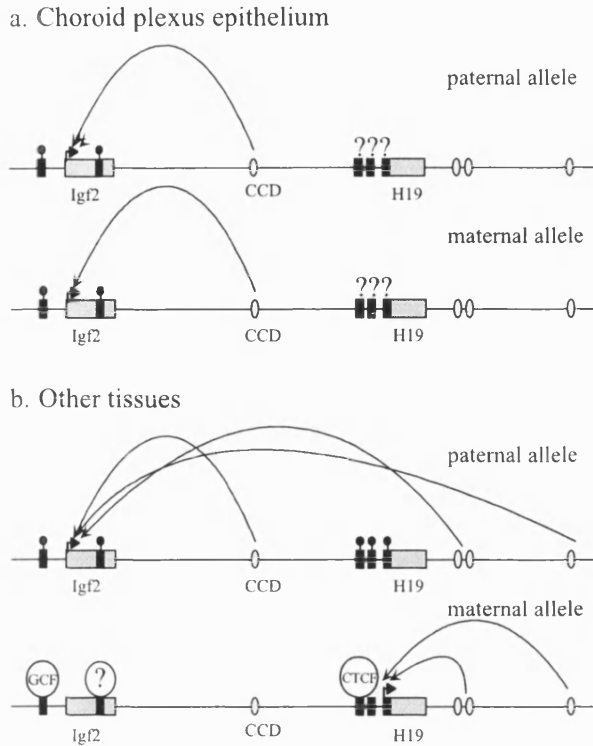


Fig. 5. Proposed model of *Igf2* expression mediated by enhancer activity of the CCD. The *Igf2* and *H19* genes (gray boxes, not to scale) are shown relative to areas that may be differentially methylated between parental alleles [black boxes, from left to right *Igf2* DMR1 and DMR2, the DMD (2 boxes) and *H19* promoter-proximal region; black lollipops above the boxes indicates regions of methylation] and enhancers (shown as gray ovals, from left, CCD, endodermal enhancers and mesodermal enhancers). Curved arrows indicate interactions between enhancers and promoters. (a) In the choroid plexus epithelium, the CCD may drive *Igf2* expression from the paternal allele and the maternal allele, as DMR1 methylation prevents the binding of *Igf2*-promoter silencing factors such as GCF. *H19* is not expressed in the choroid plexus epithelium, perhaps due to the methylation of its promoter (though this has yet to be established; see text). (b) In other tissues where the CCD is active (i.e., CP stroma, somites, tongue, eye), the *Igf2* promoter can be accessed on the paternal allele, due to methylation at DMR1. On the maternal allele, loss of DMR1 methylation allows the binding of silencing factors that prevent CCD enhancer activity. In addition, lack of methylation of the DMD on the maternal allele allows the binding of the boundary protein CTCF, and thus blocks the *Igf2* promoter from access by the distal enhancers.

opment in tissues where *Igf2* is expressed both biallelically (the choroid plexus epithelium) and monoallelically (the stroma of the choroid plexus and also discrete sites outside of the brain). It is important to note that the *Igf2* P3-LacZ-CCD transgenes did not exhibit any differences in expression when transmitted from either males or females, indicating that the isolated CCD is not sufficient to direct imprinted expression, a fact that is consistent with the absence from this region of any parental allele-specific methylation or DNaseI hypersensitivity (Koide et al., 1994). The enhancer for choroid plexus expression has previously been predicted to lie within the interval between *Igf2* and *H19*, both from transgenic experiments with CCD reporter constructs (Ward

et al., 1997), and from a 12 kb deletion, including the CCD, which showed reduced expression in the choroid plexus (Jones et al., 2001). The knockout study by Jones et al. (2001) did not report a reduction in levels of gene expression in any tissues other than the choroid plexus; however, the study measured gene expression quantitatively on dissected organs. Our study shows expression of the reporter gene in discrete tissues and developmental stages that could easily be missed by the previous approach. Likewise, deletion of the 5' 1 kb (including Region 1) of the CCD from a YAC transgene did not result in the loss of gene expression in any of the tissues that we report, and instead, CCD Region 1 was associated with a tissue-specific silencer function (Ainscough et al., 2000). Consequently, we propose that the enhancer region most likely lies in the second 1 kb of the CCD that includes Region 2 (see Fig. 1). This must be confirmed by testing smaller reporter constructs to exclude alternative explanations, such as the presence of redundant enhancers that may have obscured the role of Region 1 in the YAC experiments. Within the choroid plexus epithelium, the CCD directed transgene expression in a mosaic fashion to only a subset of cells, mimicking the endogenous *Igf2* expression pattern in this tissue. Interestingly, the silencer function of the mouse CCD was found to be conserved when it was tested in transgenic *Drosophila* and conferred variegated silencing on the mini-*white* reporter gene, with silencing dependent upon two polycomb-group proteins (Erhardt et al., 2003). This suggests a mechanism by which enhancer and silencer elements within the CCD might interact to bring about variegated expression of *Igf2* within the choroid plexus epithelium.

We propose that a mesodermal or neural crest enhancer element lies at the CCD, driving the imprinted expression of *Igf2* independently of the *Igf2*/*H19* boundary element. The *Igf2* DMRs have been shown to play a role in the imprinting of *Igf2* in the mesoderm (Constancia et al., 2000; Eden et al., 2001; Weber et al., 2001). DMR1 contains several CpG dinucleotides that are hypomethylated on the maternally derived chromosome, and hypermethylated on the paternally derived chromosome (Brandeis et al., 1993; Feil et al., 1994; Sasaki et al., 1992). Differences in the levels of methylation between parental chromosomes are most marked in tissues with a substantial mesodermal component (Weber et al., 2001). A deletion encompassing DMR1, when maternally inherited, leads to a detectable derepression of the maternal *Igf2* allele from e12 in whole embryos, and from e16 in individual mesodermal tissues (Constancia et al., 2000). The authors suggest that DMR1 contains an allele-specific silencer that represses the maternal allele in the mesoderm. An additional methylation-sensitive silencer has been mapped within DMR1, but its action is not thought to be tissue-specific (Eden et al., 2001). It would be of interest to ascertain if DMR1 can silence gene activity in the subset of mesodermal tissues stained in transgenic mice carrying the P3-LacZ-CCD reporter construct. The presence of enhancers located upstream of the DMD boundary, combined with

differential methylation at *Igf2* DMR1 and DMR2, could provide the basis of correct imprinted expression of *Igf2* in some non-endodermal tissues, including the choroid plexus epithelium (see Fig. 5).

It has been shown recently that methylation of the DMRs at this locus is coordinated in a hierarchical fashion (Lopes et al., 2003). Mutations in the DMD, when transmitted maternally, result in loss of differential methylation of both DMR1 and DMR2. Both alleles become highly methylated. Moreover, a maternally transmitted deletion encompassing DMR1 leads to a greater level of methylation of DMR2. Thus, *cis*-acting elements are present in the DMD and upstream of *Igf2* that act to protect the DMRs from methylation. This work confirms earlier experiments showing that *Igf2*-proximal DMR methylation is dependent upon DMD sequences (Forné et al., 1997), but also highlights that perturbations of DMR1 could lead to the relaxation of *Igf2* imprinting independently of the DMD. The DMRs proximal to *Igf2* provide an additional level of imprinting control. In combination with enhancers proximal to the DMD boundary, these local DMRs may provide control of *Igf2* imprinting that is independent of the DMD (Fig. 5). We propose that such an enhancer region lies at the CCD and functions to drive imprinted expression of *Igf2* in a small subset of tissues of mesodermal and neural crest origin. Other enhancer sequences may also lie within the interval between the *Igf2* promoter and the DMD boundary (Drewell et al., 2002). The presence of *Igf2*-proximal enhancers suggests that a distinct mechanism of *Igf2* imprinting has arisen in two subsets of tissues where the gene is expressed. Mutations in this DMD-independent mechanism of *Igf2* imprinting may account for some of the cases of Beckwith–Wiedemann syndrome, in which loss of imprinting of *Igf2* occurs with no modification of methylation at the DMD (Engel et al., 2000).

## Acknowledgments

We thank Tsuyoshi Koide for the 2 kb CCD clone, Haymo Kurz and the Institute of Anatomy at the University of Freiburg for assistance with *in situ* hybridization, and Catherine Skuse and 5WL1 staff for technical assistance. We are grateful to Wolf Reik (The Babraham Institute, Cambridge) for the *Igf2* *LacZ*DMR2<sup>-</sup> knock-in mouse strain. This work was supported by grants from the Association of Cancer Research, the Biotechnology and Biological Science Research Council, Cancer Research UK, and the Medical Research Council, in addition to a studentship from the University of Bath.

## References

- Ainscough, J.F.X., Koide, T., Tada, M., Barton, S., Surani, M.A., 1997. Imprinting of *Igf2* and *H19* from a 130 kb YAC transgene. *Development* 124, 3621–3632.
- Ainscough, J.F.-X., John, R.M., Barton, S.M., Surani, M.A., 2000. A skeletal muscle-specific mouse *Igf2* repressor lies 40kb downstream of the gene. *Development* 127, 3923–3930.
- Bell, A.C., Felsenfeld, G., 2000. Methylation of a CTCF-dependent boundary controls imprinted expression of the *Igf2* gene. *Nature* 405, 483–485.
- Brandeis, M., Kafri, T., Ariel, M., Chaillet, J.R., McCarrey, J., Razin, A., Cedar, H., 1993. The ontogeny of allele-specific methylation associated with imprinted genes in the mouse. *EMBO J.* 12, 3669–3677.
- Caricasole, A., Ward, A., 1993. Transactivation of the mouse insulin-like growth factor II (IGF-II) gene promoters by the AP-1 complex. *Nucleic Acids Res.* 21, 1873–1879.
- Catala, M., 1998. Embryonic and fetal development of structures associated with the cerebro-spinal fluid in man and other species. Part I: the ventricular system, meninges and choroid plexuses. *Arch. Anat. Cytol. Pathol.* 46, 153–169.
- Charalambous, M., Smith, F.M., Bennett, W.R., Crew, T.E., Mackenzie, F., Ward, A., 2003. Disruption of the imprinted *Grb10* gene leads to disproportionate overgrowth by an *Igf2*-independent mechanism. *Proc. Natl. Acad. Sci. U. S. A.* 100, 8292–8297.
- Constancia, M., Dean, W., Lopes, S., Moore, T., Kelsey, G., Reik, W., 2000. Deletion of a silencer element in the *Igf2* gene results in loss of imprinting independent of *H19*. *Nat. Genet.* 26, 203–206.
- Davies, K., Bowden, L., Smith, P., Dean, W., Hill, D., Furuumi, H., Sasaki, H., Cattanaach, B., Reik, W., 2002. Disruption of mesodermal enhancers for *Igf2* in the minute mutant. *Development* 129, 1657–1668.
- Davson, H., 1967. *Physiology of the Cerebrospinal Fluid*. J. & A. Churchill Ltd., London.
- Drewell, R.A., Arney, K.L., Arima, T., Barton, S.C., Brenton, J.D., Surani, M.A., 2002. Novel conserved elements upstream of the *H19* gene are transcribed and act as mesodermal enhancers. *Development* 129, 1205–1213.
- Eden, S., Constancia, M., Hashimshony, T., Dean, W., Goldstein, B., Johnson, A.C., Keshet, I., Reik, W., Cedar, H., 2001. An upstream repressor element plays a role in *Igf2* imprinting. *EMBO J.* 20, 3518–3525.
- Engel, J.R., Smallwood, A., Harper, A., Higgins, M.J., Oshimura, M., Reik, W., Schofield, P.N., Maher, E.R., 2000. Epigenotype-phenotype correlations in Beckwith–Wiedemann syndrome. *J. Med. Genet.* 37, 921–926.
- Erhardt, S., Lyko, F., Ainscough, J.F.-X., Surani, M.A., Paro, R., 2003. Polycomb-group proteins are involved in silencing processes caused by a transgenic element from the murine imprinted *H19/Igf2* region in *Drosophila*. *Dev. Genes Evol.* 213, 336–344.
- Feil, R., Walter, J., Allen, N.D., Reik, W., 1994. Developmental control of allelic methylation in the imprinted mouse *Igf2* and *H19* genes. *Development* 120, 2933–2943.
- Forné, T., Oswald, J., Dean, W., Saam, J.R., Bailleul, B., Dandolo, L., Tilghman, S.M., Walter, J., Reik, W., 1997. Loss of the maternal *H19* gene induces changes in *Igf2* methylation in both *cis* and *trans*. *Proc. Natl. Acad. Sci. U. S. A.* 94, 10243–10248.
- Hark, A., Schoenherr, C.J., Katz, D.J., Ingram, R.S., LeVorse, J.M., Tilghman, S.M., 2000. CTCF mediates methylation-sensitive enhancer-blocking activity at the *H19/Igf2* locus. *Nature* 405, 486–489.
- Hogan, B., Constantini, F., Lacy, E., 1986. *Manipulating The Mouse Embryo: A Laboratory Manual*. Cold Spring Harbor Press, Cold Spring Harbor, NY.
- Ishihara, K., Hatano, N., Furuumi, H., Kato, R., Iwaki, T., Miura, K., Jinno, Y., Sasaki, H., 2000. Comparative genomic sequencing identifies novel tissue-specific enhancers and sequence elements for methylation sensitive factors implicated in *Igf2/H19* imprinting. *Genome Res.* 10, 664–671.
- Jones, B.K., LeVorse, J., Tilghman, S.M., 2001. Deletion of a nuclease-sensitive region between the *Igf2* and *H19* genes leads to *Igf2* misregulation and increased adiposity. *Hum. Mol. Genet.* 10, 807–814.
- Kaffer, C.R., Srivastava, M., Park, K.-Y., Ives, E., Hsieh, S., Batlle, J., Grinberg, A., Huang, S.-P., Pfeifer, K., 2000. A transcriptional insulator at the imprinted *H19/Igf2* locus. *Genes Dev.* 14, 1908–1919.

- Kanduri, C., Pant, V., Loukinov, D., Pugacheva, E., Qi, C.F., Wolffe, A., Ohlsson, R., Lobanenkov, V.V., 2000. Functional association of CTCF with the insulator upstream of the *H19* gene is parent of origin-specific and methylation-sensitive. *Curr. Biol.* 10, 853–856.
- Koide, T., Ainscough, J., Wijgerde, M., Surani, M.A., 1994. Comparative analysis of Igf-2 H19 imprinted domain—Identification of a highly conserved intergenic DNase-I hypersensitive region. *Genomics* 24, 1–8.
- Lopes, S., Lewis, A., Hajkova, P., Dean, W., Oswald, J., Forne, T., Murrell, A., Constancia, M., Bartolomei, M., Walter, J., Reik, W., 2003. Epigenetic modifications in an imprinting cluster are controlled by a hierarchy of DMRs suggesting long-range chromatin interactions. *Hum. Mol. Genet.* 12, 295–305.
- Murakami, T., Yasuda, Y., Mita, S., Maeda, S., Shimada, K., Fujimoto, T., Araki, S., 1987. Prealbumin gene expression during mouse development studied by in situ hybridisation. *Cell Differ.* 22, 1–9.
- Murrell, A., Heeson, S., Bowden, L., Constancia, M., Dean, W., Kelsey, G., Reik, W., 2001. An intragenic methylated region in the imprinted *Igf2* augments transcription. *EMBO Rep.* 2, 1–6.
- Pant, V., Mariano, P., Kanduri, C., Mattsson, A., Lobanenkov, V., Heuchel, R., Ohlsson, R., 2003. The nucleotides responsible for the direct physical contact between the chromatin insulator protein CTCF and the H19 imprinting control region manifest parent of origin-specific long-distance insulation and methylation-free domains. *Genes Dev.* 17, 586–590.
- Ripoche, M.-A., Kress, C., Poirier, F., Dandolo, L., 1997. Deletion of the H19 transcriptional unit reveals the existence of a putative imprinting control element. *Genes Dev.* 11, 1596–1604.
- Rugh, R., 1990. *The Mouse*. Oxford Univ. Press, Oxford.
- Sambrook, J., Fritsch, E.F., Maniatis, T., 1989. *Molecular Cloning—A Laboratory Manual*. Cold Spring Harbor Univ. Press, Cold Spring Harbor.
- Sasaki, H., Jones, P.A., Chaillet, J.R., Fergusonsmith, A.C., Barton, S.C., Reik, W., Surani, M.A., 1992. Parental imprinting: potentially active chromatin of the repressed maternal allele of the mouse Insulin-like Growth Factor-II (*Igf2*) gene. *Genes Dev.* 6, 1843–1856.
- Stylianiopoulou, F., Efstratiadis, A., Herbert, J., Pintar, J., 1988a. Pattern of the insulin-like growth factor II gene expression during rat embryogenesis. *Development* 103, 497–506.
- Stylianiopoulou, F., Herbert, J., Bento-Soares, M., Efstratiadis, A., 1988b. Expression of the insulin-like growth factor II gene in the choroid plexus and the leptomeninges of the adult rat central nervous system. *Proc. Natl. Acad. Sci. U. S. A.* 85, 141–145.
- Svensson, K., Walsh, C., Fundele, R., Ohlsson, R., 1995. *H19* is imprinted in the choroid plexus and leptomeninges of the mouse foetus. *Mech. Dev.* 51, 31–37.
- Szabo, P., Tang, S.H., Rentsendorj, A., Pfeifer, G.P., Mann, J.R., 2000. Maternal-specific footprints at putative CTCF sites in the H19 imprinting control region give evidence for insulator function. *Curr. Biol.* 10, 607–610.
- Ward, A., Fisher, R., Richardson, L., Pooler, J.A., Squire, S., Bates, P., Shaposhnikov, R., Hayward, N., Thurston, M., Grayham, C.F., 1997. Genomic regions regulating imprinting and insulin-like growth factor-II promoter 3 activity in transgenics: novel enhancer and silencer elements. *Genes Funct.* 1, 25–36.
- Weber, M., Milligan, L., Delalbre, A., Antoine, E., Brunel, C., Cathala, G., Forne, T., 2001. Extensive tissue-specific variation of allele methylation in the *Igf2* gene during mouse fetal development: relation to expression and imprinting. *Mech. Dev.* 101, 133–141.